

ENANTIOSELECTIVE ADDITION OF 1,3-DICARBONYL COMPOUNDS TO  
*N*-ALKOXYCARBONYL KETIMINES DERIVED FROM ISATINS AND  
CONSTRUCTION OF SPIROCYCLIC OXINDOLES

A THESIS SUBMITTED TO  
THE GRADUATE SCHOOL OF NATURAL AND APPLIED SCIENCES  
OF  
MIDDLE EAST TECHNICAL UNIVERSITY

BY

DUYGU KARAÇAL

IN PARTIAL FULFILLMENT OF THE REQUIREMENTS  
FOR  
THE DEGREE OF DOCTOR OF PHILOSOPHY  
IN  
CHEMISTRY

DECEMBER 2022



Approval of the thesis:

**ENANTIOSELECTIVE ADDITION OF 1,3-DICARBONYL COMPOUNDS  
TO N-ALKOXYCARBONYL KETIMINES DERIVED FROM ISATINS  
AND CONSTRUCTION OF SPIROCYCLIC OXINDOLES**

submitted by **DUYGU KARAÇAL** in partial fulfillment of the requirements for the degree of **Doctor of Philosophy in Chemistry, Middle East Technical University** by,

Prof. Dr. Halil Kalıpçılar  
Dean, Graduate School of **Natural and Applied Sciences**

\_\_\_\_\_

Prof. Dr. Özdemir Doğan  
Head of the Department, **Chemistry**

\_\_\_\_\_

Prof. Dr. Cihangir Tanyeli  
Supervisor, **Chemistry, METU**

\_\_\_\_\_

**Examining Committee Members:**

Prof. Dr. Metin Zora  
Chemistry Dept., METU

\_\_\_\_\_

Prof. Dr. Cihangir Tanyeli  
Chemistry Dept., METU

\_\_\_\_\_

Prof. Dr. Özdemir Doğan  
Chemistry Dept., METU

\_\_\_\_\_

Prof. Dr. Adnan Bulut  
Chemistry Dept., Kırıkkale University

\_\_\_\_\_

Assoc.Prof. Dr. Yunus Emre Türkmen  
Chemistry Dept., Bilkent University

\_\_\_\_\_

Date: 14.12.2022

**I hereby declare that all information in this document has been obtained and presented in accordance with academic rules and ethical conduct. I also declare that, as required by these rules and conduct, I have fully cited and referenced all material and results that are not original to this work.**

Name Last name : Duygu Karaçal

Signature :

## ABSTRACT

### **ENANTIOSELECTIVE ADDITION OF 1,3-DICARBONYL COMPOUNDS TO *N*-ALKOXYCARBONYL KETIMINES DERIVED FROM ISATINS AND CONSTRUCTION OF SPIROCYCLIC OXINDOLES**

Karaçal, Duygu  
Doctor of Philosophy, Chemistry  
Supervisor : Prof. Dr. Cihangir Tanyeli

December 2022, 175 pages

Indoline-2,3-dione, commonly known as isatin, is a well-known natural product and has excellent potential to be used as an electrophile and nucleophile, making them valuable building blocks in organic synthesis. They are recognized as core structures in various bioactive molecules and pharmaceutical compounds, and the highly reactive C-3 carbonyl group of isatins makes them more applicable in organic synthesis. The reactions of the C-3 carbonyl group of isatins are mostly by nucleophilic additions and spiroannulation, resulting in the formation of C-3 substituted oxindoles. Specifically, 3-aminooxindole and heterocyclic spiro oxindole moiety have been encountered as the core structure of many architecturally complex natural products due to their highly pronounced pharmaceutical activities. In literature, several methods exist for the enantioselective formation of an amine at the C-3 position of oxindoles. Moreover, there are a few reports for the enantioselective spiro oxindole formation.

In this thesis study, in the first part, we aimed to synthesize C-3 substituted amino oxindoles by Mannich reaction of *N*-alkoxy carbonyl ketimines and

acetylacetone in the presence of chiral quinine-based bifunctional organocatalysts developed in our research group with high enantioselectivity. 2-Adamantyl substituted squaramide bifunctional organocatalyst revealed excellent enantioselectivity and yielded up to 99% and 98%, respectively.

From this methodology, in the second part of this thesis, we aimed to construct a stereoselective spirocyclic oxindole moiety at the C-3 position by Knoevenagel condensation and then Michael addition/cyclization reaction of isatins with ethyl cyanoacetate and 1,3-dicarbonyl compounds in the presence of chiral bifunctional organocatalysts. As in the Mannich reaction, 2-adamantyl squaramide-based bifunctional organocatalyst revealed the highest selectivity and yield as 99% ee and 98% yield, respectively. Optimization studies, reaction scope, and the activation modes of organocatalysts were discussed in detail.

**Keywords:** Asymmetric synthesis, bifunctional organocatalysis, squaramide, isatin, ketimine, 2-oxindole, spirooxindole

## ÖZ

### İSATİNLERDEN TÜRETİLMİŞ *N*-ALKOKSİKARBONİL KETİMİNLERİN 1,3-DİKARBONİL BİLEŞİKLERİNE ENANTİOSEÇİCİ OLARAK KATILMASI VE OKSİNDOL SİROHALKALARIN SENTEZİ

Karaçal, Duygu  
Doktora, Kimya  
Tez Yöneticisi: Prof.Dr. Cihangir Tanyeli

Aralık 2022, 175 sayfa

Genellikle isatin olarak bilinen indoline-2,3-dione, Çivit otu (*Isatis*) cinsi bitkilerde bulunan ve herkes tarafından bilinen bir doğal üründür. Isatinler, elektrofil ve nükleofil olarak kullanılma konusunda büyük potansiyele sahiptirler ve ayrıca kolaylıkla bulunabiliyor olmaları onları organik sentezde değerli yapı taşları haline getirmektedir. Çeşitli biyoaktif moleküller ve farmasötik bileşiklerde ana yapı olarak kabul edilirler ve reaktivitesi yüksek C-3 karbonil grupları onları organik sentez için daha uygulanabilir hale getirir. Isatinlerin C-3 karbonil grubunun tepkimeleri çoğunlukla nükleofilik katılmalar ve spiroanülasyon tepkimeleri olup, C-3 pozisyonunda substitüye oksindollerin oluşmasıyla sonuçlanır. Özellikle, 3-aminooksindol yapısı ve heterosiklik spirooksindol yapısı fazlaca etkili farmasötik aktivitelerinden dolayı yapısal olarak kompleks doğal ürünlerin en önemli merkezi olarak karşımıza çıkmaktadır. Literatürde, oksindollerin C-3 pozisyonunda enantioseçici olarak amin oluşmasıyla ilgili çeşitli yöntemler bulunmaktadır. Ayrıca, enantioseçici olarak spirooksindol yapısının oluşmasıyla ilgili çok az çalışma bulunmaktadır.

Bu tezin ilk kısmında, araştırma grubumuzda sentezlenen çeşitli kiral bifonksiyonel kinin bazlı organokatalizörler varlığında, 1,3-dikarbonil bileşiklerinin *N*-alkoksi karbonil ketiminlerle Mannich tepkimesinde yüksek seçicilik ve verim elde etmeyi amaçlanmaktadır. Çalışmalar sonucunda 2-adamantil skuaramit yapılı katalizör varlığında %99 enantioseçicilik ve %98 verim elde edilmiştir.

Bu metodolojiden yola çıkarak, tezin ikinci kısmında ise, kiral bifonksiyonel asit/baz organocatalizörler varlığında isatin, etil siyanoasetat ve 1,3-dikarbonil bileşiklerinin Knoevenagel kondenzasyonu, Michael katılma tepkimesi ve siklizasyon tepkimesi ile enantioseçici spirooksindol yapısının oluşturulması amaçlanmıştır. 2-Adamantil skuaramit/kinin katalizörü varlığında yapılan çalışmalar sonucunda en yüksek %99 enantioseçicilik ve %98 verim elde edilmiştir. Her iki çalışmanın da optimizasyon denemeleri, tepkime kapsamları ve organokatalizörün aktivasyon modları detaylı bir şekilde ele alınmıştır.

Anahtar Kelimeler: Asimetrik Sentez, bifonksiyonel organokatalizör, skuaramit, isatin, ketimin, 2-oksindol, spirooksindol



*To My Family, My Love and Deary Pito*

## ACKNOWLEDGEMENTS

Firstly, I would like to thank and express my sincere appreciation to my supervisor Prof. Dr. Cihangir Tanyeli for his valuable patience, guidance, support, advice, and encouragement throughout my Ph.D. study while I am working in the industry.

I am also grateful to my thesis monitoring committee, Prof. Dr. Özdemir Doğan, and Assoc. Prof. Dr. Yunus Emre Türkmen for their support and valuable feedback. I also would like to thank all faculty members of the Department of Chemistry for improving my scientific point of view throughout my education.

Besides all, I am also thankful to M.Sc. Supervisor, late Prof. Dr. Ayhan Sıtkı Demir, who teach me that ‘Chemistry is love’ and for his valuable guidance and scientific ideas. It was an honor for me to meet and work with him and to be his student. Rest in peace; I will never forget you.

Thank NMR specialist Betül Eymur, and Zeynep Erdoğan from Bilkent University for the HRMS analysis.

I want to thank my whole current and former lab members of the Tanyeli Research Group for their support, understanding, and friendship. Mainly, I would like to express my great thanks to Ezgi Bayer Kömüşdoğan, Arzu Bilgin Akdoğan, Seda Karahan, Zeynep Dilşad Susam and Esra DüNDAR for their help and support in NMR analysis and in solving some problems for me while I am working in industry throughout my Ph.D. studies.

I am also grateful to my manager and work colleagues in ROKETSAN for letting me finish my Ph.D. and supporting me endlessly. They encouraged me whenever I gave up and helped me to continue. It was a chance to work with them, and luckily I have them.

I am also very thankful to my lovely friend Seza Göker for supplying me DMSO for my NMR analyses and her everlasting support and friendship.

Apart from everything and everyone, I am very grateful to my family for their endless patience, support, understanding, and encouragement. Without their precious love and trust, it would be impossible to work and complete this Ph.D. study. Additionally, I would like to thank and send lots of love to the love of my life, my dear husband, for his endless patience and motivation throughout my life. Without you, I could not live in this city, could not work in ROKETSAN, and could not finish my Ph.D. study. I am lucky to be part of your life and love you to the moon and back.

## TABLE OF CONTENTS

ABSTRACT .....	v
ÖZ .....	vii
ACKNOWLEDGEMENTS .....	x
TABLE OF CONTENTS .....	xii
LIST OF TABLES .....	xviii
LIST OF FIGURES .....	xix
LIST OF SCHEMES .....	xxvi
LIST OF ABBREVIATIONS .....	xxvii
CHAPTERS.....	1
1. INTRODUCTION .....	1
1.1 Importance of Isatins .....	1
1.1.1 Chiral Oxindoles and Spirocyclic Oxindoles .....	3
1.2 Importance of Asymmetric Synthesis.....	8
1.2.1 Asymmetric Organocatalysis.....	9
1.2.2 Classification of Organocatalysis .....	10
1.2.3 Hydrogen Bonding Interactions and Bifunctional Organocatalysis ..	11
1.3 Importance of 1,3-Dicarbonyl Compounds .....	17
1.4 Enantioselective Strategies for Synthesis of 3,3-Disubstituted Oxindoles and Spirooxindoles .....	18
1.4.1 Mannich Reaction.....	19
1.4.2 Knoevenagel Condensation .....	22

1.4.3	Domino Knoevenagel Condensation / Michael Addition/ Cyclization Reaction .....	24
1.5	Aim of the work .....	27
2	RESULTS AND DISCUSSION .....	31
2.1	Synthesis of Starting Materials .....	31
2.1.1	Synthesis of <i>N</i> -Carbamate Protected Ketimines .....	31
2.1.2	Synthesis of Knoevenagel condensates .....	33
2.2	Asymmetric Mannich Reaction.....	35
2.2.1	Optimization of Reaction Parameters for Mannich Reaction .....	35
2.2.2	Scope of Mannich Reaction .....	38
2.3	Enantioselective Construction of Spiro Conjugated Amino-pyran-oxindoles.....	44
2.3.1	Optimization of the Reaction Parameters for Construction of Spiro Conjugated Amino-pyran-oxindoles.....	44
2.3.2	Scope of Enantioselective Construction of Spiro Conjugated Amino-pyran-oxindoles.....	51
3	EXPERIMENTAL.....	59
3.1	Materials and Methods .....	59
3.2	General Procedure A: Synthesis of <i>N</i> -Substituted Isatin Derivatives.....	60
3.2.1	<i>N</i> -Alkylation of Isatin .....	60
3.2.2	<i>N</i> -Benzylation of Isatin .....	60
3.2.3	<i>N</i> -Acetylation of Isatin.....	61
3.3	General Procedure B: Synthesis of Isatin-Derived Ketimines .....	61
3.4	General Procedure C: Racemic Synthesis of Mannich Adducts .....	61
3.5	General Procedure D: Asymmetric Synthesis of Mannich Adducts .....	62

3.5.1	( <i>S</i> )- <i>tert</i> -Butyl (3-(2,4-dioxopentan-3-yl)-1-methyl-2-oxoindolin-3-yl)carbamate (84a)	62
3.5.2	( <i>S</i> )- <i>tert</i> -Butyl (3-(2,4-dioxopentan-3-yl)-2-oxoindolin-3-yl)carbamate (84b)	63
3.5.3	( <i>S</i> )- <i>tert</i> -Butyl (1-acetyl-3-(2,4-dioxopentan-3-yl)-2-oxoindolin-3-yl)carbamate (84c)	63
3.5.4	( <i>S</i> )- <i>tert</i> -Butyl (1-benzyl-3-(2,4-dioxopentan-3-yl)-2-oxoindolin-3-yl)carbamate (84d)	64
3.5.5	( <i>S</i> )- <i>tert</i> -Butyl (3-(2,4-dioxopentan-3-yl)-1-ethyl-2-oxoindolin-3-yl)carbamate (84e)	64
3.5.6	( <i>S</i> )-Ethyl (3-(2,4-dioxopentan-3-yl)-2-oxoindolin-3-yl)carbamate (84f)	65
3.5.7	( <i>S</i> )-Benzyl (3-(2,4-dioxopentan-3-yl)-2-oxoindolin-3-yl)carbamate (84g)	65
3.5.8	( <i>S</i> )-Benzyl (3-(2,4-dioxopentan-3-yl)-1-methyl-2-oxoindolin-3-yl)carbamate (84i)	66
3.5.9	( <i>S</i> )-Ethyl (3-(2,4-dioxopentan-3-yl)-1-methyl-2-oxoindolin-3-yl)carbamate (84j)	67
3.5.10	( <i>S</i> )- <i>tert</i> -Butyl (3-(2,4-dioxopentan-3-yl)-5-methoxy-1-methyl-2-oxoindolin-3-yl)carbamate (84k)	67
3.5.11	( <i>S</i> )- <i>tert</i> -Butyl (3-(2,4-dioxopentan-3-yl)-1,5-dimethyl-2-oxoindolin-3-yl)carbamate (84l)	68
3.5.12	( <i>S</i> )- <i>tert</i> -Butyl (7-chloro-3-(2,4-dioxopentan-3-yl)-1-methyl-2-oxoindolin-3-yl)carbamate (84m)	68
3.5.13	( <i>S</i> )- <i>tert</i> -Butyl (6-chloro-3-(2,4-dioxopentan-3-yl)-1-methyl-2-oxoindolin-3-yl)carbamate (84n)	69

3.5.14	( <i>S</i> )- <i>tert</i> -Butyl (6-bromo-3-(2,4-dioxopentan-3-yl)-1-methyl-2-oxoindolin-3-yl)carbamate (84o) .....	70
3.5.15	( <i>S</i> )- <i>tert</i> -Butyl (3-(2,4-dioxopentan-3-yl)-7-fluoro-1-methyl-2-oxoindolin-3-yl)carbamate (84p) .....	70
3.5.16	( <i>S</i> )- <i>tert</i> -Butyl (5-bromo-3-(2,4-dioxopentan-3-yl)-2-oxoindolin-3-yl)carbamate (84q) .....	71
3.5.17	( <i>S</i> )- <i>tert</i> -Butyl (3-(2,4-dioxopentan-3-yl)-5-fluoro-2-oxoindolin-3-yl)carbamate (84r).....	71
3.5.18	( <i>S</i> )- <i>tert</i> -Butyl (3-(2,4-dioxopentan-3-yl)-5,7-dimethyl-2-oxoindolin-3-yl)carbamate (84s) .....	72
3.6	General Procedure E: Synthesis of 2-cyano-2-oxoindoline-alkylidene acetates .....	72
3.6.1	2-cyano-2-(1-methyl-2-oxoindolin-3-ylidene)acetate (77a) .....	73
3.6.2	ethyl 2-cyano-2-(5-methoxy-1-methyl-2-oxoindolin-3-ylidene)acetate (77b) .....	73
3.6.3	ethyl 2-cyano-2-(1,5-dimethyl-2-oxoindolin-3-ylidene)acetate (77c).. .....	74
3.6.4	ethyl 2-(5-bromo-1-methyl-2-oxoindolin-3-ylidene)-2-cyanoacetate (77d) .....	74
3.6.5	ethyl 2-cyano-2-(5-fluoro-1-methyl-2-oxoindolin-3-ylidene)acetate (77e) .....	75
3.6.6	2-cyano-2-(2-oxoindolin-3-ylidene) acetate (77g).....	75
3.6.7	ethyl 2-(1-benzyl-2-oxoindolin-3-ylidene)-2-cyanoacetate (77h) ....	76
3.6.8	ethyl 2-cyano-2-(5,7-dimethyl-2-oxoindolin-3-ylidene)acetate (77i) .....	76

3.7	General Procedure F: Racemic Synthesis of Michael Addition/Cyclization Adducts Spiro Conjugated Amino-pyran-oxindoles .....	77
3.8	General Procedure G: Asymmetric Synthesis of Michael Addition/Cyclization Adducts Spiro Conjugated Amino-pyran-oxindoles .....	77
3.8.1	( <i>S</i> )-ethyl 3'-acetyl-6'-amino-1,2'-dimethyl-2-oxospiro[indoline-3,4'-pyran]-5'-carboxylate (87a) .....	77
3.8.2	( <i>S</i> )-ethyl 3'-acetyl-6'-amino-5-methoxy-1,2'-dimethyl-2-oxospiro[indoline-3,4'-pyran]-5'-carboxylate (87b) .....	78
3.8.3	( <i>S</i> )-ethyl 3'-acetyl-6'-amino-1,2',5-trimethyl-2-oxospiro[indoline-3,4'-pyran]-5'-carboxylate (87c) .....	79
3.8.4	( <i>S</i> )-ethyl 3'-acetyl-6'-amino-5-bromo-1,2'-dimethyl-2-oxospiro[indoline-3,4'-pyran]-5'-carboxylate (87d) .....	79
3.8.5	( <i>S</i> )-ethyl 3'-acetyl-6'-amino-5-fluoro-1,2'-dimethyl-2-oxospiro[indoline-3,4'-pyran]-5'-carboxylate (87e) .....	80
3.8.6	( <i>S</i> )-ethyl 3'-acetyl-6'-amino-7-fluoro-1,2'-dimethyl-2-oxospiro[indoline-3,4'-pyran]-5'-carboxylate (87f) .....	80
3.8.7	( <i>S</i> )-ethyl 3'-acetyl-6'-amino-2'-methyl-2-oxospiro[indoline-3,4'-pyran]-5'-carboxylate (87g) .....	81
3.8.8	( <i>S</i> )-ethyl 3'-acetyl-6'-amino-1-benzyl-2'-methyl-2-oxospiro[indoline-3,4'-pyran]-5'-carboxylate .....	82
3.8.9	( <i>S</i> )-ethyl 3'-acetyl-6'-amino-2',5,7-trimethyl-2-oxospiro[indoline-3,4'-pyran]-5'-carboxylate (87i) .....	82
3.8.10	( <i>S</i> )-ethyl 2-amino-1',6,6-trimethyl-2',5-dioxo-5,6,7,8-tetrahydrospiro[chromene-4,3'-indoline]-3-carboxylate (87j) .....	83
3.8.11	( <i>S</i> )-ethyl 2-amino-1',7,7-trimethyl-2',5-dioxo-5,6,7,8-tetrahydrospiro[chromene-4,3'-indoline]-3-carboxylate (87k) .....	84



3.8.12	( <i>S</i> )-ethyl 2-amino-1'-methyl-2',5-dioxo-5,6,7,8-tetrahydrospiro[chromene-4,3'-indoline]-3-carboxylate (87l) .....	84
3.8.13	( <i>S</i> )-3'-ethyl 5'-methyl 2'-amino-1,6'-dimethyl-2-oxospiro[indoline-3,4'-pyran]-3',5'-dicarboxylate (87m) .....	85
3.8.14	( <i>S</i> )-diethyl 2'-amino-1-methyl-2-oxo-6'-phenylspiro[indoline-3,4'-pyran]-3',5'-dicarboxylate (87n).....	85
3.8.15	( <i>S</i> )-diethyl 2'-amino-6'-ethyl-1-methyl-2-oxospiro[indoline-3,4'-pyran]-3',5'-dicarboxylate (87o).....	86
3.8.16	( <i>S</i> )-diethyl 2'-amino-1,6'-dimethyl-2-oxospiro[indoline-3,4'-pyran]-3',5'-dicarboxylate (87p) .....	87
3.8.17	( <i>S</i> )-ethyl 2'-amino-5'-cyano-1-methyl-2-oxo-6'-phenylspiro[indoline-3,4'-pyran]-3'-carboxylate (87q) .....	87
4	CONCLUSION .....	89
	REFERENCES .....	91
	APPENDICES.....	97
	A.    NMR SPECTRA .....	97
	B.    HPLC CHROMATOGRAMS.....	140
	CURRICULUM VITAE .....	175

## LIST OF TABLES

### TABLES

<b>Table 1</b> Synthesized <i>N</i> -Carbamate Protected Ketimines .....	32
<b>Table 2</b> Synthesized 2-oxoindolin-3-ylidene acetate derivatives .....	33
<b>Table 3</b> Catalyst Screening for Optimization of Mannich Reaction.....	36
<b>Table 4</b> Catalyst loading and Concentration Screening.....	37
<b>Table 5</b> Solvent Screening .....	37
<b>Table 6</b> Reaction scope of Mannich reaction of isatin derived ketimine <b>76</b> and acetylacetone <b>29</b> .....	39
<b>Table 7</b> Reaction scope of Mannich reaction of isatin derived ketimine <b>76</b> and other 1,3-dicarbonyl compounds <b>85</b> .....	43
<b>Table 8</b> Optimization studies for the Enantioselective Construction of Spirooxindoles.....	44
<b>Table 9</b> Catalyst Screening .....	48
<b>Table 10</b> Temperature Screening.....	49
<b>Table 11</b> 4Å MS Effect.....	49
<b>Table 12</b> Solvent Screening .....	50
<b>Table 13</b> Concentration Screening.....	50
<b>Table 14</b> Reaction scope for the construction of Spiro Conjugated Amino-pyran-oxindoles.....	52

## LIST OF FIGURES

### FIGURES

<b>Figure 1</b> Structure of isatin and isatin derived transformations .....	2
<b>Figure 2</b> Representative examples of biologically active compounds containing 3-amino-2-oxindole skeleton.....	3
<b>Figure 3</b> Representative examples from isatin imine framework .....	5
<b>Figure 4</b> Incidence of spirooxindoles in the literature up to 2020 .....	6
<b>Figure 5</b> Catalytic asymmetric synthesis of chiral spirooxindoles from oxindole derivatives .....	8
<b>Figure 6</b> Classification of Organocatalysis .....	11
<b>Figure 7</b> Single and dual activation concept of bifunctional thiourea organocatalyst .....	12
<b>Figure 8</b> Literature examples of bifunctional organocatalysts .....	13
<b>Figure 9</b> Duality in H-bonding in Squaramides .....	14
<b>Figure 10</b> Resonance structure of i) (thio)urea, ii) squaramide .....	15
<b>Figure 11</b> Calculated i) H-bond spacing, ii) H-bond angle.....	15
<b>Figure 12</b> pK <sub>a</sub> values of squaramide analogues in DMSO.....	16
<b>Figure 13</b> Selected literature examples of Squaramide based organocatalysts.....	17
<b>Figure 14</b> Potential Reaction Sites of 1,3-Dicarbonyl Compounds .....	18
<b>Figure 15</b> Quinine-based bifunctional organocatalysts.....	28
<b>Figure 16</b> <sup>1</sup> H NMR Spectrum of <b>77a</b> .....	35
<b>Figure 17</b> <sup>1</sup> H-NMR Spectrum of <b>84a</b> .....	41
<b>Figure 18</b> <sup>13</sup> C-NMR Spectrum of <b>84a</b> .....	41
<b>Figure 19</b> Possible transition state .....	42
<b>Figure 20</b> <sup>1</sup> H NMR Spectrum of <b>87a</b> .....	55
<b>Figure 21</b> <sup>13</sup> C NMR Spectrum of <b>87a</b> .....	55
<b>Figure 22</b> Plausible reaction course model .....	57
<b>Figure A. 1</b> <sup>1</sup> H NMR spectrum of <b>84a</b> .....	97
<b>Figure A. 2</b> <sup>13</sup> C NMR spectrum of <b>84a</b> .....	97

<b>Figure A. 3</b> $^1\text{H}$ NMR spectrum of <b>84b</b> .....	98
<b>Figure A. 4</b> $^{13}\text{C}$ NMR spectrum of <b>84b</b> .....	98
<b>Figure A. 5</b> $^1\text{H}$ NMR spectrum of <b>84c</b> .....	99
<b>Figure A. 6</b> $^{13}\text{C}$ NMR spectrum of <b>84c</b> .....	99
<b>Figure A. 7</b> $^1\text{H}$ NMR spectrum of <b>84d</b> .....	100
<b>Figure A. 8</b> $^{13}\text{C}$ NMR spectrum of <b>84d</b> .....	100
<b>Figure A. 9</b> $^1\text{H}$ NMR spectrum of <b>84e</b> .....	101
<b>Figure A. 10</b> $^{13}\text{C}$ NMR spectrum of <b>84e</b> .....	101
<b>Figure A. 11</b> $^1\text{H}$ NMR spectrum of <b>84f</b> .....	102
<b>Figure A. 12</b> $^{13}\text{C}$ NMR spectrum of <b>84f</b> .....	102
<b>Figure A. 13</b> $^1\text{H}$ NMR spectrum of <b>84g</b> .....	103
<b>Figure A. 14</b> $^{13}\text{C}$ NMR spectrum of <b>84g</b> .....	103
<b>Figure A. 15</b> $^1\text{H}$ NMR spectrum of <b>84i</b> .....	104
<b>Figure A. 16</b> $^{13}\text{C}$ NMR spectrum of <b>84i</b> .....	104
<b>Figure A. 17</b> $^1\text{H}$ NMR spectrum of <b>84j</b> .....	105
<b>Figure A. 18</b> $^{13}\text{C}$ NMR spectrum of <b>84j</b> .....	105
<b>Figure A. 19</b> $^1\text{H}$ NMR spectrum of <b>84k</b> .....	106
<b>Figure A. 20</b> $^{13}\text{C}$ NMR spectrum of <b>84k</b> .....	106
<b>Figure A. 21</b> $^1\text{H}$ NMR spectrum of <b>84l</b> .....	107
<b>Figure A. 22</b> $^{13}\text{C}$ NMR spectrum of <b>84l</b> .....	107
<b>Figure A. 23</b> $^1\text{H}$ NMR spectrum of <b>84m</b> .....	108
<b>Figure A. 24</b> $^{13}\text{C}$ NMR spectrum of <b>84m</b> .....	108
<b>Figure A. 25</b> $^1\text{H}$ NMR spectrum of <b>84n</b> .....	109
<b>Figure A. 26</b> $^{13}\text{C}$ NMR spectrum of <b>84n</b> .....	109
<b>Figure A. 27</b> $^1\text{H}$ NMR spectrum of <b>84o</b> .....	110
<b>Figure A. 28</b> $^{13}\text{C}$ NMR spectrum of <b>84o</b> .....	110
<b>Figure A. 29</b> $^1\text{H}$ NMR spectrum of <b>84p</b> .....	111
<b>Figure A. 30</b> $^{13}\text{C}$ NMR spectrum of <b>84p</b> .....	111
<b>Figure A. 31</b> $^1\text{H}$ NMR spectrum of <b>84q</b> .....	112
<b>Figure A. 32</b> $^{13}\text{C}$ NMR spectrum of <b>84q</b> .....	112

<b>Figure A. 33</b> $^1\text{H}$ NMR spectrum of <b>84r</b> .....	113
<b>Figure A. 34</b> $^{13}\text{C}$ NMR spectrum of <b>84r</b> .....	113
<b>Figure A. 35</b> $^1\text{H}$ NMR spectrum of <b>84s</b> .....	114
<b>Figure A. 36</b> $^{13}\text{C}$ NMR spectrum of <b>84s</b> .....	114
<b>Figure A. 37</b> $^1\text{H}$ NMR spectrum of <b>77a</b> .....	115
<b>Figure A. 38</b> $^{13}\text{C}$ NMR spectrum of <b>77a</b> .....	115
<b>Figure A. 39</b> $^1\text{H}$ NMR spectrum of <b>77b</b> .....	116
<b>Figure A. 40</b> $^{13}\text{C}$ NMR spectrum of <b>77b</b> .....	116
<b>Figure A. 41</b> $^1\text{H}$ NMR spectrum of <b>77c</b> .....	117
<b>Figure A. 42</b> $^{13}\text{C}$ NMR spectrum of <b>77c</b> .....	117
<b>Figure A. 43</b> $^1\text{H}$ NMR spectrum of <b>77d</b> .....	118
<b>Figure A. 44</b> $^{13}\text{C}$ NMR spectrum of <b>77d</b> .....	118
<b>Figure A. 45</b> $^1\text{H}$ NMR spectrum of <b>77e</b> .....	119
<b>Figure A. 46</b> $^{13}\text{C}$ NMR spectrum of <b>77e</b> .....	119
<b>Figure A. 47</b> $^1\text{H}$ NMR spectrum of <b>77g</b> .....	120
<b>Figure A. 48</b> $^{13}\text{C}$ NMR spectrum of <b>77g</b> .....	120
<b>Figure A. 49</b> $^1\text{H}$ NMR spectrum of <b>77h</b> .....	121
<b>Figure A. 50</b> $^{13}\text{C}$ NMR spectrum of <b>77h</b> .....	121
<b>Figure A. 51</b> $^1\text{H}$ NMR spectrum of <b>77i</b> .....	122
<b>Figure A. 52</b> $^{13}\text{C}$ NMR spectrum of <b>77i</b> .....	122
<b>Figure A. 53</b> $^1\text{H}$ NMR spectrum of <b>87a</b> .....	123
<b>Figure A. 54</b> $^{13}\text{C}$ NMR spectrum of <b>87a</b> .....	123
<b>Figure A. 55</b> $^1\text{H}$ NMR spectrum of <b>87b</b> .....	124
<b>Figure A. 56</b> $^{13}\text{C}$ NMR spectrum of <b>87b</b> .....	124
<b>Figure A. 57</b> $^1\text{H}$ NMR spectrum of <b>87c</b> .....	125
<b>Figure A. 58</b> $^{13}\text{C}$ NMR spectrum of <b>87c</b> .....	125
<b>Figure A. 59</b> $^1\text{H}$ NMR spectrum of <b>87d</b> .....	126
<b>Figure A. 60</b> $^{13}\text{C}$ NMR spectrum of <b>87d</b> .....	126
<b>Figure A. 61</b> $^1\text{H}$ NMR spectrum of <b>87e</b> .....	127
<b>Figure A. 62</b> $^{13}\text{C}$ NMR spectrum of <b>87e</b> .....	127

<b>Figure A. 63</b> $^1\text{H}$ NMR spectrum of <b>87f</b> .....	128
<b>Figure A. 64</b> $^{13}\text{C}$ NMR spectrum of <b>87f</b> .....	128
<b>Figure A. 65</b> $^1\text{H}$ NMR spectrum of <b>87g</b> .....	129
<b>Figure A. 66</b> $^{13}\text{C}$ NMR spectrum of <b>87g</b> .....	129
<b>Figure A. 67</b> $^1\text{H}$ NMR spectrum of <b>87h</b> .....	130
<b>Figure A. 68</b> $^{13}\text{C}$ NMR spectrum of <b>87h</b> .....	130
<b>Figure A. 69</b> $^1\text{H}$ NMR spectrum of <b>87i</b> .....	131
<b>Figure A. 70</b> $^{13}\text{C}$ NMR spectrum of <b>87i</b> .....	131
<b>Figure A. 71</b> $^1\text{H}$ NMR spectrum of <b>87j</b> .....	132
<b>Figure A. 72</b> $^{13}\text{C}$ NMR spectrum of <b>87j</b> .....	132
<b>Figure A. 73</b> $^1\text{H}$ NMR spectrum of <b>87k</b> .....	133
<b>Figure A. 74</b> $^{13}\text{C}$ NMR spectrum of <b>87k</b> .....	133
<b>Figure A. 75</b> $^1\text{H}$ NMR spectrum of <b>87l</b> .....	134
<b>Figure A. 76</b> $^{13}\text{C}$ NMR spectrum of <b>87l</b> .....	134
<b>Figure A. 77</b> $^1\text{H}$ NMR spectrum of <b>87m</b> .....	135
<b>Figure A. 78</b> $^{13}\text{C}$ NMR spectrum of <b>87m</b> .....	135
<b>Figure A. 79</b> $^1\text{H}$ NMR spectrum of <b>87n</b> .....	136
<b>Figure A. 80</b> $^{13}\text{C}$ NMR spectrum of <b>87n</b> .....	136
<b>Figure A. 81</b> $^1\text{H}$ NMR spectrum of <b>87o</b> .....	137
<b>Figure A. 82</b> $^{13}\text{C}$ NMR spectrum of <b>87o</b> .....	137
<b>Figure A. 83</b> $^1\text{H}$ NMR spectrum of <b>87p</b> .....	138
<b>Figure A. 84</b> $^{13}\text{C}$ NMR spectrum of <b>87p</b> .....	138
<b>Figure A. 85</b> $^1\text{H}$ NMR spectrum of <b>87q</b> .....	139
<b>Figure A. 86</b> $^{13}\text{C}$ NMR spectrum of <b>87q</b> .....	139
<b>Figure B. 1</b> HPLC chromatogram of <i>rac</i> - <b>84a</b> .....	140
<b>Figure B. 2</b> HPLC chromatogram of enantiomerically enriched <b>84a</b> .....	140
<b>Figure B. 3</b> HPLC chromatogram of <i>rac</i> - <b>84b</b> .....	141
<b>Figure B. 4</b> HPLC chromatogram of enantiomerically enriched <b>84b</b> .....	141
<b>Figure B. 5</b> HPLC chromatogram of <i>rac</i> - <b>84c</b> .....	142
<b>Figure B. 6</b> HPLC chromatogram of enantiomerically enriched <b>84c</b> .....	142

<b>Figure B. 7</b> HPLC chromatogram of <i>rac</i> - <b>84d</b> .....	143
<b>Figure B. 8</b> HPLC chromatogram of enantiomerically enriched <b>84d</b> .....	143
<b>Figure B. 9</b> HPLC chromatogram of <i>rac</i> - <b>84e</b> .....	144
<b>Figure B. 10</b> HPLC chromatogram of enantiomerically enriched <b>84e</b> .....	144
<b>Figure B. 11</b> HPLC chromatogram of <i>rac</i> - <b>84f</b> .....	145
<b>Figure B. 12</b> HPLC chromatogram of enantiomerically enriched <b>84f</b> .....	145
<b>Figure B. 13</b> HPLC chromatogram of <i>rac</i> - <b>84g</b> .....	146
<b>Figure B. 14</b> HPLC chromatogram of enantiomerically enriched <b>84g</b> .....	146
<b>Figure B. 15</b> HPLC chromatogram of <i>rac</i> - <b>84i</b> .....	147
<b>Figure B. 16</b> HPLC chromatogram of enantiomerically enriched <b>84i</b> .....	147
<b>Figure B. 17</b> HPLC chromatogram of <i>rac</i> - <b>84j</b> .....	148
<b>Figure B. 18</b> HPLC chromatogram of enantiomerically enriched <b>84j</b> .....	148
<b>Figure B. 19</b> HPLC chromatogram of <i>rac</i> - <b>84k</b> .....	149
<b>Figure B. 20</b> HPLC chromatogram of enantiomerically enriched <b>84k</b> .....	149
<b>Figure B. 21</b> HPLC chromatogram of <i>rac</i> - <b>84l</b> .....	150
<b>Figure B. 22</b> HPLC chromatogram of enantiomerically enriched <b>84l</b> .....	150
<b>Figure B. 23</b> HPLC chromatogram of <i>rac</i> - <b>84m</b> .....	151
<b>Figure B. 24</b> HPLC chromatogram of enantiomerically enriched <b>84m</b> .....	151
<b>Figure B. 25</b> HPLC chromatogram of <i>rac</i> - <b>84n</b> .....	152
<b>Figure B. 26</b> HPLC chromatogram of enantiomerically enriched <b>84n</b> .....	152
<b>Figure B. 27</b> HPLC chromatogram of <i>rac</i> - <b>84o</b> .....	153
<b>Figure B. 28</b> HPLC chromatogram of enantiomerically enriched <b>84o</b> .....	153
<b>Figure B. 29</b> HPLC chromatogram of <i>rac</i> - <b>84p</b> .....	154
<b>Figure B. 30</b> HPLC chromatogram of enantiomerically enriched <b>84p</b> .....	154
<b>Figure B. 31</b> HPLC chromatogram of <i>rac</i> - <b>84q</b> .....	155
<b>Figure B. 32</b> HPLC chromatogram of enantiomerically enriched <b>84q</b> .....	155
<b>Figure B. 33</b> HPLC chromatogram of <i>rac</i> - <b>84r</b> .....	156
<b>Figure B. 34</b> HPLC chromatogram of enantiomerically enriched <b>84r</b> .....	156
<b>Figure B. 35</b> HPLC chromatogram of <i>rac</i> - <b>84s</b> .....	157
<b>Figure B. 36</b> HPLC chromatogram of enantiomerically enriched <b>84s</b> .....	157

<b>Figure B. 37</b> HPLC chromatogram of <i>rac-87a</i> .....	158
<b>Figure B. 38</b> HPLC chromatogram of enantiomerically enriched <b>87a</b> .....	158
<b>Figure B. 39</b> HPLC chromatogram of <i>rac-87b</i> .....	159
<b>Figure B. 40</b> HPLC chromatogram of enantiomerically enriched <b>87b</b> .....	159
<b>Figure B. 41</b> HPLC chromatogram of <i>rac-87c</i> .....	160
<b>Figure B. 42</b> HPLC chromatogram of enantiomerically enriched <b>87c</b> .....	160
<b>Figure B. 43</b> HPLC chromatogram of <i>rac-87d</i> .....	161
<b>Figure B. 44</b> HPLC chromatogram of enantiomerically enriched <b>87d</b> .....	161
<b>Figure B. 45</b> HPLC chromatogram of <i>rac-87e</i> .....	162
<b>Figure B. 46</b> HPLC chromatogram of enantiomerically enriched <b>87e</b> .....	162
<b>Figure B. 47</b> HPLC chromatogram of <i>rac-87f</i> .....	163
<b>Figure B. 48</b> HPLC chromatogram of enantiomerically enriched <b>87f</b> .....	163
<b>Figure B. 49</b> HPLC chromatogram of <i>rac-87g</i> .....	164
<b>Figure B. 50</b> HPLC chromatogram of enantiomerically enriched <b>87g</b> .....	164
<b>Figure B. 51</b> HPLC chromatogram of <i>rac-87h</i> .....	165
<b>Figure B. 52</b> HPLC chromatogram of enantiomerically enriched <b>87h</b> .....	165
<b>Figure B. 53</b> HPLC chromatogram of <i>rac-87i</i> .....	166
<b>Figure B. 54</b> HPLC chromatogram of enantiomerically enriched <b>87i</b> .....	166
<b>Figure B. 55</b> HPLC chromatogram of <i>rac-87j</i> .....	167
<b>Figure B. 56</b> HPLC chromatogram of enantiomerically enriched <b>87j</b> .....	167
<b>Figure B. 57</b> HPLC chromatogram of <i>rac-87k</i> .....	168
<b>Figure B. 58</b> HPLC chromatogram of enantiomerically enriched <b>87k</b> .....	168
<b>Figure B. 59</b> HPLC chromatogram of <i>rac-87l</i> .....	169
<b>Figure B. 60</b> HPLC chromatogram of enantiomerically enriched <b>87l</b> .....	169
<b>Figure B. 61</b> HPLC chromatogram of <i>rac-87m</i> .....	170
<b>Figure B. 62</b> HPLC chromatogram of enantiomerically enriched <b>87m</b> .....	170
<b>Figure B. 63</b> HPLC chromatogram of <i>rac-87n</i> .....	171
<b>Figure B. 64</b> HPLC chromatogram of enantiomerically enriched <b>87n</b> .....	171
<b>Figure B. 65</b> HPLC chromatogram of <i>rac-87o</i> .....	172
<b>Figure B. 66</b> HPLC chromatogram of enantiomerically enriched <b>87o</b> .....	172



<b>Figure B. 67</b> HPLC chromatogram of <i>rac</i> - <b>87p</b> .....	173
<b>Figure B. 68</b> HPLC chromatogram of enantiomerically enriched <b>87p</b> .....	173
<b>Figure B. 69</b> HPLC chromatogram of <i>rac</i> - <b>87q</b> .....	174
<b>Figure B. 70</b> HPLC chromatogram of enantiomerically enriched <b>87q</b> .....	174

## LIST OF SCHEMES

### SCHEMES

<b>Scheme 1</b> Organocatalytic strategies for the synthesis of chiral 3-amino-2-oxindoles. .....	4
<b>Scheme 2</b> The first asymmetric organocatalytic reaction in 1971 .....	9
<b>Scheme 3</b> Essentials of the Mannich Reaction .....	19
<b>Scheme 4</b> The first asymmetric organocatalytic Mannich reaction .....	20
<b>Scheme 5</b> Literature examples of Mannich reactions affording 3,3'-substituted oxindoles.....	22
<b>Scheme 6</b> Original Knoevenagel Condensation Reaction <b>a)</b> yielding bis adduct at 298K <b>b)</b> yielding bis adduct and condensation product at 373K .....	23
<b>Scheme 7</b> The first asymmetric organocatalytic Knoevenagel condensation reaction .....	24
<b>Scheme 8</b> Multicomponent reactions proposed by Yuan and Makaev .....	26
<b>Scheme 9</b> Enantioselective domino Michael addition/cyclization reaction proposed by Nakano.....	26
<b>Scheme 10</b> Catalytic asymmetric synthesis of chiral spiro[4 <i>H</i> -pyran-3,3'-oxindole] in the presence of water proposed by Zhao .....	27
<b>Scheme 11</b> Synthetic route for asymmetric Mannich reaction .....	28
<b>Scheme 12</b> Synthetic route for asymmetric construction of spiro[4 <i>H</i> -pyran- oxindole].....	29
<b>Scheme 13</b> <i>N</i> -Substitution of isatin and subsequent ketimine synthesis .....	31
<b>Scheme 14</b> <i>E/Z</i> configuration of 2-oxoindolin-3-ylidene acetate .....	34
<b>Scheme 15</b> Screening results for control of selectivity of the reaction.....	47
<b>Scheme 16</b> Mannich reaction of isatin derived ketimine <b>76</b> and acetylacetone <b>29</b> in the presence of 1 mol% catalyst loading .....	89
<b>Scheme 17</b> Enantioselective Construction of Spirooxindoles .....	90

## LIST OF ABBREVIATIONS

Boc	<i>tert</i> -Butoxycarbonyl
Cbz	Carboxybenzyl
DMAP	4-Dimethylaminopyridine
DCM	Dichloromethane
DABCO	1,4-diazabicyclo[2.2.2]octane
DMSO	Dimethyl sulfoxide
EWG	Electron withdrawing group
EDG	Electron donating group
FG	Functional group
NMR	Nuclear Magnetic Resonance
PMP	<i>p</i> -methoxyphenyl
PG	Protecting group



## CHAPTER 1

### INTRODUCTION

#### 1.1 Importance of Isatins

1*H*-Indole-2,3-dione, commonly known as isatin (Figure 1), is a well-known natural product found in plants of the genus *Isatis* and fruits of the cannonball tree *Couroupita guianensis Aubl.*<sup>1</sup> Isatin was a synthetic molecule for almost 160 years. It was first obtained as a product of the oxidation of indigo dye by nitric acid and chromic acids in 1841 by Erdman<sup>2</sup> and Laurent.<sup>3</sup> It can be crystallized from alcohol, acetic acid, or water in the form of red-orange monoclinic prism crystals, which melts at 200°C. Also, it is found in many plants, the secretion of animals, and human beings displaying a broad spectrum of biological activities such as a metabolic derivative of adrenaline hormone, a component of the parotid gland, and as melosatin alkaloids.<sup>4</sup> In 1869, its current structure was stated by Kekule.<sup>5</sup>

Although isatin and many of its substituted versions are commercially available, many conventional methods are used to prepare isatin and its derivatives, such as the Sandmeyer<sup>6</sup>, Stolle<sup>7</sup>, Gassman<sup>8</sup>, and Martinet<sup>9</sup> procedures. Because of possessing an indole unit with a ketone and  $\gamma$ -lactam moiety in its structure, isatin is an essential and unique structure capable of being used both as an electrophile and nucleophile (Figure 1). Due to this fact, isatins are crucial building blocks in organic synthesis. Their privileged structure revealed many interesting aspects of organic syntheses, such as N-substitutions and electrophilic aromatic substitutions at C-5 and C-7 of the phenyl ring, spiro-annulations, and nucleophilic additions onto the C-3 carbonyl group.<sup>1</sup>

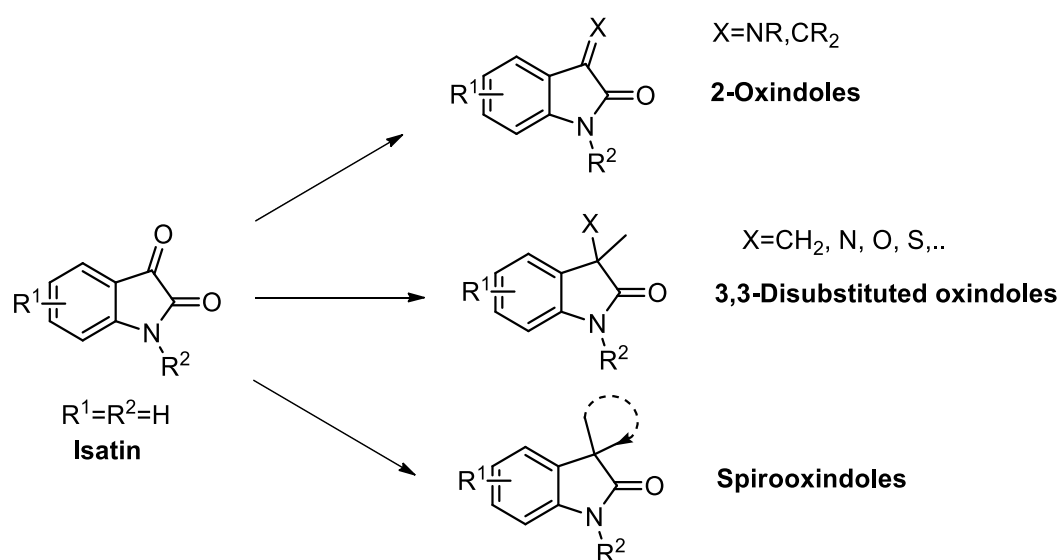


**Figure 1** Structure of isatin and isatin derived transformations

Isatins are recognized as a core structure in a variety of bioactive molecules and pharmaceutical compounds. The highly reactive prochiral C-3 carbonyl group of isatins makes them more applicable in organic synthesis.

The reactions of the prochiral C-3 center of isatins, primarily by nucleophilic additions and spiroannulation, result in the formation of C-3 substituted oxindoles, 2-oxindole derivatives. The construction of 2-oxindoles, especially 3,3-disubstituted and spiro-fused heterocyclic frameworks, have drawn significant attention in the chemical community because of the requirement of specific design-based strategies and challenging steric issues induce easy rearrangements.<sup>10</sup> This attention has led researchers to explore isatin chemistry and offer several synthetic design strategies for synthesizing various tetra-substituted and spirocyclic 2-oxindole moieties in the last few years.

### 1.1.1 Chiral Oxindoles and Spirocyclic Oxindoles

Chiral oxindoles are essential in the large family of bioactive natural products. Among the various chiral oxindoles, specifically, 3-amino-2-oxindoles have been encountered as the core structure of many architecturally complex natural products and pharmaceutical candidates such as AG-041R gastrin/CCK-B receptor agonist,<sup>11a</sup> vasopressin V<sub>1b</sub> receptor antagonist SSR-149,415 which is used in the treatment of anxiety and depression,<sup>11b</sup> an antimalarial agent NITD609,<sup>11c</sup> CRTH2 antagonist, a progesterone receptor, an anti-bacterial agent and an anti-tuberculosis agent,<sup>11d</sup> and HIV-1 protease inhibitor<sup>11e</sup> (Figure 2).

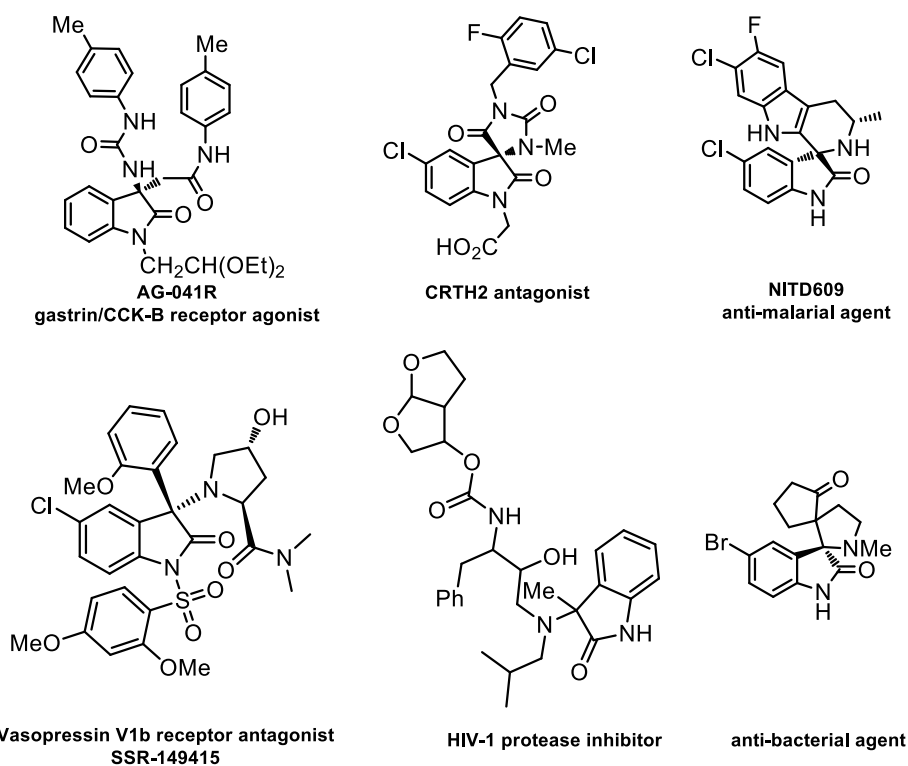
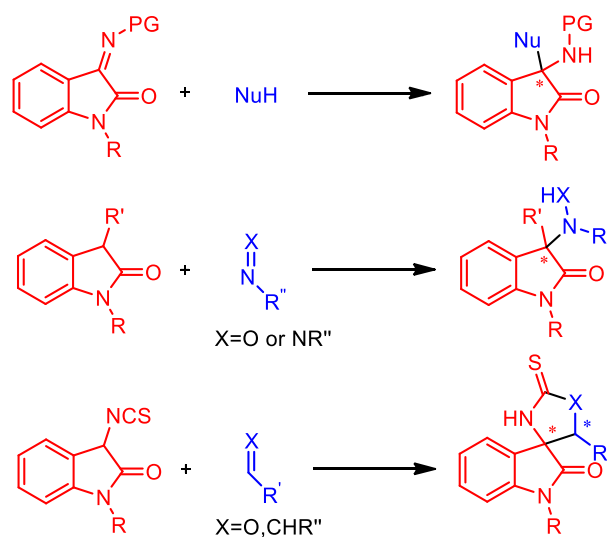


**Figure 2** Representative examples of biologically active compounds containing 3-amino-2-oxindole skeleton

Due to its importance and wide application in medicinal chemistry, considerable efforts have been devoted to designing efficient methodologies using chiral catalysts to construct 3-amino-2-oxindole derivatives bearing a tetrasubstituted stereocenter

in the past few years<sup>12</sup> (Scheme 1). These synthetic strategies include asymmetric addition to isatin imines,<sup>13</sup> intramolecular  $\alpha$ -arylation of amides,<sup>14</sup> alkylations of 3-aminooxindole,<sup>15</sup> aminations of 3-substituted oxindoles,<sup>16</sup> and multicomponent reaction<sup>17</sup> (Figure 3).



**Scheme 1** Organocatalytic strategies for the synthesis of chiral 3-amino-2-oxindoles.

Among these reactions, the most straightforward and efficient method is the asymmetric addition of a nucleophile to isatin imines. Its simplicity and efficiency arise from the ease of access to isatin imines and the possibility of using a wide range of nucleophiles that increase the resulting products' structural diversity.<sup>18</sup> For constructing 3-substituted-3-amino-2-oxindoles with a quaternary stereogenic center, various organocatalytic enantioselective reactions such as Mannich reaction, Henry reaction, aza-Friedel-Crafts reaction, Morita-Baylis Hilmann reaction, and Strecker reaction have been reported. The representative examples of these reported strategies involving addition to isatin imine framework are shown in Figure 3.<sup>19</sup>



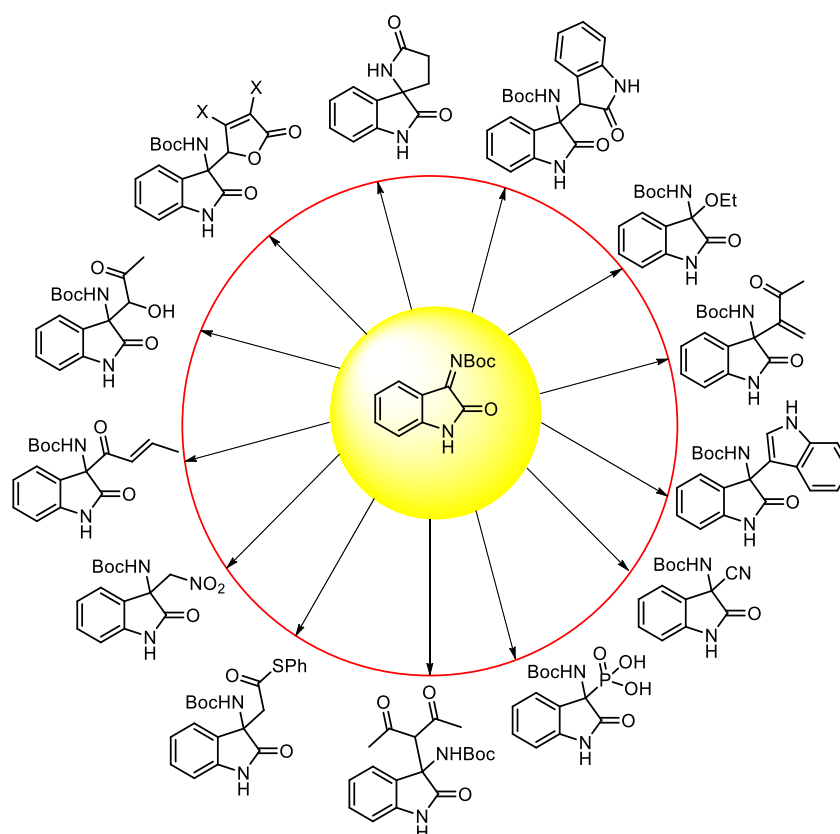


**Figure 3** Representative examples from isatin imine framework

Chiral spirooxindoles, a class of spiro-cyclic framework bearing a spiro-ring fused at the C-3 position of oxindole moiety, are as critical synthetic compounds as oxindoles according to their biological activity and applications in medicinal chemistry. In recent years, the attention to spirocyclic structures in drug discovery has dramatically increased and caused significant developments in spirocyclization chemistry. Apart from the examples given for chiral oxindoles in Figure 2, this unique spirocyclic framework has been widely found as a core structure in natural alkaloids with a broad range of pharmaceutical activities such as anti-tumor, antimicrobial, anti-HIV, antimalarial, antipyretic agents and sodium channel blockers.<sup>20</sup>

Structurally, containing a bicycle connected by a single fully-substituted carbon atom, spirooxindoles are considered rigid and dense spirocyclic systems and have an excellent affinity to three-dimensional proteins acting as biotargets compared to flat aromatic compounds.<sup>21</sup> Moreover, spirocyclic compounds have the potential to improve specific physicochemical properties such as metabolic stability, aqueous solubility, and lipophilicity concerning monocyclic structures. All these advantages of spirooxindoles have contributed to a tremendous interest in industry and academia to construct and provide spirocyclic frameworks in a controlled and stereoselective manner. Eventually, various approaches have been developed, and synthetic methods towards chiral spirooxindoles have increasingly appeared in the past several years. According to the literature, there have been 6896 publications containing spirooxindoles since 1950 and 3283 reported since 2012. To understand the importance of spirooxindoles in the organic synthesis literature, Bull and Boddy collected and analyzed publications, including stereoselective spiro-(3 to 7)-membered ring structures between 1970 and 2020. As demonstrated in Figure 4, the interest over the last 50 years has increased significantly, and the number of publications has reached above 400 per year since 2013. Especially the publications about 5- to 6- membered rings dominate the total number.<sup>22</sup>

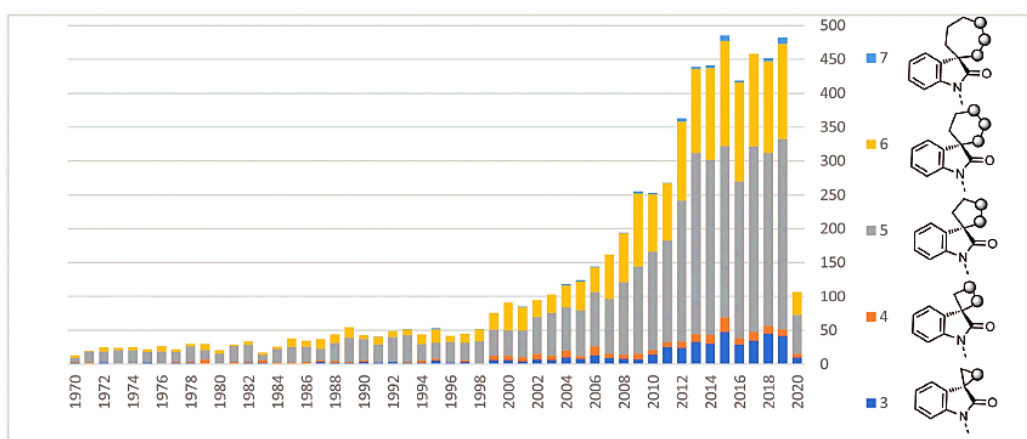


**Figure 4** Incidence of spirooxindoles in the literature up to 2020

Obviously, among the different enantioselective synthetic strategies, it is seen that organocatalytic methods are one of the most direct and efficient strategies for the asymmetric synthesis of spirooxindoles due to their stability, mild reaction conditions, and easy availability.

After the comprehensive review by Barbas, Tan, and co-workers in 2014, organocatalytic asymmetric synthesis has progressed rapidly. The construction of spirooxindoles from oxindole derivatives as starting materials has drawn significant attention. Isatins, isatin imines, and their derivatives **1** can readily react with nucleophiles due to the highly reactive carbonyl group at the C-3 position. With efficient strategies and attacking groups, a spiroannulation reaction occurs and transforms isatins into spirooxindoles. Moreover, spirooxindoles can be afforded from cycloaddition reactions of 3-alkylidene-indolinones **2**, which act as a suitable acceptor. However, controlling regioselectivity at the double bond can be a challenging issue because of the effect of substituents on the reactivity of two carbon atoms.<sup>23</sup> Additionally, indolin-2-one and its derivatives **3** are widely used as nucleophiles in spiroannulation reactions by reacting with efficient groups. Also, isatin-derived 3-indolylmethanols **4** have drawn attention in the last few years. Their ability to generate reactive intermediates under acidic conditions made them versatile reactants in various catalytic enantioselective [3+n] cyclizations and substitutions for constructing chiral spirooxindoles.

Using oxindoles and derivatives in organocatalytic reactions, various enantioenriched spirocyclic oxindoles **5-9** with 3 to 7-membered rings have been synthesized, and new examples have emerged come up growingly. Besides, multiple stereocenters and enantio-pure bispirooxindoles have also been formed according to substituents on the ring.<sup>20</sup>

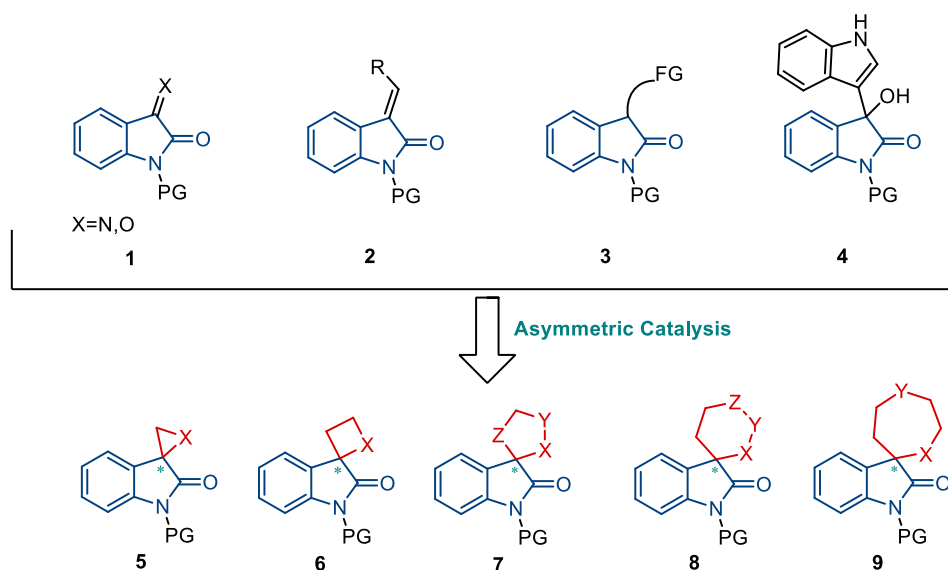


**Figure 5** Catalytic asymmetric synthesis of chiral spirooxindoles from oxindole derivatives

## 1.2 Importance of Asymmetric Synthesis

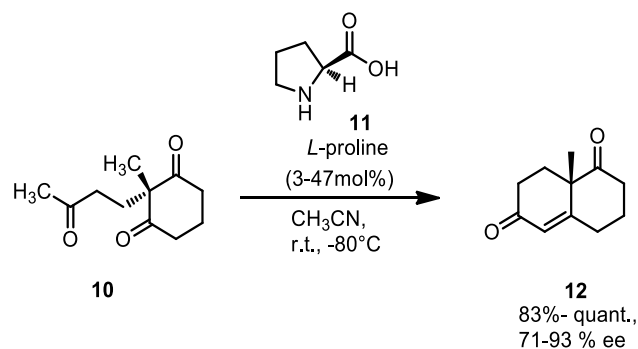
The asymmetric synthesis, also called enantioselective or chiral synthesis, is defined as a method for the preparation of stereoisomeric compounds selectively with unequal amounts. Stereoisomers are molecules with the same connectivity of atoms, but arrangements of atoms are different in three-dimensional space and thus can have other properties from one another.

The use of asymmetric synthesis plays a vital role in preparing enantioenriched and pure compounds, significantly bioactive therapeutic agents, most practically and efficiently. In chiral biologically active compounds, different enantiomers interact differently, with the target receptors showing different responses. These responses could be quite distinct and may lead to other consequences. The drug thalidomide is an excellent example for which both enantiomers display a sedative effect, but only the (-) enantiomer causes fetal deformations.<sup>24</sup> Due to this, access to enantiomerically pure molecules has gained attention. Because of this increasing

interest in getting enriched biologically active products, developments in this field are constantly growing, from metal complexes bearing chiral ligands to chiral metal-free organocatalysts. The use of catalysts is considered to be the most efficient way of asymmetric synthesis and has become an indispensable technology for the production of pharmaceutical compounds.<sup>25</sup>

### 1.2.1 Asymmetric Organocatalysis

Catalytic systems in nature have inspired chemists to seek strategies and compounds that mimic the biocatalytic processes occurring in nature. This impression led to the birth of organocatalysis, in which small, metal-free chiral organic molecules containing minimal functionalities imitate biocatalysts and affect asymmetric reactions. The first asymmetric organocatalytic reaction was reported by two industrial research groups in 1971 in which proline was used as an organocatalyst for intramolecular asymmetric aldol reactions of triketone (Scheme 2).<sup>26</sup>



**Scheme 2** The first asymmetric organocatalytic reaction in 1971

This approach has been ignored for almost three decades since the late 1990s. However, using small organic molecules to control the stereoselectivity in reactions of structurally diverse molecules has become one of the most powerful tools in the past 20 years in contemporary organic synthesis. In addition to transition-metal complexes and enzyme-mediated catalysis, asymmetric organocatalysis is

recognized as the "third pillar" of enantioselective synthesis due to advantages such as easy availability and preparation and mild, simple, and metal-free reaction conditions.<sup>27</sup> The growing attention to organocatalysis and functionalization in designing more complex reactions for synthesizing biologically active molecules, drugs, and agrochemicals has resulted in almost 1500 publications in the last decade. In consideration of these publications and efforts, IUPAC elected the enantioselective organocatalysis as one of the "10 emerging technologies in Chemistry" on its 100<sup>th</sup> anniversary of foundation in 2019.<sup>28</sup>

### 1.2.2 Classification of Organocatalysis

Over the past two decades, asymmetric organocatalysis has become an emerging technology because of the simplicity of structures and advantages and the variety of activation modes capable of promoting several reactions.<sup>29</sup> These significant properties can play a crucial role in the outcome of stereoselectivity and the prediction of mechanistic working models of reactions. In other words, they have mainly two functions; one is the activation of electrophile or nucleophile or both, and the other is the creation of an asymmetric environment for setting the chirality of the product. From the mechanistic way, the activation modes of organocatalysts can be classified according to their interaction with the substrate or 'mode of action' as covalent and noncovalent catalysts and secondly according to the chemical nature of the catalyst as Lewis base, Lewis acid, Brønsted base, and Brønsted acid. Moreover, it should be noted that many organocatalysts can display dual characters like bifunctional organocatalysts and work through covalent and noncovalent interactions such as amino acids and phosphoric acids.

In the case of covalent catalysis, the formation of a new covalent bond result from the interaction between the catalyst and the substrate. Aminocatalysis and carbenes can be given as an example of this interaction. Moreover, in noncovalent catalysis, the activation is based on weak binding such as hydrogen bonding (thioureas,

squaramides, and phosphoric acids) or ionic interactions (cinchona alkaloids, phase transfer catalysts, counter-ion catalysts). The general classification of organocatalysis is summarized in Figure 6.<sup>30</sup>

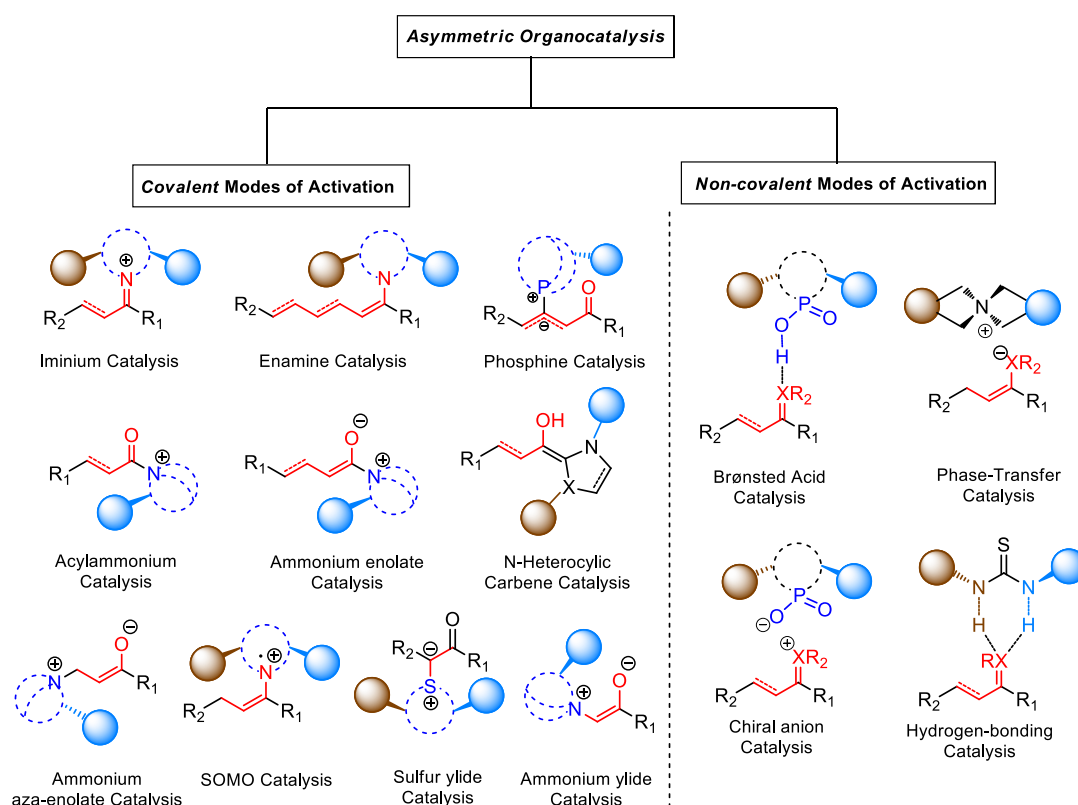


**Figure 6** Classification of Organocatalysis

### 1.2.3 Hydrogen Bonding Interactions and Bifunctional Organocatalysis

Since the rebirth of organocatalysis in 2000, research in this field has grown rapidly and become one of the fascinating fields in organic chemistry. Then, the organocatalysis field was dominated by nucleophilic aminocatalysis, where the iminium/enamine intermediates governed most enantioselective carbon-carbon bond-forming reactions. However, as time progressed, various research groups

studied and made efforts to develop new, efficient and improved organocatalysts useful for different asymmetric reactions. *N*-heterocyclic carbenes (NHCs), bifunctional-hydrogen bonding catalysts such as urea/thioureas, Cinchona alkaloids, guanidines, and phosphate-derived Brønsted acids, joined the field of organocatalysts to facilitate several enantioselective reactions.

In particular, the H-bond donor catalysts based on thiourea/urea core have received specific attention, and bifunctional catalysts possessing a combination of urea/thiourea and amine groups that activates the reactants synergistically dominate the asymmetric catalysis field (Figure 7).<sup>31</sup>

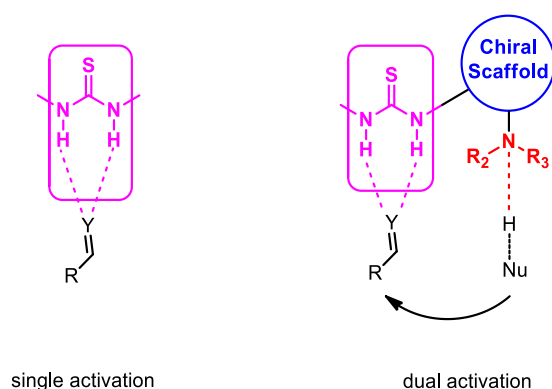


**Figure 7** Single and dual activation concept of bifunctional thiourea organocatalyst

The first reliable and general strategy on dual activation of thiourea and tertiary amine groups was reported by Takemoto and co-workers in 2003.<sup>32</sup> In this work, the efficiency of the dual activation of thiourea/amine moiety has been proved in catalytic reactions as monofunctional thioureas. It is assumed that the double hydrogen bonding interaction of the N-H of thiourea/urea with a reactant plays a significant role in efficient catalysis and stereocontrol of the reaction.

After this pioneering work, the concept of multifunctional asymmetric synthesis and the dual activation of organocatalysis has increased impressively. Several research groups have designed various novel bifunctional organocatalysts in the following



years. Some selected examples concerning bifunctional organocatalysts are given in Figure 8.

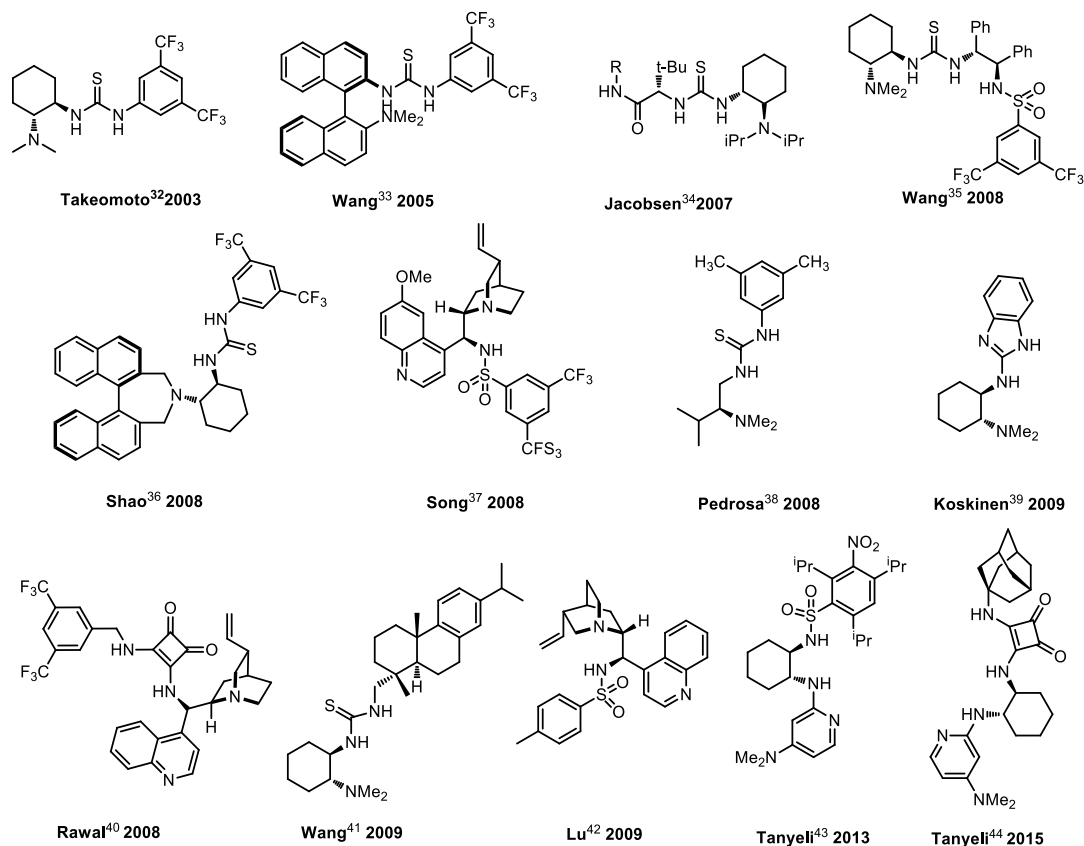


**Figure 8** Literature examples of bifunctional organocatalysts

In 2008, pioneering research was introduced by Rawal's group on the development of chiral squaramides derived from Cinchona alkaloids. This work has opened new opportunities for the asymmetric synthesis of complex structures and is recognized as an efficient alternative to the thiourea/urea and guanidine organocatalysts. Compared to thiourea/urea, the functionality of squaramides differ in many ways, such as duality in binding, rigidity in conformation, H-bond spacing, H-bond angle, and acidity.<sup>45</sup>

In the case of duality in binding, despite the anion binding affinity of ureas and thioureas being excellent, their capability to recognize cations is much more limited. However, squaramides exhibit perfect duality in recognition of anion and cation

binding. Besides that, in addition to ditopic binding, containing two H-bond donors (N-H) unit and two H-bond acceptors (C=O) units make squaramides more “bifunctional” in their H-bonding properties than thioureas and ureas. Due to this ambivalent nature, squaramides possess three possible H-bonding patterns.

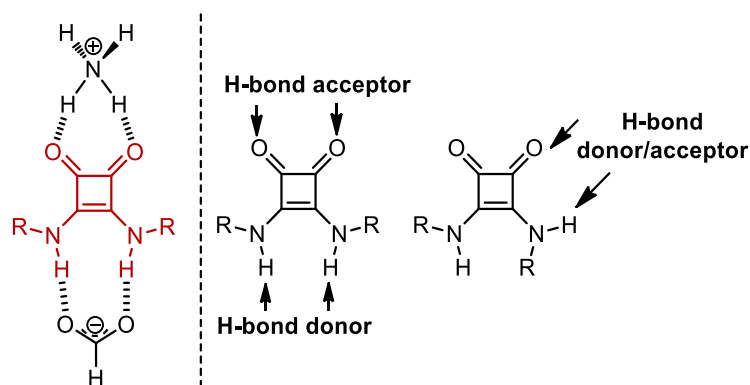


**Figure 9** Duality in H-bonding in Squaramides

Beyond the dual binding ability, thioureas/ureas and squaramides can delocalize the lone pair on the nitrogen atom through the carbon-oxygen/carbon-sulfur double bond, thereby restricting the rotation of the C-N bond. However, only the squaramides can undergo further delocalization through the cyclobutenedione system, which has two positive charges in the ring. By computational methods, the partial aromatic character of these systems has been analyzed. It is indicated that this structure fulfills the geometric, energetic, and magnetic criteria of aromaticity which accounts for the rigidity of the catalyst (Figure 10).<sup>46</sup>

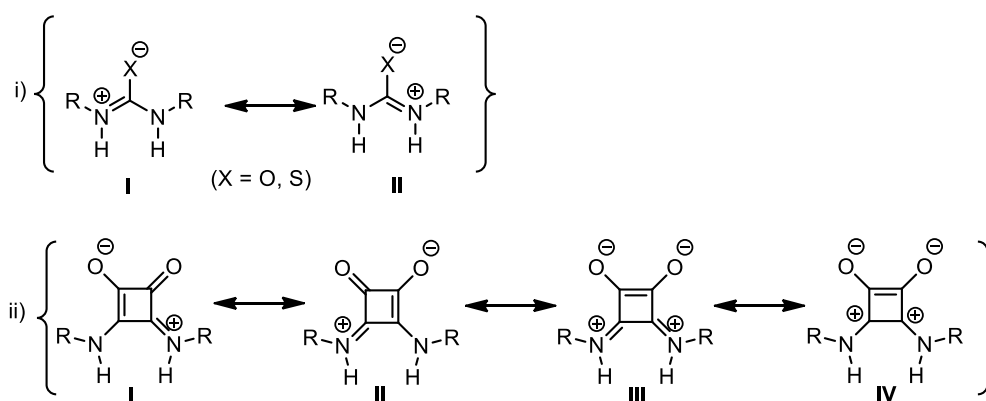


**Figure 10** Resonance structure of i) (thio)urea, ii) squaramide

The most significant difference between thioureas and squaramides is the relative distance and bond spacing between the two N-H groups attached to the same carbon. The calculated distances for *N,N'*-dimethyl thiourea and *N,N'*-dimethylsquaramide is approximately 2.13 Å and 2.72 Å, respectively. The calculated length of H-bonding in squaramides is one-third larger than in thiourea. This larger distance empowers the squaramides to form stronger hydrogen bonds with the substrates bearing nitro, carbonyl, imino, and nitrile functionalities, etc.<sup>31</sup> Furthermore, “the square structure” of cyclobutendione ring induces the convergent orientation of the N-H groups and brings the difference in the value of the dihedral angle values of N-H bonds between thioureas and squaramides as 6~8° (Figure 11).

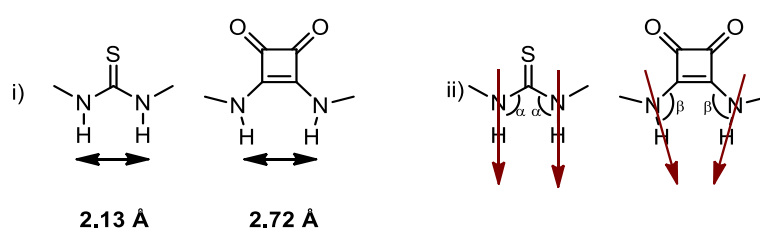


**Figure 11** Calculated i) H-bond spacing, ii) H-bond angle

In addition to the structural differences, the distinctly different acidity values of N-H bonds between squaramide and (thio)urea compounds are one of the most important parameters when considering the superior performance of squaramides. Unfortunately, the  $pK_a$  values for squaramides are still unknown, which excludes the

ability of direct comparison. As an analogy, the acidities of (thio)urea and squaramide can be compared with carbonic acid,  $\text{H}_2\text{CO}_3$  ( $\text{pK}_{\text{a}1}$ : 3.62;  $\text{pK}_{\text{a}2}$ : 10.3), and squaric acid ( $\text{pK}_{\text{a}1}$ : 1.5;  $\text{pK}_{\text{a}2}$ : 3.4). Remarkably, the acidity of the catalyst can guide the design and the selection of the appropriate catalyst. Because of this importance, several studies were done to understand the  $\text{pK}_{\text{a}}$  value of the squaramide catalysts. In 2004, Li and Cheng established a study to evaluate the acidity value of commonly used bifunctional squaramide catalysts that involved measurements in DMSO (Figure 12).

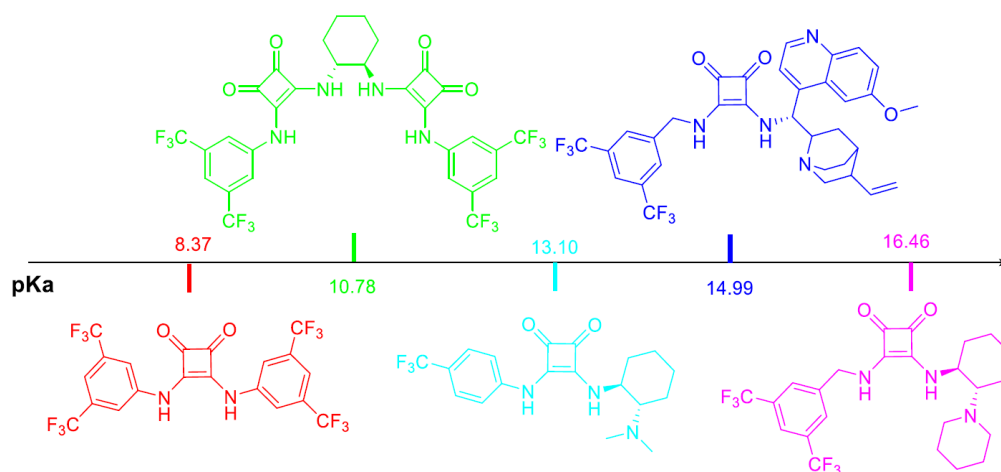


**Figure 12**  $\text{pK}_{\text{a}}$  values of squaramide analogues in DMSO

Due to their more acidic character, squaramides engage in much stronger hydrogen bonds than (thio)ureas. Thus, this result can explain the higher activity and efficiency of squaramides in asymmetric transformations even with lower loading of catalysts.<sup>47</sup>

Up to now, along with other bifunctional organocatalysts, squaramide-hydrogen-bonding catalysts have been developed and applied to a wide range of asymmetric reactions, including Friedel-Crafts reactions, Mannich reactions, Michael addition reactions, Aldol reactions, cycloaddition reactions, Strecker reactions and so on.<sup>48</sup> Some selected literature examples of squaramide catalysts are shown in Figure 13.

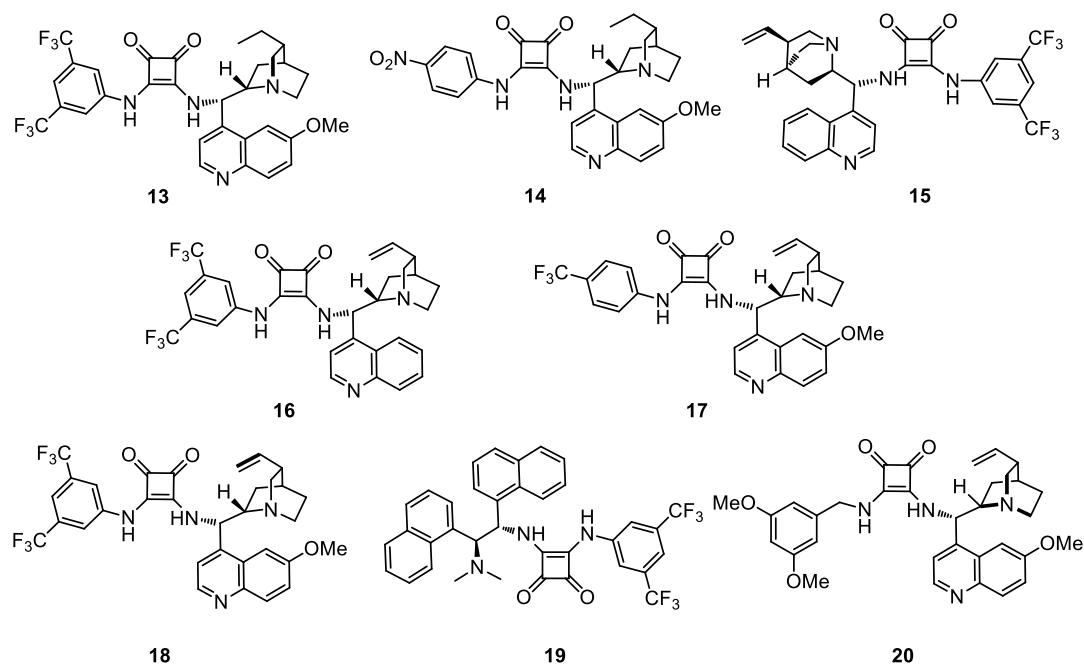


**Figure 13** Selected literature examples of Squaramide based organocatalysts

### 1.3 Importance of 1,3-Dicarbonyl Compounds

1,3-Dicarbonyl compounds as an important class and an excellent synthetic platform in organic chemistry due to their functionality. They bear multi-centers reaction sites with an alternative nucleophilic and electrophilic character. Thus, nucleophiles and electrophiles can undergo new bond forming reactions with 1,3-dicarbonyl compounds. They are valuable building blocks for heterocyclic potentially bioactive compounds. According to the nature and type of substituents, 1,3-dicarbonyl compounds can undergo various addition, domino, and multicomponent reactions with their unsaturated bonds for the synthesis of a wide variety of bioactive compounds.

1,3-dicarbonyl compounds have four contiguous reaction sites in which two of them exhibit electrophilic character and the other exhibit nucleophilic character, as depicted in Figure 14. As mentioned before, under suitable conditions, they can react

selectively. There are exceptional studies in which 1,3-dicarbonyl compounds are used as nucleophiles and electrophiles. Generally, these reactions are well-known reactions or derived from them, such as the Hantzsch reaction, Michael addition reaction, Biginelli reaction, Knoevenagel reaction, and Mannich reaction.<sup>49</sup>

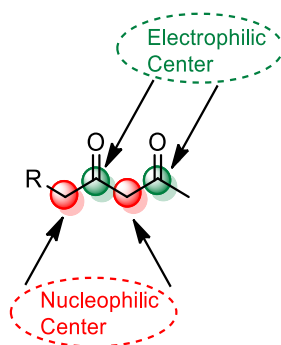


**Figure 14** Potential Reaction Sites of 1,3-Dicarbonyl Compounds

#### 1.4 Enantioselective Strategies for Synthesis of 3,3-Disubstituted Oxindoles and Spirooxindoles

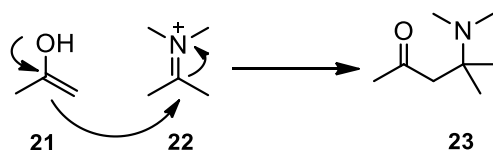
The oxindole scaffold bearing a tetra-substituted stereocenter at the C-3 position has been identified as a privileged structure. It serves as a key intermediate in the total synthesis of biologically active indole-containing alkaloids. Significantly, 3,3-disubstituted oxindoles have increased the attention of researchers in the last few years, and considerable efforts have been devoted to developing new methodologies to synthesize 3,3-disubstituted oxindoles and spirocyclization reactions of oxindoles as mentioned before. Among the methods for obtaining chiral oxindoles and spirooxindoles, nucleophilic addition to isatin imines has been considered one of the most intriguing methods in which the number of publications has grown over the years.<sup>12</sup>

Aiming the synthesis of 3,3-disubstituted oxindoles and construction of spirocyclic framework in this thesis, the organocatalytic approaches as Mannich reaction and as

Knoevenagel condensation, Michael addition/cyclization reactions will be discussed preferentially on this section.

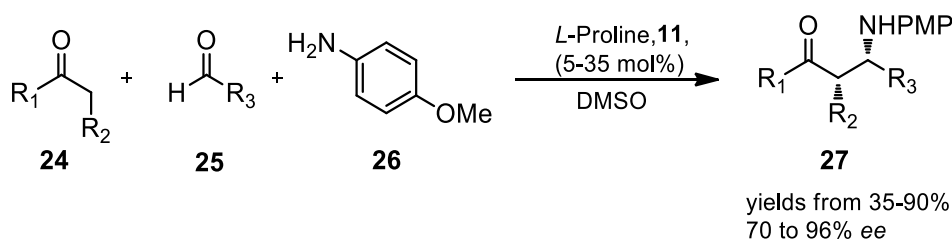
### 1.4.1 Mannich Reaction

Mannich reaction, first recognized and named by Carl Mannich in the early 19th century, is a valuable method for constructing  $\beta$ -aminoketones and aldehydes (Mannich bases). As such, in organic chemistry is one of the most important C-C bond-forming reaction types. In practice, enolizable ketones or aldehydes **21** serve as the CH-acidic substrate (nucleophiles), and the critical element in this reaction is the formation of an iminium intermediate **22** (Scheme 3). Thus, the Mannich reaction is a crucial step in synthesizing numerous natural alkaloids and pharmaceuticals. It can be used as a part of a tandem reaction sequence for constructing complex target molecules<sup>50</sup>.



**Scheme 3** Essentials of the Mannich Reaction

Benjamin List reported the first example of an organocatalytic asymmetric Mannich reaction in 2000. List hypothesized that chiral amines or amino acids might catalyze the Mannich reaction as they did in the asymmetric aldol reaction by using proline. It was reported that a one-pot three-component Mannich reaction of acetone, an aliphatic or aromatic aldehyde, and *p*-anisidine (**26**) in the presence of *L*-proline (**11**) provided the desired Mannich products in highly enantiopure form (70-96 %ee) with moderate yields due to the aldol addition and condensation products as side products (Scheme 4).<sup>51</sup>



**Scheme 4** The first asymmetric organocatalytic Mannich reaction

After this pioneering discovery, structurally diverse aldehydes and ketones have been examined with various organocatalytic approaches, such as catalysis by chiral amines (enamine catalysis), chiral Brønsted acids, and chiral Brønsted bases. Both one-pot three components (direct) reactions and reactions with preformed imines (indirect) have increasingly been investigated to get enantio- and diastereomerically pure Mannich products.<sup>50</sup>

Among a broad range of Mannich reactions, due to the versatility and the potential, the direct synthesis of 3-amino-2-oxindoles using a protected isatin imine and enolizable carbonyl compounds has gotten attention and inspired chemists in recent years.

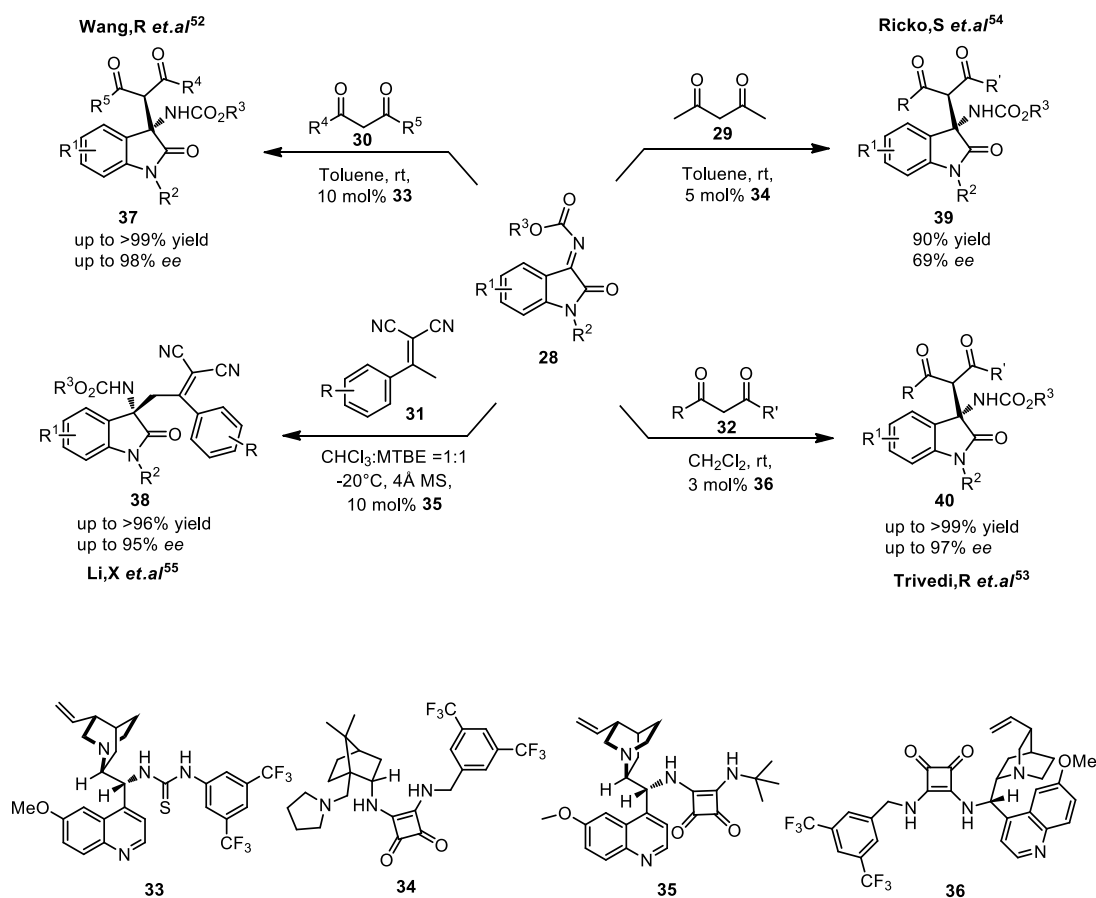
Initially, Wang et al.<sup>52</sup> reported the asymmetric addition of 1,3-dicarbonyl compounds to isatin-derived ketimines **28** in which quinine-thiourea organocatalyst **33** afforded products in good yields and enantioselectivities up to 98% ee in 2012. Then, Trivedi and co-workers<sup>53</sup> accomplished the same work in satisfying enantiopurity and chemical yields using chiral Cinchona-derived squaramide catalyst **36** in 2016. For examination of squaramide organocatalysis in the reaction of 1,3 dicarbonyl compound to ketimines, authors screened the different substituted *N*-Boc protected ketimine substrates, symmetrical and unsymmetrical 1,3-dicarbonyl compounds and afforded Mannich adducts in 78 to 99% yield with 90 to 98% ee and up to 95:5 dr with only 3 mol% of the catalyst.



Also, in the same year, Ricko and co-workers<sup>54</sup> tested a series of camphor-derived 1,3-diamine bifunctional squaramide organocatalyst **34** in a reaction of acetylacetone **29** and *N*-methyl substituted Boc-protected ketimine **28**, but only 69% ee was achieved.

Moreover, the vinylogous Mannich reaction has also become an important method for the preparation and synthesis of multifunctional 3-substituted-2-oxindole products in addition to the simple Mannich reaction. In 2016, Li et al.<sup>55</sup> demonstrated the vinylogous Mannich reaction of  $\alpha,\alpha$ -dicyanoolefins **31** with isatin-derived ketimines **28** catalyzed by Cinchona alkaloid-derived *tert*-butyl substituted squaramide catalyst **35** to provide the 3,3'-substituted oxindoles **38** in high yields (80-96%) and enantiopurity (88-96% ee) (Scheme 5).

With the known potential of squaramides and isatins, Mannich reaction of isatin derived ketimines with an enolizable 1,3-dicarbonyl compounds has been investigated as a part of this thesis study.<sup>56</sup>

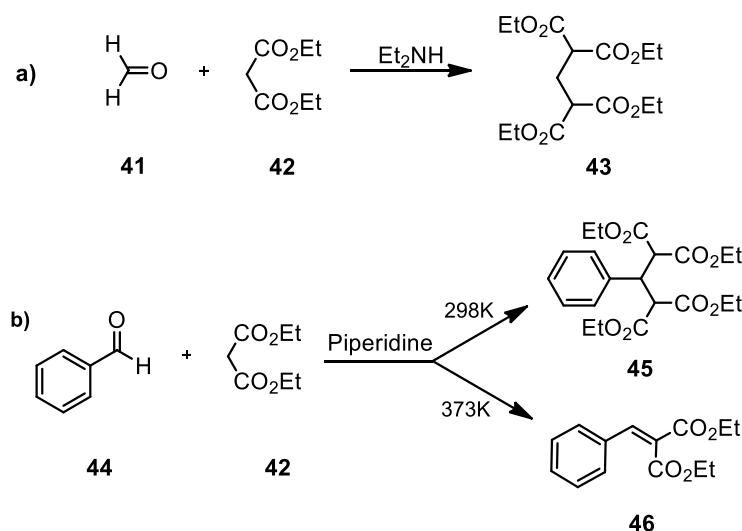


**Scheme 5** Literature examples of Mannich reactions affording 3,3'-substituted oxindoles

#### 1.4.2 Knoevenagel Condensation

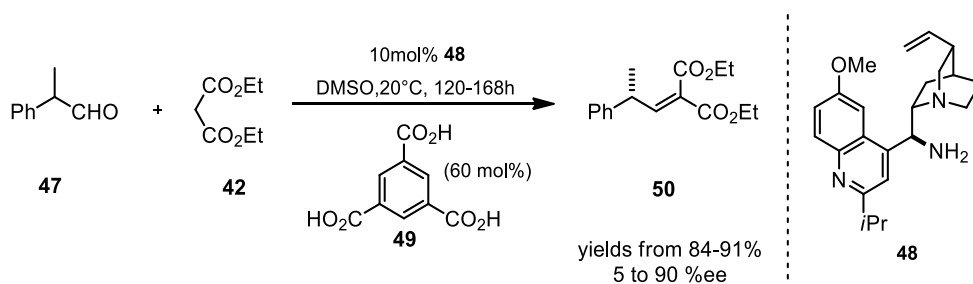
The Knoevenagel reaction is an efficient general method for synthesizing electrophilic olefins from active methylene and carbonyl compounds. Emil Knoevenagel first reported it in 1894<sup>57</sup> and was regarded as a pioneer in the field of the C-C bond formation reactions with the reaction of formaldehyde with diethyl malonate in the presence of diethyl amine as the catalyst that afforded the bis product. The bis adduct resulted from addition followed by a Michael reaction and was not considered an actual Knoevenagel product of present times. Two years later, in 1896, Knoevenagel could manage to produce the desired conventional

condensation product using aromatic aldehyde compounds with piperidine as a catalyst (Scheme 6).<sup>58</sup>



**Scheme 6** Original Knoevenagel Condensation Reaction a) yielding bis adduct at 298K b) yielding bis adduct and condensation product at 373K

Almost 126 years later, several active methylene units and weak basic catalysts such as primary, secondary, tertiary amines, and ammonium salts were examined to develop the industry's efficient and eco-friendly condensation reactions. In addition to numerous industrial applications of the Knoevenagel reaction, an asymmetric version using chiral auxiliaries or catalysts was not reported until 2011. In 2011, Benjamin List and co-workers published the first asymmetric example of Knoevenagel condensation that proceeds through a dynamic kinetic resolution of  $\alpha$ -branched aldehydes using a Cinchona-derived primary amine catalyst (Scheme 7).<sup>59</sup>



**Scheme 7** The first asymmetric organocatalytic Knoevenagel condensation reaction

Through time, various molecules directly used in products or indirectly as half-products are synthesized via modifications of the Knoevenagel reaction for the complex larger synthetic schemes. Moreover, the functionalization of the Knoevenagel condensation products has shifted the interest of academia to use Knoevenagel condensation in synthesizing biologically active molecules such as stilbenes, spiropyrans, and dispiropyrans via domino or cascade reactions.<sup>60</sup>

**1.4.3 Domino Knoevenagel Condensation / Michael Addition/ Cyclization Reaction**

The growing interest in forming stereogenic carbon centers and optically active biologically complex molecules using atom-economical and eco-friendly methods has led researchers to focus on developing cascade and multicomponent reactions (MCR), particularly organocatalyzed transformations, in a consecutive one-pot way. In nature, the synthesis of natural products and complex molecules occurs in this fashion with the help of enzymes. In this regard, the aim for the efficient synthesis of biosynthetic products and construction of cyclic frameworks is to mimic the nature and to resemble the processes with an organocascade or domino reactions in highly chemo-, regio- and stereoselective way.<sup>61</sup> Domino or multicomponent reactions are generally defined as reactions in which two or more bond formations occur under the same reaction conditions where the functionality of the previous step contributes to the formation of the target product. These reactions are considered a green protocol in synthesizing natural products because of atom-economical and time-consuming steps with minimal waste generation.

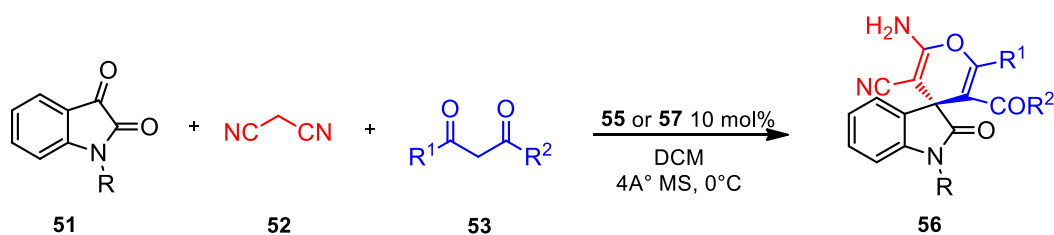
Over the past twenty years, the synthesis of biologically active products with the MCR or cascade methodology using organocatalysts has progressed. Several

reviews and studies have been published about their great potential and development in this area.

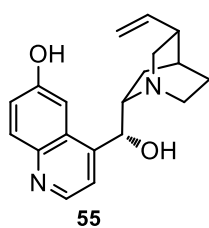
Significantly, synthesizing the privileged spirooxindole moiety using the organocascade or domino strategy has become essential. Several methods have been devised in the last decade, including double or triple cascade reactions and cyclizations. Despite these advances, there have been limited examples of stereoselective synthesis of spirooxindoles, especially spiro[4*H*-pyran-3,3'-oxindole], in which isatins or isatin-imines used as a starting material and most of the reported methods generally focus on the synthesis of racemic products.

The first enantioselective example of domino Knoevenagel/Michael/cyclization sequence catalyzed by a cinchona alkaloid, Cupreine (6'-hydroxycinchonidine) **55**, has been reported by Yuan and co-workers<sup>62</sup> to prepare stereochemically complex spiro[4*H*-pyran-3,3'-oxindoles] **56** in excellent yields (up to 99%) and good to excellent enantioselectivities (72-97% ee) in 2010. A wide range of spiropyran derivatives was synthesized using *N*-protected isatins **51**, malononitrile **52**, and 1,3-dicarbonyl compounds **54**. Moreover, they demonstrated that this reaction could also proceed starting directly from an isatylidene malononitrile, the Knoevenagel condensate.

Soon after, in 2011, Macaev and co-workers<sup>63</sup> also reported a similar three-component reaction using (-)-(*S*)-brevicolline [(*S*)-1-methyl-4-(1-methyl-2-pyrrolidinyl)-9*H*-pyrido[3,4-*b*]indole] **57** as an alternate catalyst which affords the same spirooxindole pyrans **56** with good enantioselectivities up to 94% ee. To compare Yuan's work, the enantioselectivities are low, and yields are modest, even some racemic examples reported (Scheme 8).

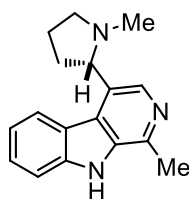


Yuan, W.-C. *et al.*<sup>62</sup>



72-99% ee  
87-98% yield

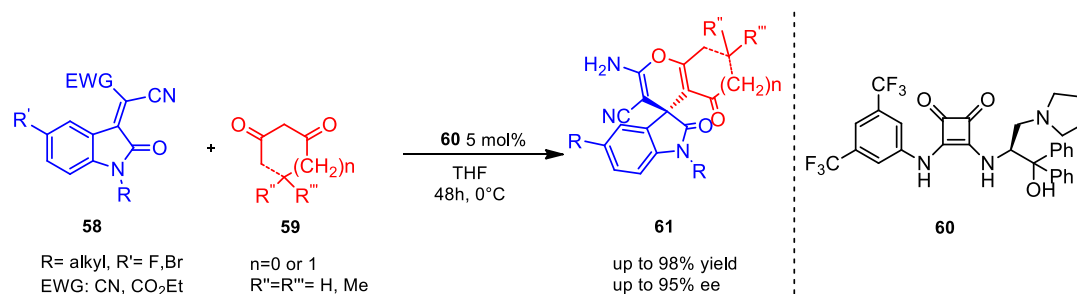
Makaev, F. *et al.*<sup>63</sup>



12-93% ee  
50-98% yield

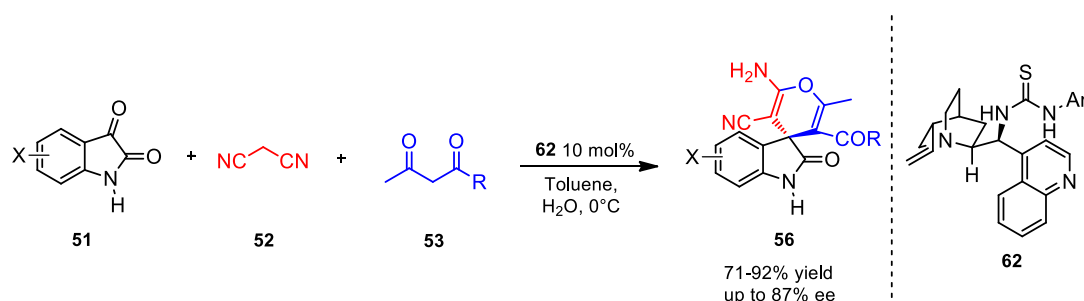
**Scheme 8** Multicomponent reactions proposed by Yuan and Makaev

Most recently, Nakano and co-workers<sup>64</sup> tested their newly developed hybrid-type type squaramide-fused amino alcohol (SFAA) organocatalyst **60** in enantioselective domino Michael addition/cyclization reaction of oxindoles **58** with cyclic 1,3-diketones **59** to afford the chiral spiro-conjugated oxindoles with 2-aminopyrans **61** in excellent chemical yields (up to 98%) and enantioselectivities (up to 95% ee) in 2018. In this study, they demonstrated the functionality of their newly SFAA organocatalyst **60** and achieved to afford spiro compounds highly selectively by using cyclic 1,3-diketones, unlike Yuan's work (Scheme 9).



**Scheme 9** Enantioselective domino Michael addition/cyclization reaction proposed by Nakano

After one year, Zhao and co-workers<sup>65</sup> examined the efficiency of water in the catalytic asymmetric synthesis of chiral spiro[4*H*-pyran-3,3'-oxindole] derivatives using the three-component reaction of isatin **51**, malononitrile **52**, and 1,3-dicarbonyl compounds **53** catalyzed by cinchonidine-derived thiourea **62** in 2019. In this study, they took advantage of the known significant impact of water in many organocatalytic reactions and tested it in the synthesis of spiropyran derivatives. Under the optimized conditions, it was realized that using water as an additive improved the product ee values significantly, and they achieved synthesizing the desired spiro[4*H*-pyran-3,3'-oxindole] **56** derivatives in good yields (71-92%) and in moderate to high enantioselectivity (up to 84% ee) (Scheme 10).



**Scheme 10** Catalytic asymmetric synthesis of chiral spiro[4*H*-pyran-3,3'-oxindole] in the presence of water proposed by Zhao

## 1.5 Aim of the work

The main objective of this thesis is the enantioselective synthesis of 2-oxindole derivatives and the construction of spirocyclic oxindoles, which are unique core structures in many natural products and biologically active compounds. They also have significant importance in medicinal chemistry, and due to this importance, the new synthetic methodologies to synthesize this core structural motif have been rapidly growing. In line with this growing interest, to synthesize 2-oxindole derivatives and construct a spirocyclic framework with high selectivity was aimed. Moreover, we benefited from the efficiency of chiral bifunctional organocatalysts designed in our research group to activate substrates and achieve high

stereoselectivity. After an extensive literature survey, it was realized that the sterically hindered hydrocarbon substituents on squaramides also significantly influence asymmetric synthesis in addition to the common N-H acidity concept. Therefore, newly designed quinine-based organocatalysts (Figure 15) were synthesized and tested to explore the scope of hydrocarbon substituents in the enantioselective addition of 1,3-dicarbonyl compounds to isatin-derived *N*-alkoxy carbonyl ketimines.

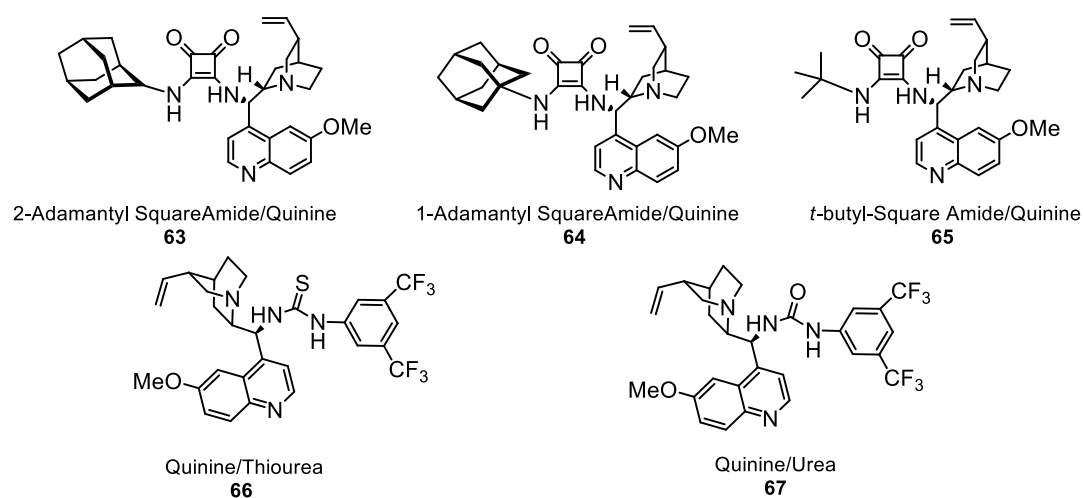
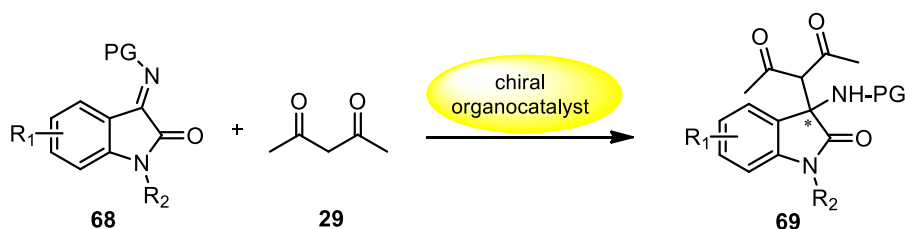


**Figure 15** Quinine-based bifunctional organocatalysts

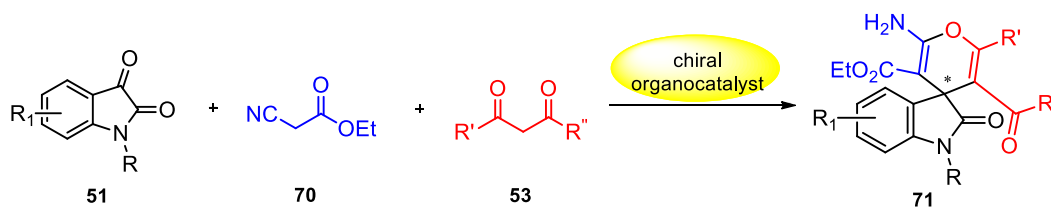
Among diverse reactions and transformations of isatins and isatin-imines, the Mannich reaction was preferred to afford the highly selective 3,3'-disubstituted oxindoles due to its importance and versatility in synthesizing natural products, drugs, and related analogs (Scheme 11).



**Scheme 11** Synthetic route for asymmetric Mannich reaction



The second part of the study aimed to develop a simple and efficient method for synthesizing spiro-fused pyran-oxindole heterocycles. In literature, stereoselective synthesis of spiro-pyran derivatives was very limited, and almost all studies comprise the multicomponent or domino reactions based on malononitrile as a nucleophile. Contrary to common studies conducted with malononitrile **52** or isatylidene malononitrile, a new strategy based on ethyl cyanoacetate oxindolines with cyclic and acyclic 1,3-dicarbonyl compounds was examined. Inspired by the efficiency of newly designed quinine-based squaramide organocatalysts and their results in our preliminary study, we would also like to investigate their efficiency in the stereoselective synthesis of spiro[4*H*-pyran-oxindole] derivatives aiming to afford them in high enantioselectivity (Scheme 12).



**Scheme 12** Synthetic route for asymmetric construction of spiro[4*H*-pyran-oxindole]



## CHAPTER 2

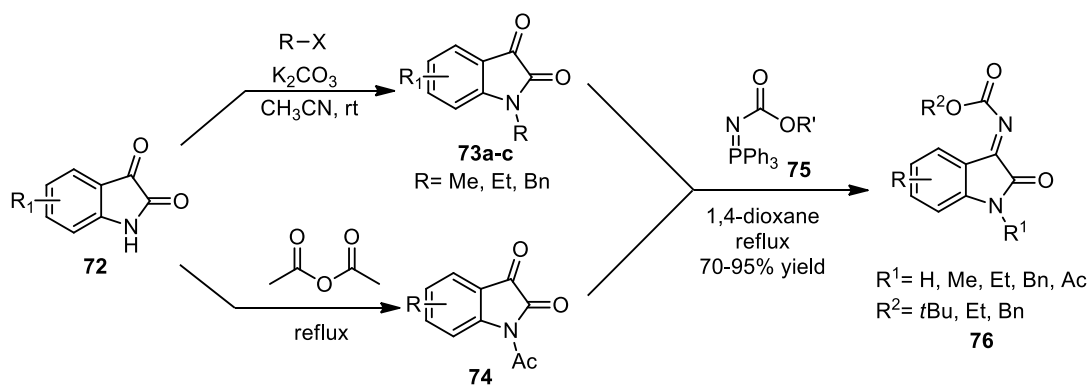
### RESULTS AND DISCUSSION

#### 2.1 Synthesis of Starting Materials

##### 2.1.1 Synthesis of *N*-Carbamate Protected Ketimines

To achieve the efficient asymmetric addition of nucleophiles to isatin-imines, the C-3 position of the isatin reacted with some protecting groups to form isatin-imines. Initially, *N*-alkoxy carbonyl moiety was preferred because of the ease of deprotection procedures.

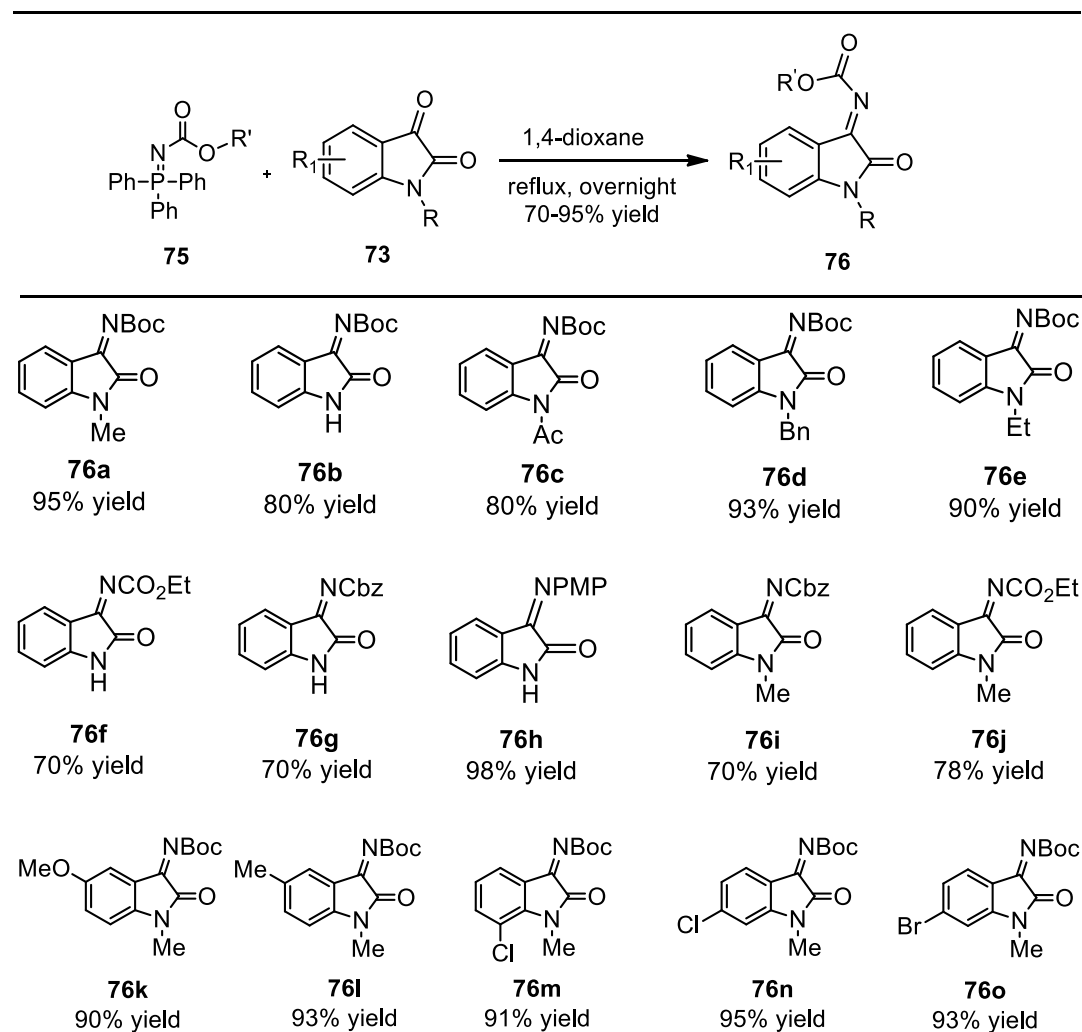
According to the literature procedure, various iminophosphane **75** derivatives, such as *t*-butyl, ethyl, and benzyl triphenyliminophosphane, were synthesized in our group. Then, isatins **72**, readily available, reacted with those iminophosphane reagents **75**, and synthesis of *N*-carbamate-protected ketimines **76** was achieved by the aza-Wittig process presented in the literature (Scheme 13).<sup>66</sup>

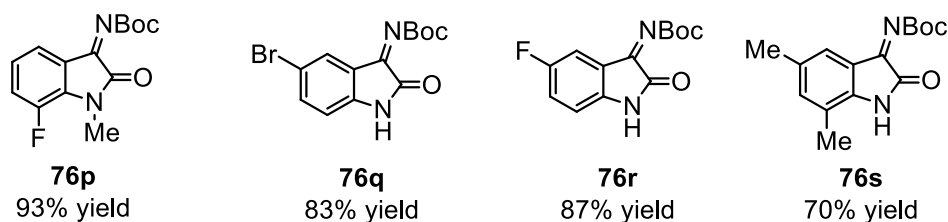


**Scheme 13** *N*-Substitution of isatin and subsequent ketimine synthesis

Furthermore, the derivatization of the *N*-H amide moiety of isatins was conducted through *N*-substitution reactions. According to the literature, *N*-alkylation and benzylation reactions were carried out with corresponding alkyl and benzyl halides (X=Br, I) using potassium carbonate (K<sub>2</sub>CO<sub>3</sub>) as a base. In addition, the *N*-acetylation of isatin was achieved by the reflux of isatin **72** in an acetic anhydride solution. After *N*-substitution reactions of isatins, all isatin derivatives (*N*-substituted and unsubstituted) were reacted with corresponding triphenyliminophosphane reagent **75** by aza-Wittig reaction and yielded the 19 different carbamates protected isatin derived ketimines **76** (70-95% yield) (Scheme 13).

**Table 1** Synthesized *N*-Carbamate Protected Ketimines\*

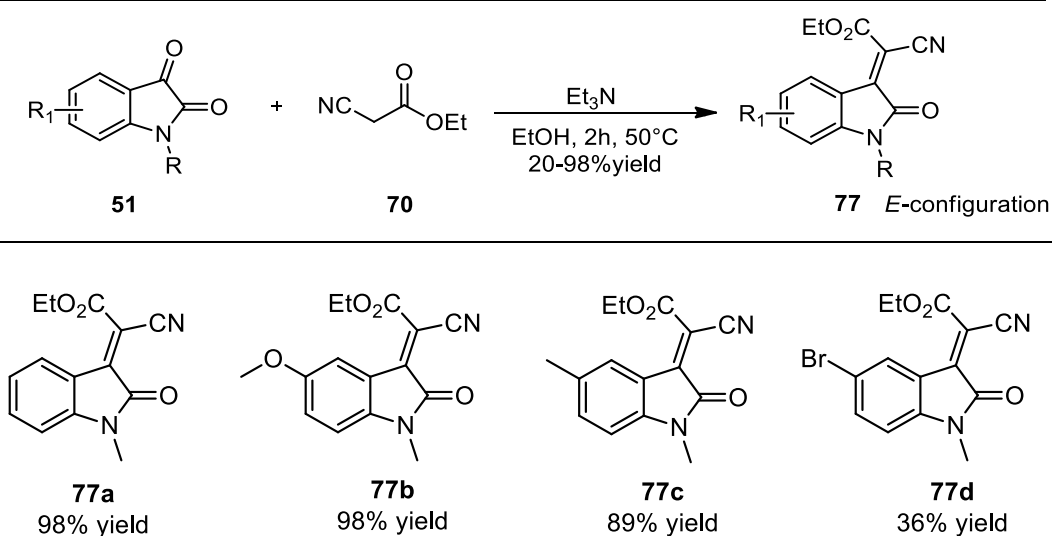


**Table 1** Continued

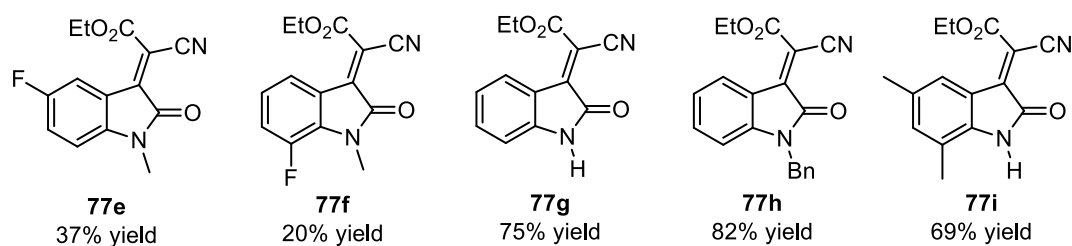
\*Isolated yields

### 2.1.2 Synthesis of Knoevenagel condensates

To develop a simple and efficient method for synthesizing spiro-fused oxindole moiety, the C-3 position of isatins was reacted with an active methylene unit to form a C-C bond and become a reactive center for the cyclization reaction. To achieve this goal, commercially available isatin derivatives reacted with ethyl cyanoacetate in the presence of triethylamine as a base. Up to now, nine different isatins **51** (*N*-substituted and unsubstituted, C-5 and C-7 substituted) reacted with ethyl cyanoacetate **70**, and the condensation products **77** were synthesized and isolated according to the protocol mentioned below (Table 2).

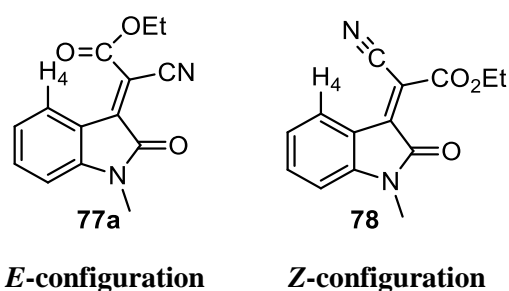
**Table 2** Synthesized 2-oxoindolin-3-ylidene acetate derivatives\*

**Table 2** Continued



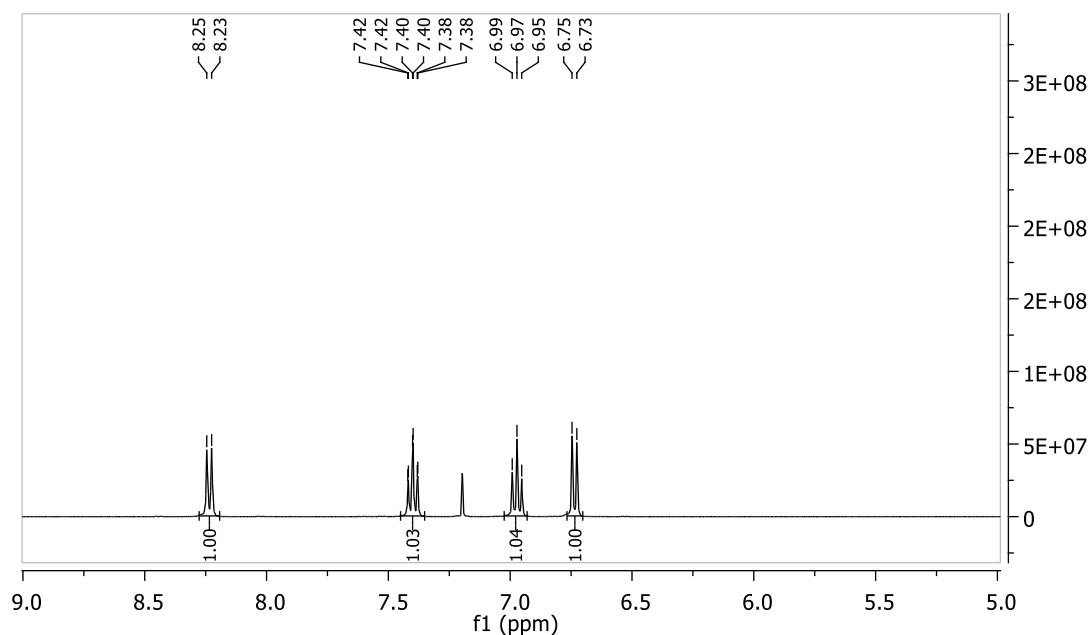
\*Isolated yields. R<sub>1</sub>,R=5MeO,Me (**88**),5Me,Me (**89**), 5Br,Me (**90**), 5F,Me (**91**), 7F,Me (**92**), 5,7-Dimethyl,H (**93**)

According to literature studies, we predicted the *E/Z* configuration of the condensation products by comparing <sup>1</sup>H NMR signals of the ortho (H<sub>4</sub>) protons. It is explained that, either the cyanide group or ester carbonyl group in the structure of **77a-78** lie across the ortho proton in a deshielding position, electron withdrawing groups could cause differing in de-shielding effects.<sup>67</sup> For *Z*-configuration in which the cyanide group lies across the ortho proton, H<sub>4</sub> resonates 0.7-0.8 ppm downfield from other aromatic protons. However, when the ester carbonyl group lies across the H<sub>4</sub> proton as in *E*-configuration, it would cause a more deshielding effect than the cyanide group, and the signal of the H<sub>4</sub> proton shifts around 1.0 ppm to downfield.<sup>68</sup>



**Scheme 14** *E/Z* configuration of 2-oxoindolin-3-ylidene acetate

To clarify the configuration of the condensation product, the <sup>1</sup>H NMR spectrum of the **77a** is given in Figure 16. As shown in the spectrum, the signal of the H<sub>4</sub> proton resonates at 8.24 ppm and shifts downfield according to the H<sub>5</sub> proton that resonates at 6.99 ppm.

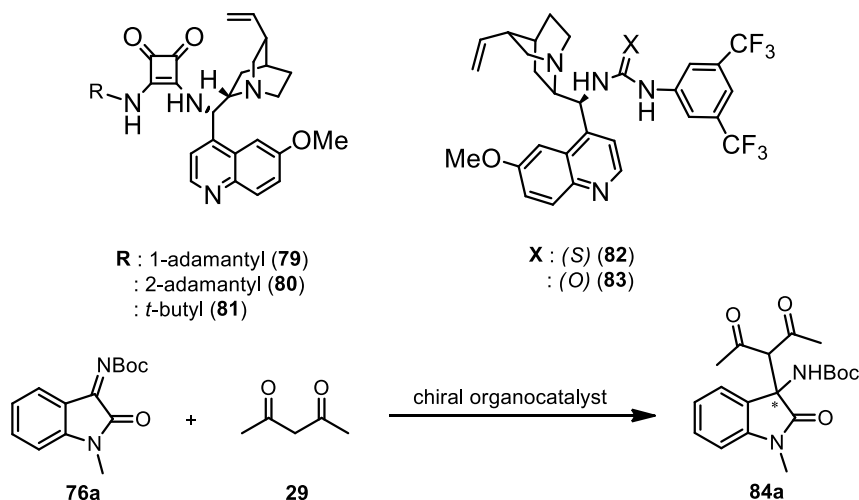


**Figure 16**  $^1\text{H}$  NMR Spectrum of **77a**

## 2.2 Asymmetric Mannich Reaction

### 2.2.1 Optimization of Reaction Parameters for Mannich Reaction

To optimize the reaction parameters, we initiated the studies with the quinine-based bifunctional catalysts screening, which were synthesized in our group in the enantioselective addition of acetylacetone to *N*-methyl substituted ketimine (Table 3). At first, the catalyst loading was chosen as 5 mol%, and reactions were carried out in dichloromethane solvent at room temperature and monitored each hour. The results are depicted in Table 3.

**Table 3** Catalyst Screening for Optimization of Mannich Reaction

entry	Catalyst	Catalyst Loading	Solvent	Conc. (M)	time	yield%**	ee%***
1	<b>79</b>	5 mol%	DCM	0.1	24	98	96
2	<b>80</b>	5 mol%	DCM	0.1	2	99	99
3	<b>81</b>	5 mol%	DCM	0.1	24	87	97
4	<b>82</b>	5 mol%	DCM	0.1	24	94	89
5	<b>83</b>	5 mol%	DCM	0.1	24	92	93

Reaction conditions: ketimine **76a** (0.05 mmol, 0.1 M in solvent) and acetylacetone **29** (0.05 mmol).

\*Isolated yields are reported. \*\*Determined by HPLC equipped with chiral column. Desired product precipitates in the solvent.

According to obtained results, in the catalysis of all quinine-derived squaramides **79–81**, thiourea **82** and urea **83** reaction proceeded smoothly to afford **84a** in high yields (87–99%) and enantioselectivities (89–99% ee). Due to product **84a** in a very short time and excellent yield and enantioselectivity (99% yield and 99% ee, entry 2), further optimization studies continued with 2-adamantyl substituted squaramide **80** as the best organocatalyst in hand.

For continuation of optimization reactions, as a second parameter, lower catalyst loadings (2, 1, 0.5 mol%) were examined to offer a protocol synthetically more atom



economical. Decreasing the amount of catalyst from 5 mol% to 1 mol% caused no loss in the yield nor stereoselectivity at room temperature (Table 4, entries 1 and 3, respectively). The use of low-loading catalysts is very rare in organocatalysis. Such good results obtained with 1 mol% level ensure organocatalysis field attains the advantage of metal complex catalysts in terms of efficiency.<sup>69</sup> Although different substrate concentrations are examined with 0.5 mol% catalyst loading of **80**, 99% ee could not be achieved in these cases (entries 4–6, Table 4).

**Table 4** Catalyst loading and Concentration Screening

entry	Catalyst	Catalyst Loading	Solvent	Conc. (M)	time	yield%**	ee%***
1	80	5 mol%	DCM	0.1	2	99	99
2	80	2 mol%	DCM	0.1	3h	99	99
3	80	1 mol%	DCM	0.1	8h	99	99
4	80	0.5 mol%	DCM	0.1	22h	88	93
5	80	0.5 mol%	DCM	0.2	22h	99	98
6	80	0.5 mol%	DCM	0.3	22h	99	98

After checking the influence of loaded catalysts and the change in concentration, various solvents were tried as another parameter. Upon those trials, besides yielding adduct in a shorter time than it was with DCM, diethyl ether brought along the advantage of simple isolation of readily precipitated product **84a** from the reaction medium (Table 5, entry 3).

**Table 5** Solvent Screening

entry	Catalyst	Catalyst Loading	Solvent	Conc. (M)	time	yield%**	ee%***
1	80	1 mol%	DCM	0.1	8h	99	99
2	80	1 mol%	Toluene	0.1	7h	97	99

3	80	1 mol%	Et <sub>2</sub> O*	0.1	3h	92	99
4	80	1 mol%	EtOAc	0.1	7h	93	98
5	80	1 mol%	CH <sub>3</sub> CN	0.1	24h	92	98
6	80	1 mol%	THF	0.1	24h	90	94

\*as reaction proceeds, product precipitates in ether, \*\* isolated yields are reported, \*\*\* Determined by HPLC equipped with chiral column

As a result of screening studies, optimum conditions for the Mannich reaction of acetylacetone **29** to *N*-methyl substituted ketimine **76a** was determined to be 1 mol% catalyst, 0.1M concentration, diethyl ether as a reaction solvent, and room temperature.

### 2.2.2 Scope of Mannich Reaction

Having decided the optimum reaction condition, to determine the reaction scope, several isatin ketimines with different substituents at amide nitrogen, electron withdrawing and donating groups on aryl part, and various *N*-carbamoyl protecting groups were reacted with acetylacetone in the presence of organocatalyst **80**.

Initially, the effect of different substituents (-H, -Me, -Et, -Bn, -Ac) at 1-position of isatin was investigated and in all cases, catalyst **80** induced high stereoselectivity (92–99% ee) in adducts **84a–e** (Table 6). However, lower reactivity was observed for the ketimines having acetyl and ethyl substituents (**76c** and **76e**, respectively). Then compatibility of protecting groups, *N*-Cbz, -CO<sub>2</sub>Et, and -PMP, were tested. Although the first two yielded adducts (**76f**, **76g**, **76i**, and **76j**) with high enantioselectivities (91–98% ee), PMP-protected ketimine revealed no reactivity. This consequence indicates that the *N*-carbamoyl unit is indispensable in the activation of electrophile by H-bond donor squaramide moiety in organocatalyst **80**.

Lastly, by derivatization on the aryl part of the isatin ketimine, corresponding adducts (**76k–s**) were obtained in high yields (84–98%) and with excellent enantioselectivities (85- >99% ee), except for the 5-bromo substituted derivative

**76q**. Being sterically bulky and at a close position to the imine part of the starting ketimine, bromine may restrain the formation of a rigid transition state so that it causes a lack of enantioselectivity of **76q** (41% ee).

**Table 6** Reaction scope of Mannich reaction of isatin derived ketimine **76** and acetylacetone **29**

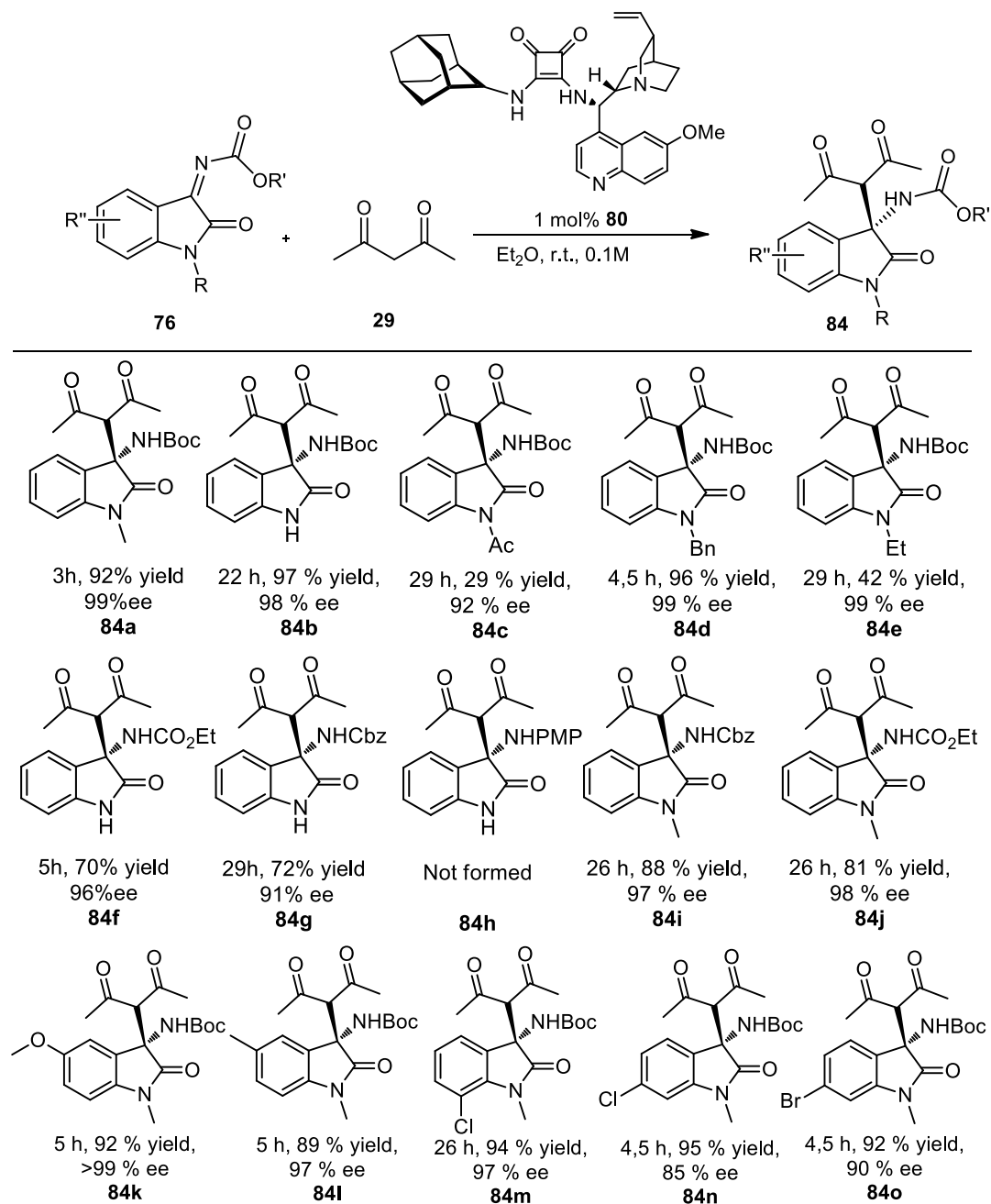
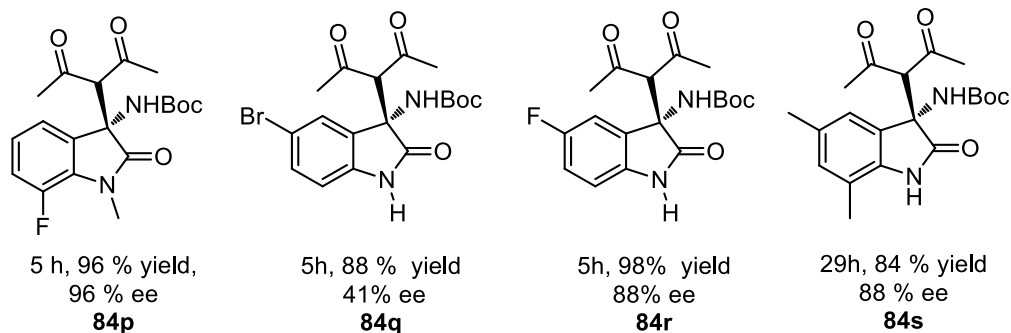


**Table 6** Continued



Reaction conditions: ketimine **76** (0.05 mmol, 1eq.) and acetylacetone **29** (0.05 mmol, 1 eq), catalyst **80**, diethyl ether (0.5 mL). \*Isolated yields are reported. \*\*Determined by HPLC equipped with chiral column. Desired product precipitates in the solvent.

As an illustrative example;  $^1\text{H}$  and  $^{13}\text{C}$  NMR spectra of compound **84a** are given in Figures 17 and 18, respectively. The most indicative signals in the  $^1\text{H}$  NMR spectrum belong to  $-\text{NH}$  and  $-\text{CH}$  protons adjacent to the quaternary center that resonate at 6.43 ppm as a singlet and 4.01 ppm as a broad singlet, respectively. In the  $^{13}\text{C}$  NMR spectrum, a newly formed quaternary carbon atom resonating at 68.6 ppm was also a decisive signal for the bond formation. Additionally, signals of the  $-\text{CH}_3$  group of acetylacetone resonating at 2.22 ppm and 2.10 ppm as singlet also represent the addition of the acetylacetone group. *N*-Me and *t*-butoxy methyl protons give singlet at 3.18 and 1.20 ppm, respectively, and 4 aromatic protons are observed in the range of 7.26-6.43 ppm.

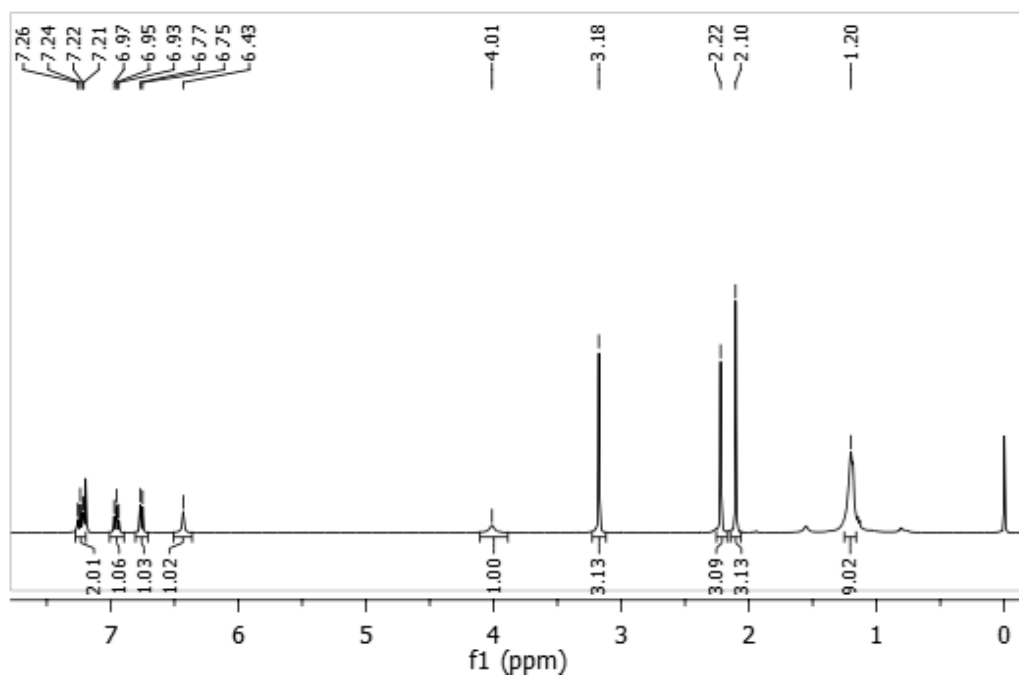


Figure 17 <sup>1</sup>H-NMR Spectrum of 84a

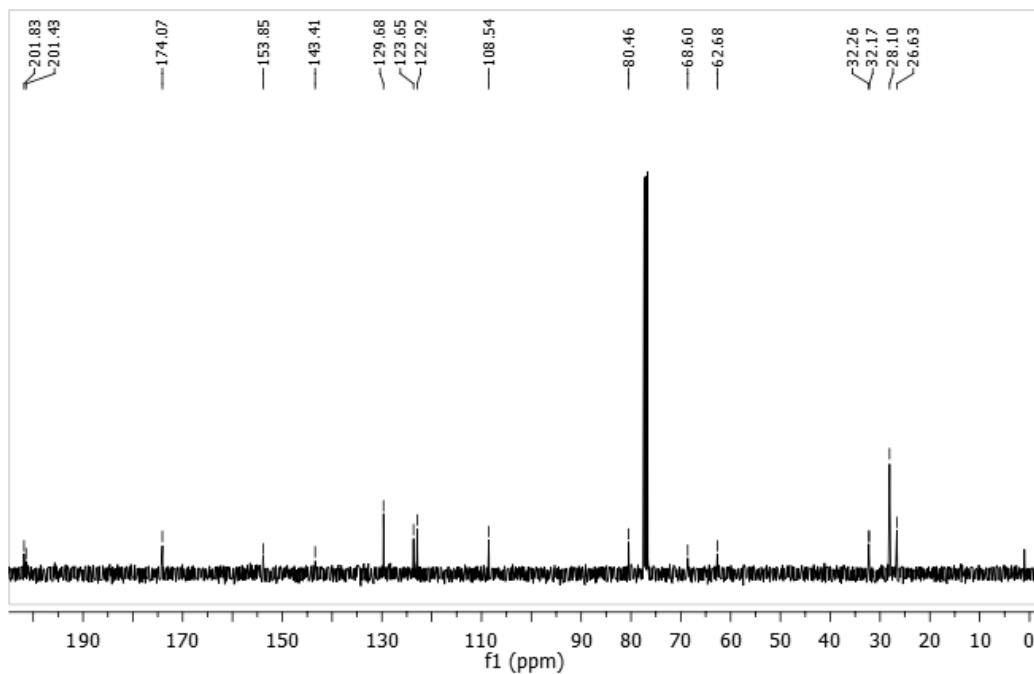
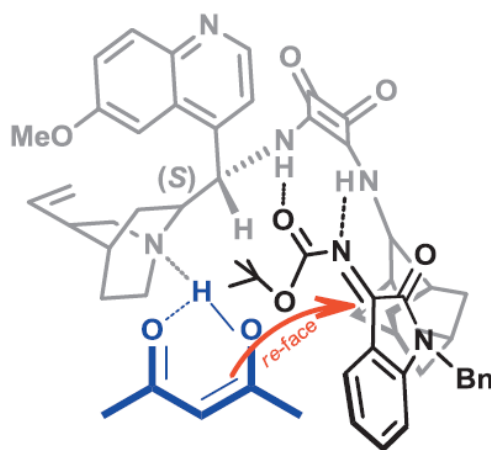


Figure 18 <sup>13</sup>C-NMR Spectrum of 84a

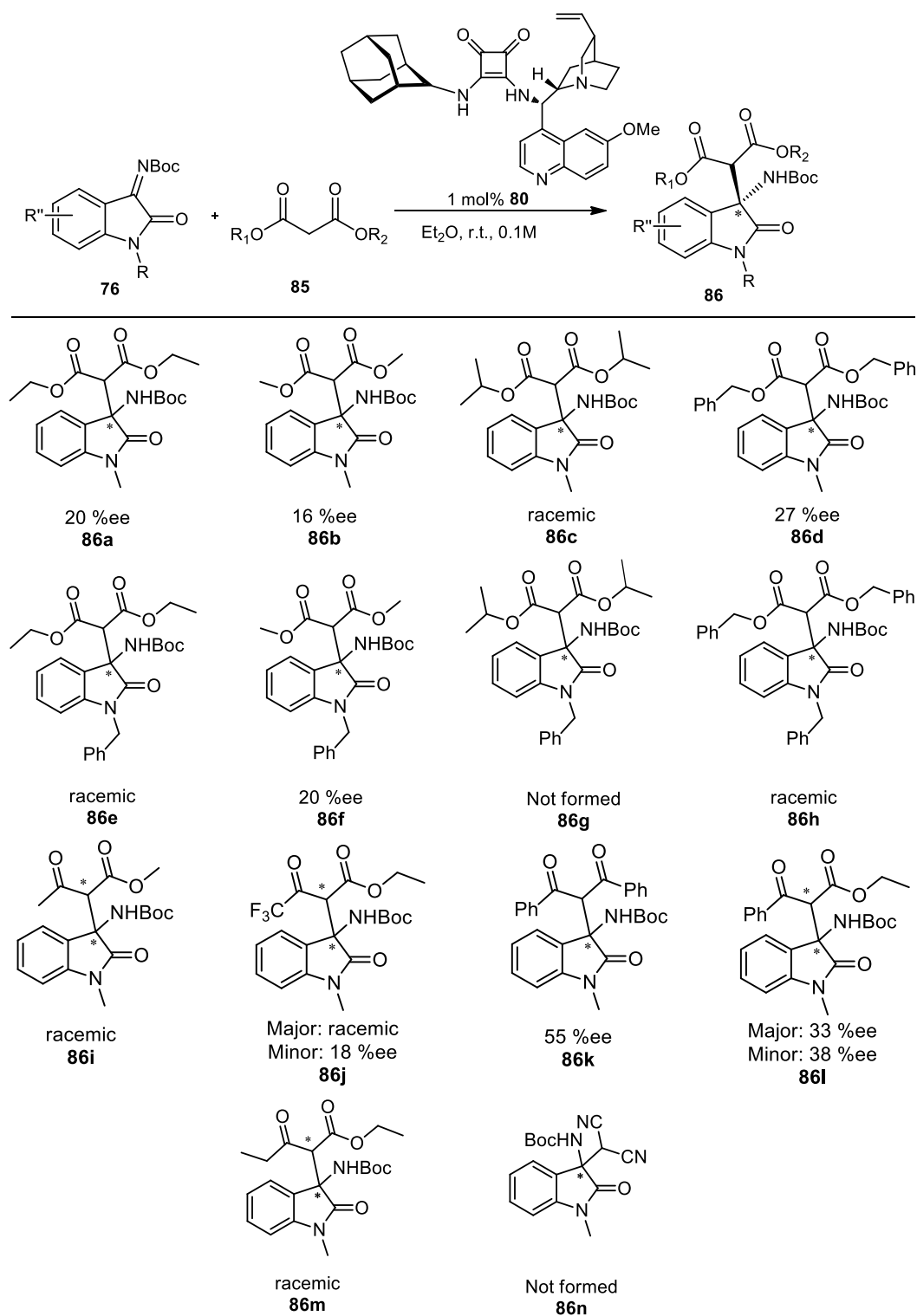
Furthermore, the absolute configuration of the products was assigned as *S*-enantiomer according to previously reported studies.<sup>13d,53</sup> Regarding this structure, a possible transition state model is given in Figure 19. The tertiary amine of the quinuclidine unit of organocatalyst **80** activates the 1,3-dicarbonyl compound upon deprotonation, and resulting enol gets closer to the ketimine interacting with squaramide unit through H-bonding. In addition, the sterically bulky adamantyl group hinders the *si*-face of ketimine and favors the attack of enol from *re*-face selectively.<sup>56</sup>



**Figure 19** Possible transition state

In addition to derivatization studies, other 1,3-dicarbonyl compounds were examined with two different ketimines (*N*-methyl, *N*-benzyl substituted) under the optimized reaction condition. In earlier reactions, although acetylacetone as an active methylene unit showed excellent results, selectivities were not satisfied with other 1,3-dicarbonyl compounds. (Table 7).

**Table 7** Reaction scope of Mannich reaction of isatin derived ketimine **76** and other 1,3-dicarbonyl compounds **85**



Reaction conditions: ketimine **76** (0.05 mmol, 1eq.) and 1,3-dicarbonyl compound **85** (0.05 mmol, 1 eq), catalyst **80**, diethyl ether (0.5 mL). \*Determined by HPLC equipped with chiral column.

A decrement in the selectivity in the reaction of malonates with ketimines could have resulted from the lower reactivities of methylene unit in malonates than acetylacetone's methylene unit. Moreover, sterically bulky groups in phenyl and benzyl-substituted dicarbonyls could also block one side and make the approach of malonates to ketimines difficult, which caused the low selectivity with low yield. Lastly, in addition to malonates, malononitrile was checked in this reaction.

However, the expected Mannich addition reaction did not form, and the presence of malononitrile resulted in the condensation of protecting group (Table 7). Surprisingly, after some research, the resulting condensation product led us to another point in which the construction of spirooxindoles was investigated.

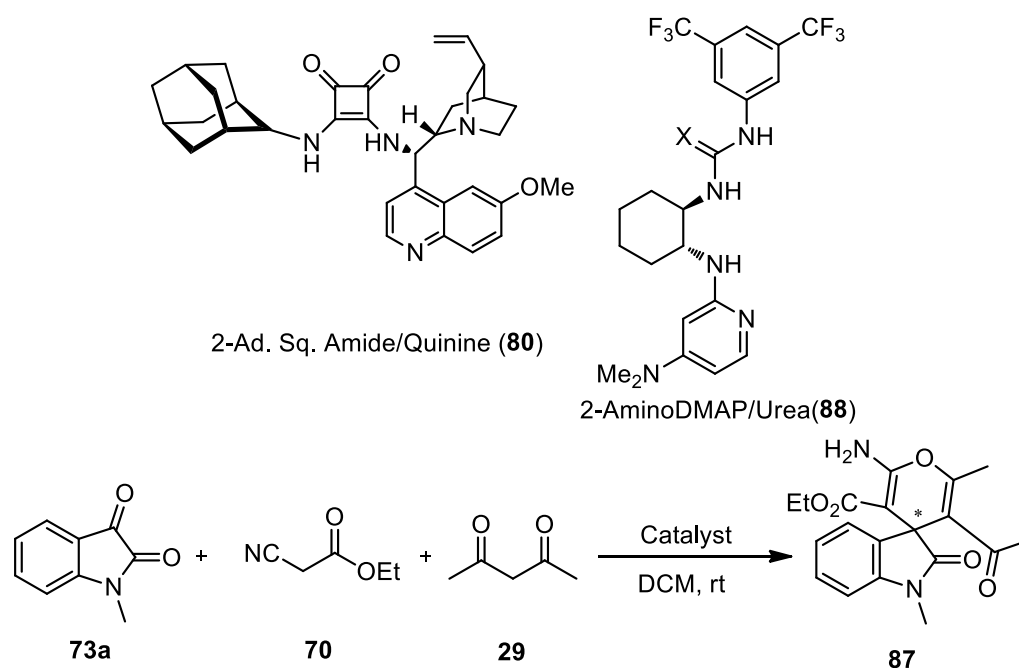
## **2.3 Enantioselective Construction of Spiro Conjugated Amino-pyran-oxindoles**

### **2.3.1 Optimization of the Reaction Parameters for Construction of Spiro Conjugated Amino-pyran-oxindoles**

To investigate the utility of the formation of the spiro-oxindole moiety, studies were initiated with the one-pot reaction of *N*-Me substituted isatin, ethyl cyanoacetate, and acetylacetone by checking 2 different bifunctional organocatalyst system (2-AminoDMAP/Urea **88** and 2 Ad. Sq. Amide/Quinine **80**) and catalyst loading. The reaction was monitored each hour to determine the reaction time according to selectivity and checked both in 24h and 48hours. The results are expressed in Table 8.



**Table 8** Optimization studies for the Enantioselective Construction of Spirooxindoles



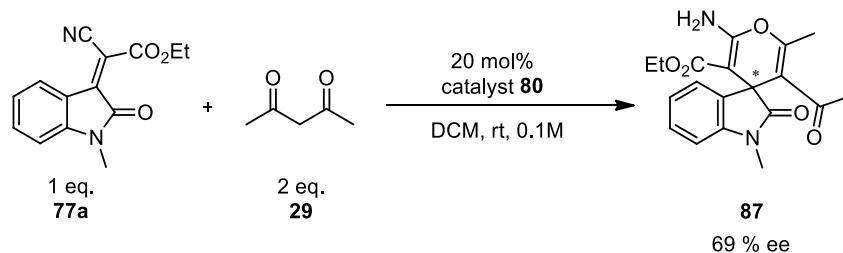
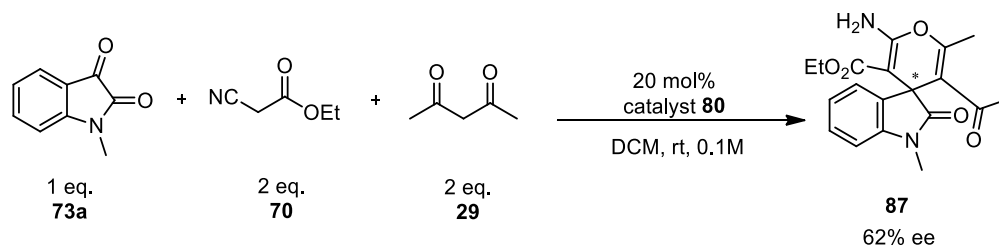
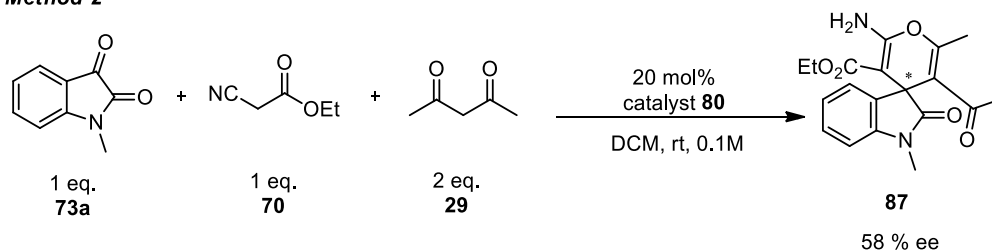
entry	Catalyst	Catalyst Loading	Conc.(M)	time	ee%*
1	<b>88</b>	5 mol%	0.1	24h	rac
2	<b>88</b>	5 mol%	0.1	48h	rac
3	<b>80</b>	5 mol%	0.1	24h	11
4	<b>80</b>	5 mol%	0.1	48h	25
5	<b>80</b>	20 mol%	0.1	24h	40
6	<b>80</b>	20 mol%	0.1	48h	62

Reaction conditions: isatin **73a** (0.05 mmol, 0.1 M in DCM), ethyl cyanoacetate **70** (0.1 mmol) and acetylacetone **29** (0.1 mmol). \*Determined by HPLC equipped with chiral column

According to results depicted in Table 8, the highest selectivity was obtained in the presence of 20 mol% 2-adamantyl substituted squaramide **80** catalyst in DCM at 48h.

In literature, there are several reports about one-pot domino type reactions in which isatins or indole derivatives, malononitrile, and 1,3-dicarbonyl compounds are used to get spirooxindoles. Besides, there are reports in which Knoevenagel condensates are used as starting material. However, examples of the organocatalytic and asymmetric versions of those transformations are scarcely any. From this point of view, for further optimization, the control of selectivity of the reaction for the formation of spirooxindole was checked by trying both domino-type and initially synthesizing the Knoevenagel condensate. At the start, the reactions were designed by using 2 different amounts of ethyl cyanoacetate in a one-pot domino type reaction in terms of the rate of the formation of the condensation product. In other methods, Knoevenagel condensates were already synthesized, purified, and characterized as mentioned above and then reacted with acetylacetone. In all processes, the cyclization reactions and formation of the spirooxindole occurred with similar selectivities but in different yields. In line with our aim in this transformation, optimization studies proceeded by using Knoevenagel condensates as starting material due to the yield of the reaction.

---

**Method 1****Method 2****Scheme 15** Screening results for control of selectivity of the reaction

For the continuation of optimization studies, other bifunctional organocatalysts, which are quinine-derived squaramide **80-91**, thiourea **90** and 2-amino DMAP derived urea **88** and thiourea **89** that synthesized in our group were examined in the model reaction of 2-cyano-2-(1-methyl-2-oxoindolin-3-ylidene) acetate **77a** with acetylacetone in DCM (Table 9).

According to obtained results, in the catalysis of quinine-derived 2-adamantyl squaramide catalyst **80**, the reaction proceeded more smoothly than other quinine-derived and amino DMAP derived catalysts to afford **87**. Since the highest selectivity was obtained with catalyst **80** (Table 9, entry 1), further optimization studies were continued with 2-adamantyl substituted squaramide catalyst **80** as the best catalyst in hand.

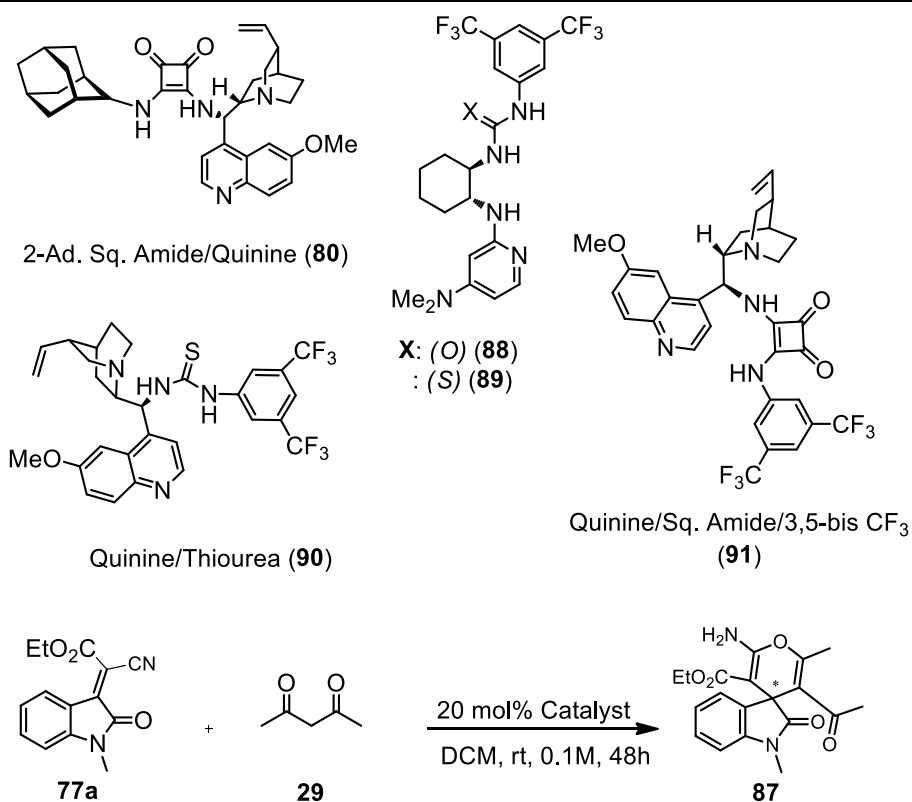


**Table 9** Catalyst Screening

entry	Catalyst	Temperature (°C)	Conc. (M)	Time (h)	ee%
1	<b>80</b>	RT	0.1	48	69
2	<b>88</b>	RT	0.1	48	5
3	<b>89</b>	RT	0.1	48	45
4	<b>90</b>	RT	0.1	48	31
5	<b>91</b>	RT	0.1	48	49

Reaction conditions 2-cyano-2-(1-methyl-2-oxoindolin-3-ylidene)acetate **77a** (0.05 mmol) and acetylacetone **29** (0.1 mmol). \*Determined by HPLC equipped with chiral column.

As another parameter, the effect of temperature, which plays an important role in asymmetric transformations in selectivity, was screened. Three different temperature conditions were applied in addition to ambient conditions to understand the effect on selectivity. Generally, decreasing temperatures in which reactivities also drop will

cause an increase in selectivity. As known in our reaction, lowering the temperature from ambient conditions to 22°C increases the yield and the selectivity of the reaction (Table 10, entry 2). However, reducing the temperature to 20°C and 15°C also decreases the selectivity. In light of these results, other parameters in the reaction were screened at 22°C.

**Table 10** Temperature Screening

entry	Catalyst	Temperature (°C)	Solvent	Conc. (M)	Time (h)	ee%*	Yield**
1	<b>80</b>	Ambient	DCM	0.1	48	70	40
2	<b>80</b>	22	DCM	0.1	48	87	53
3	<b>80</b>	20	DCM	0.1	48	73	56
4	<b>80</b>	15	DCM	0.1	48	63	54

\*Determined by HPLC equipped with chiral column.\*\*Isolated yields

Further, the effect of adding 4Å molecular sieves to the reaction medium was analyzed. To understand the impact of the particle size, sieves were added as a crushed particles. The results obtained with crushed molecular sieves could indicate that increasing the particle surface area increases the activity and efficacy of the molecular sieve and the reactivity of the reaction (Table 11).

**Table 11** 4Å MS Effect

entry	Catalyst	Temp. (°C)	4Å MS	Solvent	Conc. (M)	Time (h)	ee%*	Yield**
1	<b>80</b>	22	particle	DCM	0.1	48	70	52
2	<b>80</b>	22	crushed	DCM	0.1	48	85	50

\*Determined by HPLC equipped with chiral column.\*\*Isolated yields

As another parameter, various solvents were screened in the reaction of 2-cyano-2-(1-methyl-2-oxoindolin-3-ylidene) acetate **77a** with acetylacetone **29**. Among the 8

different solvents, the highest selectivity was attained in toluene at 89% ee, as shown in Table 12.

**Table 12** Solvent Screening

entry	Catalyst	Temp. (°C)	4Å MS	Solvent	Conc. (M)	Time (h)	ee%*	Yield**
1	80	22	crushed	Hexane	0.1	48	71	60
2	80	22	crushed	Toluene	0.1	48	89	77
3	80	22	crushed	CH <sub>3</sub> CN	0.1	48	39	71
4	80	22	crushed	EtOAc	0.1	48	64	75
5	80	22	crushed	Et <sub>2</sub> O	0.1	48	8	88
6	80	22	crushed	1,4-Dioxane	0.1	48	25	59
7	80	22	crushed	1,2-Dichloro benzene	0.1	48	41	69
8	80	22	crushed	1,2-Dichloro ethane	0.1	48	41	48
9	80	22	crushed	α,α,α-trifluoro toluene	0.1	48	8	43

\*Determined by HPLC equipped with chiral column.\*\*Isolated yields

After selecting the solvent, the final parameter concentration of the reaction medium was controlled. Increasing the concentration of the reaction medium drastically diminished the reaction's selectivity (Table 13).

**Table 13** Concentration Screening

entry	Catalyst	Temp. (°C)	4Å MS	Solvent	Conc. (M)	Time (h)	ee%	Yield
1	<b>80</b>	22	crushed	Toluene	0.1	48	89	77
2	<b>80</b>	22	crushed	Toluene	0.2	48	11	62
3	<b>80</b>	22	crushed	Toluene	0.3	48	rac	40

As consequence of the optimization studies, the best condition was obtained with 2-adamantyl squaramide catalyst **80**, toluene as a solvent, in the presence crushed 4Å molecular sieves at 22°C in 48h for this reaction.

### 2.3.2 Scope of Enantioselective Construction of Spiro Conjugated Amino-pyran-oxindoles

To examine the scope of the reaction, with the optimum condition in hand, several isatyridine acetate derivatives and 1,3-dicarbonyl compounds were checked for the construction of spirooxindole moiety.

The effect of different substituents **77g**, **77h** (-H, -Bn) at 1-position of isatyridine acetate was studied. Although lower reactivity was observed in all cases, for benzyl substituted isatyridine acetate **77h**, moderate selectivity (as 62% ee) was obtained at **87h**. In addition to the 1-position substitution, the effect of different substituents on the aryl part was also investigated. Related products (**87b-87i**) were obtained generally in low yields (up to 41%) but moderate to excellent enantioselectivities (52-99% ee), except for 5-fluoro substituted derivative **87e**. Due to its highest electronegativity and close position to the newly formed quaternary center, fluorine may restrain the cyclization reaction so that it causes a decrease in enantioselectivity (16% ee).

Moreover, to analyze the compatibility of the 1,3-dicarbonyl compounds in the construction of spirooxindole moiety, various 1,3-dicarbonyl compounds were

examined with 2-cyano-2-(1-methyl-2-oxoindolin-3-ylidene) acetate **77a** and ethyl cyanoacetate **70**. In this trial, 16 different substances with different reactivities were checked. As shown in Table 14, almost all products **87a-q** gave the corresponding spirooxindole generally in low yields and low to moderate enantioselectivities (up to 52%ee). Among all the dicarbonyl compounds, although racemic products were easily synthesized with 1,3-diphenylpropane-1,3-dione and 1,3-bis(4-methoxyphenyl)propane-1,3-dione, corresponding spirooxindoles **87r-s** did not form selectively. Regarding the mechanism of the Michael addition/ cyclization reaction, the sterically bulky adamantyl unit of the catalyst may hinder the possible approach of the sterically bulky phenyl unit in the transition state.

Further, in the designed reaction with 1,1,1-trifluoropentane-2,4-dione **87t** and ethyl 4,4,4-trifluoro acetoacetate **87u**, both racemic and enantioselective reactions did not occur. Also, there was a gas evolution shortly after adding the substrates to the reaction medium. Besides, various malonate derivatives **87v-y** were examined with *N*-Methyl substituted isatylidene acetate. However, in all cases, instead of cyclization and formation of spirooxindole moiety, malonate derivatives did nucleophilic substitution to the substrate, which could easily be characterized from <sup>1</sup>H NMR spectroscopy.

**Table 14** Reaction scope for the construction of Spiro Conjugated Amino-pyran-oxindoles

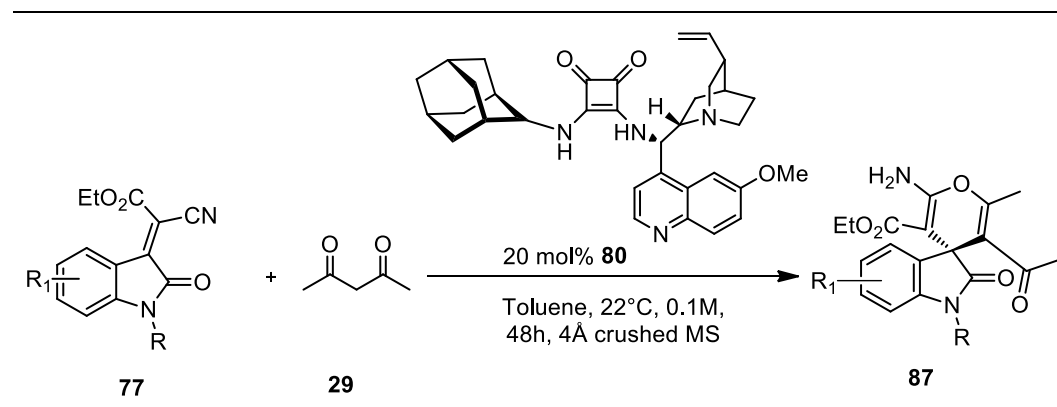




**Table 14 Continued**

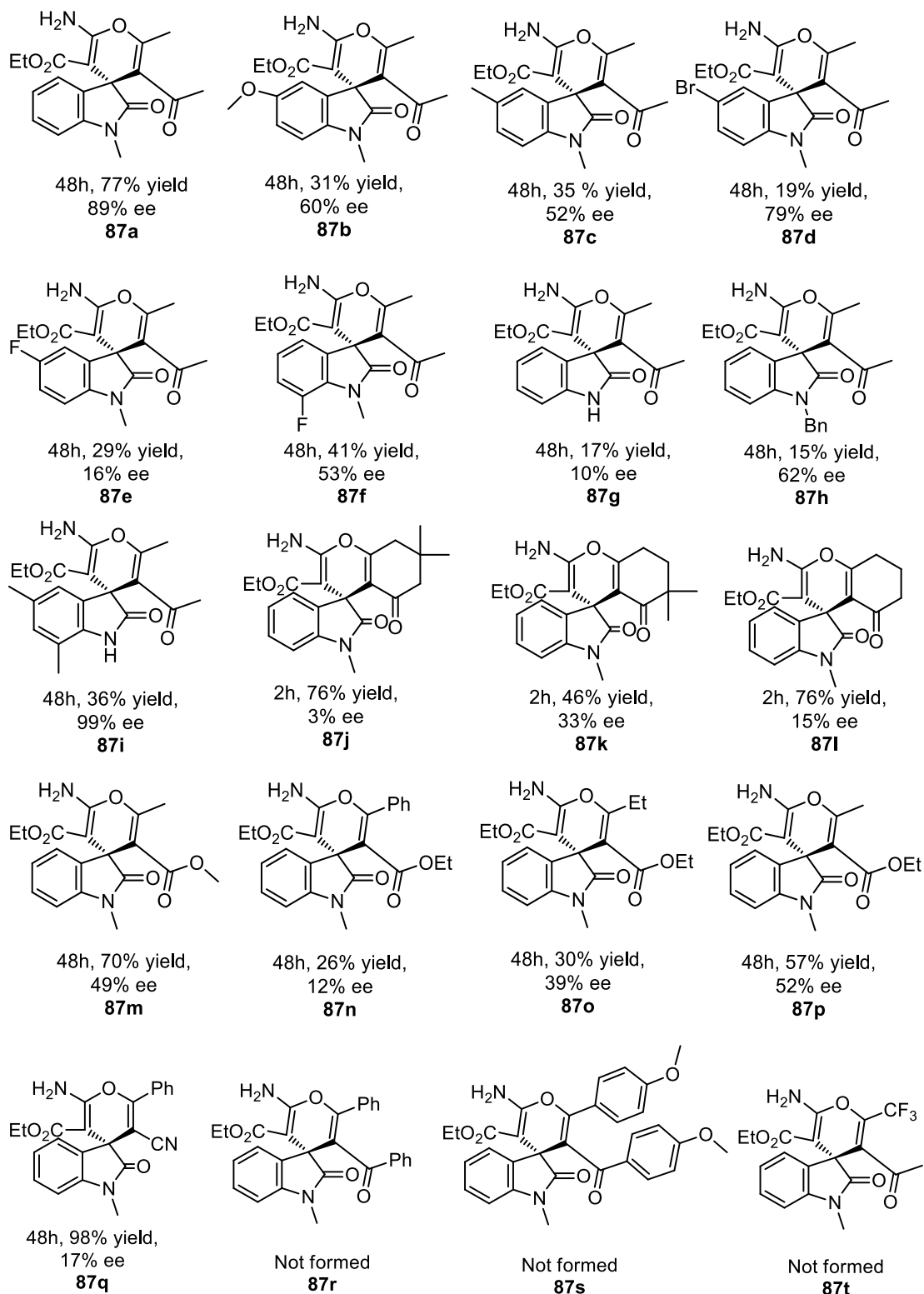
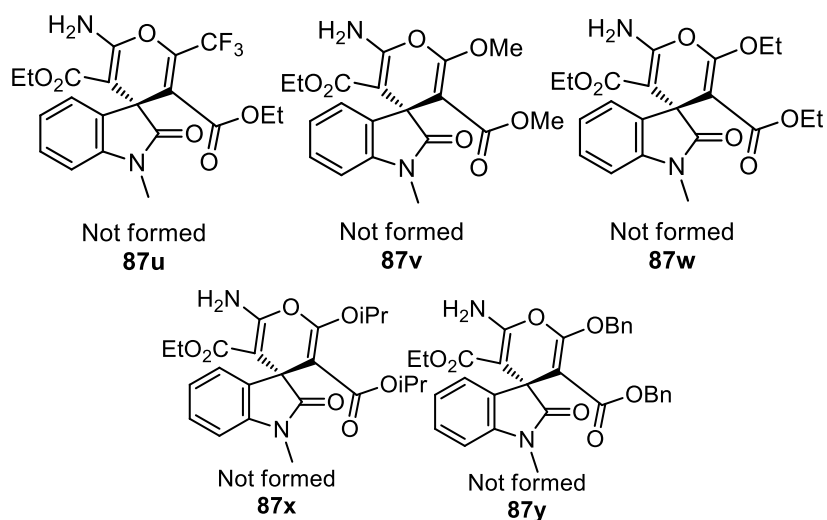


**Table 14** Continued



Reaction conditions corresponding isatynylidene acetate **77** (0.05 mmol) and acetylacetone **29** (0.1 mmol). \*Isolated yields.\*\*Determined by HPLC equipped with chiral column.

As an illustrative example;  $^1\text{H}$  and  $^{13}\text{C}$  NMR spectra of compound **87a** are given in Figures 20 and 21, respectively. In  $^1\text{H}$  NMR spectroscopy, the distinctive signal that addresses the formation of the spirooxindole belongs to  $-\text{NH}_2$  signal of the oxindole, which resonates around 7.8-7.9 ppm as a singlet. In addition to  $-\text{NH}_2$  signal, the ethoxy ( $-\text{OCH}_2\text{CH}_3$ ) group attached to the nearby  $-\text{NH}_2$  group resonated at 3.69 ppm as a quartet and 0.7 ppm as a triplet, respectively. In the  $^{13}\text{C}$  NMR spectrum, the characteristic signal that proves the construction of the spirooxindole moiety belongs to a newly formed quaternary carbon atom, which resonates at 74.4 ppm. Additionally, signals of the double bond carbons of the newly formed spirooxindole unit resonated at around 107 ppm to 122 ppm.

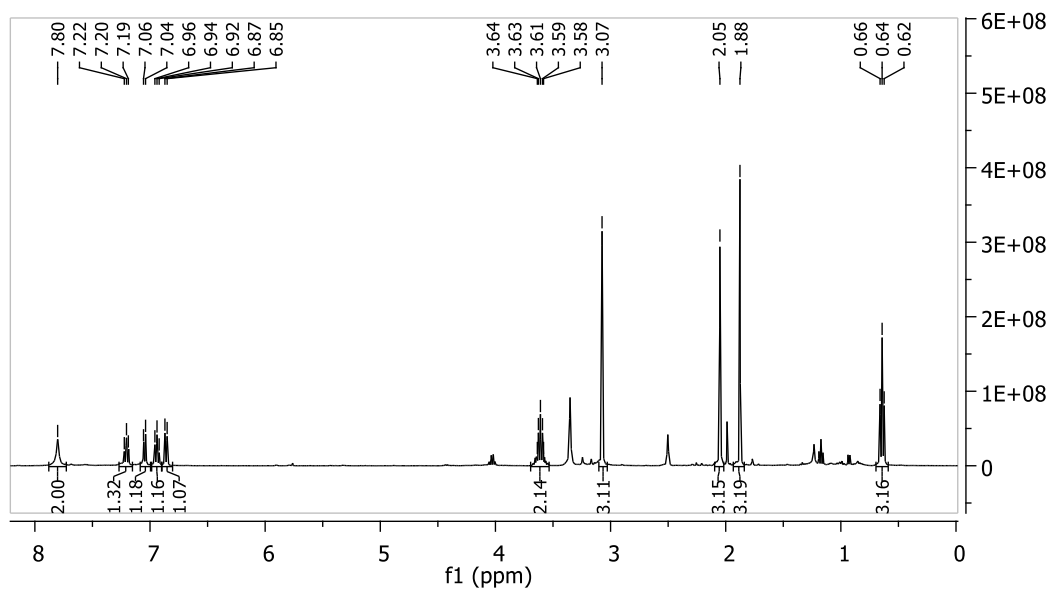


**Figure 20**  $^1\text{H}$  NMR Spectrum of **87a**

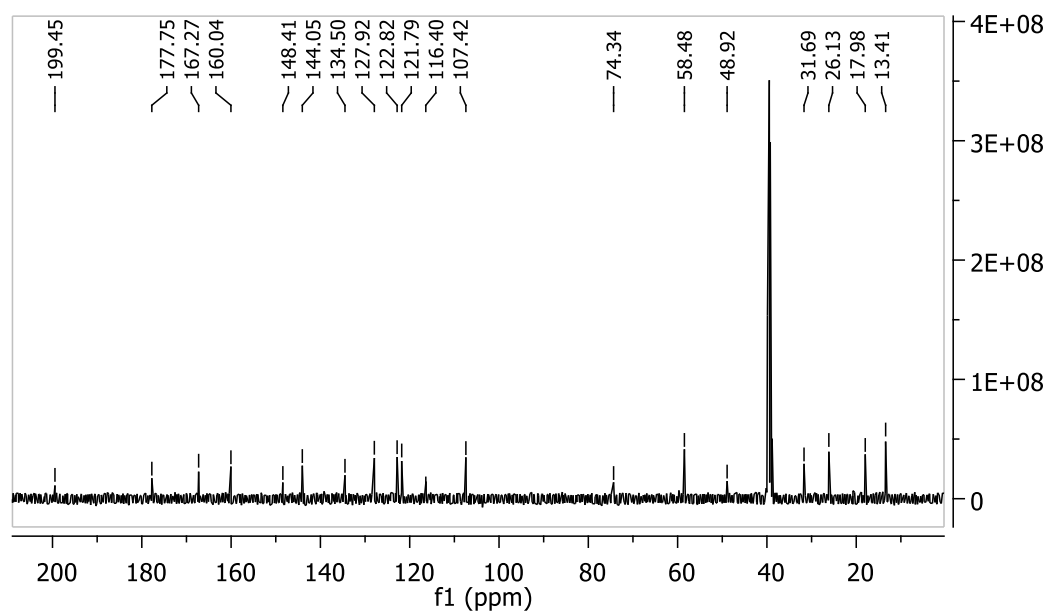


**Figure 21**  $^{13}\text{C}$  NMR Spectrum of **87a**

The absolute configuration of the spirocyclic products was decided as *S*-enantiomer according to the literature's retention time comparison and then generalized for the

others.<sup>64</sup> The plausible reaction course model was proposed regarding S-selectivity, as shown in Figure 20. 1,3-Dicarbonyl compound is activated by the tertiary amine of quinuclidine unit of organocatalyst **80** by abstracting a proton and generated enolate species forms H-bond with the ammonium site of organocatalyst **80**. In addition, the isatinyldine acetate unit also interacts with squaramide through H-bonding. Thus, Michael addition reaction might proceed from the less sterically hindered side and favors the attack of enolate of the 1,3-dicarbonyl compound from *si*-face since the sterically bulky adamantyl unit hinders the *re*-face of isatinyldine acetate. After Michael addition, subsequent intramolecular cyclization and then tautomerization afford the formation of **87a**.

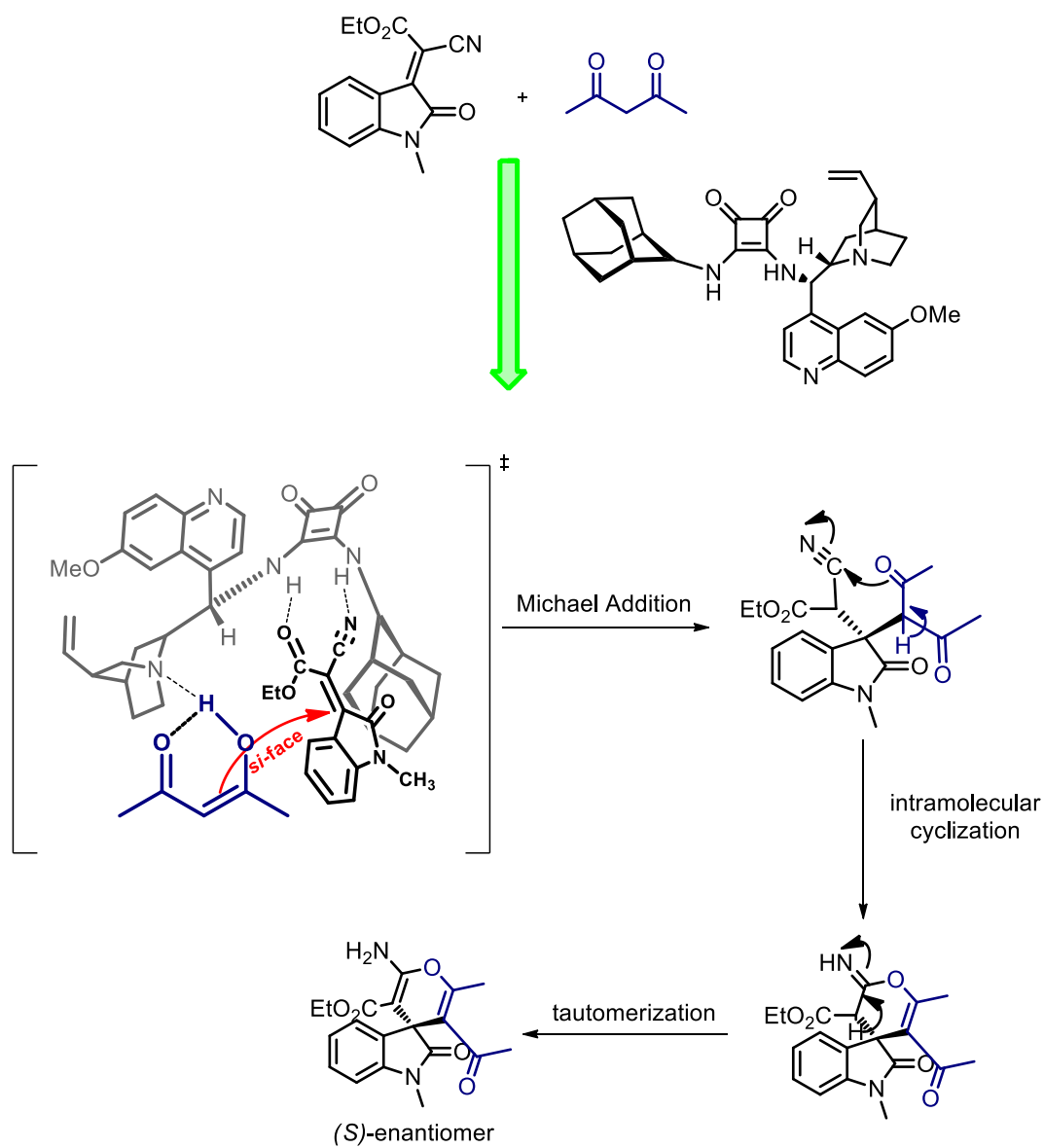


**Figure 22** Plausible reaction course model



## CHAPTER 3

### EXPERIMENTAL

#### 3.1 Materials and Methods

$^1\text{H}$  NMR and  $^{13}\text{C}$  NMR spectra were recorded on Bruker Spectrospin Avance DPX 400 spectrometer at 400 MHz and 100 MHz in  $\text{CDCl}_3$  and  $\text{DMSO-d}_6$ . TMS used as an internal standard and residual nondeuterated solvent peaks recorded at  $\delta$  7.26 and 77.0 ppm, or 2.50 and 39.5 ppm, respectively. Chemical shifts are reported in ppm, coupling constants (J) are given in Hertz (Hz) and data are specified as s (singlet), brs (broad singlet), d (doublet), dd (doublet of doublet), dt (doublet of triplet), t (triplet), q (quartet) and m (multiplet).  $^1\text{H}$  and  $^{13}\text{C}$  NMR spectra of products which are unknown in literature are given in appendix A. All reactions were monitored by thin layer chromatography (TLC) on Merck silica gel 60, F-254 TLC and plates were visualized by UV light using *p*-anisaldehyde stain. Column chromatography purifications were carried out using glass columns with a silica gel (230-400 mesh). Polarimetric measurements were carried out by Rudolph Scientific Autopol III polarimeter at sodium D-line (589nm) and reported as  $[\alpha]_D^T$  (c in g/100mL in solvent). Melting points were measured by capillary tubes. Infrared Spectra (IR) were recorded on Bruker Alpha Platinum ATR and data were reported in wavenumbers ( $\text{cm}^{-1}$ ). High Resolution Mass (HRMS) data were recorded on Agilent 6224 TOF LC/MS with ESI method. HPLC analysis were carried out with Daicell AD-H, AS-H, OD-H and IA chiral columns (0.46 cm  $\varnothing$  x 25 cm) with hexane:*i*-PrOH eluent. HPLC chromatograms of chiral and racemic products were given in appendix B. All compounds were named by using ChemDraw Ultra 12.0.

## 3.2 General Procedure A: Synthesis of N-Substituted Isatin Derivatives

### 3.2.1 N-Alkylation of Isatin

According to procedure in the literature,<sup>70</sup> isatin (1*H*-indole-2,3-dione) (**72**) (30.0 mmol, 4.4 g) and potassium carbonate, K<sub>2</sub>CO<sub>3</sub> (60.0 mmol, 8.3 g) was dissolved in 100 mL acetonitrile, CH<sub>3</sub>CN at room temperature. Then, alkyl halide (33.0 mmol) was added and the reaction mixture was stirred overnight at room temperature. The completion of the reaction was monitored by TLC and upon the completion, the reaction was quenched by distilled water. After the evaporation of the reaction solvent, the crude solid product was dissolved in EtOAc and organic phase was extracted with 5% (w/v) aqueous NaHCO<sub>3</sub> solution and brine three times for compounds **73a**, **73b**. For **73b**, extraction was done only with water and brine solution. The organic layer was dried over anhydrous MgSO<sub>4</sub> and concentrated in vacuo. The crude product was recrystallized multiple times from ethyl acetate and hexane at room temperature to afford compounds **73a-b** in good yields (80-92%) as needle-like crystals. The spectral data agreed with literature.<sup>70-71</sup>

### 3.2.2 N-Benzoylation of Isatin

In a similar manner with *N*-alkylation procedure, Isatin (1*H*-indole-2,3-dione) (**72**) (30.0 mmol, 4.4 g), potassium carbonate (60.0 mmol, 8.3 g) and potassium iodide (3.0 mmol, 0.5 g) were mixed in 100 mL of acetonitrile. Then, benzyl bromide (33.0 mmol, 3.92 mL) was added and the mixture was stirred overnight at room temperature. Upon the completion, solvent was evaporated and standard work-up procedure was done with aqueous NaHCO<sub>3</sub> and purification by recrystallization afforded orange needle-like solid with 88% yield. The spectral data agreed with literature.<sup>70</sup>



### 3.2.3 *N*-Acetylation of Isatin

According to the literature,<sup>72</sup> isatin (1H-indole-2,3-dione) (**72**) (3.4 mmol, 0.5 g) and acetic anhydride (20 mL) were placed in a flask and refluxed for 6 h. Then, the solution was cooled to room temperature and after cooling the reaction mixture was poured into the cold water and filtrated. After filtration, the precipitate afforded *N*-acetylisatin **74** as yellow powder crystals with 90% yield. The crude product does not need any further purification and was used in later steps without purification.

### 3.3 General Procedure B: Synthesis of Isatin-Derived Ketimines

According to literature procedure,<sup>66</sup> related triphenyliminophosphane **75** (2.9 mmol) and isatin derivative **72** (2.6 mmol) were placed in an oven-dried Schlenk flask and dissolved in 4 mL of dry 1,4-dioxane. The mixture was refluxed under argon atmosphere until completion of the reaction. After completion of the reaction, organic solvent was evaporated and the mixture was purified by column chromatography over silica gel column with hexane: EtOAc (3:1) eluent. Characterization of compounds **76a-s** was done by comparing with previously reported <sup>1</sup>H and <sup>13</sup>C NMR spectra.

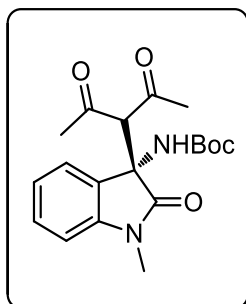
### 3.4 General Procedure C: Racemic Synthesis of Mannich Adducts

To a solution of *N*-alkoxycarbonyl ketimine (0.1mmol) **76** and acetylacetone **29** (0.1 mmol) in DCM (1mL), DABCO (30 mol%) was added at room temperature. Reaction was monitored by TLC and upon the completion, the reaction mixture directly loaded on silica gel and purified by column chromatography with 4:1 Hexane/EtOAc eluent.

### 3.5 General Procedure D: Asymmetric Synthesis of Mannich Adducts

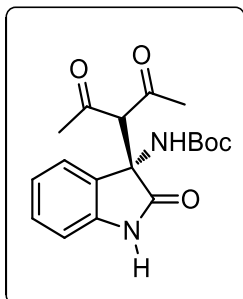
In a 5-mL vial, 2-Adamantyl squaramide catalyst **80** (1 mol%) and *N*-alkoxycarbonyl ketimine **76** (0.05 mmol) were placed. After injection of diethyl ether solvent (0.5 mL), 0.05 mmol (1eq.) acetylacetone **29** was added and the mixture was stirred until complete disappearance of the ketimine. In some cases, *N*-alkoxycarbonyl ketimine was not dissolved totally in diethylether and to overcome this problem DCM was added drop by drop until all ketimine was dissolved. Completion of the reaction was monitored with TLC and also with precipitation of product as a white solid while the reaction proceeds. After that, the mixture was purified by coloumn chromatography with 4:1 Hexane/EtOAc eluent and afforded the resulting product as described below.

#### 3.5.1 (*S*)-*tert*-Butyl (3-(2,4-dioxopentan-3-yl)-1-methyl-2-oxoindolin-3-yl)carbamate (**84a**)



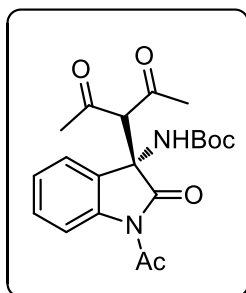
The use of (*E*)-*tert*-butyl (1-methyl-2-oxoindolin-3-ylidene)carbamate **76a** and acetylacetone **29** in general procedure afforded chiral adduct **84a** in 99% yield. mp 165–168 °C;  $[\alpha]_D^{34} = -12.0$  (*c* 1.00, CHCl<sub>3</sub>). Enantiomeric excess was determined as 99% ee by Chiralpak OD-H column (hexane/2-propanol = 80:20, 254 nm, 1 mL/min,  $t_{\text{major}} = 8.19$  min,  $t_{\text{minor}} = 6.88$  min). <sup>1</sup>H NMR (400 MHz, CDCl<sub>3</sub>) δ 7.33 – 7.20 (m, 2H), 6.95 (t, *J* = 11.0, 4.2 Hz, 1H), 6.76 (d, *J* = 7.8 Hz, 1H), 6.43 (s, 1H), 3.97 (s, 1H), 3.18 (s, 3H), 2.24 (s, 3H), 2.10 (s, 3H), 1.19 (s, 9H). <sup>13</sup>C NMR (100 MHz, CDCl<sub>3</sub>) δ 201.8, 201.4, 174.2, 153.8, 143.5, 129.7, 123.6, 123.5, 122.9, 108.5, 80.5, 68.6, 62.6, 32.3, 32.2, 28.1, 26.6. IR (neat): 3425, 3185, 2919, 2850, 1707, 1615, 1491, 1472, 1255, 1151, 755 cm<sup>-1</sup>.

### 3.5.2 (S)-tert-Butyl (3-(2,4-dioxopentan-3-yl)-2-oxoindolin-3-yl)carbamate (84b)



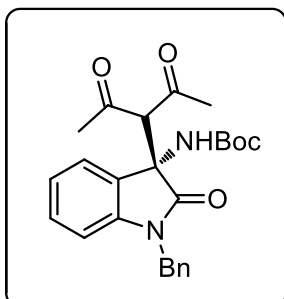
The use of (*E*)-*tert*-butyl (2-oxoindolin-3-ylidene)carbamate **76b** and acetylacetone **29** in general procedure afforded chiral adduct **84b** in 97% yield. mp 164-167 °C;  $[\alpha]_D^{20} = +6.0$  (*c* 0.90, CHCl<sub>3</sub>). Enantiomeric excess was determined as 98% ee by Chiralpak OD-H column (hexane/2-propanol = 80:20, 254 nm, 1 mL/min,  $t_{\text{major}} = 6.77$  min,  $t_{\text{minor}} = 9.24$  min). <sup>1</sup>H NMR (400 MHz, CDCl<sub>3</sub>) δ 7.98 (s, 1H), 7.19-7.10 (m, 2H), 6.92 (td, *J* = 7.6 Hz, 1H), 6.77 (d, *J* = 7.7 Hz, 1H), 6.64 (s, 1H), 4.02 (s, 1H), 2.26 (s, 3H), 2.10 (s, 3H), 1.24 (s, 9H). <sup>13</sup>C NMR (100 MHz, CDCl<sub>3</sub>) 200.3, 200.1, 174.5, 153.1, 139.7, 128.6, 127.6, 122.9, 121.8, 109.7, 79.7, 66.9, 62.2, 31.5, 31.4, 27.2. IR (neat): 3418, 2922, 1738, 1686, 1620, 1496, 1392, 1358, 1163, 753 cm<sup>-1</sup>

### 3.5.3 (S)-tert-Butyl (1-acetyl-3-(2,4-dioxopentan-3-yl)-2-oxoindolin-3-yl)carbamate (84c)



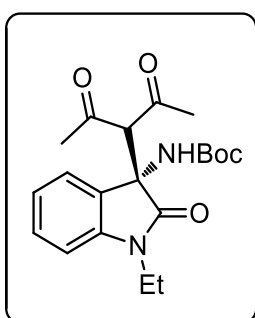
The use of (*E*)-*tert*-butyl (1-acetyl-2-oxoindolin-3-ylidene)carbamate **76c** and acetylacetone **29** in general procedure afforded chiral adduct **84c** in 29% yield. mp 145-147 °C;  $[\alpha]_D^{34} = -3.0$  (*c* 0.30, CHCl<sub>3</sub>). Enantiomeric excess was determined as 92% ee by Chiralpak OD-H column (hexane/2-propanol = 80:20, 254 nm, 0.7 mL/min,  $t_{\text{major}} = 8.44$  min,  $t_{\text{minor}} = 9.74$  min). <sup>1</sup>H NMR (400 MHz, CDCl<sub>3</sub>) δ 8.24 (d, *J* = 8.0 Hz, 1H), 7.41-7.32 (m, 1H), 7.30-7.22 (m, 1H), 7.22 – 7.12 (m, 1H), 6.65 (s, 1H), 4.07 (s, 1H), 2.71 (s, 3H), 2.24 (s, 3H), 2.18 (s, 3H), 1.34 (s, 9H). <sup>13</sup>C NMR (100 MHz, CDCl<sub>3</sub>) δ 201.7, 200.7, 174.9, 170.4, 153.7, 140.0, 129.9, 127.5, 125.3, 122.5, 116.7, 81.2, 69.8, 62.9, 31.9, 31.8, 29.6, 27.9, 26.4. IR (neat): 3417, 2918, 1760, 1704, 1607, 1467, 1335, 1270, 1160, 765 cm<sup>-1</sup>.

### 3.5.4 (S)-tert-Butyl (1-benzyl-3-(2,4-dioxopentan-3-yl)-2-oxoindolin-3-yl)carbamate (**84d**)



The use of (*E*)-tert-butyl (1-benzyl-2-oxoindolin-3-ylidene)carbamate **76d** and acetylacetone **29** in general procedure afforded chiral adduct **84d** in 96% yield. mp 144–147 °C;  $[\alpha]_D^{34} = -0.4$  (*c* 0.90, CHCl<sub>3</sub>). Enantiomeric excess was determined as 99% ee by Chiralpak OD-H column (hexane/2-propanol = 90:10, 254 nm, 1 mL/min,  $t_{\text{major}} = 10.05$  min,  $t_{\text{minor}} = 12.73$  min). <sup>1</sup>H NMR (400 MHz, CDCl<sub>3</sub>) δ 7.33 (d, *J* = 7.2 Hz, 2H), 7.28 (dd, *J* = 10.0, 4.7 Hz, 2H), 7.23 – 7.15 (m, 2H), 7.11 (td, *J* = 7.8, 1.1 Hz, 1H), 6.91 (td, *J* = 7.6, 0.8 Hz, 1H), 6.64 (d, *J* = 7.8 Hz, 1H), 6.51 (s, 1H), 4.97 (d, *J* = 15.5 Hz, 1H), 4.76 (s, 1H), 4.03 (s, 1H), 2.24 (s, 3H), 2.11 (s, 3H), 1.23 (s, 9H). <sup>13</sup>C NMR (100 MHz, CDCl<sub>3</sub>) δ 201.6, 201.3, 174.3, 153.9, 142.6, 135.6, 129.5, 128.8, 128.3, 127.7, 127.5, 123.7, 122.9, 109.5, 80.5, 68.7, 62.8, 44.4, 32.2, 32.1, 29.7, 28.2 IR (neat): 3378, 2919, 1729, 1706, 1616, 1497, 1357, 1275, 1249, 1163, 751 cm<sup>-1</sup>.

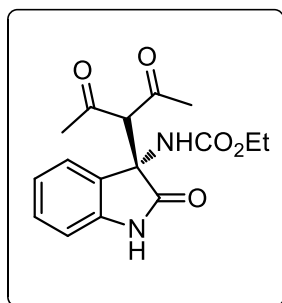
### 3.5.5 (S)-tert-Butyl (3-(2,4-dioxopentan-3-yl)-1-ethyl-2-oxoindolin-3-yl)carbamate (**84e**)



The use of (*E*)-tert-butyl (1-ethyl-2-oxoindolin-3-ylidene)carbamate **76e** and acetylacetone **29** in general procedure afforded chiral adduct **84e** in 42% yield. mp 102–102 °C;  $[\alpha]_D^{34} = -10.2$  (*c* 1.00, CHCl<sub>3</sub>). Enantiomeric excess was determined as 99% ee by Chiralpak OD-H column (hexane/2-propanol = 90:10, 254 nm, 1 mL/min,  $t_{\text{major}} = 29.92$  min,  $t_{\text{minor}} = 16.42$  min). <sup>1</sup>H NMR (400 MHz, CDCl<sub>3</sub>) δ 7.27–7.20 (m, 2H), 6.94 (t, *J* = 7.5 Hz, 1H), 6.77 (d, *J* = 7.7 Hz, 1H), 6.31 (s, 1H), 4.06 (s, 1H), 3.83 (dd, *J* = 14.1, 7.1 Hz, 1H), 3.60 (s, 1H), 2.19 (s, 3H), 2.12 (s, 3H), 1.25 – 1.20 (m, 9H). <sup>13</sup>C NMR (100 MHz, CDCl<sub>3</sub>) δ 201.7, 201.6, 173.8, 153.5, 142.1, 129.5, 128.5, 123.9,

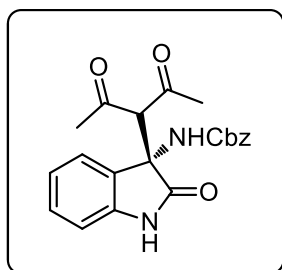
122.6, 108.6, 80.4, 68.6, 62.6, 35.1, 32.3, 32.1, 28.1, 12.3. IR (neat): 3276, 2920, 1712, 1697, 1590, 1370, 1286, 1151, 1084, 787, 684  $\text{cm}^{-1}$ .

**3.5.6 (S)-Ethyl (3-(2,4-dioxopentan-3-yl)-2-oxoindolin-3-yl)carbamate (84f)**



The use of (*E*)-ethyl (2-oxoindolin-3-ylidene)carbamate **76f** and acetylacetone **29** in general procedure afforded chiral adduct **84f** in 70% yield. mp 167-170 °C;  $[\alpha]_D^{34} = +11.0$  (*c* 0.90,  $\text{CHCl}_3$ ). Enantiomeric excess was determined as 96% ee by Chiralpak OD-H column (hexane/2-propanol = 90:10, 254 nm, 1 mL/min,  $t_{\text{major}} = 22.04$  min,  $t_{\text{minor}} = 18.84$  min).  $^1\text{H}$  NMR (400 MHz,  $\text{CDCl}_3$ )  $\delta$  7.95 (s, 1H), 7.14 (dd,  $J = 13.2, 7.6$  Hz, 2H), 6.92 (dd,  $J = 14.3, 6.5$  Hz, 2H), 6.79 (d,  $J = 7.8$  Hz, 1H), 4.01 (s, 1H), 3.98 – 3.83 (m, 2H), 2.28 (s, 3H), 2.10 (s, 3H), 1.10 (s, 3H).  $^{13}\text{C}$  NMR (100 MHz,  $\text{CDCl}_3$ )  $\delta$  199.3, 198.9, 173.5, 152.9, 138.7, 127.8, 126.3, 122.1, 121.0, 108.6, 66.0, 61.2, 59.5, 30.6, 30.4, 12.4. IR (neat): 3319, 2920, 1729, 1619, 1466, 1357, 1255, 1174, 1066, 753  $\text{cm}^{-1}$ . HRMS (ESI)  $m/z$ : calcd for  $\text{C}_{16}\text{H}_{18}\text{N}_2\text{NaO}_5$   $[\text{M}+\text{Na}]^+$ : 341.1113; found:341.1119.

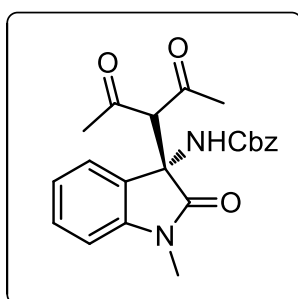
**3.5.7 (S)-Benzyl (3-(2,4-dioxopentan-3-yl)-2-oxoindolin-3-yl)carbamate (84g)**



The use of (*E*)-benzyl (2-oxoindolin-3-ylidene)carbamate **76g** and acetylacetone **29** in general procedure afforded chiral adduct **84g** in 72% yield. mp 154-157 °C;  $[\alpha]_D^{34} = +30.0$  (*c* 1.00,  $\text{CHCl}_3$ ). Enantiomeric excess was determined as 91% ee by Chiralpak OD-H column (hexane/2-propanol = 80:20, 254 nm, 1 mL/min,  $t_{\text{major}} = 22.94$  min,  $t_{\text{minor}} = 14.99$  min).  $^1\text{H}$  NMR (400 MHz,  $\text{CDCl}_3$ )  $\delta$  8.14 (s, 1H), 7.23 (s,

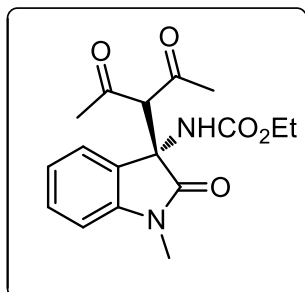
4H), 7.19 – 7.06 (m, 3H), 7.03 (s, 1H), 6.93 (td,  $J = 7.6, 0.9$  Hz, 1H), 6.73 (d,  $J = 7.6$  Hz, 1H), 4.91 (s, 2H), 4.03 (s, 1H), 2.27 (s, 3H), 2.08 (s, 3H).  $^{13}\text{C}$  NMR (100 MHz,  $\text{CDCl}_3$ )  $\delta$  201.1, 200.8, 175.4, 154.7, 140.7, 135.7, 129.9, 128.5, 128.1, 128.0, 124.2, 123.0, 110.8, 67.3, 63.3, 32.7, 32.5, 32.4, 29.7. IR (neat): 3393, 2922, 1707, 1618, 1496, 1350, 1259, 1060, 749, 696  $\text{cm}^{-1}$ . HRMS (ESI)  $m/z$ : calcd for  $\text{C}_{21}\text{H}_{20}\text{N}_2\text{NaO}_5$   $[\text{M}+\text{Na}]^+$ : 403.1270; found: 403.1294.

### 3.5.8 (S)-Benzyl (3-(2,4-dioxopent-3-yl)-1-methyl-2-oxindolin-3-yl)carbamate (**84i**)



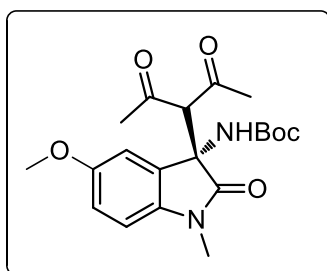
The use of (*E*)-benzyl (1-methyl-2-oxindolin-3-ylidene)carbamate **76i** and acetylacetone **29** in general procedure afforded chiral adduct **84i** in 88% yield. mp 127-129 °C;  $[\alpha]_D^{34} = +30.5$  ( $c$  0.90,  $\text{CHCl}_3$ ). Enantiomeric excess was determined as 97% ee by Chiralpak OD-H column (hexane/2-propanol = 80:20, 254 nm, 1 mL/min,  $t_{\text{major}} = 14.76$  min,  $t_{\text{minor}} = 13.09$  min).  $^1\text{H}$  NMR (400 MHz,  $\text{CDCl}_3$ )  $\delta$  7.38 – 7.07 (m, 6H), 6.96 (td,  $J = 7.6, 0.9$  Hz, 1H), 6.87 (s, 1H), 6.75 (s, 1H), 4.96 (s, 2H), 4.01 (s, 1H), 3.18 (s, 3H), 2.24 (s, 3H), 2.12 (s, 3H).  $^{13}\text{C}$  NMR (100 MHz,  $\text{CDCl}_3$ )  $\delta$  200.6, 200.1, 172.7, 153.5, 142.4, 134.6, 128.9, 127.5, 127.2, 127.1, 122.7, 122.1, 107.7, 67.3, 66.2, 61.8, 31.3, 31.2, 28.7. IR (neat): 3417, 2921, 2851, 1713, 1611, 1492, 1357, 1306, 1255, 1161, 753  $\text{cm}^{-1}$ .

### 3.5.9 (S)-Ethyl (3-(2,4-dioxopentan-3-yl)-1-methyl-2-oxoindolin-3-yl)carbamate (**84j**)



The use of (*E*)-ethyl (1-methyl-2-oxoindolin-3-ylidene)carbamate **76j** and acetylacetone **29** in general procedure afforded chiral adduct **84j** in 81% yield. mp 151-154 °C;  $[\alpha]_D^{34} = +17.0$  (*c* 0.80, CHCl<sub>3</sub>). Enantiomeric excess was determined as 98% ee by Chiralpak OD-H column (hexane/2-propanol = 70:30, 254 nm, 1 mL/min,  $t_{\text{major}} = 8.68$  min,  $t_{\text{minor}} = 6.44$  min). <sup>1</sup>H NMR (400 MHz, CDCl<sub>3</sub>) δ 7.25 (t, *J* = 7.7, 1H), 7.17 (d, *J* = 7.5 Hz, 1H), 6.96 (t, *J* = 7.6 Hz, 1H), 6.77 (d, *J* = 7.9 Hz, 2H), 3.97 (s, 1H), 3.95- 3.81 (m, 2H), 3.19 (s, 3H), 2.25 (s, 3H), 2.11 (s, 3H), 1.19 (s, 3H). <sup>13</sup>C NMR (100 MHz, CDCl<sub>3</sub>) δ 201.7, 201.2, 173.8, 154.7, 143.6, 129.9, 127.7, 123.7, 123.0, 108.6, 68.3, 62.7, 61.3, 32.3, 32.2, 26.7, 14.3. IR (neat): 3414, 2907, 1720, 1710, 1610, 1495, 1470, 1347, 1256, 755 cm<sup>-1</sup>.

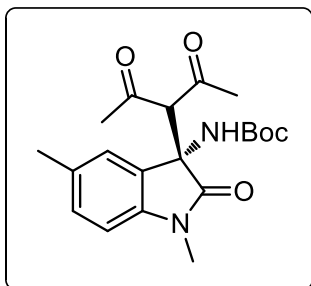
### 3.5.10 (S)-*tert*-Butyl (3-(2,4-dioxopentan-3-yl)-5-methoxy-1-methyl-2-oxoindolin-3-yl)carbamate (**84k**)



The use of (*E*)-*tert*-butyl (5-methoxy-1-methyl-2-oxoindolin-3-ylidene)carbamate **76k** and acetylacetone **29** in general procedure afforded chiral adduct **84k** in 92% yield. mp 147-150 °C;  $[\alpha]_D^{34} = -6.0$  (*c* 4.00, CHCl<sub>3</sub>). Enantiomeric excess was determined as >99% ee by Chiralpak AS-H column (hexane/2-propanol = 80:20, 254 nm, 1 mL/min,  $t_{\text{major}} = 7.39$  min,  $t_{\text{minor}} = 9.41$  min). <sup>1</sup>H NMR (400 MHz, CDCl<sub>3</sub>) δ 6.85 (d, *J* = 2.3 Hz, 1H), 6.76 (dd, *J* = 8.5, 2.5 Hz, 1H), 6.67 (d, *J* = 8.0 Hz, 1H), 6.41 (s, 1H), 4.02 (s, 1H), 3.69 (s, 3H), 3.15 (s, 3H), 2.25 (s, 3H), 2.11 (s, 3H), 1.20 (s, 9H). <sup>13</sup>C NMR (100 MHz, CDCl<sub>3</sub>) δ 201.62, 201.4, 173.7, 156.2, 153.8,

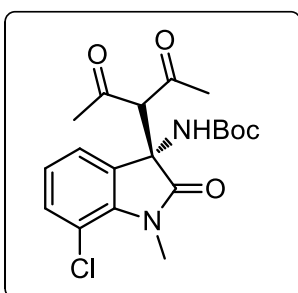
136.8, 129.5, 113.9, 111.2, 108.8, 80.4, 68.5, 62.9, 55.8, 32.2, 32.1, 28.1, 26.7. IR (neat): 3417, 2975, 1707, 1607, 1495, 1355, 1257, 1161, 1038, 756, 701  $\text{cm}^{-1}$ .

### 3.5.11 (*S*)-*tert*-Butyl (3-(2,4-dioxopentan-3-yl)-1,5-dimethyl-2-oxoindolin-3-yl)carbamate (**84l**)



The use of (*E*)-*tert*-butyl (1,5-dimethyl-2-oxoindolin-3-ylidene)carbamate **76l** and acetylacetone **29** in general procedure afforded chiral adduct **84l** in 89% yield. mp 148-151  $^{\circ}\text{C}$ ;  $[\alpha]_D^{34} = -20.0$  ( $c$  0.90,  $\text{CHCl}_3$ ). Enantiomeric excess was determined as 97% ee by Chiralpak OD-H column (hexane/2-propanol = 80:20, 254 nm, 1 mL/min,  $t_{\text{major}} = 7.93$  min,  $t_{\text{minor}} = 6.35$  min).  $^1\text{H}$  NMR (400 MHz,  $\text{CDCl}_3$ )  $\delta$  7.03 (d,  $J = 8.6$  Hz, 2H), 6.64 (d,  $J = 7.8$  Hz, 1H), 6.42 (s, 1H), 4.00 (s, 1H), 3.15 (s, 3H), 2.23 (s, 6H), 2.10 (s, 3H), 1.20 (s, 9H).  $^{13}\text{C}$  NMR (100 MHz,  $\text{CDCl}_3$ )  $\delta$  201.8, 201.4, 173.9, 153.8, 141.0, 132.5, 129.9, 128.3, 124.4, 108.3, 80.4, 68.6, 62.8, 32.2, 32.1, 28.1, 26.6, 21.1. IR (neat): 3413, 2923, 1704, 1607, 1494, 1348, 1255, 1160, 822, 636  $\text{cm}^{-1}$ .

### 3.5.12 (*S*)-*tert*-Butyl (7-chloro-3-(2,4-dioxopentan-3-yl)-1-methyl-2-oxoindolin-3-yl)carbamate (**84m**)

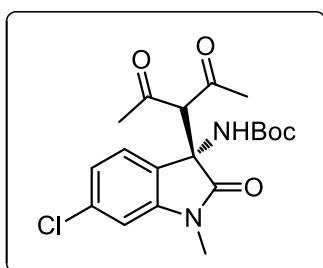


The use of (*E*)-*tert*-butyl (7-chloro-1-methyl-2-oxoindolin-3-ylidene)carbamate **76m** and acetylacetone **29** in general procedure afforded chiral adduct **84m** in 94% yield. mp 148-151  $^{\circ}\text{C}$ ;  $[\alpha]_D^{34} = +40.0$  ( $c$  0.90,  $\text{CHCl}_3$ ). Enantiomeric excess was determined as 97% ee by Chiralpak OD-H column (hexane/2-propanol = 90:10, 254 nm, 1 mL/min,  $t_{\text{major}} = 10.59$  min,  $t_{\text{minor}} = 9.38$  min).  $^1\text{H}$  NMR (400 MHz,  $\text{CDCl}_3$ )  $\delta$  7.16 (dd,  $J = 8.2, 0.9$  Hz, 1H), 7.11 – 7.04 (m, 1H), 6.86 (t,  $J = 7.8$  Hz, 1H), 6.49



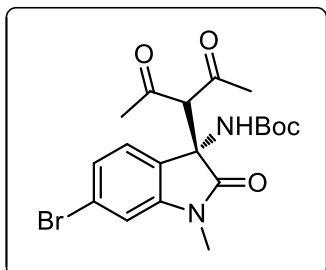
(s, 1H), 3.95 (s, 1H), 3.54 (s, 3H), 2.22 (s, 3H), 2.09 (s, 3H), 1.22 (s, 9H).  $^{13}\text{C}$  NMR (100 MHz,  $\text{CDCl}_3$ )  $\delta$  201.5, 200.9, 174.5, 153.7, 139.3, 131.9, 131.3, 123.6, 121.9, 116.0, 80.7, 68.3, 62.4, 32.3, 30.1, 28.1. IR (neat): 3412, 2921, 1704, 1607, 1463, 1360, 1255, 1113, 738, 705  $\text{cm}^{-1}$ . HRMS (ESI)  $m/z$ : calcd for  $\text{C}_{19}\text{H}_{23}\text{ClN}_2\text{NaO}_5$   $[\text{M}+\text{Na}]^+$ : 417.1193; found: 417.1230.

### 3.5.13 (S)-*tert*-Butyl (6-chloro-3-(2,4-dioxopentan-3-yl)-1-methyl-2-oxoindolin-3-yl)carbamate (**84n**)



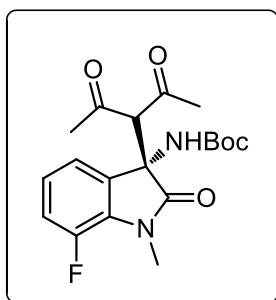
The use of (*E*)-*tert*-butyl (6-chloro-1-methyl-2-oxoindolin-3-ylidene)carbamate **76n** and acetylacetone **29** in general procedure afforded chiral adduct **84n** in 95% yield. mp 144-147 °C;  $[\alpha]_D^{34} = -61.0$  ( $c$  0.80,  $\text{CHCl}_3$ ). Enantiomeric excess was determined as 85% ee by Chiralpak OD-H column (hexane/2-propanol = 80:20, 254 nm, 1 mL/min,  $t_{\text{major}} = 9.99$  min,  $t_{\text{minor}} = 7.15$  min).  $^1\text{H}$  NMR (400 MHz,  $\text{CDCl}_3$ )  $\delta$  7.15 (d,  $J = 8.0$  Hz, 1H), 6.92 (dd,  $J = 8.0, 1.8$  Hz, 1H), 6.75 (d,  $J = 1.8$  Hz, 1H), 6.33 (s, 1H), 4.02 (s, 1H), 3.16 (s, 3H), 2.21 (s, 3H), 2.11 (s, 3H), 1.23 (s, 9H).  $^{13}\text{C}$  NMR (100 MHz,  $\text{CDCl}_3$ )  $\delta$  201.3, 201.2, 174.1, 153.8, 144.8, 135.5, 126.6, 124.8, 122.7, 109.3, 80.7, 68.5, 62.2, 32.3, 31.9, 28.1, 26.7. IR (neat): 3381, 3067, 2922, 1712, 1610, 1478, 1362, 1255, 1159, 734, 704  $\text{cm}^{-1}$ . HRMS (ESI)  $m/z$ : calcd for  $\text{C}_{19}\text{H}_{23}\text{ClN}_2\text{NaO}_5$   $[\text{M}+\text{Na}]^+$ : 417.1193; found: 417.1199.

### 3.5.14 (S)-tert-Butyl (6-bromo-3-(2,4-dioxopentan-3-yl)-1-methyl-2-oxoindolin-3-yl)carbamate (**84o**)



The use of (*E*)-*tert*-butyl (6-bromo-1-methyl-2-oxoindolin-3-ylidene)carbamate **76o** and acetylacetone **29** in general procedure afforded chiral adduct **84o** in 92% yield. mp 167-169 °C;  $[\alpha]_D^{34} = +38.0$  (*c* 0.60, CHCl<sub>3</sub>). Enantiomeric excess was determined as 90% ee by Chiralpak OD-H column (hexane/2-propanol = 80:20, 254 nm, 1 mL/min,  $t_{\text{major}} = 10.22$  min,  $t_{\text{minor}} = 7.23$  min). <sup>1</sup>H NMR (400 MHz, CDCl<sub>3</sub>) δ 7.11 – 7.03 (m, 2H), 6.90 (dd, *J* = 3.2, 2.3 Hz, 1H), 6.33 (s, 1H), 4.02 (s, 1H), 3.15 (s, 3H), 2.20 (s, 3H), 2.10 (s, 3H), 1.23 (s, 9H). <sup>13</sup>C NMR (100 MHz, CDCl<sub>3</sub>) δ 200.3, 200.2, 173.0, 152.8, 143.9, 126.2, 124.7, 124.2, 122.4, 111.1, 79.7, 67.4, 61.3, 31.3, 30.9, 27.1, 25.7. IR (neat): 3374, 2922, 1712, 1606, 1474, 1361, 1254, 1157, 730, 697 cm<sup>-1</sup>. HRMS (ESI) *m/z*: calcd for C<sub>19</sub>H<sub>23</sub>BrN<sub>2</sub>NaO<sub>5</sub> [M+Na]<sup>+</sup>: 461.0688; found: 461.0705.

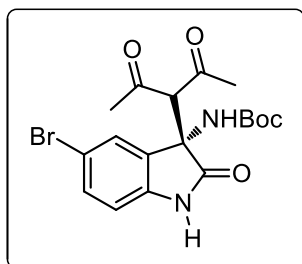
### 3.5.15 (S)-tert-Butyl (3-(2,4-dioxopentan-3-yl)-7-fluoro-1-methyl-2-oxoindolin-3-yl)carbamate (**84p**)



The use of (*E*)-*tert*-butyl (7-fluoro-1-methyl-2-oxoindolin-3-ylidene)carbamate **76p** and acetylacetone **29** in general procedure afforded chiral adduct **84p** in 96% yield. mp 153-156 °C;  $[\alpha]_D^{34} = +2.0$  (*c* 1.00, CHCl<sub>3</sub>). Enantiomeric excess was determined as 96% ee by Chiralpak AS-H column (hexane/2-propanol = 80:20, 254 nm, 1 mL/min,  $t_{\text{major}} = 5.76$  min,  $t_{\text{minor}} = 7.33$  min). <sup>1</sup>H NMR (400 MHz, CDCl<sub>3</sub>) δ 7.01 – 6.92 (m, *J* = 10.9, 9.3 Hz, 2H), 6.92 – 6.84 (m, 1H), 6.47 (s, 1H), 4.03 (s, 1H), 3.38 (d, *J* = 2.7 Hz, 3H), 2.22 (s, 3H), 2.11 (s, 3H), 1.21 (s, 9H). <sup>13</sup>C NMR (100 MHz, CDCl<sub>3</sub>) δ 201.5, 201.1, 173.8, 153.7, 147.9 (d, *J*<sub>C-F</sub> = 244.3 Hz) 131.1, 130.2, 123.6 (d, *J*<sub>C-F</sub> = 6.1 Hz), 119.4,

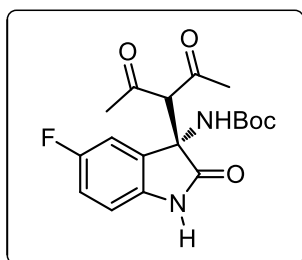
119.3, 117.8 (d,  $J_{C-F} = 19.2$  Hz), 80.7, 68.4, 62.7, 32.3, 32.2, 29.2, 29.1, 28.1. IR (neat): 3420, 2918, 1708, 1630, 1481, 1357, 1239, 1162, 777, 732  $\text{cm}^{-1}$ . HRMS (ESI)  $m/z$ : calcd for  $\text{C}_{19}\text{H}_{23}\text{FN}_2\text{NaO}_5$   $[\text{M}+\text{Na}]^+$ : 401.1489; found: 401.1519.

### 3.5.16 (S)-*tert*-Butyl (5-bromo-3-(2,4-dioxopentan-3-yl)-2-oxoindolin-3-yl)carbamate (**84q**)



The use of (*E*)-*tert*-butyl (5-bromo-2-oxoindolin-3-ylidene)carbamate **76q** and acetylacetone **29** in general procedure afforded chiral adduct **84q** in 88% yield. mp 195-197 °C;  $[\alpha]_D^{34} = -8.0$  ( $c$  0.60,  $\text{CHCl}_3$ ). Enantiomeric excess was determined as 41% ee by Chiralpak AD-H column (hexane/2-propanol = 90:10, 254 nm, 0.8 mL/min,  $t_{\text{major}} = 34.51$  min,  $t_{\text{minor}} = 28.12$  min).  $^1\text{H}$  NMR (400 MHz,  $\text{CDCl}_3$ )  $\delta$  8.49 (s, 1H), 7.31 – 7.23 (m, 2H), 6.64 (s, 1H), 6.62 (d,  $J = 8.2$  Hz, 1H), 4.01 (s, 1H), 2.27 (s, 3H), 2.11 (s, 3H), 1.28 (s, 9H).  $^{13}\text{C}$  NMR (100 MHz,  $\text{CDCl}_3$ )  $\delta$  198.7, 198.6, 173.2, 152.0, 137.7, 130.5, 128.7, 125.2, 113.4, 110.1, 79.0, 63.7, 60.9, 30.6, 30.1, 26.1. IR (neat): 3393, 2922, 1708, 1618, 1497, 1349, 1259, 1060, 749, 696  $\text{cm}^{-1}$ .

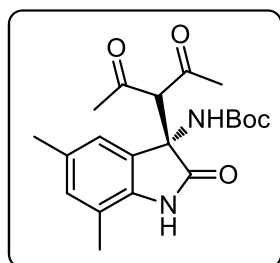
### 3.5.17 (S)-*tert*-Butyl (3-(2,4-dioxopentan-3-yl)-5-fluoro-2-oxoindolin-3-yl)carbamate (**84r**)



The use of (*E*)-*tert*-butyl (5-fluoro-2-oxoindolin-3-ylidene)carbamate **76r** and acetylacetone **29** in general procedure afforded chiral adduct **84r** in 98% yield. mp 149-152 °C;  $[\alpha]_D^{34} = +2.0$  ( $c$  0.90,  $\text{CHCl}_3$ ). Enantiomeric excess was determined as 88% ee by Chiralpak AS-H column (hexane/2-propanol = 90:10, 254 nm, 1 mL/min,  $t_{\text{major}} = 11.06$  min,  $t_{\text{minor}} = 6.67$  min).  $^1\text{H}$  NMR (400 MHz,  $\text{CDCl}_3$ )  $\delta$  8.05 (s, 1H), 6.94 (dd,  $J = 8.0, 2.5$  Hz, 1H), 6.86 (td,  $J = 8.8, 2.5$  Hz, 1H), 6.68 (dd,  $J = 8.5, 4.2$

Hz, 1H), 6.59 (s, 1H), 4.03 (s, 1H), 2.27 (s, 3H), 2.11 (d,  $J = 4.6$  Hz, 3H), 1.28 (s, 9H).  $^{13}\text{C}$  NMR (100 MHz,  $\text{CDCl}_3$ )  $\delta$  199.9, 199.7, 174.6, 158.1 (d,  $J_{\text{C-F}} = 241.7$  Hz), 153.1, 135.6, 135.5, 129.1, 129.0, 115.1 (d,  $J_{\text{C-F}} = 23.6$  Hz), 111.3 (d,  $J_{\text{C-F}} = 25.6$  Hz), 110.2 (d,  $J_{\text{C-F}} = 7.5$  Hz), 80.0, 66.9, 62.3, 31.6, 31.2, 27.2. IR (neat): 3424, 2921, 1729, 1617, 1488, 1369, 1257, 1158, 755  $\text{cm}^{-1}$ . HRMS (ESI)  $m/z$ : calcd for  $\text{C}_{18}\text{H}_{21}\text{FN}_2\text{NaO}_5$   $[\text{M}+\text{Na}]^+$ : 387.1332; found: 387.1351.

### 3.5.18 (S)-*tert*-Butyl (3-(2,4-dioxopentan-3-yl)-5,7-dimethyl-2-oxoindolin-3-yl)carbamate (**84s**)



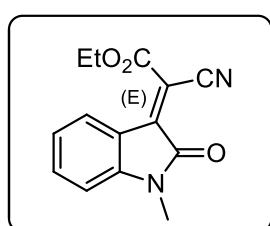
The use of (*E*)-*tert*-butyl (5,7-dimethyl-2-oxoindolin-3-ylidene)carbamate **76s** and acetylacetone **29** in general procedure afforded chiral adduct **84s** in 84% yield. mp 192–194 °C;  $[\alpha]_D^{34} = +38.0$  ( $c$  0.70,  $\text{CHCl}_3$ ). Enantiomeric excess was determined as 88% ee by Chiralpak OD-H column (hexane/2-propanol = 90:10, 254 nm, 1 mL/min,  $t_{\text{major}} = 10.45$  min,  $t_{\text{minor}} = 8.42$  min).  $^1\text{H}$  NMR (400 MHz,  $\text{CDCl}_3$ )  $\delta$  8.57 (s, 1H), 6.79 (s, 1H), 6.76 (s, 1H), 6.65 (s, 1H), 3.97 (s, 1H), 2.27 (s, 3H), 2.17 (s, 3H), 2.11 (s, 3H), 2.08 (s, 3H), 1.22 (s, 9H).  $^{13}\text{C}$  NMR (100 MHz,  $\text{CDCl}_3$ )  $\delta$  199.2, 198.6, 174.1, 151.6, 134.2, 129.9, 129.1, 119.4, 117.0, 78.2, 65.9, 61.3, 30.1, 30.0, 25.7, 18.7, 13.7. IR (neat): 3357, 2922, 1707, 1629, 1483, 1356, 1260, 1161, 861, 799  $\text{cm}^{-1}$ . HRMS (ESI)  $m/z$ : calcd for  $\text{C}_{20}\text{H}_{26}\text{N}_2\text{NaO}_5$   $[\text{M}+\text{Na}]^+$ : 397.1739; found: 397.1767.

## 3.6 General Procedure E: Synthesis of 2-cyano-2-oxoindoline-alkylidene acetates

According to literature procedure,<sup>73</sup> to the solution of isatins (**72**) (1 eq.) in dry ethanol (20.0 mL), ethylcyanoacetate **70** (1.1 eq.) and triethylamine (1eq.) were added. The reaction mixture was heated to 50°C nearly 2h. The completion of the

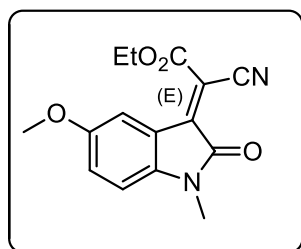
reaction was monitored by TLC and also precipitation of product while reaction proceeds. Upon the completion, the mixture was allowed to cool to the room temperature, crystalline products of **77** precipitated. The precipitated solids were filtered off and washed several times with cold ethanol to afford analytically pure compounds as described below.

### 3.6.1 2-cyano-2-(1-methyl-2-oxoindolin-3-ylidene)acetate (**77a**)



The use of 1-methylindoline-2,3-dione **73a** and ethyl cyanoacetate **70** in general procedure afforded **77a** in 98% isolated yield. mp 175-177 °C. <sup>1</sup>H NMR (400 MHz, CDCl<sub>3</sub>) δ 8.24 (d, *J* = 7.9 Hz, 1H), 7.40 (td, *J* = 7.8, 0.9 Hz, 1H), 6.98 (t, *J* = 7.8 Hz, 1H), 6.74 (d, *J* = 7.9 Hz, 1H), 4.38 (q, *J* = 7.1 Hz, 2H), 3.18 (s, 3H), 1.37 (t, *J* = 7.1 Hz, 3H). <sup>13</sup>C NMR (101 MHz, CDCl<sub>3</sub>) δ 164.3, 161.5, 146.6, 144.7, 135.7, 129.9, 123.1, 118.7, 114.0, 108.8, 106.4, 63.4, 26.3, 13.9. IR (neat): 3119, 3054, 2962, 2214, 1712, 1607, 1582, 1469 cm<sup>-1</sup>. HRMS (ESI) *m/z*: calcd for C<sub>14</sub>H<sub>13</sub>N<sub>2</sub>O<sub>3</sub> [M+H]<sup>+</sup>: 257.09207; found: 257.09252.

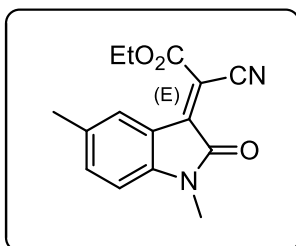
### 3.6.2 ethyl 2-cyano-2-(5-methoxy-1-methyl-2-oxoindolin-3-ylidene)acetate (**77b**)



The use of 5-methoxy-1-methylindoline-2,3-dione **88** and ethyl cyanoacetate **70** in general procedure afforded condensation adduct **77b** in 98% isolated yield. mp 165-167 °C. <sup>1</sup>H NMR (400 MHz, DMSO) δ 7.77 (s, 1H), 7.16 (d, *J* = 8.5, 2.6 Hz, 1H), 6.98 (d, *J* = 8.6 Hz, 1H), 4.42 (q, *J* = 14.1, 7.0 Hz, 2H), 3.74 (s, 3H), 3.12 (s, 3H), 1.34 (t, *J* = 7.1 Hz, 3H). <sup>13</sup>C NMR (101 MHz, DMSO) δ 163.6, 161.1, 154.8, 144.8, 140.5, 121.2, 118.6, 114.9, 114.0, 110.1, 105.3, 63.2, 55.6, 26.2, 13.7. IR (neat): 3121, 3059, 2962, 2212, 1704, 1612,

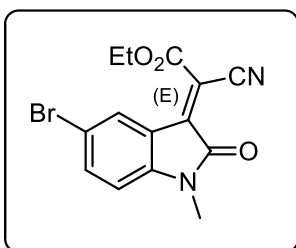
1576, 1465  $\text{cm}^{-1}$ . HRMS (ESI)  $m/z$ : calcd for  $\text{C}_{15}\text{H}_{15}\text{N}_2\text{O}_4$   $[\text{M}+\text{H}]^+$ : 287.10263; found: 287.10316.

### 3.6.3 ethyl 2-cyano-2-(1,5-dimethyl-2-oxoindolin-3-ylidene)acetate (77c)



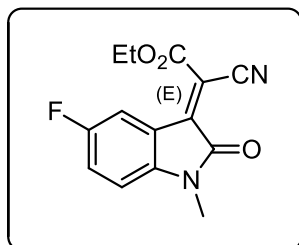
The use of 1,5-dimethylindoline-2,3-dione **89** and ethyl cyanoacetate **70** in general procedure afforded adduct **77c** in 89% isolated yield. mp 164-167  $^{\circ}\text{C}$ .  $^1\text{H}$  NMR (400 MHz,  $\text{CDCl}_3$ )  $\delta$  8.05 (s, 1H), 7.20 (d,  $J = 7.3$  Hz, 1H), 6.62 (d,  $J = 8.0$  Hz, 1H), 4.39 (q,  $J = 7.1$  Hz, 2H), 3.15 (s, 3H), 2.26 (s, 3H), 1.39 – 1.35 (m, 3H).  $^{13}\text{C}$  NMR (101 MHz,  $\text{CDCl}_3$ )  $\delta$  164.3, 161.6, 145.0, 144.4, 136.3, 132.7, 130.3, 118.7, 114.1, 108.5, 105.9, 63.3, 26.3, 21.1, 14.0. IR (neat): 3121, 3059, 2962, 2212, 1704, 1612, 1576, 1465  $\text{cm}^{-1}$ . HRMS (ESI)  $m/z$ : calcd for  $\text{C}_{15}\text{H}_{15}\text{N}_2\text{O}_3$   $[\text{M}+\text{H}]^+$ : 271.10772; found: 271.10831.

### 3.6.4 ethyl 2-(5-bromo-1-methyl-2-oxoindolin-3-ylidene)-2-cyanoacetate (77d)



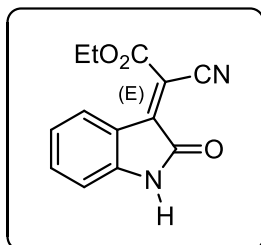
The use of 5-bromo-1-methylindoline-2,3-dione **90** and ethyl cyanoacetate **70** in general procedure afforded condensation adduct **77c** in 36% isolated yield. mp 183-185  $^{\circ}\text{C}$ .  $^1\text{H}$  NMR (400 MHz,  $\text{CDCl}_3$ )  $\delta$  8.44 (s, 1H), 7.52 (d,  $J = 8.4, 1.9$  Hz, 1H), 6.64 (d,  $J = 8.4$  Hz, 1H), 4.41 (q,  $J = 7.1$  Hz, 2H), 3.17 (s, 3H), 1.38 (t,  $J = 7.1$  Hz, 3H).  $^{13}\text{C}$  NMR (101 MHz,  $\text{CDCl}_3$ )  $\delta$  163.6, 161.1, 145.3, 143.5, 137.9, 132.6, 120.0, 115.6, 113.5, 110.0, 107.8, 63.6, 26.3, 13.8. IR (neat): 3133, 3063, 2989, 2215, 1727, 1605, 1580, 1462  $\text{cm}^{-1}$ . HRMS (ESI)  $m/z$ : calcd for  $\text{C}_{14}\text{H}_{11}\text{BrN}_2\text{NaO}_3$   $[\text{M}+\text{Na}]^+$ : 356.98453; found: 356.98418.

**3.6.5 ethyl 2-cyano-2-(5-fluoro-1-methyl-2-oxoindolin-3-ylidene)acetate (77e)**



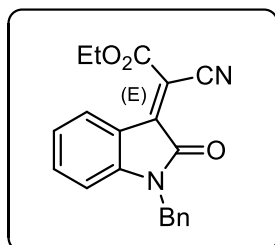
The use of 5-fluoro-1-methylindoline-2,3-dione **91** and ethyl cyanoacetate **70** in general procedure afforded condensation adduct **77e** in 37% isolated yield. mp 175-177 °C. <sup>1</sup>H NMR (400 MHz, CDCl<sub>3</sub>) δ 8.10 (dd, *J* = 9.4, 2.6 Hz, 1H), 7.14 (td, *J* = 8.5, 2.6 Hz, 1H), 6.68 (dd, *J* = 8.6, 4.2 Hz, 1H), 4.40 (q, *J* = 7.1 Hz, 2H), 3.17 (s, 3H), 1.38 (t, *J* = 7.1 Hz, 3H). <sup>13</sup>C NMR (101 MHz, CDCl<sub>3</sub>) δ 163.9, 161.1, 159.8, 157.4, 144.3, 142.7, 121.9 (d, *J*<sub>C-F</sub> = 24.3 Hz), 119.3 (d, *J*<sub>C-F</sub> = 9.5 Hz), 117.4 (d, *J*<sub>C-F</sub> = 27.6 Hz), 113.5, 109.1, 63.5, 26.3, 13.8. IR (neat): 3309, 2586, 2218, 2204, 1705, 1584, 1469 cm<sup>-1</sup>. HRMS (ESI) *m/z*: calcd for C<sub>14</sub>H<sub>11</sub>FN<sub>2</sub>NaO<sub>3</sub> [M+Na]<sup>+</sup>: 297.06459; found: 297.06511.

**3.6.6 2-cyano-2-(2-oxoindolin-3-ylidene) acetate (77g)**



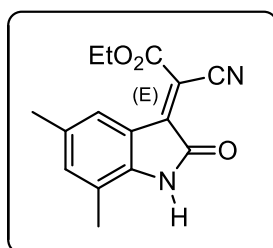
The use of isatin **72** and ethyl cyanoacetate **70** in general procedure afforded condensation adduct **77g** in 75% isolated yield. mp 188-190 °C. <sup>1</sup>H NMR (400 MHz, DMSO) δ 11.08 (s, 1H), 8.09 (d, *J* = 7.8 Hz, 1H), 7.51 – 7.39 (m, 1H), 7.05 – 6.94 (m, 1H), 6.90 – 6.78 (m, 1H), 4.40 (q, *J* = 10.1, 5.1 Hz, 2H), 1.33 (t, *J* = 14.2, 7.0 Hz, 3H). <sup>13</sup>C NMR (101 MHz, DMSO) δ 165.1, 161.3, 145.8, 145.3, 135.9, 129.2, 122.1, 118.7, 114.1, 110.8, 104.4, 63.1, 13.7. IR (neat): 3366, 3242, 2986, 2215, 1717, 1615, 1580, 1461 cm<sup>-1</sup>. HRMS (ESI) *m/z*: calcd for C<sub>13</sub>H<sub>10</sub>N<sub>2</sub>NaO<sub>3</sub> [M+Na]<sup>+</sup>: 265.05836; found: 265.05909.

### 3.6.7 ethyl 2-(1-benzyl-2-oxoindolin-3-ylidene)-2-cyanoacetate (**77h**)



The use of 1-benzylindoline-2,3-dione **73c** and ethyl cyanoacetate **70** in general procedure afforded condensation adduct **77h** in 82% isolated yield. mp 160-162 °C. <sup>1</sup>H NMR (400 MHz, DMSO) δ 8.17 (d, *J* = 7.5 Hz, 1H), 7.52 – 7.45 (m, 1H), 7.41 – 7.31 (m, 5H), 7.13 – 7.02 (m, 1H), 6.99 (d, *J* = 7.9 Hz, 1H), 4.95 (s, 2H), 4.44 (q, *J* = 7.0 Hz, 2H), 1.34 (t, 3H). <sup>13</sup>C NMR (101 MHz, DMSO) δ 164.0, 161.1, 145.5, 135.7, 135.5, 129.0, 128.7, 128.7, 127.6, 127.2, 122.8, 118.3, 114.1, 110.6, 110.2, 105.5, 63.2, 42.9, 13.7. IR (neat): 3673, 3065, 2982, 2215, 1719, 1610, 1585, 1468 cm<sup>-1</sup>. HRMS (ESI) *m/z*: calcd for C<sub>20</sub>H<sub>16</sub>N<sub>2</sub>NaO<sub>3</sub> [M+Na]<sup>+</sup>: 355.10531; found: 355.10597.

### 3.6.8 ethyl 2-cyano-2-(5,7-dimethyl-2-oxoindolin-3-ylidene)acetate (**77i**)



The use of 5,7-dimethylindoline-2,3-dione **93** and ethyl cyanoacetate **70** in general procedure afforded condensation adduct **77i** in 69% isolated yield. mp 223-225 °C. <sup>1</sup>H NMR (400 MHz, DMSO) δ 10.98 (s, 1H), 7.72 (s, 1H), 7.10 (s, 1H), 4.41 (q, 2H), 2.19 (s, 3H), 2.13 (s, 3H), 1.34 (t, *J* = 11.5, 4.4 Hz, 3H). <sup>13</sup>C NMR (101 MHz, DMSO) δ 165.6, 161.4, 145.6, 142.2, 137.8, 130.7, 126.6, 119.9, 118.4, 114.3, 103.8, 63.0, 20.5, 16.0, 13.7. IR (neat): 3278, 2981, 2210, 1711, 1625, 1571, 1474, cm<sup>-1</sup>. HRMS (ESI) *m/z*: calcd for C<sub>15</sub>H<sub>15</sub>N<sub>2</sub>O<sub>3</sub> [M+H]<sup>+</sup>: 271.10772; found: 271.10829.



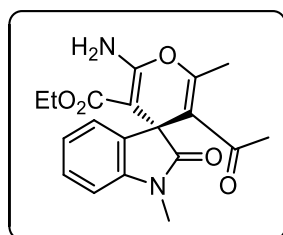
### 3.7 General Procedure F: Racemic Synthesis of Michael Addition/Cyclization Adducts Spiro Conjugated Amino-pyran-oxindoles

To a solution of corresponding 2-cyano-2-oxoindolin-3-ylidene)acetate **77** (1eq.) and corresponding 1,3-dicarbonyl compounds (2 eq.) in DCM (1mL), triethylamine (0.2 mL) was added at room temperature. Reaction was monitored by TLC and being colored by *p*-anisaldehyde stain. Products on TLC plate were observed as white spots and according to TLC monitoring purification was done by column chromatography on silica gel as described for asymmetric synthesis.

### 3.8 General Procedure G: Asymmetric Synthesis of Michael Addition/Cyclization Adducts Spiro Conjugated Amino-pyran-oxindoles

In a 5-mL vial, 2-Adamantyl squaramide catalyst **80** (20 mol%), corresponding 2-cyano-2-oxoindolin-3-ylidene)acetate **77** (0.05 mmol) and crushed 4Å molecular sieves were placed. After injection of dry toluene solvent (~0.5 mL), corresponding 1,3 dicarbonyl compound (0.1 mmol) was added at room temperature. The reaction mixture was stirred at 22°C for 48h and monitored with TLC. After 48h, purification was done by column chromatography on silica gel with 4:1 Hexane/EtOAc eluent then 40:1 (DCM:MeOH) to give the desired product as described below.

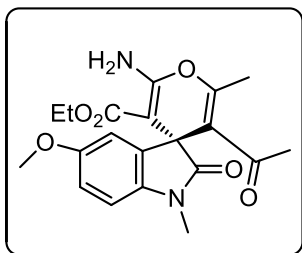
#### 3.8.1 (*S*)-ethyl 3'-acetyl-6'-amino-1,2'-dimethyl-2-oxospiro[indoline-3,4'-pyran]-5'-carboxylate (**87a**)



The use of 2-cyano-2-(1-methyl-2-oxoindolin-3-ylidene)acetate **77a** and acetylacetone **29** in general procedure afforded chiral adduct **87a** in 77% isolated yield. mp 215-217 °C;  $[\alpha]_D^{32} = -19$  (*c* 0.8, CHCl<sub>3</sub>).

Enantiomeric excess was determined as 89% ee by Chiralpak AD-H column (hexane/2-propanol = 80:20, 254 nm, 1 mL/min,  $t_{\text{major}} = 25.588$  min,  $t_{\text{minor}} = 15.020$  min).  $^1\text{H}$  NMR (400 MHz, DMSO)  $\delta$  7.80 (s,  $J = 20.1$  Hz, 2H), 7.21 (td,  $J = 7.7$ , 1.2 Hz, 1H), 7.05 (d,  $J = 6.5$  Hz, 1H), 6.94 (t,  $J = 7.4$  Hz, 1H), 6.86 (d,  $J = 7.7$  Hz, 1H), 3.69 – 3.54 (m, 2H), 3.07 (s,  $J = 10.5$  Hz, 3H), 2.05 (s, 3H), 1.88 (s, 3H), 0.64 (t,  $J = 7.1$  Hz, 3H).  $^{13}\text{C}$  NMR (101 MHz, DMSO)  $\delta$  199.5, 177.7, 167.3, 160.1, 148.4, 144.1, 134.5, 127.92, 122.8, 121.8, 116.3, 107.4, 74.3, 58.5, 48.9, 31.7, 26.1, 17.9, 13.4. IR (neat): 3352, 3260, 3202, 2923, 1689, 1626, 1607  $\text{cm}^{-1}$ . HRMS (ESI)  $m/z$ : calcd for  $\text{C}_{19}\text{H}_{21}\text{N}_2\text{O}_5$   $[\text{M}+\text{H}]^+$ : 357.1445; found: 357.14506.

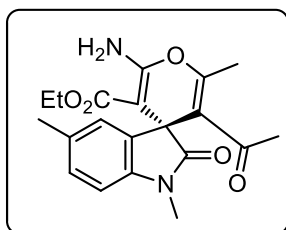
### 3.8.2 (S)-ethyl 3'-acetyl-6'-amino-5-methoxy-1,2'-dimethyl-2-oxospiro[indoline-3,4'-pyran]-5'-carboxylate (**87b**)



The use of ethyl 2-cyano-2-(5-methoxy-1-methyl-2-oxoindolin-3-ylidene)acetate **77b** and acetylacetone **29** in general procedure afforded chiral adduct **87b** in 31% isolated yield. mp 221-223 °C;  $[\alpha]_D^{33} = -221.6$  ( $c$  0.025,  $\text{CHCl}_3$ ). Enantiomeric excess was determined as 60% ee

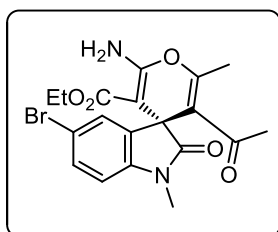
by Chiralpak AD-H column (hexane/2-propanol = 70:30, 254 nm, 1 mL/min,  $t_{\text{major}} = 20.127$  min,  $t_{\text{minor}} = 13.560$  min).  $^1\text{H}$  NMR (400 MHz, DMSO)  $\delta$  7.80 (s, 2H), 6.82 – 6.73 (m, 2H), 6.67 (s, 1H), 3.67 (s, 3H), 3.66 – 3.55 (m, 2H), 3.04 (s, 3H), 2.04 (s, 3H), 1.89 (s, 3H), 0.67 (t,  $J = 7.1$  Hz, 3H).  $^{13}\text{C}$  NMR (101 MHz, DMSO)  $\delta$  199.5, 177.4, 167.3, 160.0, 155.2, 148.2, 137.6, 135.8, 116.3, 112.2, 110.2, 107.8, 74.3, 58.5, 55.4, 49.4, 31.7, 26.2, 17.9, 13.4. IR (neat): 3347, 3261, 3201, 2987, 2925, 1688, 1628, 1600  $\text{cm}^{-1}$ . HRMS (ESI)  $m/z$ : calcd for  $\text{C}_{20}\text{H}_{23}\text{N}_2\text{O}_6$   $[\text{M}+\text{H}]^+$ : 387.15506; found: 387.15581.

### 3.8.3 (S)-ethyl 3'-acetyl-6'-amino-1,2',5-trimethyl-2-oxospiro[indoline-3,4'-pyran]-5'-carboxylate (**87c**)



The use of ethyl 2-cyano-2-(1,5-dimethyl-2-oxoindolin-3-ylidene)acetate **77c** and acetylacetone **29** in general procedure afforded chiral adduct **87c** in 35% isolated yield. mp 221-223 °C;  $[\alpha]_D^{33} = -93.3$  (*c* 0.06, CHCl<sub>3</sub>). Enantiomeric excess was determined as 52% ee by Chiralpak AD-H column (hexane/2-propanol = 80:20, 254 nm, 1 mL/min,  $t_{\text{major}} = 21.845$  min,  $t_{\text{minor}} = 14.585$  min). <sup>1</sup>H NMR (400 MHz, DMSO) δ 7.76 (s, 2H), 7.01 (d, *J* = 7.8 Hz, 1H), 6.87 (s, 1H), 6.75 (d, *J* = 7.8 Hz, 1H), 3.72 – 3.51 (m, 2H), 3.07 (s, 3H), 2.23 (s, 3H), 2.04 (s, 3H), 1.90 (s, 3H), 0.67 (t, *J* = 7.1 Hz, 3H). <sup>13</sup>C NMR (101 MHz, DMSO) δ 199.4, 177.4, 167.3, 160.0, 148.0, 141.7, 134.5, 130.7, 128.1, 123.6, 116.6, 107.2, 74.2, 58.5, 48.9, 31.7, 26.1, 20.6, 17.9, 13.5. IR (neat): 3361, 3270, 3198, 2918, 2851, 1681, 1621, 1602 cm<sup>-1</sup>. HRMS (ESI) *m/z*: calcd for C<sub>20</sub>H<sub>23</sub>N<sub>2</sub>O<sub>5</sub> [M+H]<sup>+</sup>: 371.16015; found: 371.16116.

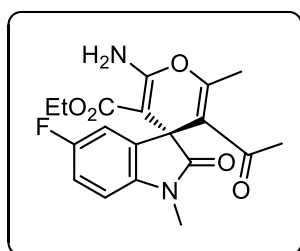
### 3.8.4 (S)-ethyl 3'-acetyl-6'-amino-5-bromo-1,2'-dimethyl-2-oxospiro[indoline-3,4'-pyran]-5'-carboxylate (**87d**)



The use of ethyl 2-(5-bromo-1-methyl-2-oxoindolin-3-ylidene)-2-cyanoacetate **77d** and acetylacetone **29** in general procedure afforded chiral adduct **87d** in 19% isolated yield. mp 253-255 °C;  $[\alpha]_D^{34} = -36.5$  (*c* 0.16, CHCl<sub>3</sub>). Enantiomeric excess was determined as 79% ee by Chiralpak AD-H column (hexane/2-propanol = 90:10, 254 nm, 0.75 mL/min,  $t_{\text{major}} = 56.43$  min,  $t_{\text{minor}} = 49.91$  min). <sup>1</sup>H NMR (400 MHz, DMSO) δ 7.86 (s, 2H), 7.39 (dd, *J* = 8.2, 1.8 Hz, 1H), 7.19 (s, 1H), 6.85 (d, *J* = 8.2 Hz, 1H), 3.66 (dt, *J* = 7.0, 3.9 Hz, 2H), 3.07 (s, 3H), 2.12 (s, 3H), 1.99 (s, 3H), 0.70 (t, *J* = 7.1 Hz, 3H). <sup>13</sup>C NMR (101 MHz, DMSO) δ 199.5, 177.9, 167.4, 160.4, 150.8, 143.9, 137.6, 130.9, 125.9,

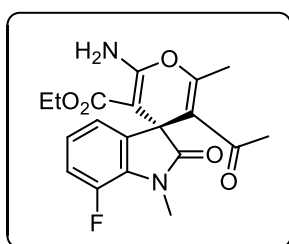
116.2, 113.7, 109.7, 74.4, 59.0, 49.4, 32.2, 26.6, 18.8, 13.8. IR (neat): 3356, 3264, 3198, 3130, 2921, 1732, 1702, 1684, 1603  $\text{cm}^{-1}$ . HRMS (ESI)  $m/z$ : calcd for  $\text{C}_{19}\text{H}_{20}\text{BrN}_2\text{O}_5$   $[\text{M}+\text{H}]^+$ : 435.05501; found: 435.05566.

### 3.8.5 (S)-ethyl 3'-acetyl-6'-amino-5-fluoro-1,2'-dimethyl-2-oxospiro[indoline-3,4'-pyran]-5'-carboxylate (**87e**)



The use of ethyl 2-cyano-2-(5-fluoro-1-methyl-2-oxoindolin-3-ylidene) acetate **77e** and acetylacetone **29** in general procedure afforded chiral adduct **87e** in 29% isolated yield. mp 214-216  $^{\circ}\text{C}$ ;  $[\alpha]_D^{32} = -14.1$  ( $c$  0.28,  $\text{CHCl}_3$ ). Enantiomeric excess was determined as 16% ee by Chiralpak AD-H column (hexane/2-propanol = 80:20, 254 nm, 1 mL/min,  $t_{\text{major}} = 15.68$  min,  $t_{\text{minor}} = 13.39$  min).  $^1\text{H}$  NMR (400 MHz, DMSO)  $\delta$  7.92 (s, 2H), 7.14 – 7.06 (m, 1H), 7.04 (dd,  $J = 8.0, 2.6$  Hz, 1H), 6.93 (dd,  $J = 8.5, 4.2$  Hz, 1H), 3.75 – 3.65 (m, 2H), 3.13 (s, 3H), 2.14 (s,  $J = 14.2$  Hz, 3H), 2.02 (s, 3H), 0.73 (t,  $J = 7.1$  Hz, 3H).  $^{13}\text{C}$  NMR (101 MHz, DMSO)  $\delta$  199.7, 178.1, 167.5, 160.4, 149.7, 140.8, 136.8 (d,  $J_{\text{C-F}} = 7.3$  Hz), 131.9 (d,  $J_{\text{C-F}} = 12.8$  Hz), 116.3, 114.2 (d,  $J_{\text{C-F}} = 23.1$  Hz), 111.1 (d,  $J_{\text{C-F}} = 24.6$  Hz), 108.4 (d,  $J_{\text{C-F}} = 7.9$  Hz), 74.4, 58.9, 49.7, 32.1, 26.7, 18.5, 13.8. IR (neat): 3743, 3362, 3262, 3199, 2919, 1705, 1681, 1622  $\text{cm}^{-1}$ . HRMS (ESI)  $m/z$ : calcd for  $\text{C}_{19}\text{H}_{20}\text{FN}_2\text{O}_5$   $[\text{M}+\text{H}]^+$ : 375.13508; found: 375.13608.

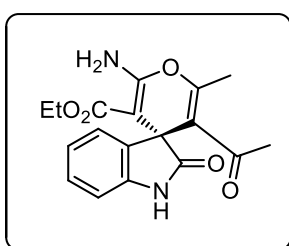
### 3.8.6 (S)-ethyl 3'-acetyl-6'-amino-7-fluoro-1,2'-dimethyl-2-oxospiro[indoline-3,4'-pyran]-5'-carboxylate (**87f**)



The use of ethyl 2-cyano-2-(7-fluoro-1-methyl-2-oxoindolin-3-ylidene)acetate **77f** and acetylacetone **29** in general procedure afforded chiral adduct **87f** in 41% isolated yield. mp 204-207  $^{\circ}\text{C}$ ;  $[\alpha]_D^{34} = -35.6$  ( $c$  0.09,  $\text{CHCl}_3$ ). Enantiomeric excess was determined as 53% ee

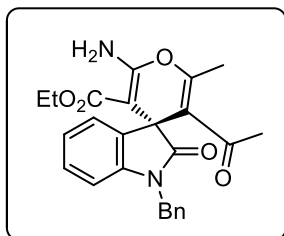
by Chiralpak AD-H column (hexane/2-propanol = 80:20, 254 nm, 1 mL/min,  $t_{\text{major}} = 11.38$  min,  $t_{\text{minor}} = 15.71$  min).  $^1\text{H}$  NMR (400 MHz,  $\text{CDCl}_3$ )  $\delta$  6.98 – 6.68 (m, 2H), 6.49 (s, 1H), 3.74 (q,  $J = 7.1$  Hz, 1H), 3.37 (d,  $J = 2.5$  Hz, 2H), 2.01 (s,  $J = 13.5$  Hz, 2H), 1.95 (s, 2H), 0.78 (t,  $J = 7.1$  Hz, 2H).  $^{13}\text{C}$  NMR (101 MHz,  $\text{CDCl}_3$ )  $\delta$  197.6, 176.7, 166.0, 157.8, 147.5, 146.7, 144.3, 135.8 (d,  $J_{\text{C-F}} = 2.9$  Hz), 129.0 (d,  $J_{\text{C-F}} = 8.3$  Hz), 120.9 (d,  $J_{\text{C-F}} = 6.3$  Hz), 117.4 (d,  $J_{\text{C-F}} = 2.9$  Hz), 115.1, 114.3 (d,  $J_{\text{C-F}} = 19.6$  Hz), 57.7, 48.1, 30.1, 27.2, 16.7, 11.7. IR (neat): 3851, 3732, 3646, 2945, 1710, 1627, 1595  $\text{cm}^{-1}$ . HRMS (ESI)  $m/z$ : calcd for  $\text{C}_{19}\text{H}_{20}\text{FN}_2\text{O}_5$   $[\text{M}+\text{H}]^+$ : 375.13508; found: 375.13496.

### 3.8.7 (S)-ethyl 3'-acetyl-6'-amino-2'-methyl-2-oxospiro[indoline-3,4'-pyran]-5'-carboxylate (**87g**)



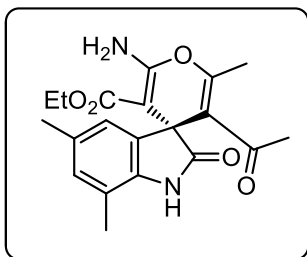
The use of 2-cyano-2-(2-oxoindolin-3-ylidene)acetate **77g** and acetylacetone **29** in general procedure afforded chiral adduct **87g** in 17% isolated yield. mp 212-214 °C;  $[\alpha]_D^{33} = -10.0$  ( $c$  0.31,  $\text{CHCl}_3$ ). Enantiomeric excess was determined as 10% ee by Chiralpak IA column (hexane/2-propanol = 80:20, 254 nm, 1 mL/min,  $t_{\text{major}} = 16.02$  min,  $t_{\text{minor}} = 51.95$  min).  $^1\text{H}$  NMR (400 MHz, DMSO)  $\delta$  10.22 (s, 1H), 7.76 (s, 2H), 7.10 (dd,  $J = 11.0, 4.2$  Hz, 1H), 7.00 (d,  $J = 7.2$  Hz, 1H), 6.86 (t,  $J = 7.4$  Hz, 1H), 6.68 (d,  $J = 7.6$  Hz, 1H), 3.76 – 3.53 (m, 2H), 1.99 (s,  $J = 19.4$  Hz, 3H), 1.88 (s,  $J = 9.4$  Hz, 3H), 0.69 (t,  $J = 7.1$  Hz, 3H).  $^{13}\text{C}$  NMR (101 MHz, DMSO)  $\delta$  199.8, 179.4, 167.4, 160.1, 147.0, 142.6, 135.3, 127.7, 123.2, 121.1, 116.5, 108.7, 74.4, 58.6, 49.5, 40.1, 39.8, 39.6, 39.4, 39.2, 39.0, 38.8, 31.8, 17.7, 13.1. IR (neat): 3374, 3177, 3075, 2979, 2924, 1729, 1691, 1614  $\text{cm}^{-1}$ . HRMS (ESI)  $m/z$ : calcd for  $\text{C}_{18}\text{H}_{19}\text{N}_2\text{O}_5$   $[\text{M}+\text{H}]^+$ : 343.12885; found: 343.12896.

### 3.8.8 (S)-ethyl 3'-acetyl-6'-amino-1-benzyl-2'-methyl-2-oxospiro[indoline-3,4'-pyran]-5'-carboxylate



The use of ethyl 2-(1-benzyl-2-oxoindolin-3-ylidene)-2-cyanoacetate **77h** and acetylacetone **29** in general procedure afforded chiral adduct **87h** in 15% isolated yield. mp 220-222 °C;  $[\alpha]_D^{31} = -19.8$  (*c* 0.28, CHCl<sub>3</sub>). Enantiomeric excess was determined as 62% ee by Chiralpak AD-H column (hexane/2-propanol = 80:20, 254 nm, 1 mL/min,  $t_{\text{major}} = 28.01$  min,  $t_{\text{minor}} = 18.58$  min. <sup>1</sup>H NMR (400 MHz, DMSO) δ 7.62 (s, 2H), 7.26 (d, *J* = 7.4 Hz, 2H), 7.07 (dt, *J* = 28.4, 7.2 Hz, 3H), 6.93 – 6.80 (m, 2H), 6.69 (t, *J* = 7.4 Hz, 1H), 6.54 (d, *J* = 7.7 Hz, 1H), 4.63 (d, *J* = 15.5 Hz, 1H), 4.50 (d, *J* = 15.5 Hz, 1H), 3.13 – 3.04 (m, 2H), 1.82 (s, 3H), 1.63 (s, 3H), 0.16 (t, *J* = 7.1 Hz, 3H). <sup>13</sup>C NMR (101 MHz, DMSO) δ 199.8, 177.9, 167.3, 160.2, 147.9, 143.5, 136.7, 134.6, 128.3, 127.9, 127.8, 127.2, 122.9, 121.9, 116.1, 108.1, 74.4, 58.3, 48.9, 43.8, 31.9, 17.9, 13.3. IR (neat): 3615, 3261, 3191, 2979, 2924, 1688, 1667, 1607 cm<sup>-1</sup>. HRMS (ESI) *m/z*: calcd for C<sub>25</sub>H<sub>25</sub>N<sub>2</sub>O<sub>5</sub> [M+H]<sup>+</sup>: 433.1758; found: 433.17601.

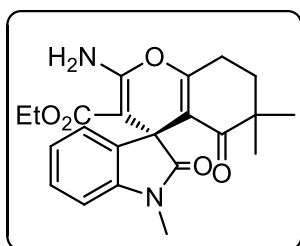
### 3.8.9 (S)-ethyl 3'-acetyl-6'-amino-2',5,7-trimethyl-2-oxospiro[indoline-3,4'-pyran]-5'-carboxylate (**87i**)



The use of ethyl 2-cyano-2-(5,7-dimethyl-2-oxoindolin-3-ylidene)acetate **77i** and acetylacetone **29** in general procedure afforded chiral adduct **87i** in 36% isolated yield. mp 245-247 °C;  $[\alpha]_D^{34} = -54.2$  (*c* 0.44, CHCl<sub>3</sub>). Enantiomeric excess was determined as 99% ee by Chiralpak IA column (hexane/2-propanol = 80:20, 254 nm, 1 mL/min,  $t_{\text{major}} = 10.49$  min,  $t_{\text{minor}} = 25.02$  min. <sup>1</sup>H NMR (400 MHz, DMSO) δ 10.18 (s, 1H), 7.71 (s, 2H), 6.73 (s, 1H), 6.63 (s, 1H), 3.64 (q, *J* = 6.9 Hz, 2H), 2.15 (s, 3H), 2.07 (s, 3H), 1.98 (s, 3H), 1.91 (s, 3H), 0.71 (t, *J* = 7.1 Hz, 3H). <sup>13</sup>C NMR

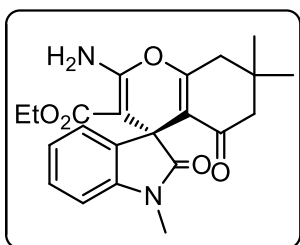
(101 MHz, DMSO)  $\delta$  199.7, 179.8, 167.5, 159.9, 146.8, 138.7, 134.9, 129.7, 129.4, 121.3, 117.4, 116.7, 74.7, 58.6, 49.8, 31.9, 20.5, 17.7, 16.1, 12.8. IR (neat): 3635, 3382, 3181, 2975, 2923, 1680, 1608  $\text{cm}^{-1}$ . HRMS (ESI)  $m/z$ : calcd for  $\text{C}_{20}\text{H}_{23}\text{N}_2\text{O}_5$   $[\text{M}+\text{H}]^+$ : 371.16015; found: 371.15933.

**3.8.10 (S)-ethyl 2-amino-1',6,6-trimethyl-2',5-dioxo-5,6,7,8-tetrahydrospiro[chromene-4,3'-indoline]-3-carboxylate (87j)**



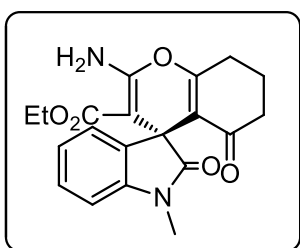
The use of 2-cyano-2-(1-methyl-2-oxoindolin-3-ylidene)acetate **77a** and 4,4-Dimethyl-1,3-Cyclohexanedione in general procedure afforded chiral adduct **87j** in 76% isolated yield. mp 212-214  $^{\circ}\text{C}$ ;  $[\alpha]_D^{34} = -21.3$  ( $c$  0.17,  $\text{CHCl}_3$ ). Enantiomeric excess was determined as 3% ee by Chiralpak AD-H column (hexane/2-propanol = 80:20, 254 nm, 1 mL/min,  $t_{\text{major}} = 8.96$  min,  $t_{\text{minor}} = 26.81$  min).  $^1\text{H}$  NMR (400 MHz, DMSO)  $\delta$  7.93 (s, 2H), 7.14 (t,  $J = 7.5$  Hz, 1H), 6.92 (d,  $J = 7.2$  Hz, 1H), 6.83 (t,  $J = 6.8$  Hz, 2H), 3.73 – 3.55 (m, 2H), 3.11 (s, 3H), 2.80 – 2.66 (m, 1H), 2.61 (dt,  $J = 11.8, 5.7$  Hz, 1H), 1.30 (t,  $J = 7.6$  Hz, 1H), 1.17 (t,  $J = 7.1$  Hz, 1H), 0.88 (s, 3H), 0.79 (s,  $J = 14.5$  Hz, 3H), 0.72 (t,  $J = 7.1$  Hz, 3H).  $^{13}\text{C}$  NMR (101 MHz, DMSO)  $\delta$  199.4, 178.3, 167.6, 161.9, 159.1, 145.3, 135.1, 127.4, 121.9, 121.2, 114.1, 112.1, 106.7, 75.8, 58.7, 46.4, 32.4, 26.1, 23.9, 23.8, 23.5, 13.5. IR (neat): 3392, 3299, 3057, 2974, 1679, 1601  $\text{cm}^{-1}$ . HRMS (ESI)  $m/z$ : calcd for  $\text{C}_{22}\text{H}_{25}\text{N}_2\text{O}_5$   $[\text{M}+\text{H}]^+$ : 397.1758; found: 397.17483.

**3.8.11 (S)-ethyl 2-amino-1',7,7-trimethyl-2',5-dioxo-5,6,7,8-tetrahydrospiro[chromene-4,3'-indoline]-3-carboxylate (87k)**



The use of 2-cyano-2-(1-methyl-2-oxoindolin-3-ylidene)acetate **77a** and 5,5-Dimethyl-1,3-Cyclohexanedione in general procedure afforded chiral adduct **87k** in 46% isolated yield. mp 214-216 °C;  $[\alpha]_D^{33} = -16.5$  (*c* 0.13, CHCl<sub>3</sub>). Enantiomeric excess was determined as 30% ee by Chiralpak AD-H column (hexane/2-propanol = 75:25, 254 nm, 1 mL/min,  $t_{\text{major}} = 29.32$  min,  $t_{\text{minor}} = 10.87$  min). <sup>1</sup>H NMR (400 MHz, DMSO)  $\delta$  7.94 (s, 2H), 7.15 (t, *J* = 7.3 Hz, 1H), 6.88 (dd, *J* = 24.8, 5.8 Hz, 3H), 5.26 (d, *J* = 46.3 Hz, 1H), 3.75 – 3.57 (m, 2H), 3.11 (s, *J* = 17.6 Hz, 3H), 2.64 – 2.44 (m, 2H), 2.00 (d, *J* = 15.8 Hz, 1H), 1.00 (s, 3H), 0.93 (s, 3H), 0.73 (t, *J* = 6.9 Hz, 3H). <sup>13</sup>C NMR (101 MHz, DMSO)  $\delta$  194.7 178.1, 167.5, 162.6, 159.2, 145.2, 134.9, 127.4, 122.0, 121.3, 112.9, 106.8, 102.3, 75.8, 58.7, 50.5, 46.0, 31.5, 27.9, 26.7, 26.1, 13.5. IR (neat): 3359, 3272, 2953, 2867, 1999, 1693, 1672, 1576 cm<sup>-1</sup>.

**3.8.12 (S)-ethyl 2-amino-1'-methyl-2',5-dioxo-5,6,7,8-tetrahydrospiro[chromene-4,3'-indoline]-3-carboxylate (87l)**

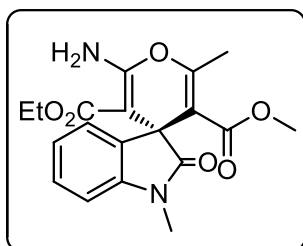


The use of 2-cyano-2-(1-methyl-2-oxoindolin-3-ylidene)acetate **77a** and 1,3-Cyclohexanedione in general procedure afforded chiral adduct **87l** in 76% isolated yield. mp 221-224 °C;  $[\alpha]_D^{34} = -13.4$  (*c* 0.28, CHCl<sub>3</sub>). Enantiomeric excess was determined as 5% ee by Chiralpak AD-H column (hexane/2-propanol = 80:20, 254 nm, 1 mL/min,  $t_{\text{major}} = 36.77$  min,  $t_{\text{minor}} = 12.39$  min). <sup>1</sup>H NMR (400 MHz, DMSO)  $\delta$  7.92 (s, 2H), 7.15 (t, *J* = 7.2 Hz, 1H), 7.01 – 6.71 (m, 3H), 3.74 – 3.53 (m, 2H), 3.10 (s, 3H), 2.64 (t, *J* = 5.7 Hz, 2H), 2.25 – 2.04 (m, 2H), 1.96 – 1.73 (m, 2H), 0.72 (t, *J* = 7.1 Hz, 3H). <sup>13</sup>C NMR (101 MHz, DMSO)  $\delta$  194.9, 178.2, 167.5, 164.4, 159.1, 145.2, 135.1, 127.4,



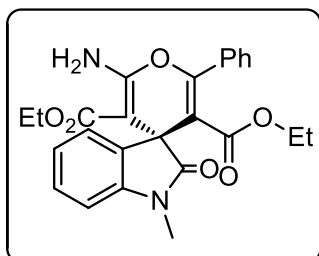
122.2, 121.3, 114.1, 106.7, 75.9, 58.7, 46.1, 36.9, 26.8, 26.0, 19.6, 13.5. IR (neat): 3359, 3243, 3183, 2940, 1672, 1610  $\text{cm}^{-1}$ . HRMS (ESI)  $m/z$ : calcd for  $\text{C}_{20}\text{H}_{21}\text{N}_2\text{O}_5$   $[\text{M}+\text{H}]^+$ : 369.1445; found: 369.14355.

**3.8.13 (S)-3'-ethyl 5'-methyl 2'-amino-1,6'-dimethyl-2-oxospiro[indoline-3,4'-pyran]-3',5'-dicarboxylate (87m)**



The use of 2-cyano-2-(1-methyl-2-oxoindolin-3-ylidene)acetate **77a** and Methyl acetoacetate in general procedure afforded chiral adduct **87m** in 70% isolated yield. mp 221-223  $^{\circ}\text{C}$ ;  $[\alpha]_D^{34} = -16.5$  ( $c$  0.30,  $\text{CHCl}_3$ ). Enantiomeric excess was determined as 49% ee by Chiralpak AD-H column (hexane/2-propanol = 70:30, 254 nm, 1 mL/min,  $t_{\text{major}} = 15.92$  min,  $t_{\text{minor}} = 5.93$  min.  $^1\text{H}$  NMR (400 MHz, DMSO)  $\delta$  7.89 (s, 2H), 7.26 (t,  $J = 7.6$  Hz, 1H), 7.04 (d,  $J = 7.2$  Hz, 1H), 6.95 (dd,  $J = 16.4, 7.7$  Hz, 2H), 3.80 – 3.60 (m, 2H), 3.35 (s, 3H), 3.16 (s, 3H), 2.24 (s, 3H), 0.73 (t,  $J = 7.1$  Hz, 3H).  $^{13}\text{C}$  NMR (101 MHz, DMSO)  $\delta$  178.2, 167.3, 165.3, 159.5, 154.6, 144.6, 134.9, 127.8, 122.7, 121.6, 107.7, 107.1, 74.8, 58.6, 51.4, 48.3, 26.1, 18.5, 13.4. IR (neat): 3482, 3305, 2957, 1695, 1603  $\text{cm}^{-1}$ . HRMS (ESI)  $m/z$ : calcd for  $\text{C}_{19}\text{H}_{21}\text{N}_2\text{O}_6$   $[\text{M}+\text{H}]^+$ : 373.13941; found: 373.13830.

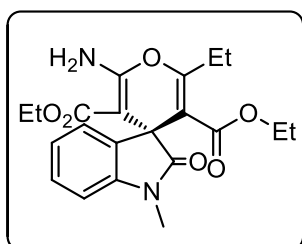
**3.8.14 (S)-diethyl 2'-amino-1-methyl-2-oxo-6'-phenylspiro[indoline-3,4'-pyran]-3',5'-dicarboxylate (87n)**



The use of 2-cyano-2-(1-methyl-2-oxoindolin-3-ylidene)acetate **77a** and Ethyl benzoylacetate in general procedure afforded chiral adduct **87n** in 26% isolated yield. mp 159-161  $^{\circ}\text{C}$ ;  $[\alpha]_D^{33} = -28.2$  ( $c$  0.20,  $\text{CHCl}_3$ ). Enantiomeric excess was determined as 12% ee by Chiralpak AD-H column (hexane/2-propanol = 80:20,

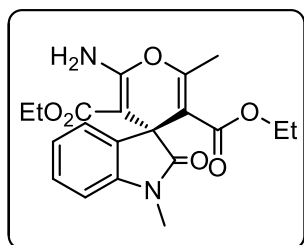
254 nm, 1 mL/min,  $t_{\text{major}} = 16.45$  min,  $t_{\text{minor}} = 13.26$  min  $^1\text{H}$  NMR (400 MHz, DMSO)  $\delta$  7.93 (s, 2H), 7.56 – 7.36 (m, 5H), 7.22 (tt,  $J = 10.3, 5.2$  Hz, 1H), 7.11 (d,  $J = 7.1$  Hz, 1H), 6.93 (dd,  $J = 17.3, 7.6$  Hz, 2H), 3.76 – 3.60 (m, 2H), 3.61 – 3.43 (m, 2H), 3.13 (s,  $J = 12.7$  Hz, 3H), 0.68 (t,  $J = 7.1$  Hz, 3H), 0.56 (t,  $J = 7.1$  Hz, 3H).  $^{13}\text{C}$  NMR (101 MHz, DMSO)  $\delta$  177.5, 167.2, 165.0, 160.2, 151.5, 144.5, 134.2, 132.5, 130.2, 128.3, 128.1, 127.8, 123.1, 121.8, 109.2, 107.4, 74.4, 60.2, 58.6, 49.2, 26.2, 13.4, 12.9. IR (neat): 3345, 3365, 3262, 3193, 2975, 1701, 1677, 1656, 1610  $\text{cm}^{-1}$ . HRMS (ESI)  $m/z$ : calcd for  $\text{C}_{25}\text{H}_{25}\text{N}_2\text{O}_6$   $[\text{M}+\text{H}]^+$ : 449.17071; found: 449.16945.

**3.8.15** (S)-diethyl 2'-amino-6'-ethyl-1-methyl-2-oxospiro[indoline-3,4'-pyran]-3',5'-dicarboxylate (**87o**)



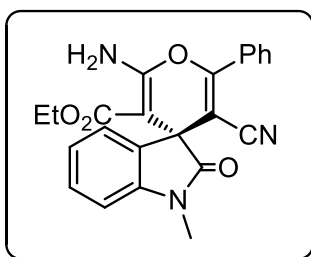
The use of 2-cyano-2-(1-methyl-2-oxoindolin-3-ylidene)acetate **77a** and Ethyl propionylacetate in general procedure afforded chiral adduct **87o** in 30% isolated yield. mp 101-103 °C;  $[\alpha]_D^{34} = -18.6$  ( $c$  0.25,  $\text{CHCl}_3$ ). Enantiomeric excess was determined as 39% ee by Chiralpak AD-H column (hexane/2-propanol = 80:20, 254 nm, 1 mL/min,  $t_{\text{major}} = 10.93$  min,  $t_{\text{minor}} = 5.85$  min.  $^1\text{H}$  NMR (400 MHz, DMSO)  $\delta$  7.82 (s, 2H), 7.20 (t,  $J = 7.5$  Hz, 1H), 7.00 – 6.74 (m, 3H), 3.82 – 3.68 (m, 2H), 3.68 – 3.56 (m, 2H), 3.10 (s, 2H), 2.45 (dd,  $J = 13.6, 6.7$  Hz, 2H), 1.16 (t,  $J = 7.4$  Hz, 3H), 0.82 (t,  $J = 7.1$  Hz, 3H), 0.68 (t,  $J = 7.1$  Hz, 3H).  $^{13}\text{C}$  NMR (101 MHz, DMSO)  $\delta$  178.0, 167.3, 164.8, 159.7, 158.1, 144.7, 134.9, 127.8, 122.7, 121.7, 107.1, 107.1, 74.8, 60.2, 58.6, 48.2, 26.1, 25.1, 13.4, 13.3, 11.6. IR (neat): 3365, 3265, 3197, 2986, 2937, 1703, 1678, 1653, 1612  $\text{cm}^{-1}$ . HRMS (ESI)  $m/z$ : calcd for  $\text{C}_{21}\text{H}_{25}\text{N}_2\text{O}_6$   $[\text{M}+\text{H}]^+$ : 401.17071; found: 401.16960.

**3.8.16 (S)-diethyl 2'-amino-1,6'-dimethyl-2-oxospiro[indoline-3,4'-pyran]-3',5'-dicarboxylate (87p)**



The use of 2-cyano-2-(1-methyl-2-oxindolin-3-ylidene)acetate **77a** and Ethyl acetoacetate in general procedure afforded chiral adduct **87p** in 57% isolated yield. mp 163-165 °C;  $[\alpha]_D^{31} = -4.3$  (*c* 0.30, CHCl<sub>3</sub>). Enantiomeric excess was determined as 52% ee by Chiralpak AD-H column (hexane/2-propanol = 70:30, 254 nm, 1 mL/min,  $t_{\text{major}} = 12.45$  min,  $t_{\text{minor}} = 5.90$  min. <sup>1</sup>H NMR (400 MHz, DMSO) δ 7.82 (s, 2H), 7.20 (dd, *J* = 9.1, 4.9 Hz, 1H), 7.05 – 6.80 (m, 3H), 3.89 – 3.69 (m, 2H), 3.69 – 3.54 (m, 2H), 3.10 (s, 3H), 2.18 (s, 3H), 0.82 (t, *J* = 5.1 Hz, 3H), 0.68 (t, *J* = 5.1 Hz, 3H). <sup>13</sup>C NMR (101 MHz, DMSO) δ 178.1, 167.3, 164.8, 159.5, 154.5, 144.8, 134.9, 127.8, 122.7, 121.6, 107.5, 107.1, 74.9, 60.1, 58.6, 48.2, 26.1, 18.5, 13.5, 13.3. IR (neat): 3378, 3241, 3190, 2977, 2931, 1715, 1697, 1606 cm<sup>-1</sup>. HRMS (ESI) *m/z*: calcd for C<sub>20</sub>H<sub>23</sub>N<sub>2</sub>O<sub>6</sub> [M+H]<sup>+</sup>: 387.15506; found: 387.15425.

**3.8.17 (S)-ethyl 2'-amino-5'-cyano-1-methyl-2-oxo-6'-phenylspiro[indoline-3,4'-pyran]-3'-carboxylate (87q)**



The use of 2-cyano-2-(1-methyl-2-oxindolin-3-ylidene)acetate **77a** and Benzoylacetonitrile in general procedure afforded chiral adduct **87q** in 98% isolated yield. mp 183-185 °C;  $[\alpha]_D^{31} = -16.7$  (*c* 1, CHCl<sub>3</sub>). Enantiomeric excess was determined as 17% ee by Chiralpak AD-H column (hexane/2-propanol = 80:20, 254 nm, 1 mL/min,  $t_{\text{major}} = 31.82$  min,  $t_{\text{minor}} = 15.05$  min. <sup>1</sup>H NMR (400 MHz, DMSO) δ 8.09 (s, 2H), 7.79 (d, *J* = 7.2 Hz, 2H), 7.59 (dt, *J* = 14.5, 6.7 Hz, 3H), 7.40 – 7.26 (m, 2H), 7.07 (t, *J* = 7.1 Hz, 2H), 3.78 – 3.63 (m, 2H), 3.19 (s, *J* = 19.7 Hz, 3H), 0.69 (t, *J* = 7.0 Hz, 3H). <sup>13</sup>C NMR (101 MHz, DMSO) δ 176.6, 166.6, 159.4, 158.3, 143.4, 133.6, 131.9, 129.6,

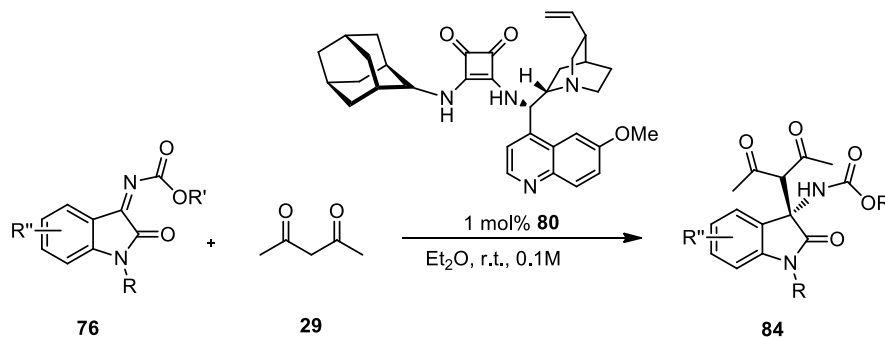
128.9, 128.7, 127.8, 123.5, 122.8, 115.4, 108.2, 89.4, 72.2, 58.9, 49.3, 26.4, 13.4. IR (neat): 3744, 3348, 3242, 3201, 1686, 1655, 1607  $\text{cm}^{-1}$ . HRMS (ESI)  $m/z$ : calcd for  $\text{C}_{23}\text{H}_{20}\text{N}_3\text{O}_4$   $[\text{M}+\text{H}]^+$ : 402.14483; found: 402.13393.

## CHAPTER 4

### CONCLUSION

In conclusion, we developed an efficient way for the formation of the stereogenic quaternary center at the C-3 position of oxindoles and also 3,3' substituted spirocyclic oxindoles by utilizing 2-adamantyl substituted quinine based squaramide organocatalyst.

In the first part of this study, the efficiency of 2-adamantyl substituted quinine based squaramide organocatalyst **80** was presented in the enantioselective reaction of pentane-2,4-dione with *N*-alkoxycarbonyl ketimines derived from isatins. The corresponding products **84** were obtained in high yields up to 98% yield and excellent enantioselectivities up to greater than 99% ee. This methodology is featured by the use of very low (1 mol%) catalyst loading which is noteworthy in organocatalysis.

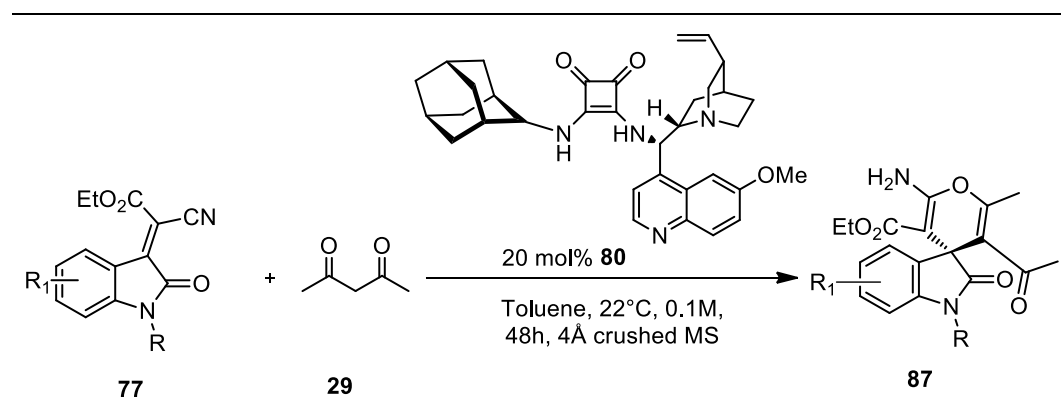


**Scheme 16** Mannich reaction of isatin derived ketimine **76** and acetylacetone **29** in the presence of 1 mol% catalyst loading

In the second part of this thesis, emerging from the methodology of the formation of stereogenic C-3 oxindoles, enantioselective construction of spirocyclic oxindoles in

the presence of chiral bifunctional acid/base organocatalysts was examined. The aim is the formation of stereogenic 3,3' substituted spirooxindoles with high yield and high selectivity by using the reaction pathway of Domino Knoevenagel Condensation/ Michael Addition/Cyclization reactions. In line with this purpose, starting from isatins, ethyl cyanoacetate and various 1,3-dicarbonyl compounds, spiro conjugated amino pyran derivatives **87** were synthesized in the presence of 2-adamantyl substituted quinine based squaramide organocatalyst **80** with low to high yield (up to 98%) and low to excellent enantioselectivity (up to 99% ee).

In brief, there are a few study reported in the literature for the formation of stereoselective spirooxindole moiety using ethyl cyanoacetate and some corresponding spirooxindole derivatives haven't reported yet. In this study, we achieved to construct spirooxindole moiety with good selectivity for the first time in the literature.



**Scheme 17** Enantioselective Construction of Spirooxindoles

## REFERENCES

1. Singh, G. S.; Desta, Z. Y. *Chem. Rev.* **2012**, *112*(11), 6104-6155.
2. Erdmann, O. L., *J. Prakt. Chem*, **1840**, *19*(1), 321-362.
3. Laurent, A. *Ann. Chim. Phys.*, **1840**, *3*(3), 393-434
4. Kakkar, R., *MedChemComm*, **2019** *10*(3), 351-368.
5. Kekulé, A., *Chem. Ber.* **1869**, *2*, 748-749
6. Sandmeyer, T. *Helv. Chim. Acta*, **1919**. *2*(1), 234-242.
7. Stollé, R., *Ber.* **1913**, *46*(3), 3915-3916.
8. Gassman, P.G.; Cue Jr.; B.W.; Luh, T.Y.; *J. Org. Chem.* **1977**, *42*, 1344.  
Gassman, P.G.; Cue, B.W. *Ger. Offen.* **1978**, *2*, 815.
9. Martinet, J. *Compt. Rend.* **1918**, *166*, 851-853.
10. Borad, M. A., Bhoi, M. N., Prajapati, N. P., Patel, H. D.; **2014**, *44*(7), 897-922.
11. (a) Kitamura, H., Kato, A., Esaki, T.; *Eur. J. Pharmacol.* **2001**, *418*(3), 225-230.  
(b) Griebel, G., Simiand, J., Serradeil-Le Gal, C., Wagnon, J., Pascal, M., Scatton, B., Soubrié, P.; *PNAS.* **2002**. *99*(9), 6370-6375.  
(c) Yeung, B. K., Zou, B., Rottmann, M., Lakshminarayana, S. B., Ang, S. H., Leong, S. Y., Keller, T. H.; *J Med.Chem.* **2010**, *53*(14), 5155-5164.  
(d) Crosignani, S., Jorand-Lebrun, C., & Grippi-Vallotton, T.; **2012**, US Patent 20120115895.  
(e) Ghosh, A. K., Schiltz, G., Perali, R. S., Leshchenko, S., Kay, S., Walters, D. E., Mitsuya, H.; *Bioorg. Med. Chem. Lett.* **2006**, *16*(7), 1869-1873.
12. Kaur, J., Kaur, B. P., Chimni, S. S.; *Org. Biomol. Chem.* **2020**, *18*(25), 4692-4708.
13. (a) Liu, Y. L., Zhou, F., Cao, J. J., Ji, C. B., Ding, M., Zhou, J.; *Org. Biomol. Chem.* **2010**, *8*(17), 3847-3850.  
(b) Liu, Y. L., Zhou, J.; *Chem. Commun.* **2013**. *49*(39), 4421-4423.  
(c) Wang, D., Liang, J., Feng, J., Wang, K., Sun, Q., Zhao, L., Wang, R.; *Adv. Synth. Catal.* **2013**, *355*(2-3), 548-558.

- (d) Yan, W., Wang, D., Feng, J., Li, P., Zhao, D., Wang, R.; *Org. Lett.* **2012**, *14*(10), 2512-2515.
- (e) Hara, N., Nakamura, S., Sano, M., Tamura, R., Funahashi, Y., Shibata, N.; *Chem. Eur. J.* **2012**, *18*(30), 9276-9280.
- (f) Guo, Q. X., Liu, Y. W., Li, X. C., Zhong, L. Z., Peng, Y. G.; *J. Org. Chem.* **2012**, *77*(7), 3589-3594.
- (g) Feng, J., Yan, W., Wang, D., Li, P., Sun, Q., Wang, R.; *Chem. Commun.* **2012**, *48*(64), 8003-8005.
- (h) Duce, S., Pesciaioli, F., Gramigna, L., Bernardi, L., Mazzanti, A., Ricci, A., Bencivenni, G.; *Adv. Synth. Catal.* **2011**, *353*(6), 860-864.
- (i) JJ, B. Silva-Garcia A. Shupe BH. Fettinger JC. Franz AK. *Tetrahedron Lett.* **2011**, *52*, 5550.
- (j) Shi, F., Xing, G. J., Zhu, R. Y., Tan, W., & Tu, S.; *Org. Lett.* **2013**, *15*(1), 128-131.
- (k) Zhang, B., Feng, P., Sun, L. H., Cui, Y., Ye, S., Jiao, N.; *Chem. Eur. J.* **2012**, *18*(30), 9198-9203.
- (l) Lv, H., Tiwari, B., Mo, J., Xing, C., Chi, Y. R.; *Org. Lett.* **2012**, *14*(21), 5412-5415.
- (m) Cheng, X., Vellalath, S., Goddard, R., List, B.; *J. Am. Chem. Soc.* **2008**, *130*(47), 15786-15787.
14. (a) Jia, Y. X., Hillgren, J. M., Watson, E. L., Marsden, S. P., Kündig, E. P.; *Chem. Commun.* **2008**, (34), 4040-4042.
- (b) Marsden, S. P., Watson, E. L., Raw, S. A.; *Org. Lett.* **2008**, *10*(13), 2905-2908.
- (c) Watson, E. L., Marsden, S. P., Raw, S. A.; *Tetrahedron Lett.* **2009**, *50*(26), 3318-3320.
15. (a) Emura, T., Esaki, T., Tachibana, K., Shimizu, M.; *J. Org. Chem.* **2006**, *71*(22), 8559-8564.
- (b) Zhao, H., Thurkauf, A., Braun, J., Brodbeck, R., Kieltyka, A. *Bioorg. Med. Chem. Lett.* **2000**, *10*(18), 2119-2122.



16. (a) Cheng, L., Liu, L., Wang, D., Chen, Y. J.; *Org. Lett.* **2009**, *11*(17), 3874-3877.
- (b) Qian, Z. Q., Zhou, F., Du, T. P., Wang, B. L., Ding, M., Zhao, X. L., Zhou, J.; *Chem. Commun.* **2009**, (44), 6753-6755.
- (c) Bui, T., Borregan, M., Barbas III, C. F.; *J. Org. Chem.* **2009**, *74*(23), 8935-8938.
- (d) Mouri, S., Chen, Z., Mitsunuma, H., Furutachi, M., Matsunaga, S., Shibasaki, M.; *J. Am. Chem. Soc.* **2010**, *132*(4), 1255-1257.
- (e) Yang, Z., Wang, Z., Bai, S., Shen, K., Chen, D., Liu, X., Feng, X.; *Chem. Eur. J.* **2010**, *16*(22), 6632-6637.
17. (a) Shi, F., Tao, Z. L., Luo, S. W., Tu, S. J., Gong, L. Z.; *Chem. Eur. J.* **2012**, *18*(22), 6885-6894.
- (b) Ren, L., Lian, X. L., Gong, L. Z.; *Chem. Eur. J.* **2013**, *19*(10), 3315-3318.
18. Pellissier, H. *Beil. J. Org. Chem.* **2018**, *14*(1), 1349-1369.
19. Kaur, J., Chimni, S. S., Mahajan, S., Kumar, A; *RSC Adv.* **2015**, *5*(65), 52481-52496.
20. Mei, G. J., & Shi, F. (2018). Catalytic asymmetric synthesis of spirooxindoles: recent developments. *Chemical Communications*, *54*(50), 6607-6621.
21. Pavlovska, T. L., Redkin, R. G., Lipson, V. V., Atamanuk, D. V.; *Mol. Diversity*, **2016**, *20*(1), 299-344.
22. Boddy, A. J., Bull, J. A.; *Org. Chem. Front.* **2021**, *8*(5), 1026-1084.
23. Cheng, D., Ishihara, Y., Tan, B., & Barbas III, C. F.; *ACS Catalysis*, **2014**, *4*(3), 743-762.
24. Aitken, A., Kilényi, S. N.; *Asymmetric synthesis*, CRC Press., **1992**
25. Chinchilla, R. *Molecules*, **2017**, *22*(9), 1504.
26. (a) Hajos, Z. G., Parrish, D. R.; *J. Org. Chem.* **1974**, *39*(12), 1615-1621.
- (b) Eder, U., Sauer, G., Wiechert, R.; *Angew. Chem.* **1971**, *83*(13), 492-493.
27. Giacalone, F., Gruttadauria, M., Agrigento, P., Noto, R.; *Chem. Soc. Rev.* **2012**, *41*(6), 2406-2447.
28. Xiang, S. H., Tan, B.; *Nature Communications*, **2020**, *11*(1), 1-5.

29. Torres, R. R. *Stereoselective organocatalysis: bond formation methodologies and activation modes*. John Wiley & Sons., **2013**, Vol. 2, pp 11-81
30. Abbasov, M. E., Romo, D.; *Nat. Prod. Rep.* **2014**, *31*(10), 1318-1327.
31. Zhao, B. L., Li, J. H., Du, D. M.; *Chem. Rec.* **2017**, *17*(10), 994-1018.
32. Okino, T., Hoashi, Y., Takemoto, Y.; *J. Am. Chem. Soc.* **2003**, *125*(42), 12672-12673.
33. Wang, J.; Li, H.; Duan, W.; Zu, L.; Wang, W. *Org. Lett.* **2005**, *7*, 4713-4716.
34. Zuend, S. J.; Jacobsen, E. N. *J. Am. Chem. Soc.* **2007**, *129* (51), 15872-15883.
35. a) Wang, C.-J.; Zhang, Z.-H.; Dong, X.-Q.; Wu, X.-J. *Chem. Commun.* **2008**, 1431-1433. b) Wang, C.-J.; Zhang, Z.-H.; Dong, X.-Q.; Xue, Z.-Y.; Teng, H.-L. *J. Am. Chem. Soc.* **2008**, *130*, 8606-8607.
36. Peng, F.-Z.; Shao, Z.-H.; Fan, B.-M.; Song, H.; Li, G.-P.; Zhang, H.-B. *J. Org. Chem.* **2008**, *73* (13), 5202-5205.
37. Oh, S. H.; Rho, H. S.; Lee, J. W.; Lee, J. E.; Youk, S. H.; Chin, J.; Song, C. E. *Angew. Chem. Int. Ed.* **2008**, *47*(41), 7872-7875.
38. Andrés, J. M.; Manzano, R.; Pedrosa, R. *Chem. Eur. J.* **2008**, *14* (17), 5116-5119.
39. Malerich, J. P.; Hagihara, K.; Rawal, V. H. *J. Am. Chem. Soc.* **2008**, *130* (44), 14416-14417.
40. Jiang, X.; Zhang, Y.; Liu, X.; Zhang, G.; Lai, L.; Wu, L.; Zhang, J.; Wang, R. *J. Org. Chem.* **2009**, *74*(15), 5562-5567.
41. Bassas, O.; Huuskonen, J.; Rissanen, K.; Koskinen, A. M. P. *Eur. J. Org. Chem.* **2009**, 1340-1351.
42. Luo, J.; Xu, L.-W.; Hay, R. A. S.; Lu, Y. *Org. Lett.* **2009**, *11*(12), 437-440.
43. Tanyeli, C.; Isik, M. *J. Org. Chem.* **2013**, *78*(4), 1604-1611.
44. Işık, M.; Ünver, M. Y.; Tanyeli, C. *J. Org. Chem.* **2015**, *80*(2), 828-835.
45. Chauhan, P., Mahajan, S., Kaya, U., Hack, D., Enders, D.; *Adv. Synth. Catal.* **2015**, *357*(2-3), 253-281.
46. Alemán, J., Parra, A., Jiang, H., Jørgensen, K. A.; *Chem. Eur. J.* **2011**, *17*(25), 6890-6899.
47. Ni, X., Li, X., Wang, Z., Cheng, J. P.; *Org. Lett.* **2014**, *16*(6), 1786-1789.

48. Hou, X. Q., Du, D. M.; *Adv. Synth. Catal.* **2020**, 362(21), 4487-4512.
49. Bugaut X., Constantieux T., Coquerel Y., Rodriguez J., *In Multicomponent Reactions in Organic Synthesis*, **2015** Wiley-VCH Weinheim, Germany, 109-151.
50. Arend, M., Westermann, B., Risch, N.; *Angew. Chem.* **1998**, 37(8), 1044-1070.
51. List, B. *J. Am. Chem. Soc.* **2000**, 122(38), 9336-9337.
52. W. Yan, D. Wang, J. Feng, P. Li, D. Zhao, R. Wang, *Org. Lett.* **2012**, 14(10), 2512-2515.
53. Rao, K. S., Ramesh, P., Chowhan, L. R., Trivedi, R.; *RSC Adv.* **2016**, 6(87), 84242-84247.
54. Ričko, S., Svete, J., Štefane, B., Perdih, A., Golobič, A., Meden, A., Grošelj, U.; *Adv. Synth. Catal.* **2016**, 358(23), 3786-3796.
55. Zhu, Y., Li, Y., Meng, Q., Li, X.; *Org. Chem. Front.*, **2016**, 3(6), 709-713.
56. İşibol, D.; Karahan, S.; Tanyeli, C. *Tetrahedron Lett.* **2018**, 59, 541-545.
57. Knoevenagel, E. *Ber.Dtsch. Chem. Ges.* **1894**, 27(2), 2345-2346.
58. van Beurden, K., de Koning, S., Molendijk, D., van Schijndel, J.; *Green Chem. Lett. Rev.* **2020**, 13(4), 349-364.
59. Lee, A., Michrowska, A., Sulzer-Mosse, S., List, B.; *Angew. Chem.Int. Ed.* **2011**, 50(7), 1707-1710.
60. Suresh, Sandhu, J. S.; *Green Chem.Lett.Rev.* **2009**, 2(3), 189-192.
61. Volla, C. M., Atodiresei, I., Rueping, M. *Chem. Rev.* **2014**, 114(4), 2390-2431.
62. Chen, W. B., Wu, Z. J., Pei, Q. L., Cun, L. F., Zhang, X. M., Yuan, W. C.; *Org. Lett.* **2010**, 12(14), 3132-3135.
63. Macaev, F., Sucman, N., Shepeli, F., Zveaghintseva, M., Pogrebnoi, V.; *Symmetry*, **2011**, 3(2), 165-170.
64. Chennapuram, M., Owolabi, I. A., Seki, C., Okuyama, Y., Kwon, E., Uwai, K., Nakano, H.; *ACS Omega*, **2018**, 3(9), 11718-11726.
65. Konda, S., Jakkampudi, S., Arman, H. D., Zhao, J. C. G.; *Synth. Commun.* **2019**, 49(21), 2971-2982.

66. Yan, W., Wang, D., Feng, J., Li, P., Zhao, D., Wang, R.; *Org. Lett.* **2012**, *14*(10), 2512-2515.
67. Jones, G., Rae, W. J.; *Tetrahedron*, **1966**, *22*(9), 3021-3026.
68. Morales-Rios, M. S., Mora-Pérez, Y., Joseph-Nathan, P.; *Magn. Reson. Chem.* **1992**, *30*(12), 1153-1157.
69. Giacalone, F., Gruttadauria, M., Agrigento, P., Noto, R. *Chem. Soc. Rev.* **2012**, *41*(6), 2406-2447.
70. Furdas, S. D., Shekfeh, S., Kannan, S., Sippl, W., Jung, M.; *Med. Chem. Comm.* **2012**, *3*(3), 305-311.
71. Tang, B. X., Song, R. J., Wu, C. Y., Liu, Y., Zhou, M. B., Wei, W. T., Li, J. H.; *J. Am. Chem. Soc.* **2010**, *132*(26), 8900-8902.
72. Boraiei, A. T., El Tamany, E. S. H., Ali, I. A., Gebriel, S. M.; *J. Heterocyclic Chem.* **2017**, *54*(5), 2881-2888.
73. Abdel-Latif, F. F., Mekheimer, R. A., Mashaly, M. M., Ahmed, E. K.; *Collect. Czech. Chem. Commun.* **1994**, *59*(5), 1235-1240.

## APPENDICES

### A. NMR SPECTRA

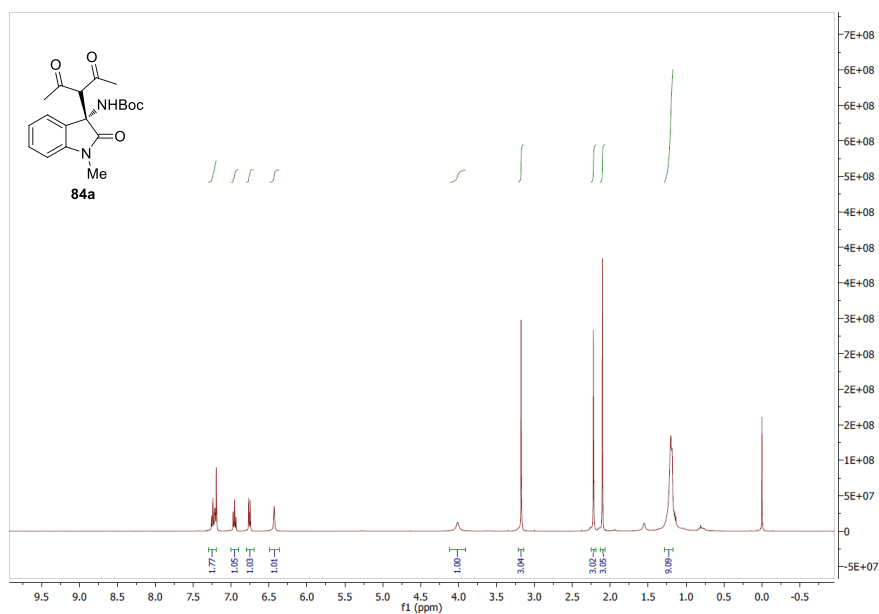


Figure A. 1 <sup>1</sup>H NMR spectrum of 84a

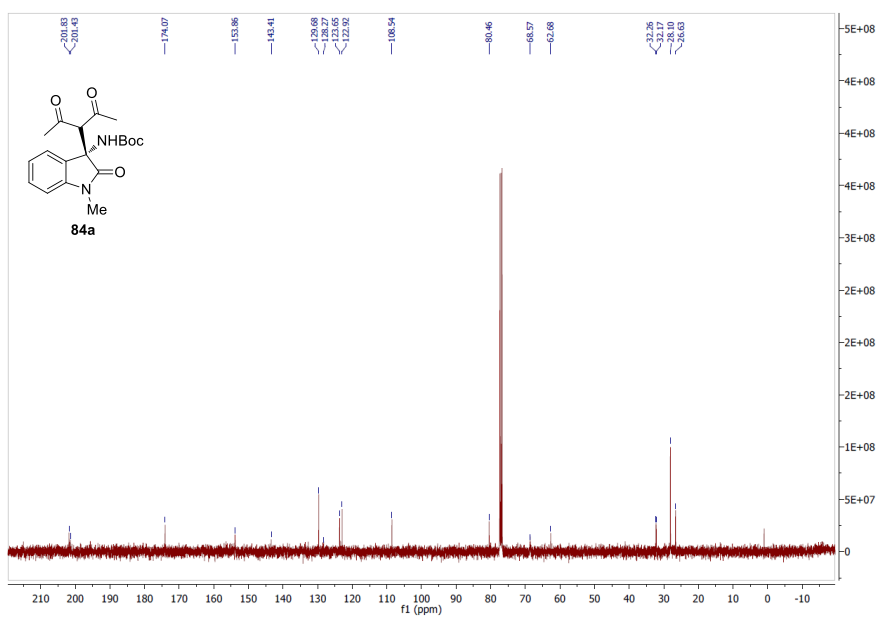


Figure A. 2 <sup>13</sup>C NMR spectrum of 84a

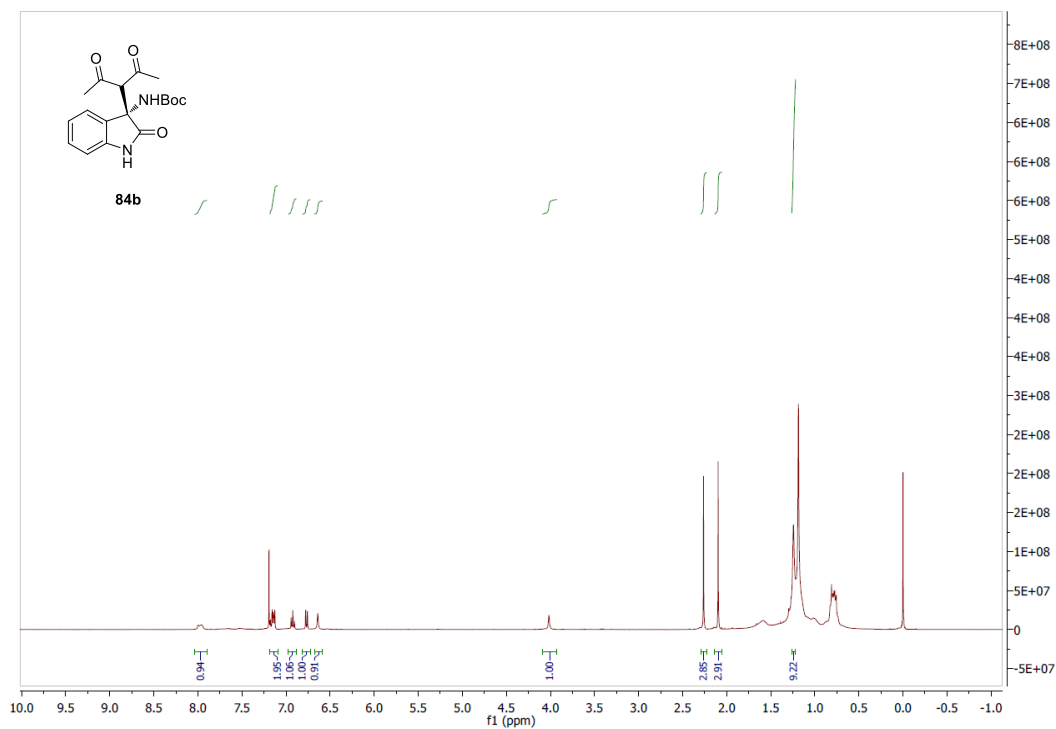


Figure A. 3  $^1\text{H}$  NMR spectrum of **84b**

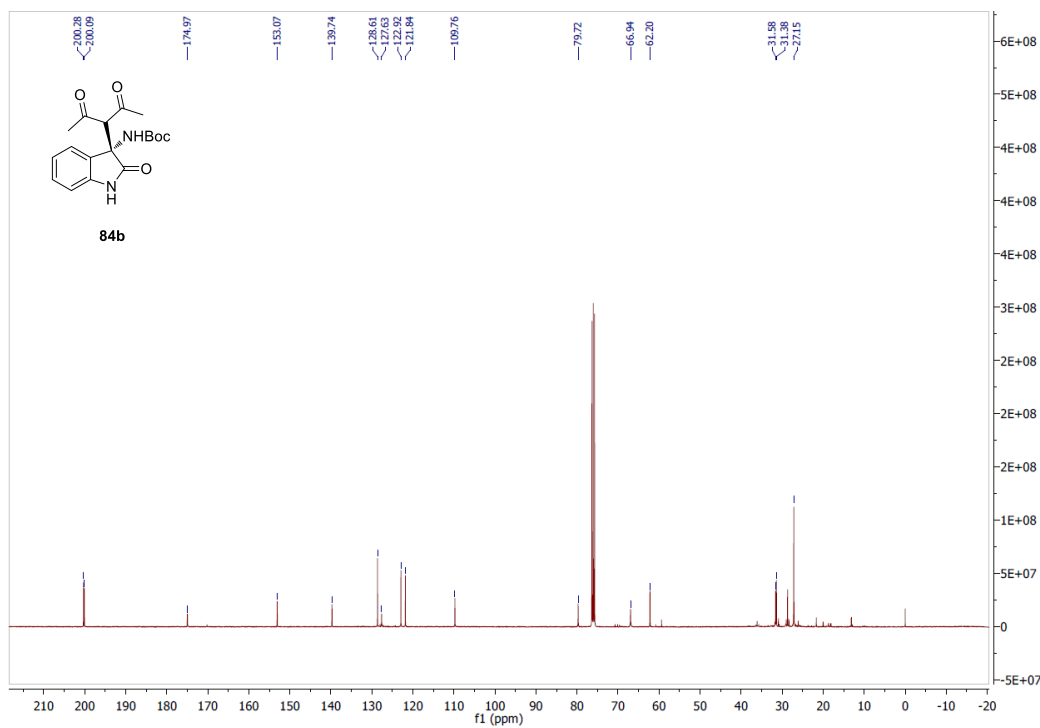


Figure A. 4  $^{13}\text{C}$  NMR spectrum of **84b**

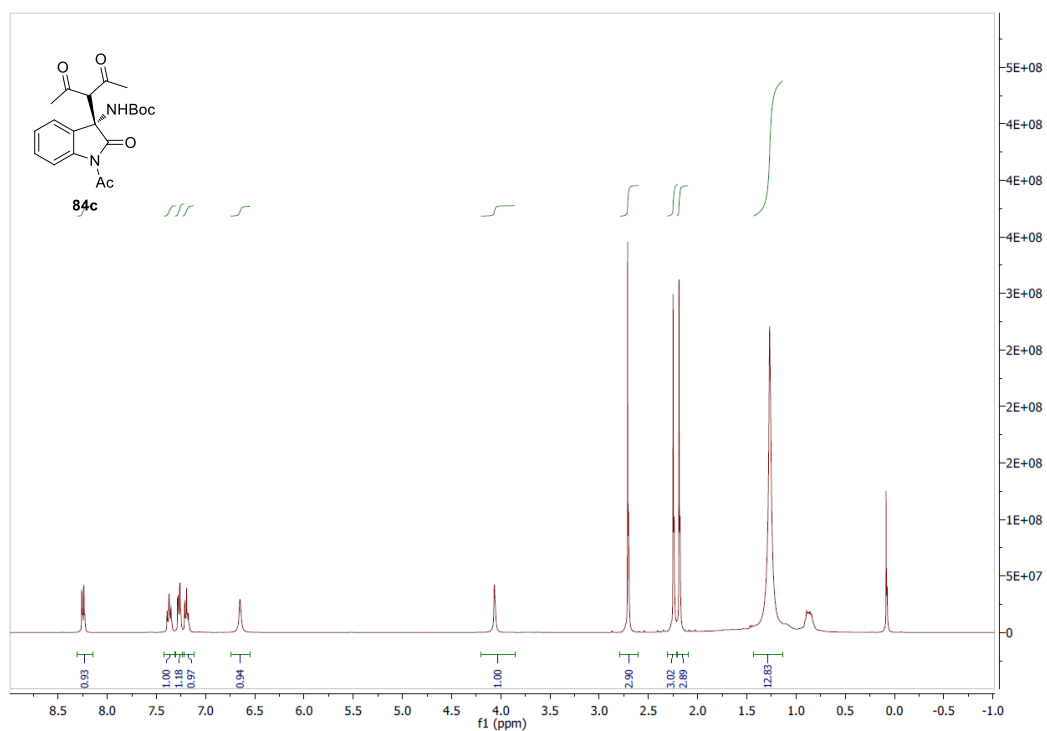


Figure A. 5  $^1\text{H}$  NMR spectrum of **84c**

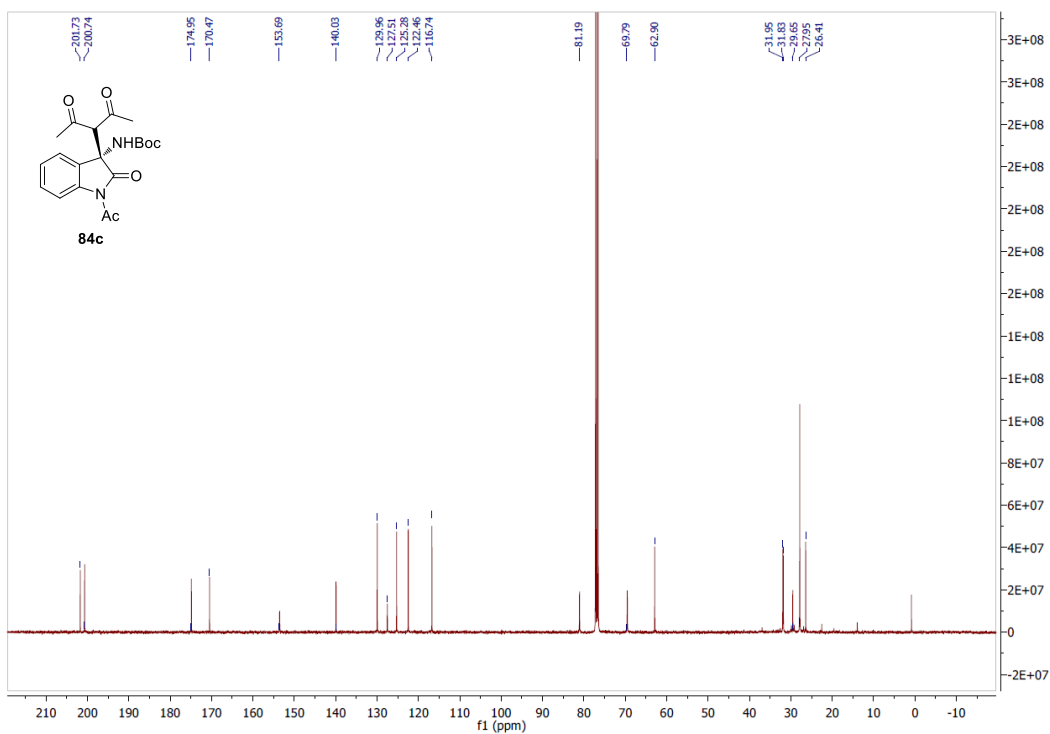
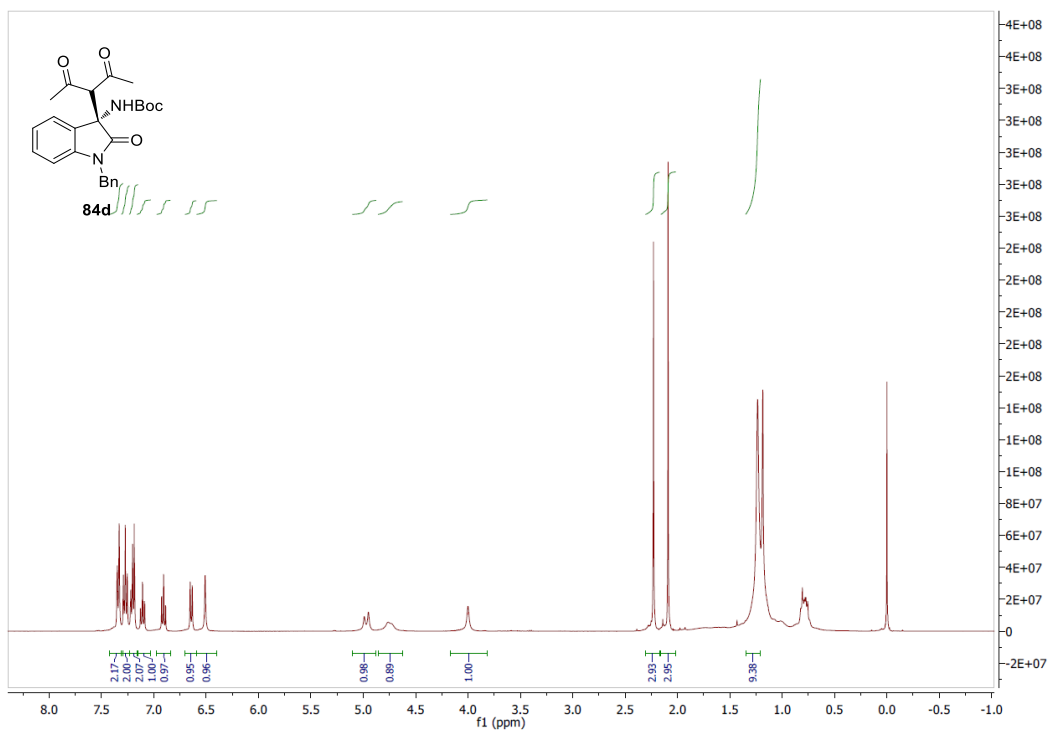
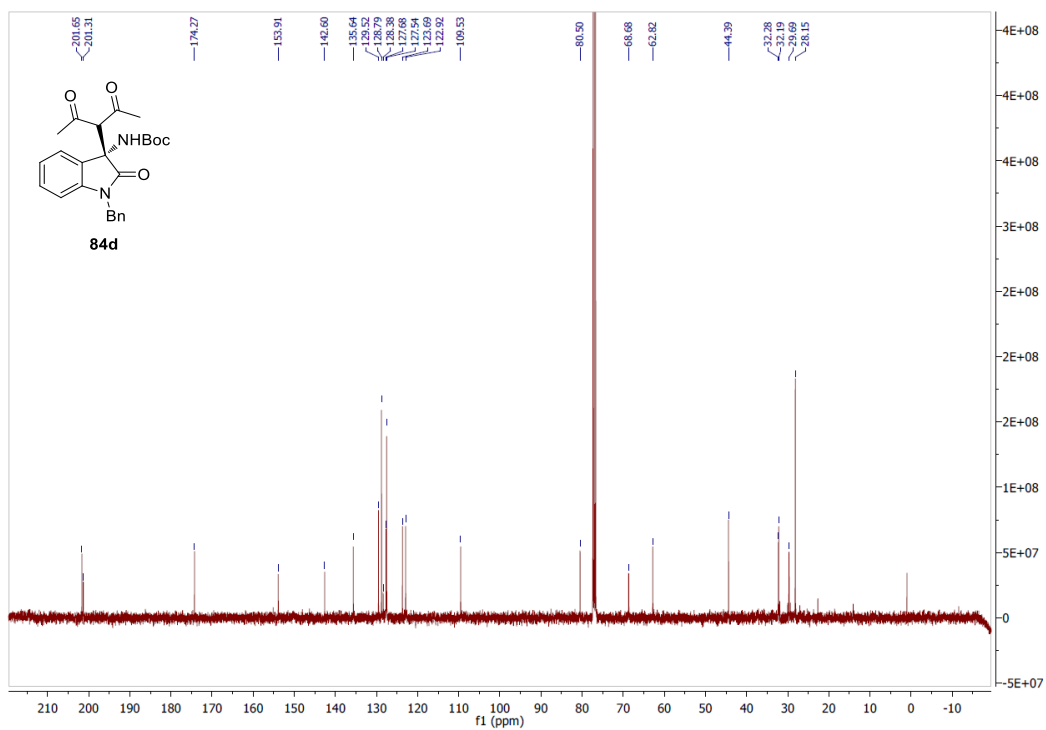


Figure A. 6  $^{13}\text{C}$  NMR spectrum of **84c**

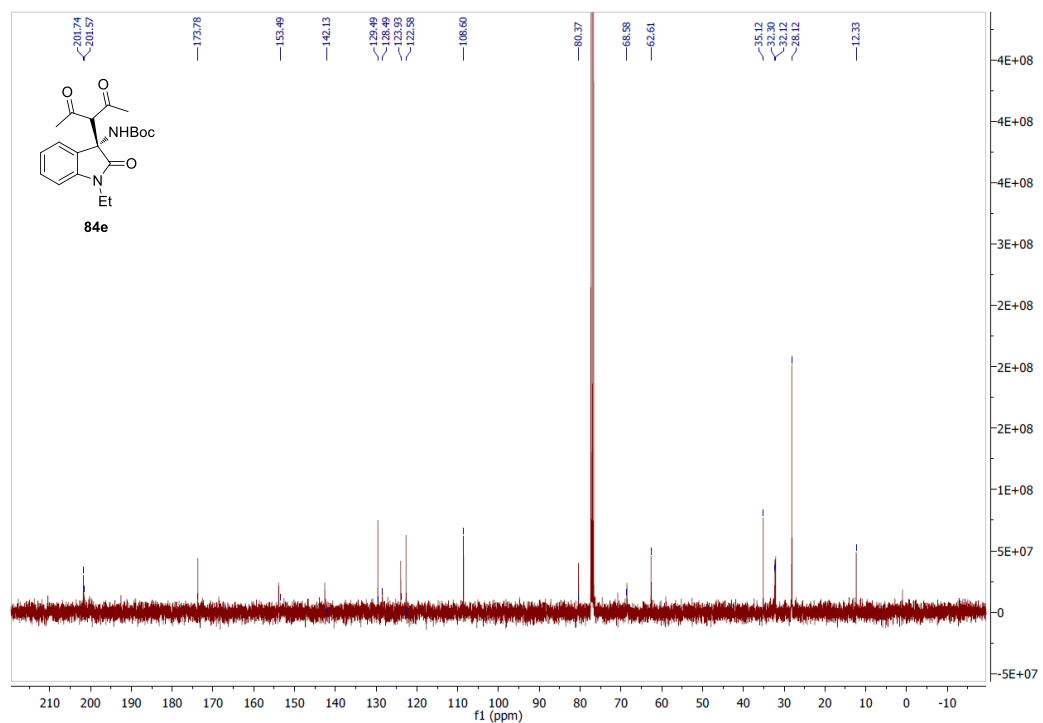
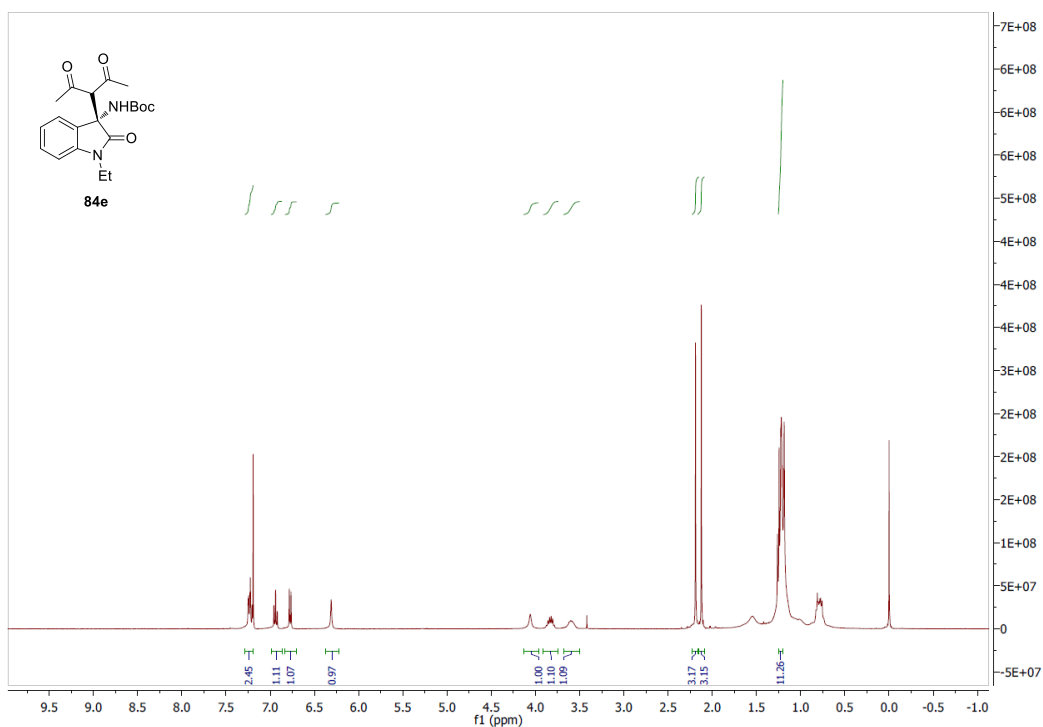


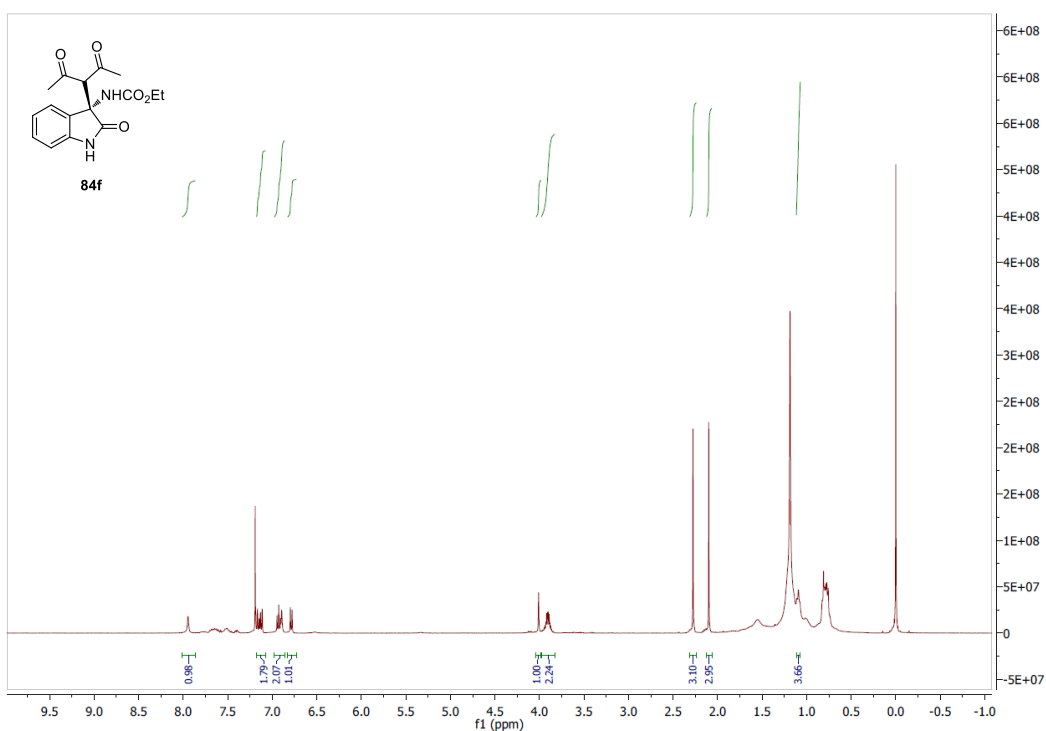
**Figure A. 7**  $^1\text{H}$  NMR spectrum of **84d**



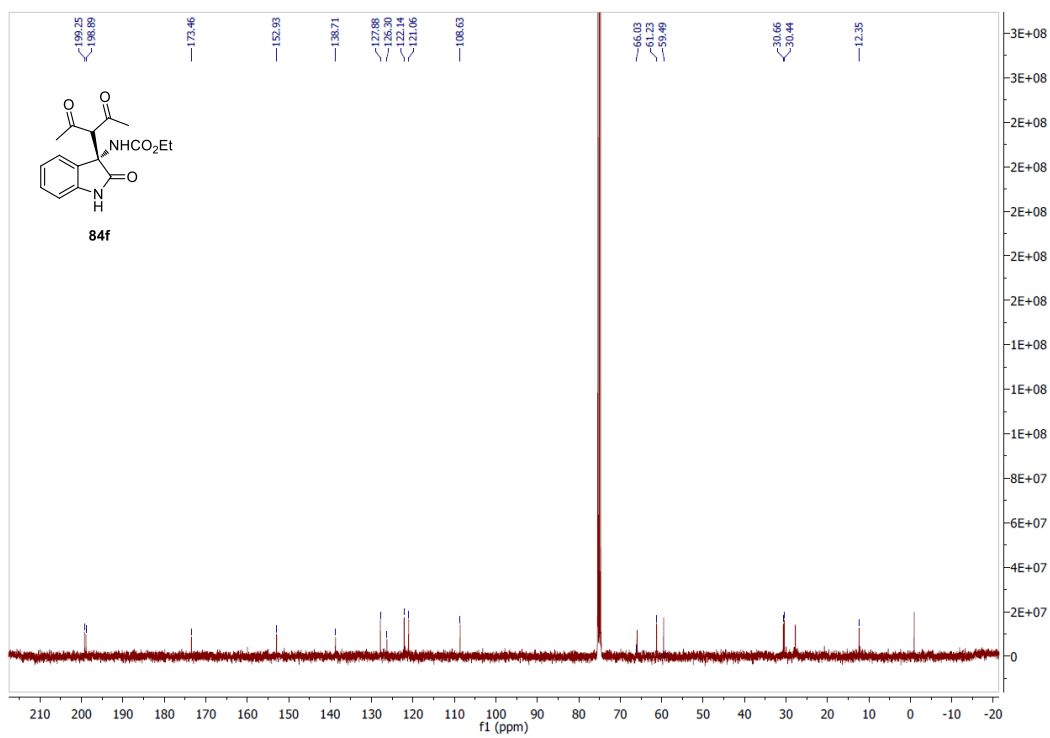
**Figure A. 8**  $^{13}\text{C}$  NMR spectrum of **84d**



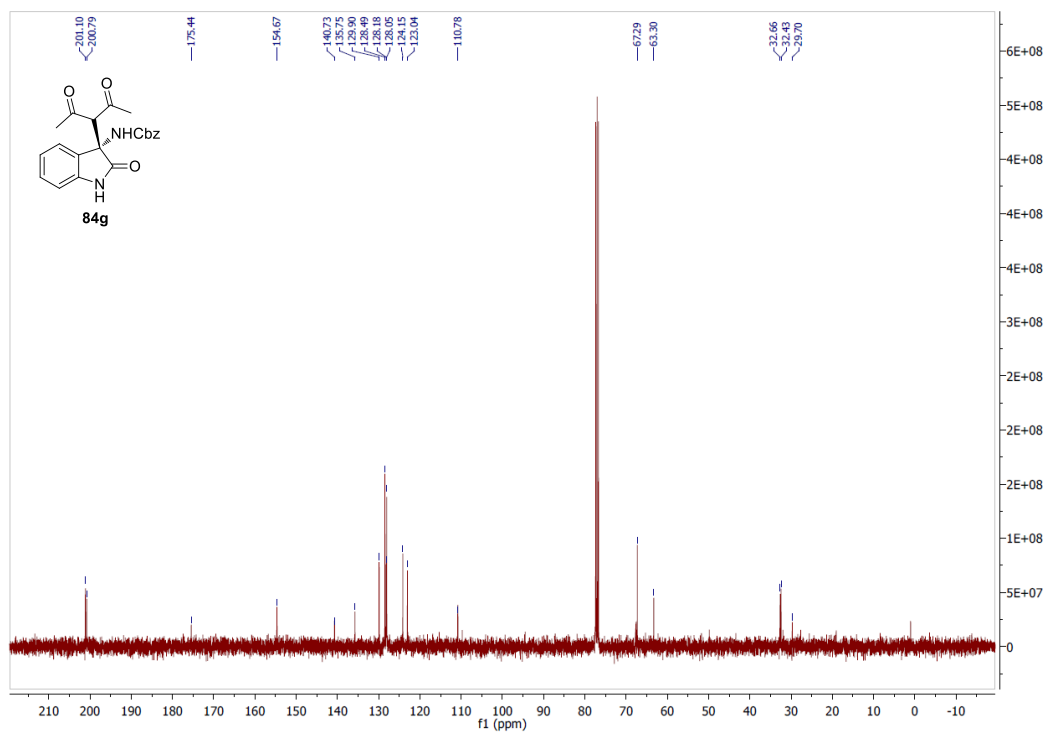
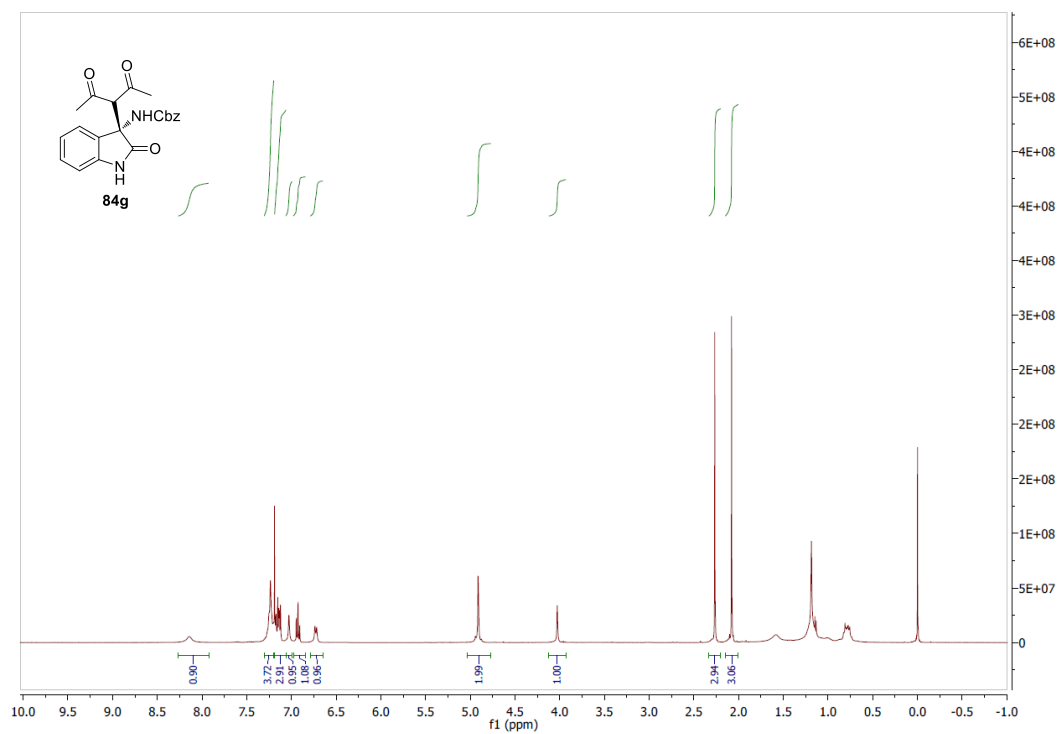




**Figure A. 11**  $^1\text{H}$  NMR spectrum of **84f**



**Figure A. 12**  $^{13}\text{C}$  NMR spectrum of **84f**



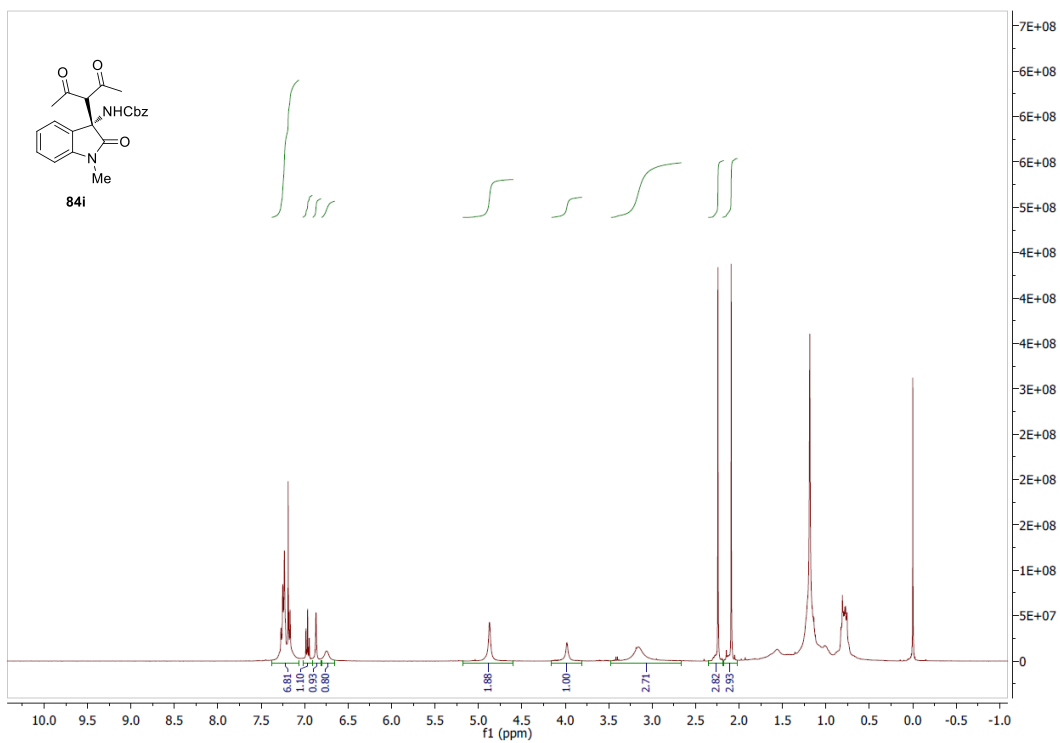


**Figure A. 15** <sup>1</sup>H NMR spectrum of **84i**

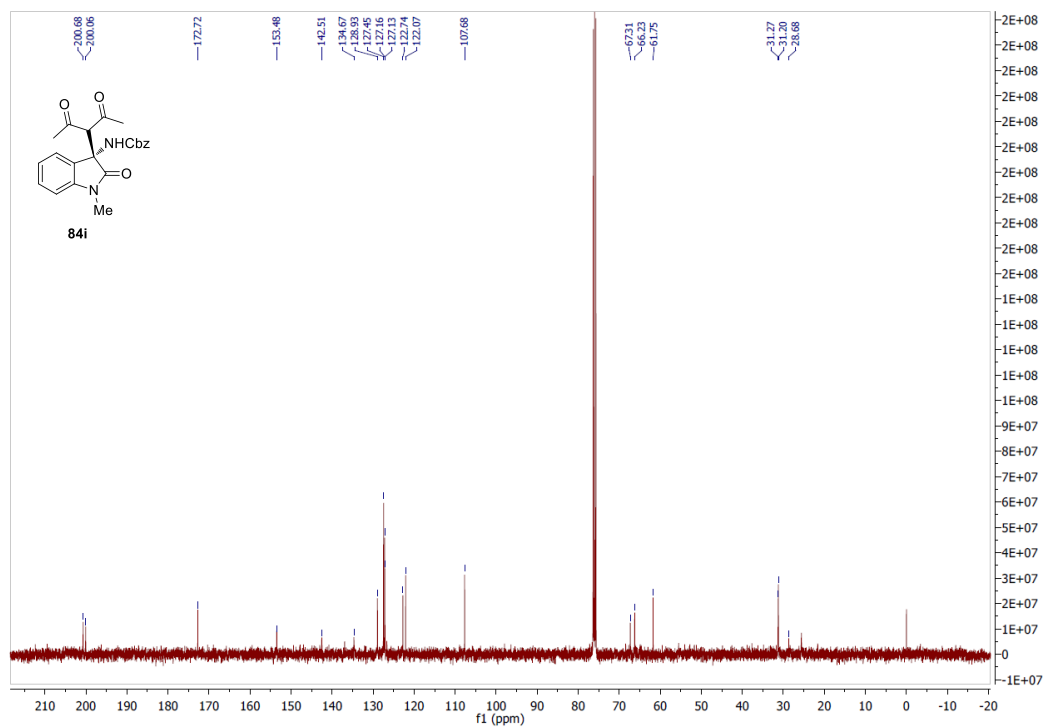


**Figure A. 16** <sup>13</sup>C NMR spectrum of **84i**

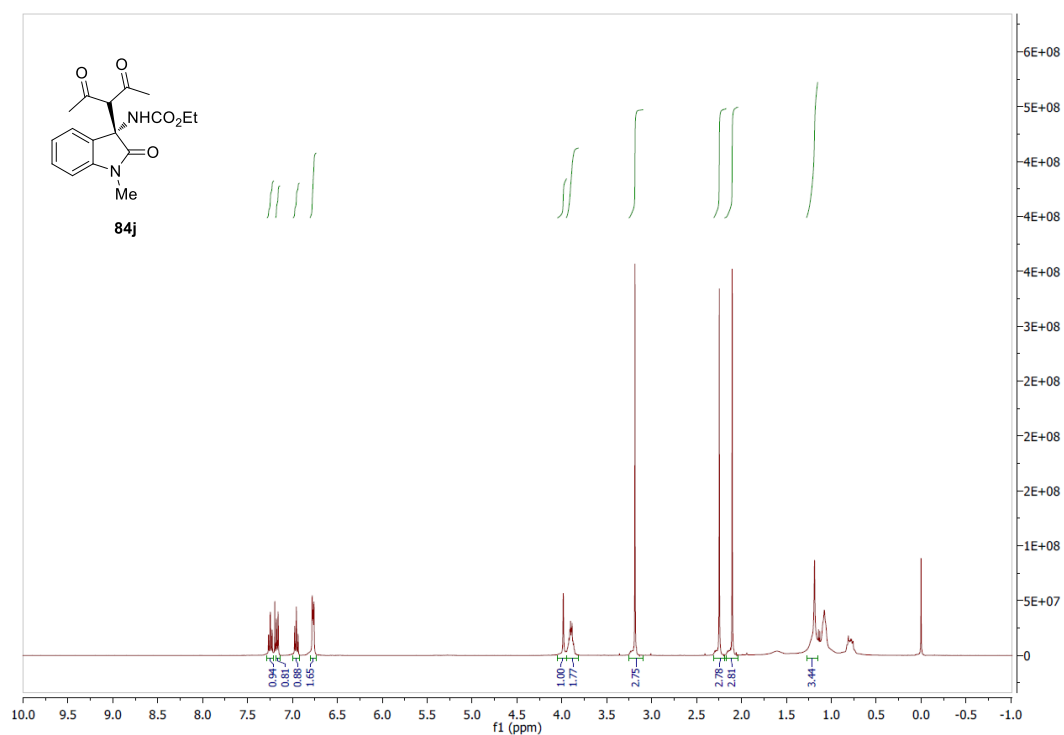


Figure A. 17 <sup>1</sup>H NMR spectrum of **84j**

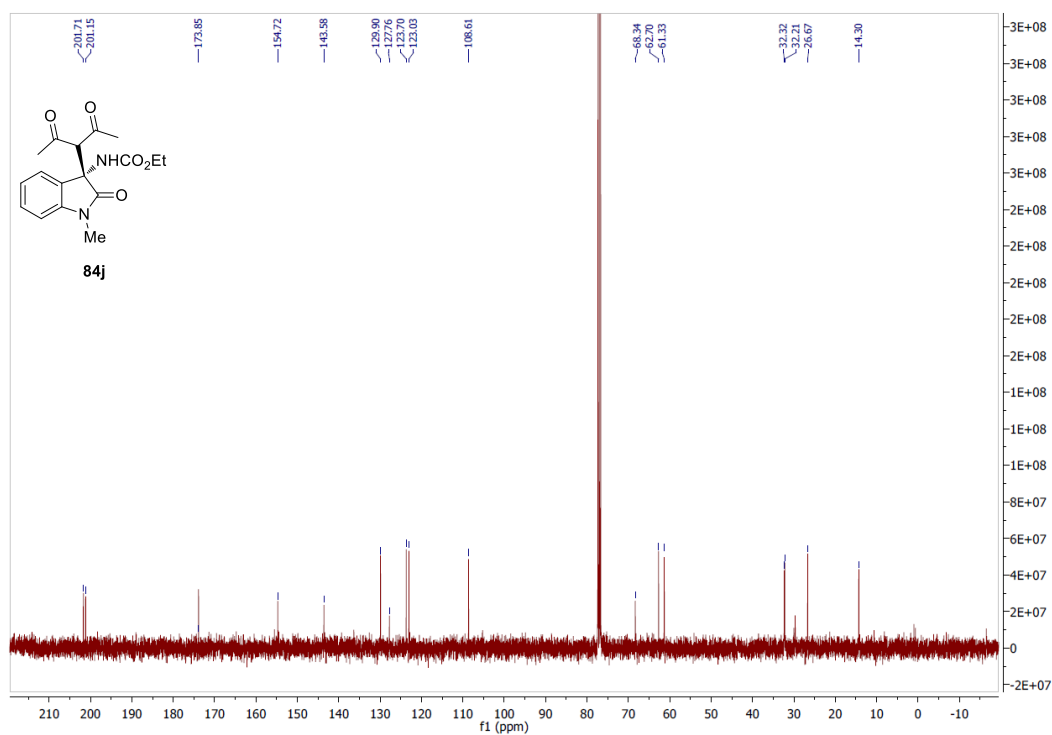


Figure A. 18 <sup>13</sup>C NMR spectrum of **84j**

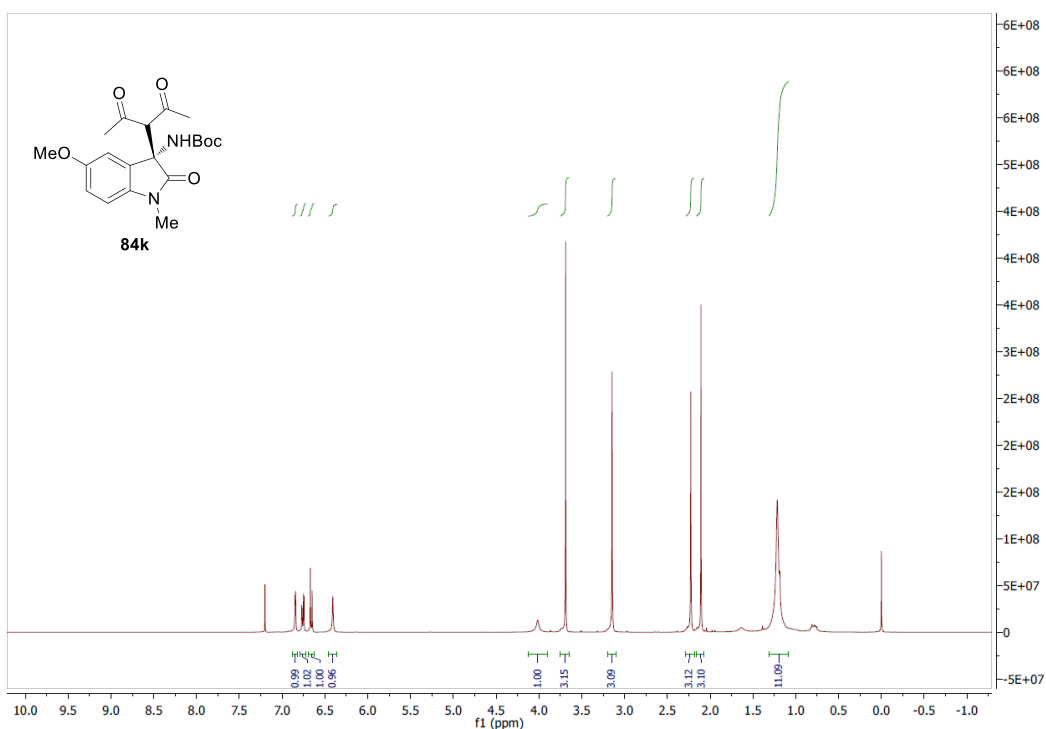


Figure A. 19  $^1\text{H}$  NMR spectrum of **84k**

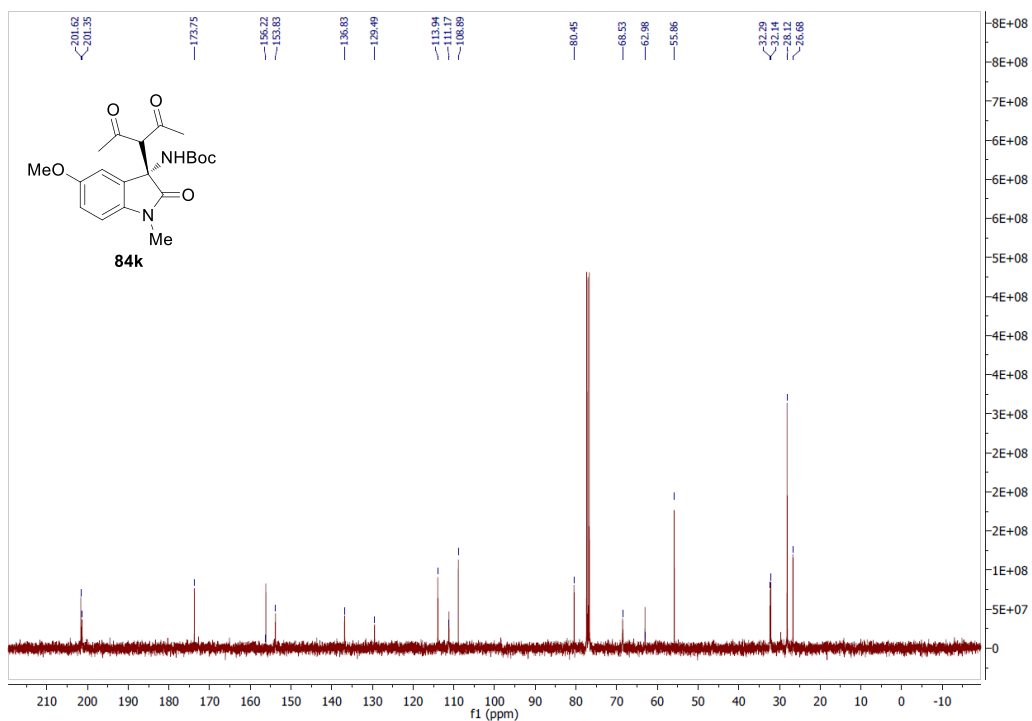
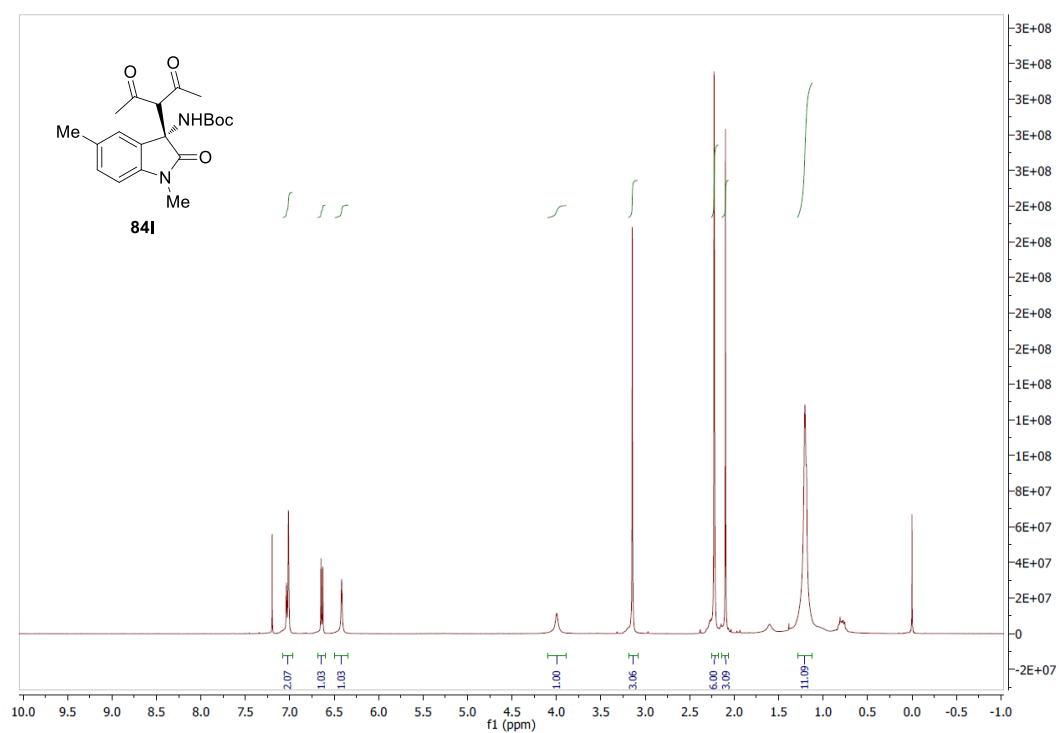
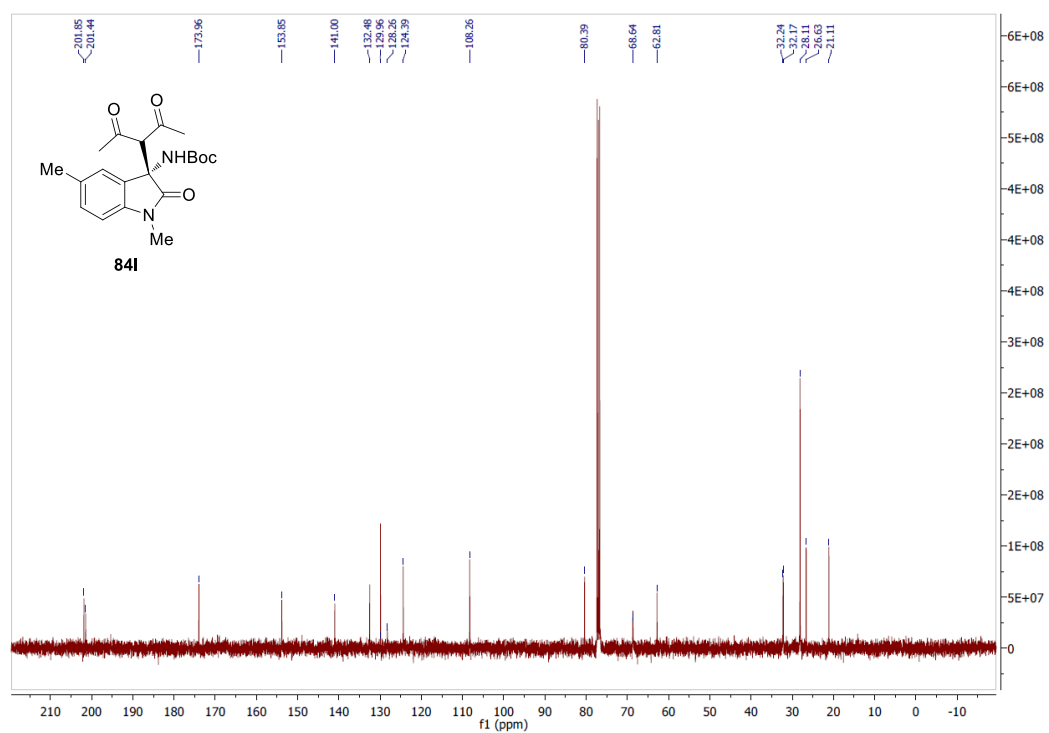


Figure A. 20  $^{13}\text{C}$  NMR spectrum of **84k**



**Figure A. 21**  $^1\text{H}$  NMR spectrum of **84I**



**Figure A. 22**  $^{13}\text{C}$  NMR spectrum of **84I**

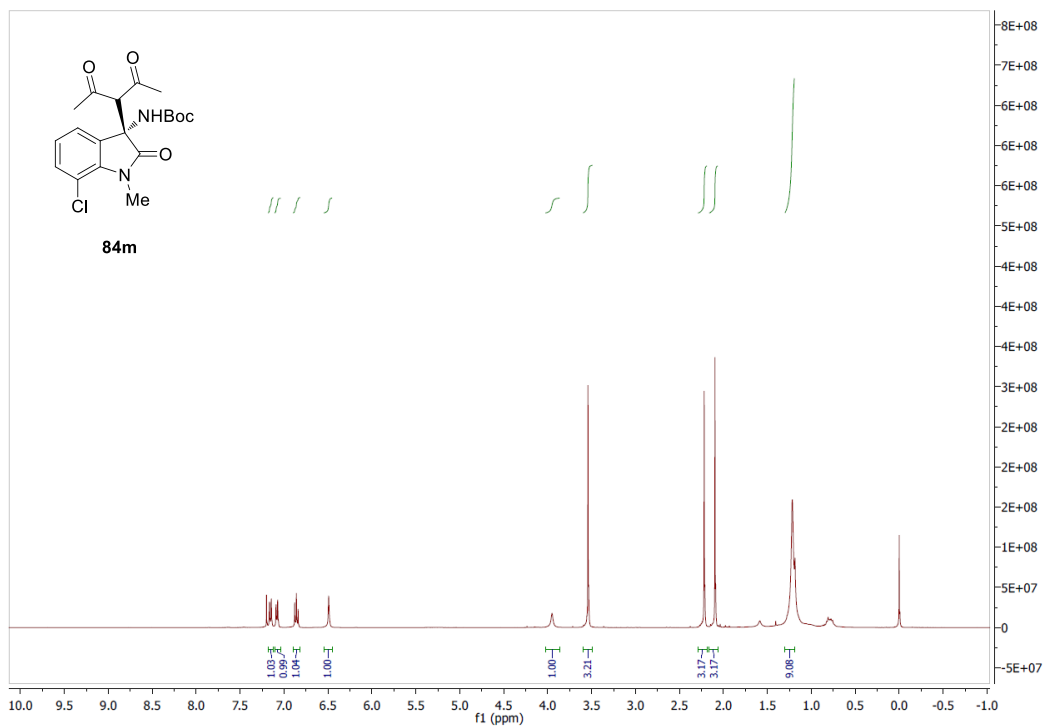


Figure A. 23  $^1\text{H}$  NMR spectrum of **84m**

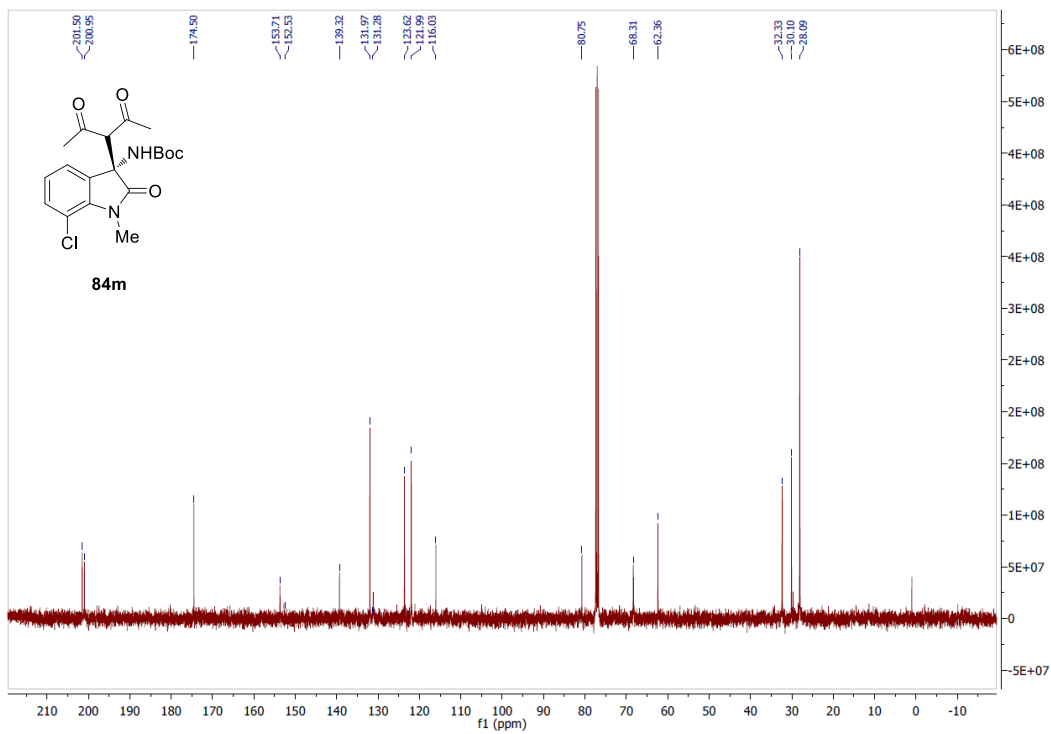


Figure A. 24  $^{13}\text{C}$  NMR spectrum of **84m**



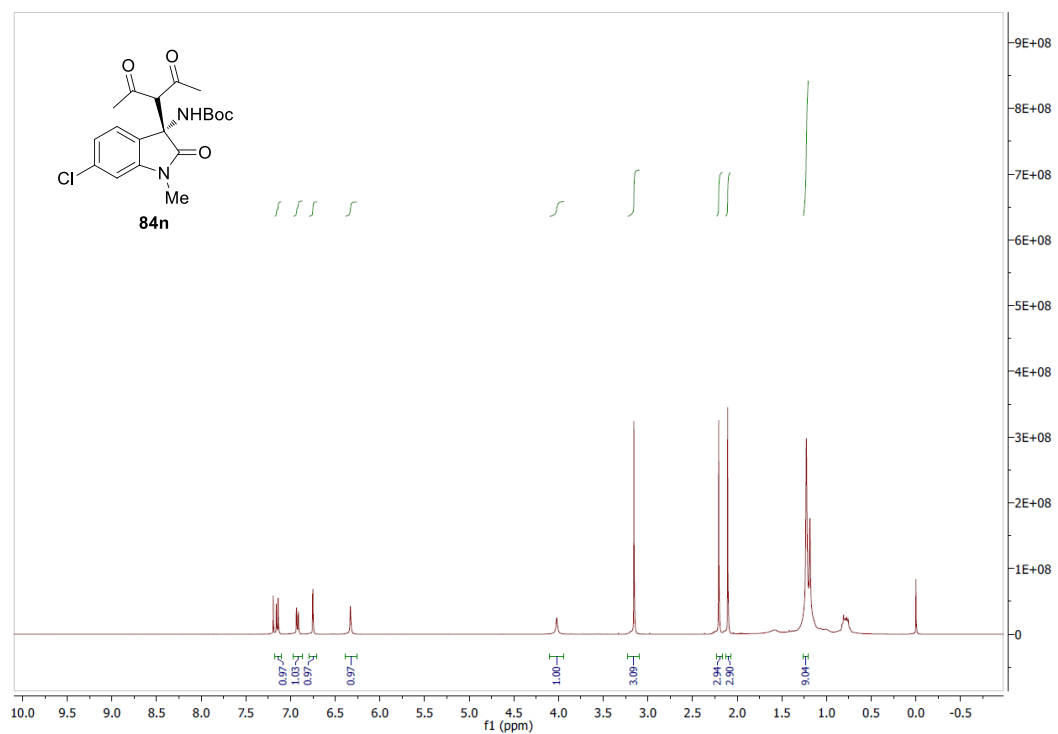


Figure A. 25 <sup>1</sup>H NMR spectrum of **84n**

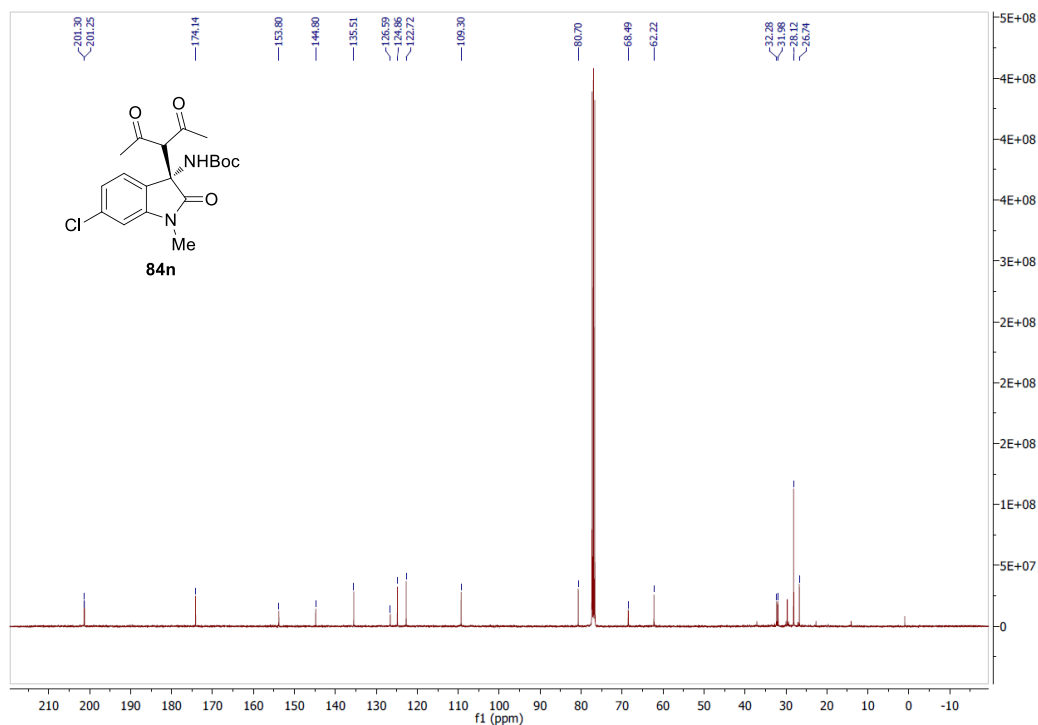
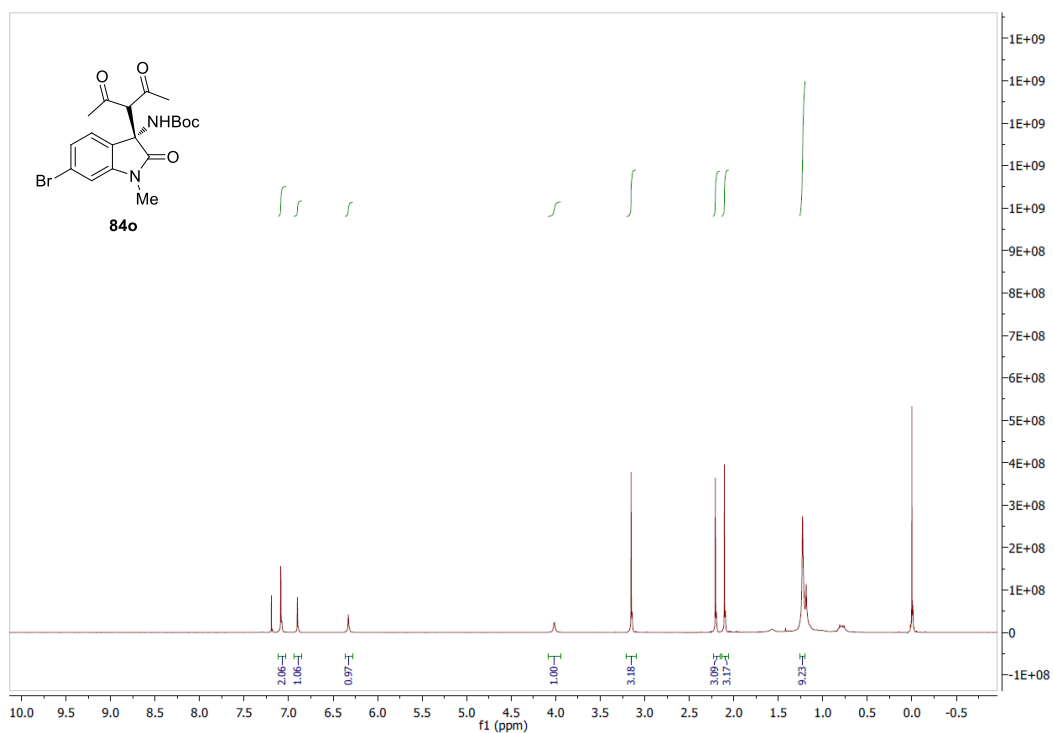
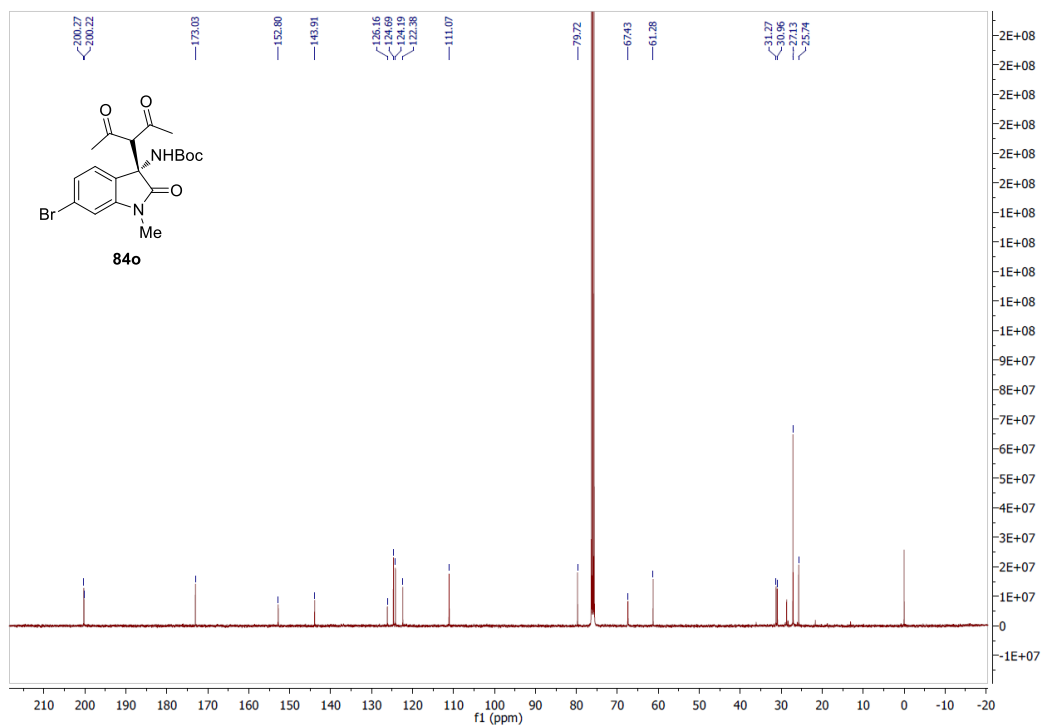


Figure A. 26 <sup>13</sup>C NMR spectrum of **84n**



**Figure A. 27** <sup>1</sup>H NMR spectrum of **84o**



**Figure A. 28** <sup>13</sup>C NMR spectrum of **84o**

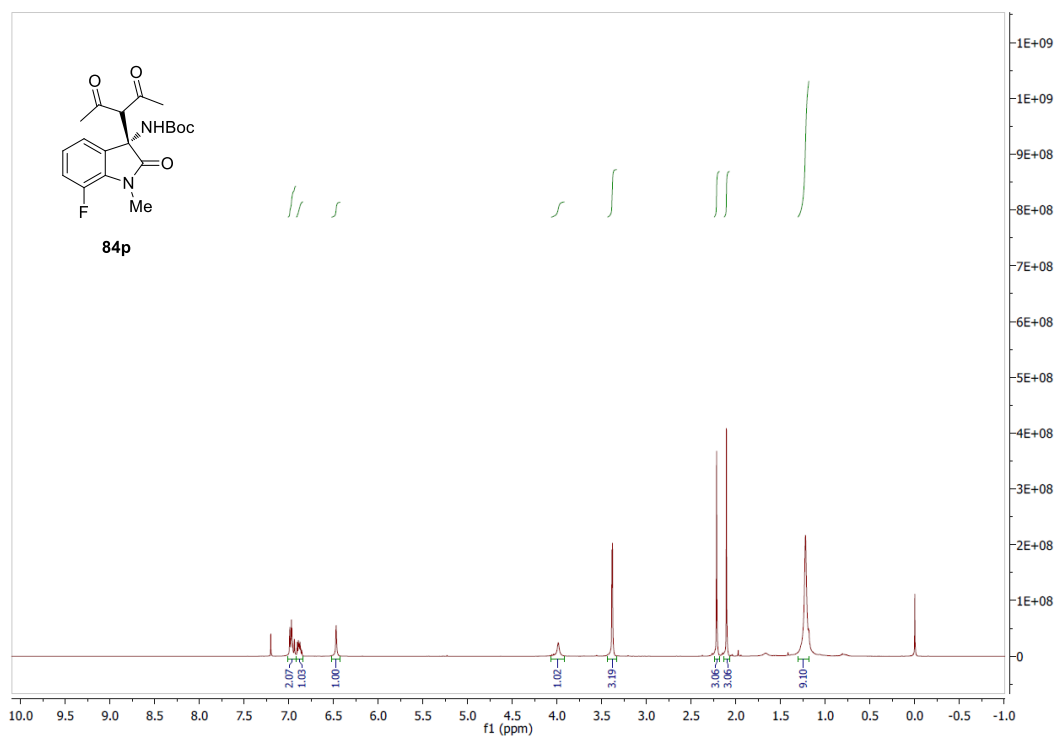


Figure A. 29  $^1\text{H}$  NMR spectrum of **84p**

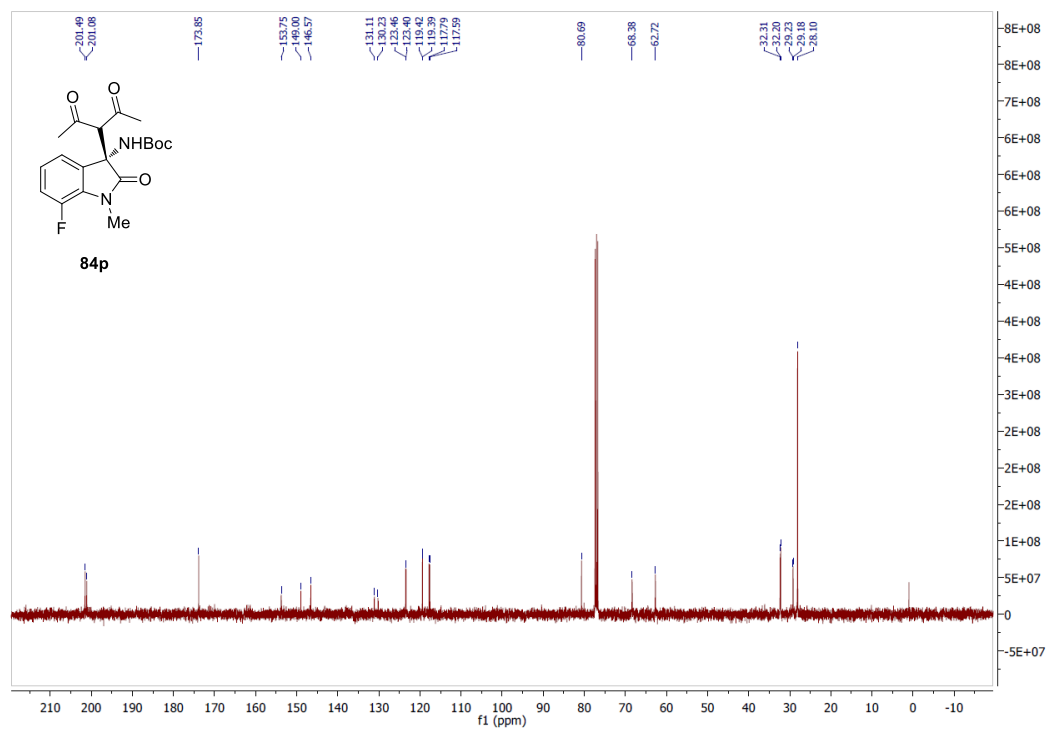


Figure A. 30  $^{13}\text{C}$  NMR spectrum of **84p**

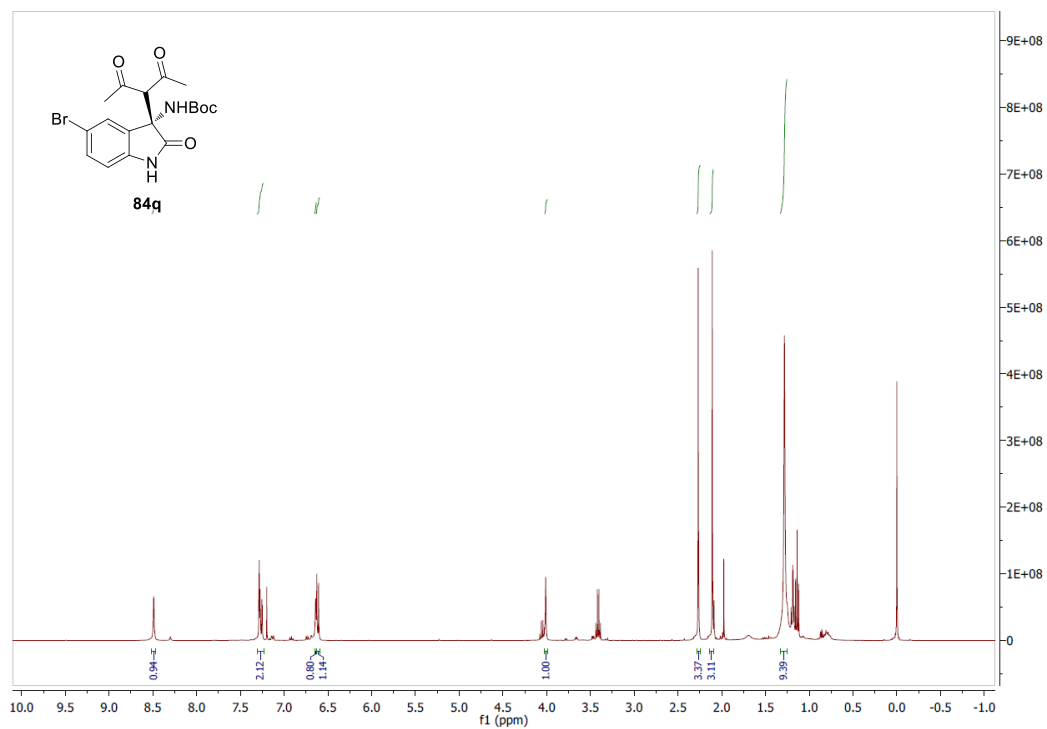


Figure A. 31 <sup>1</sup>H NMR spectrum of **84q**

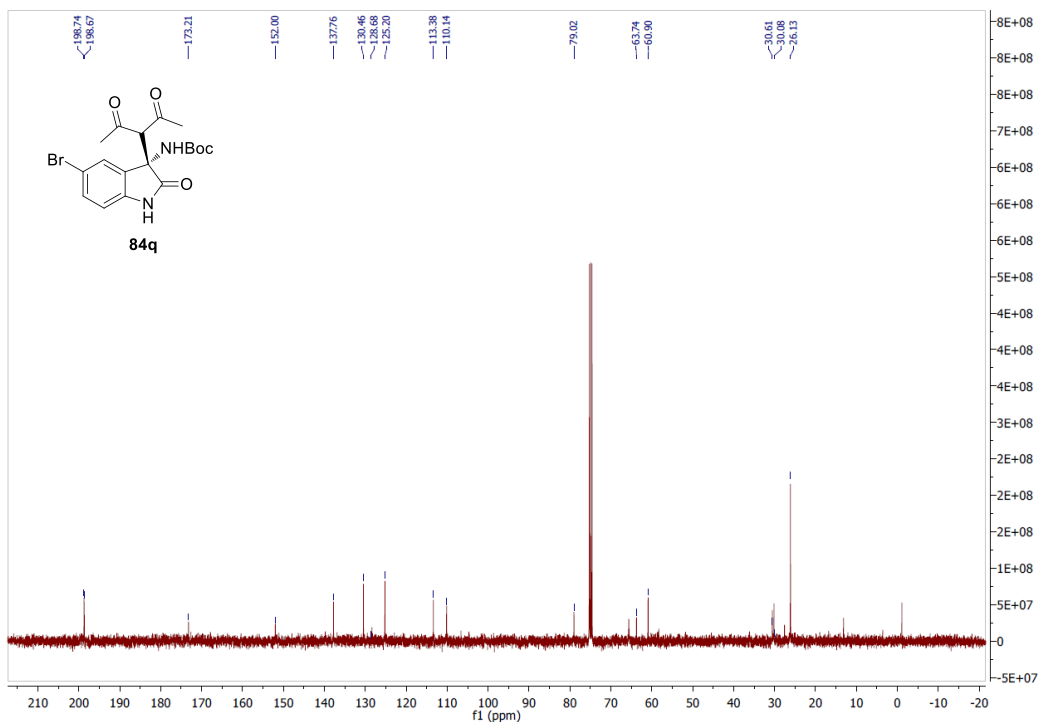
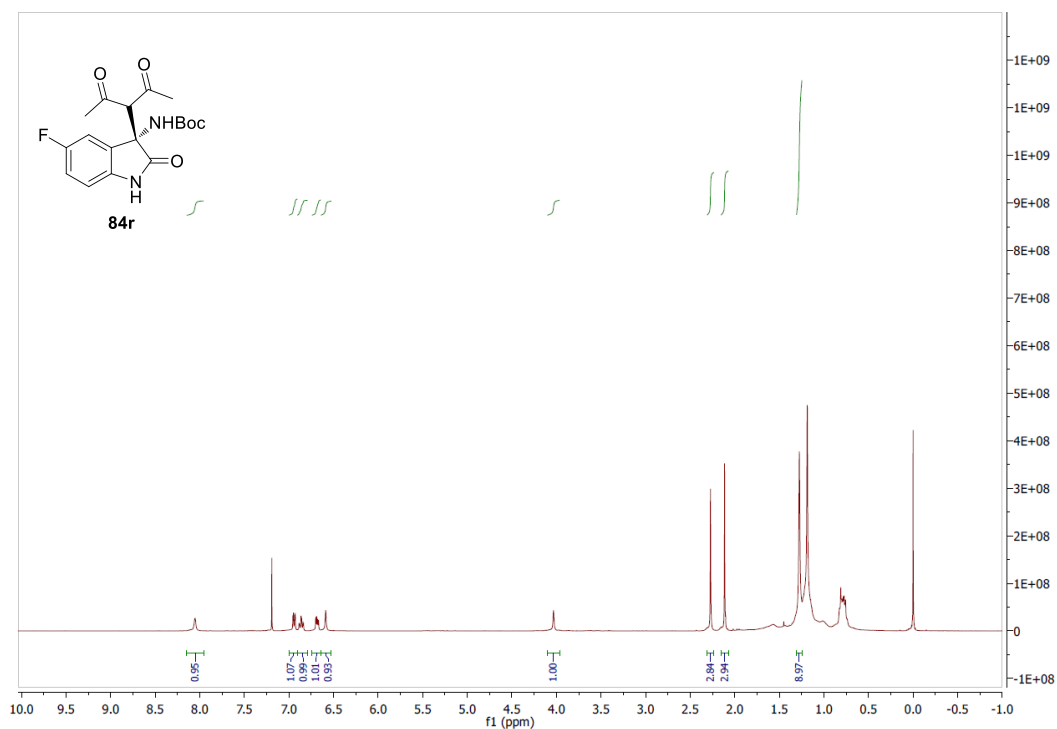
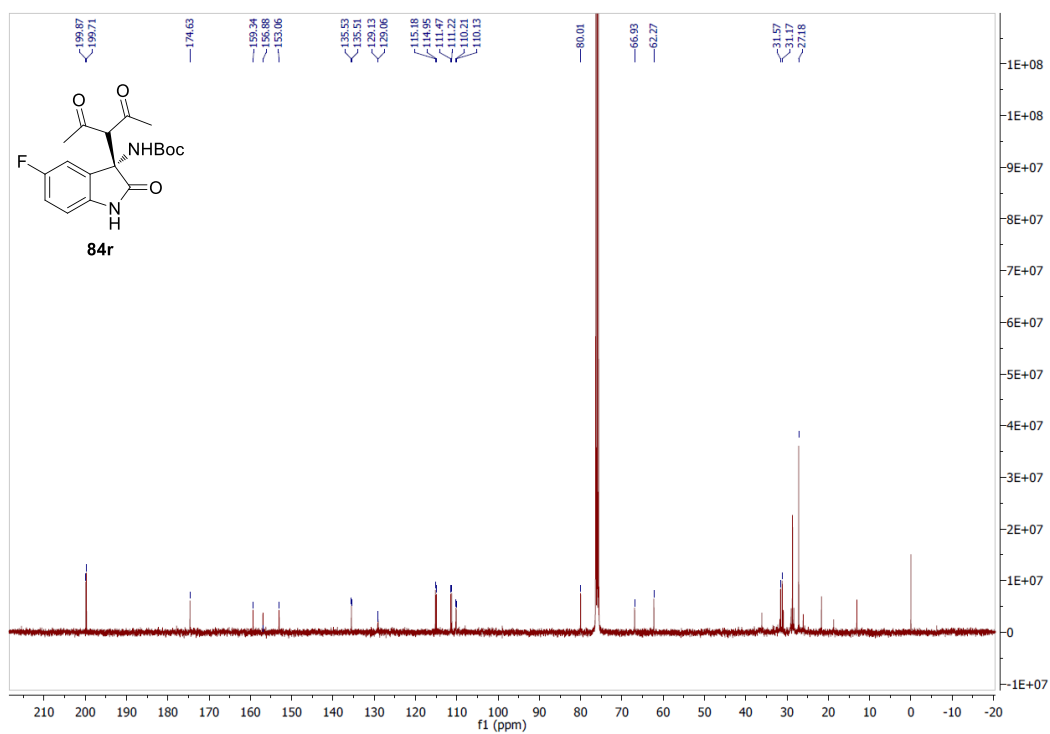


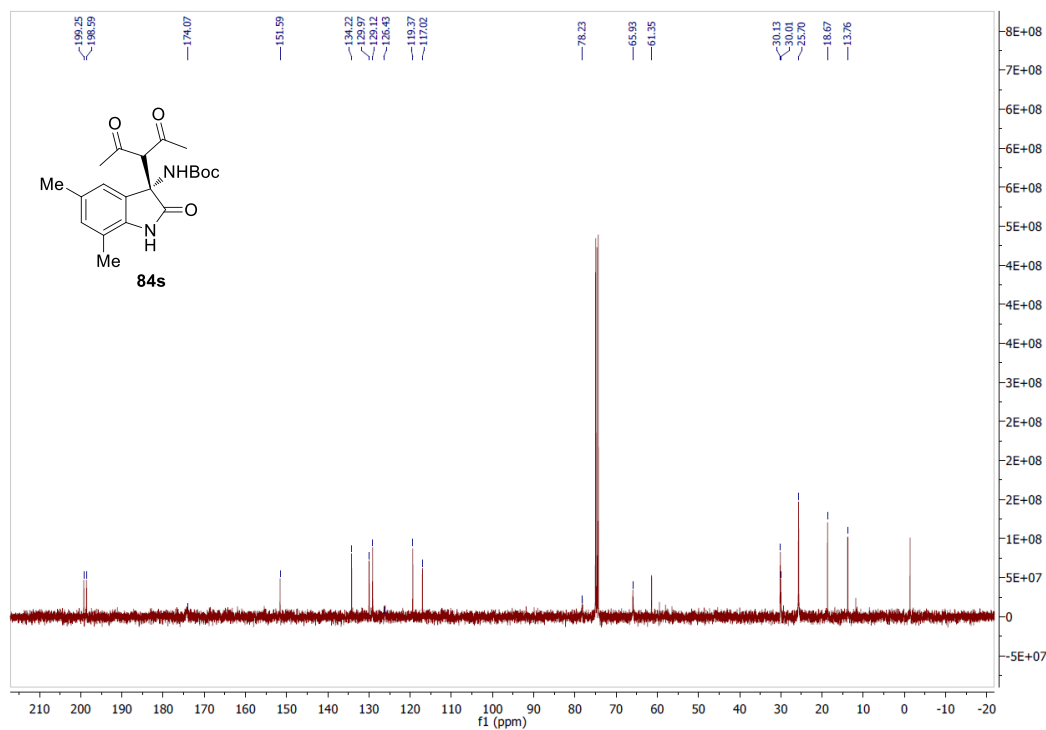
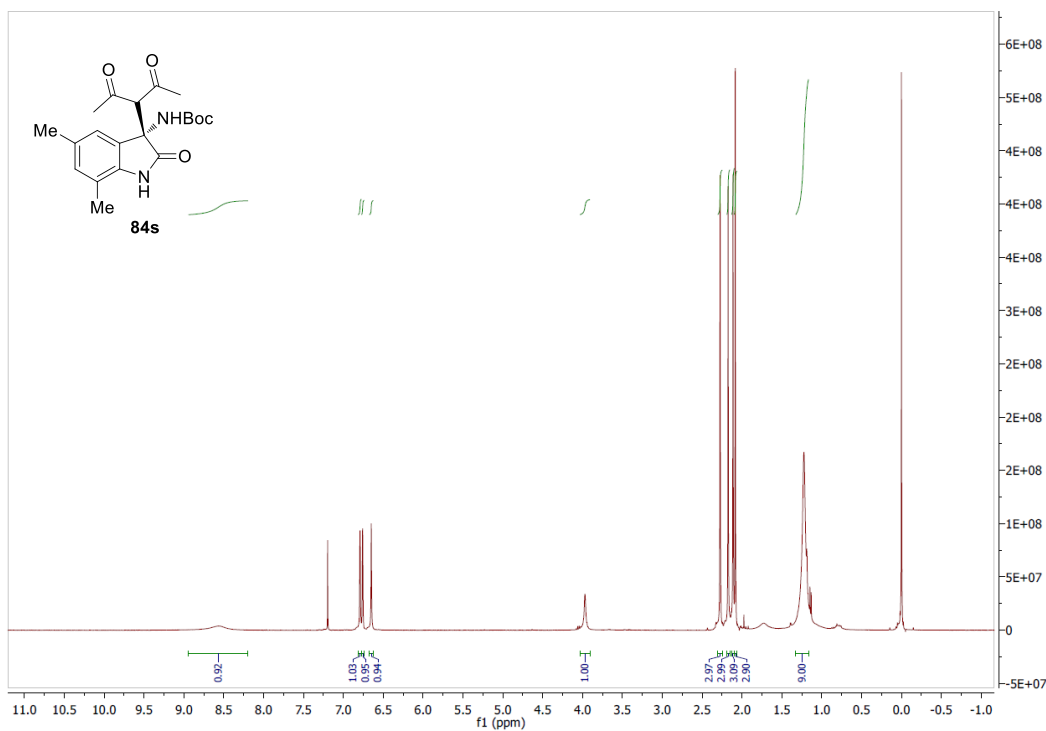
Figure A. 32 <sup>13</sup>C NMR spectrum of **84q**



**Figure A. 33** <sup>1</sup>H NMR spectrum of **84r**



**Figure A. 34** <sup>13</sup>C NMR spectrum of **84r**



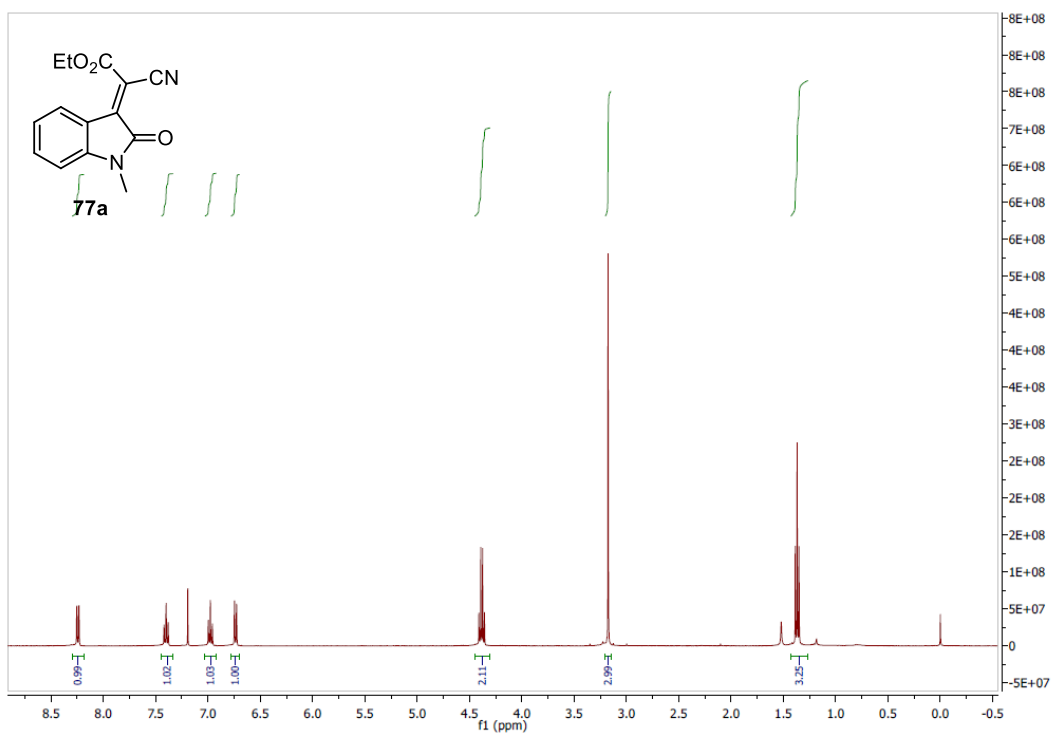


Figure A. 37 <sup>1</sup>H NMR spectrum of **77a**

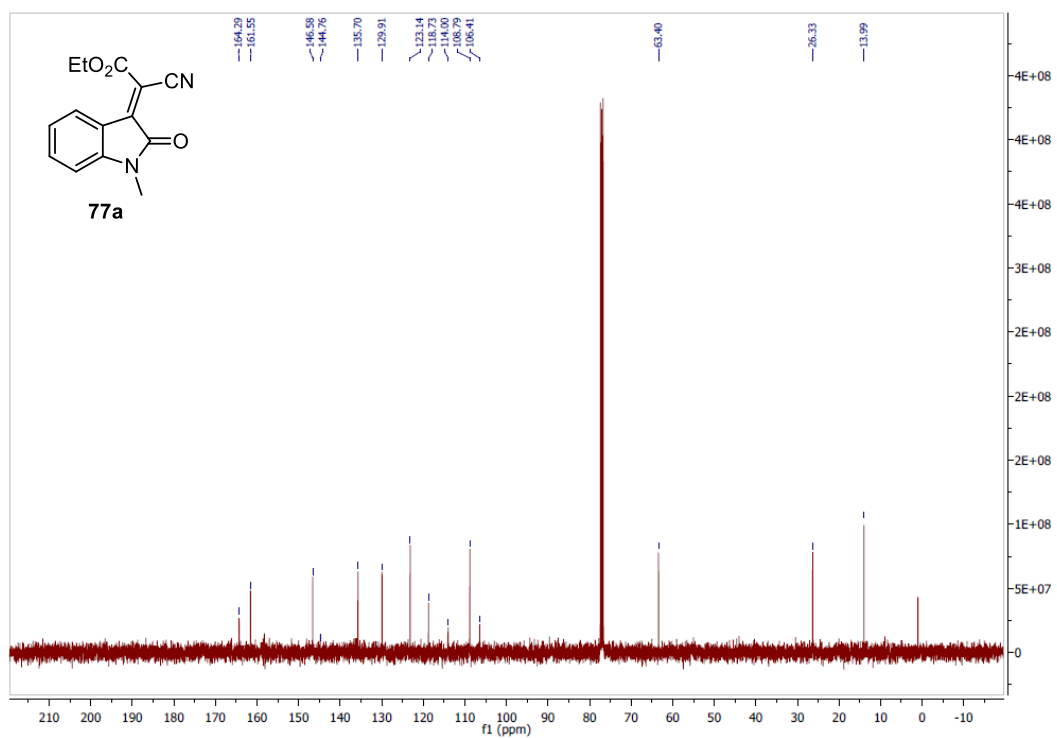


Figure A. 38 <sup>13</sup>C NMR spectrum of **77a**

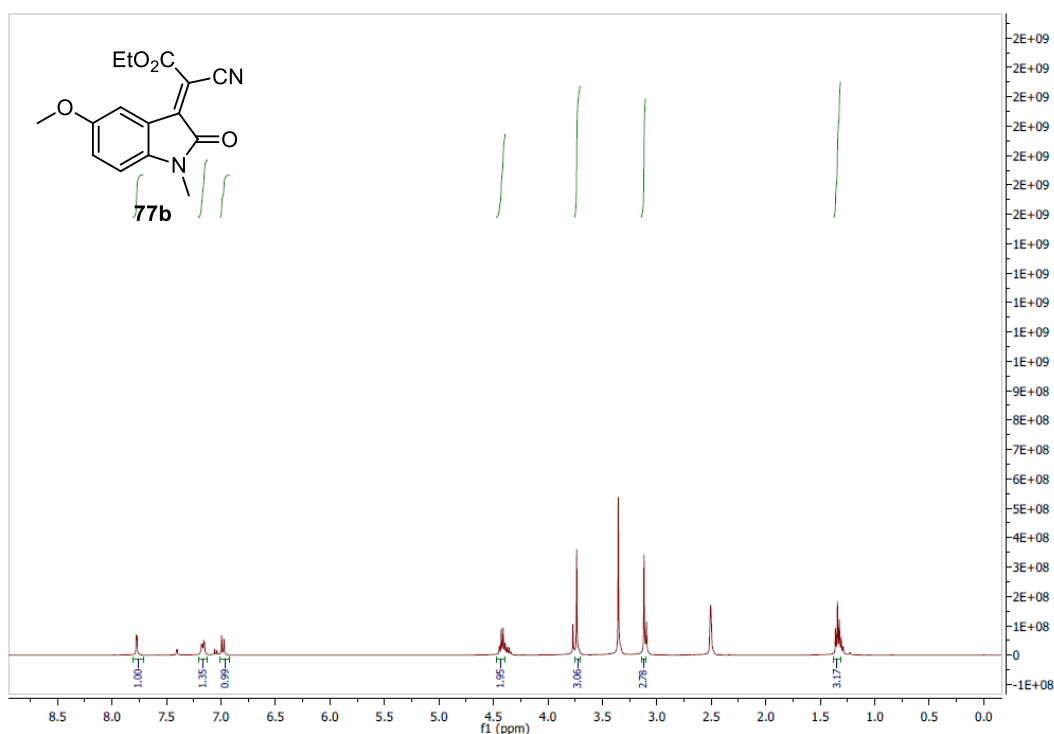


Figure A. 39 <sup>1</sup>H NMR spectrum of **77b**

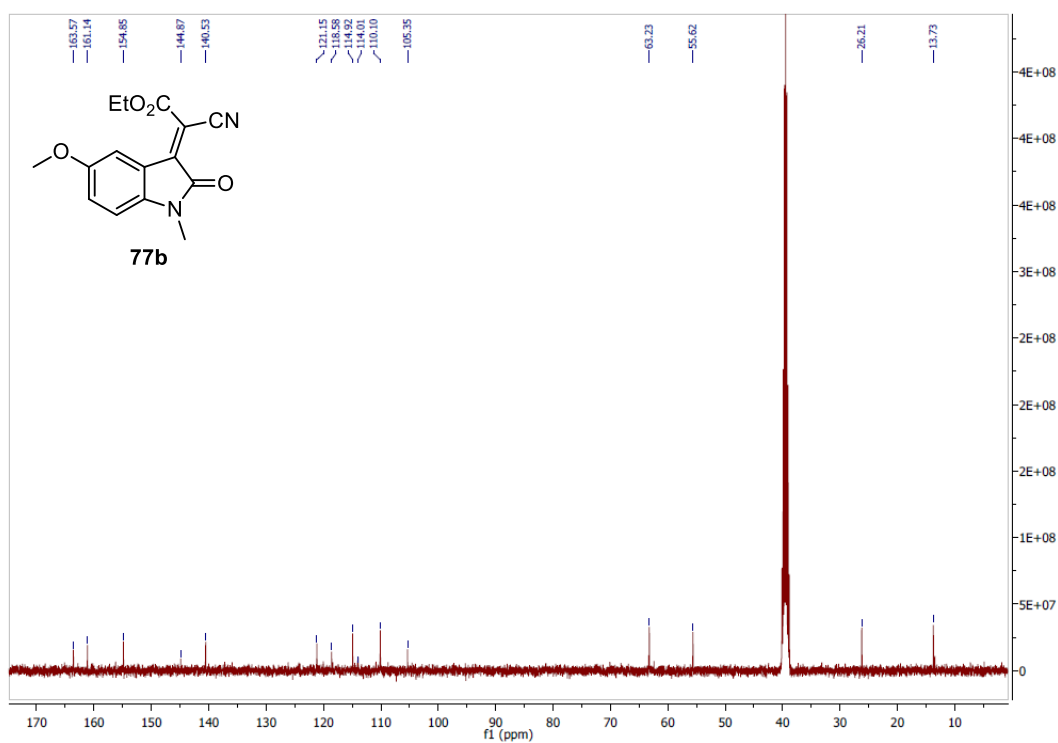


Figure A. 40 <sup>13</sup>C NMR spectrum of **77b**



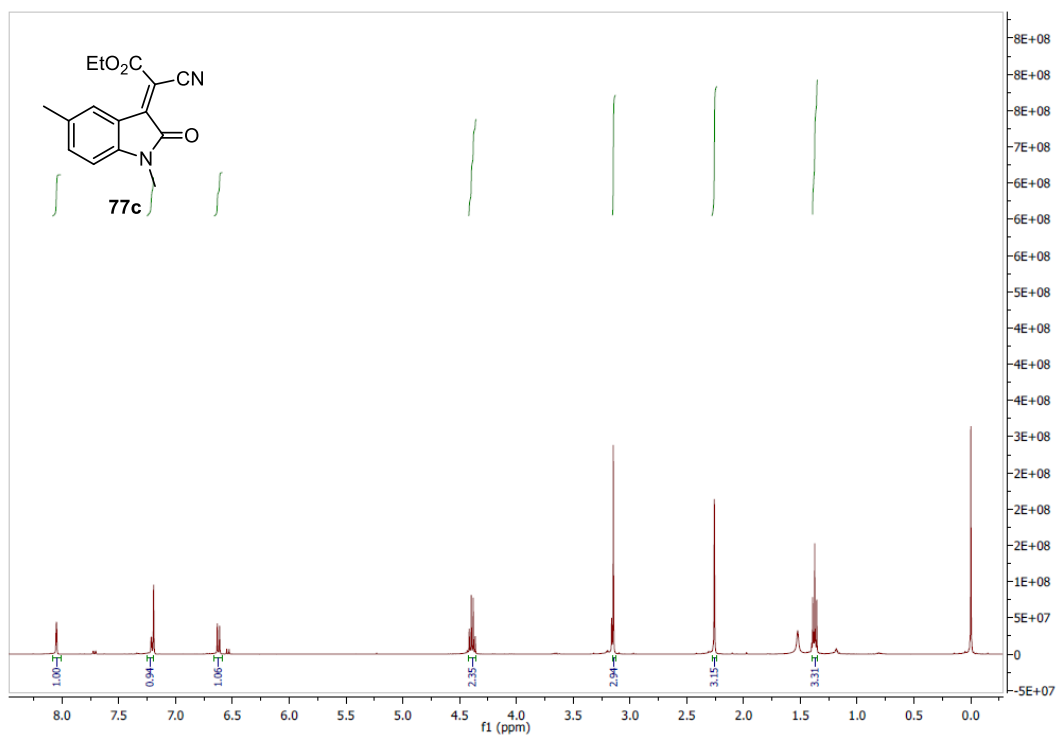


Figure A. 41 <sup>1</sup>H NMR spectrum of **77c**

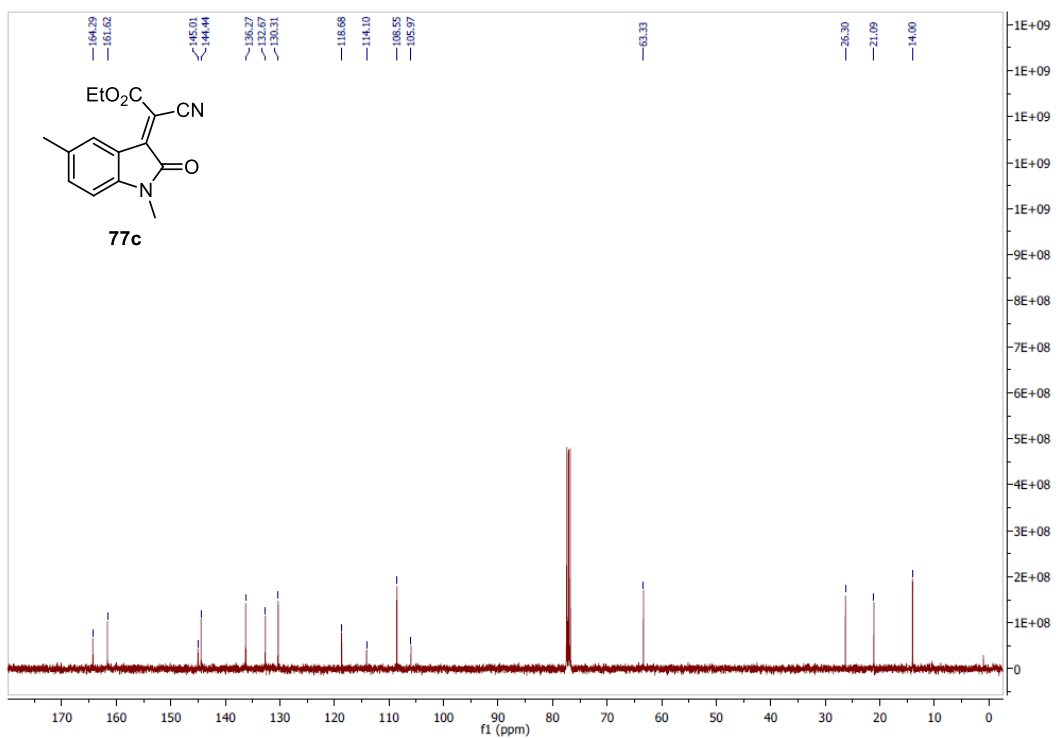
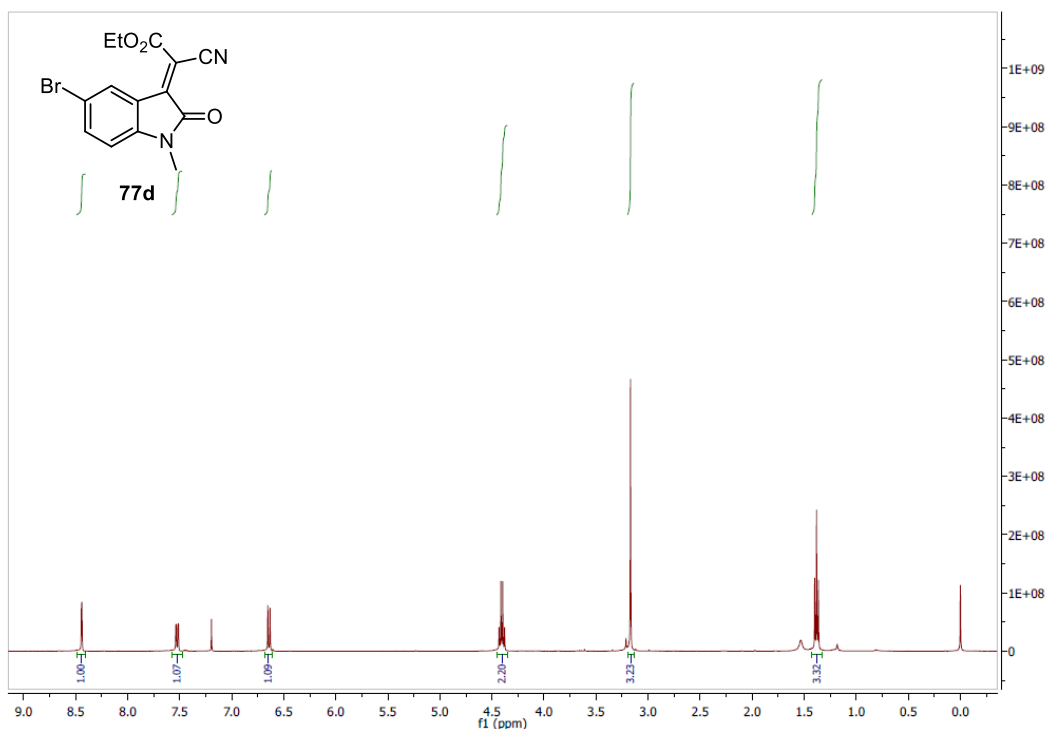
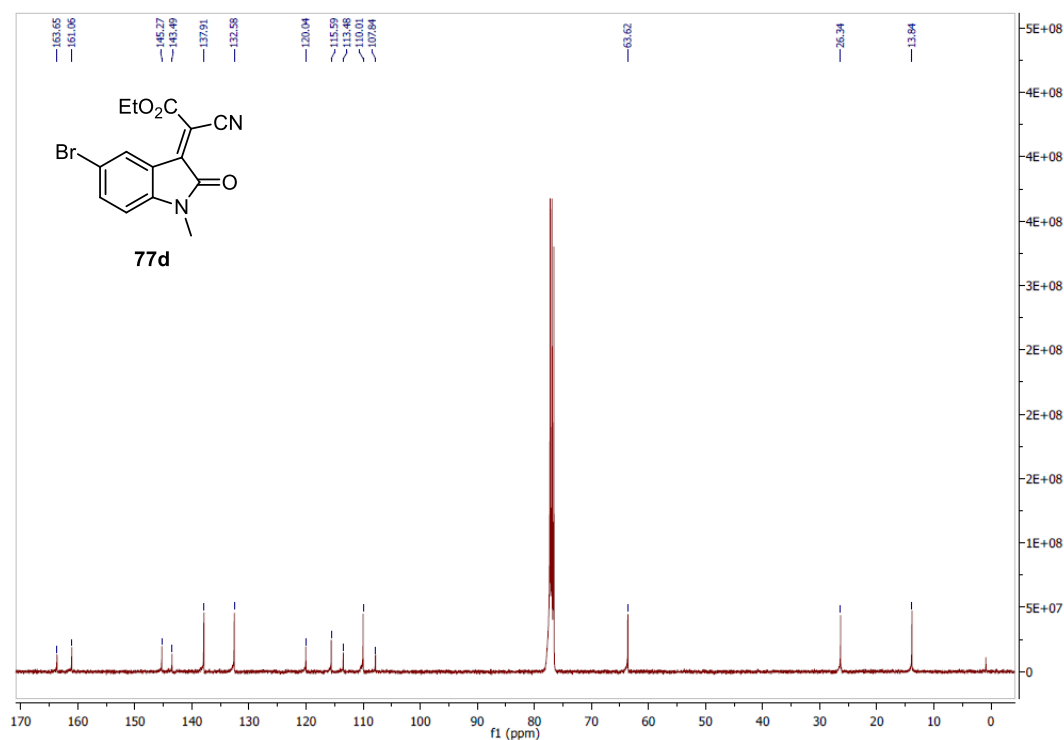


Figure A. 42 <sup>13</sup>C NMR spectrum of **77c**



**Figure A. 43** <sup>1</sup>H NMR spectrum of **77d**



**Figure A. 44** <sup>13</sup>C NMR spectrum of **77d**

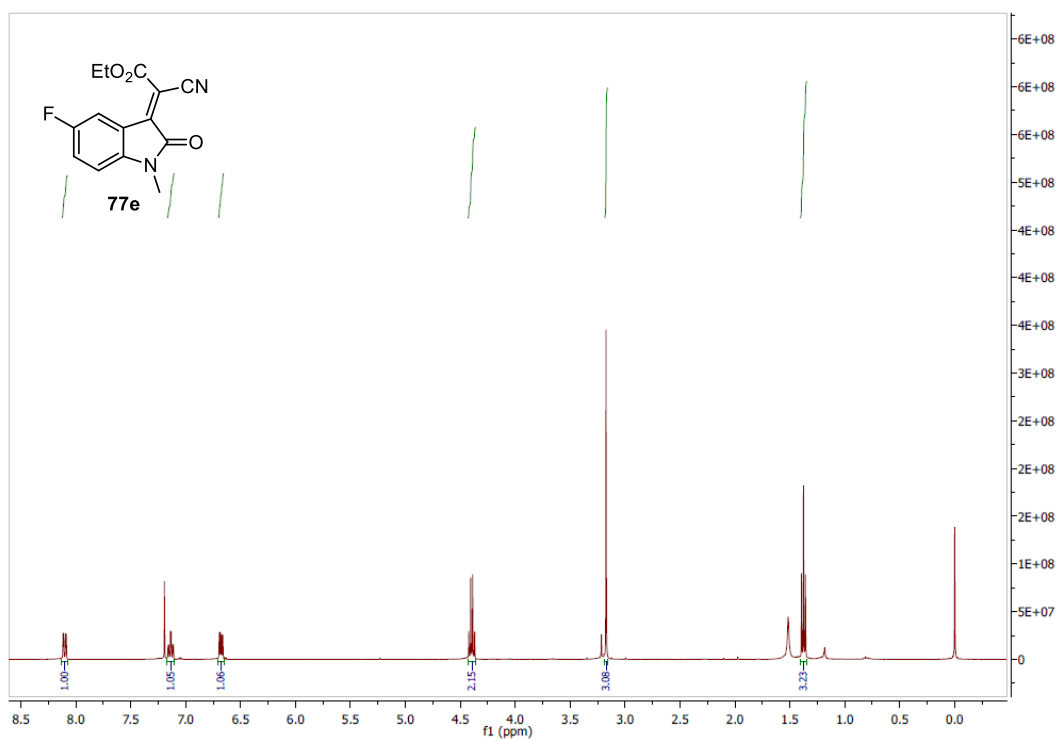


Figure A. 45 <sup>1</sup>H NMR spectrum of **77e**

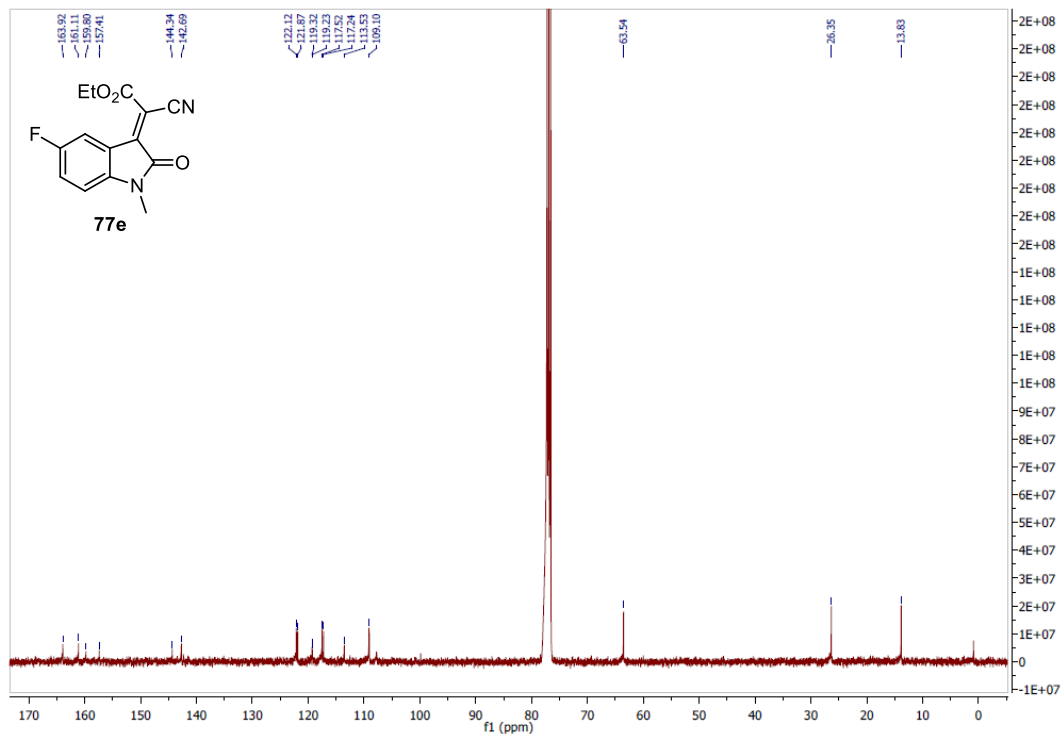


Figure A. 46 <sup>13</sup>C NMR spectrum of **77e**

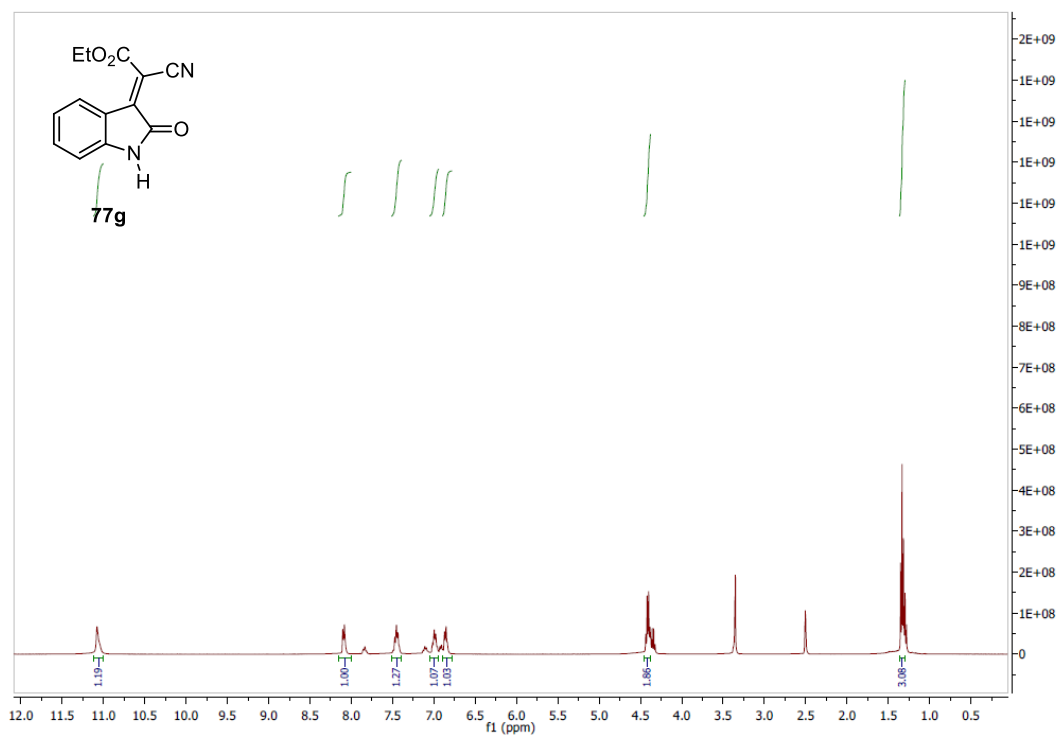


Figure A. 47 <sup>1</sup>H NMR spectrum of **77g**

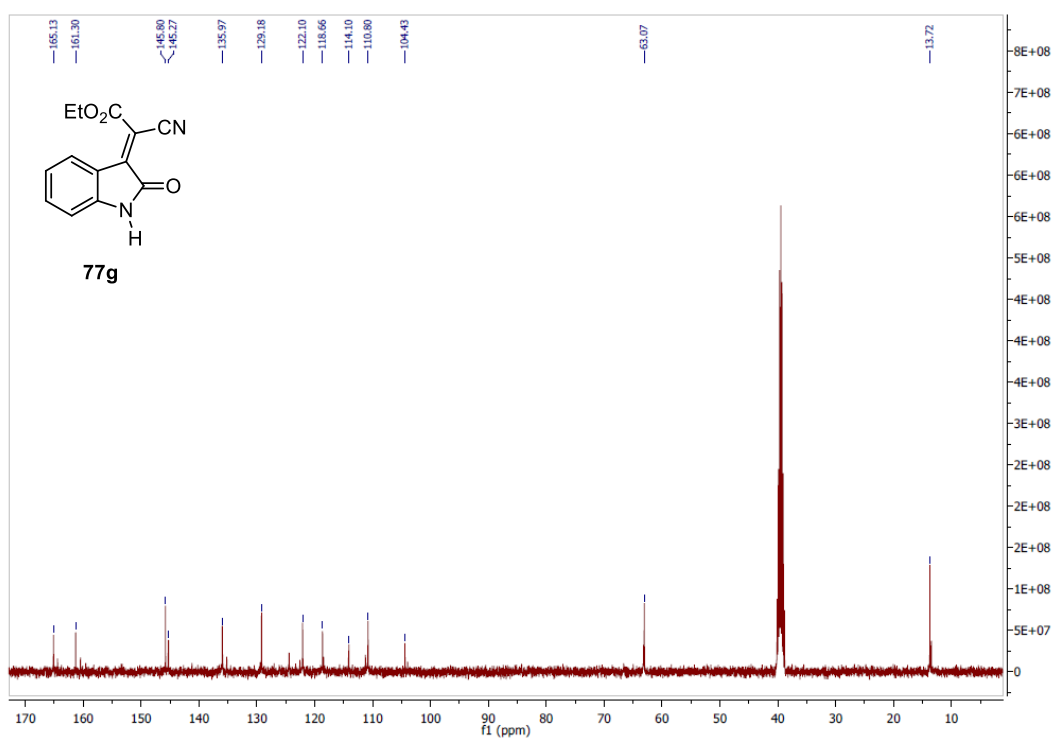


Figure A. 48 <sup>13</sup>C NMR spectrum of **77g**

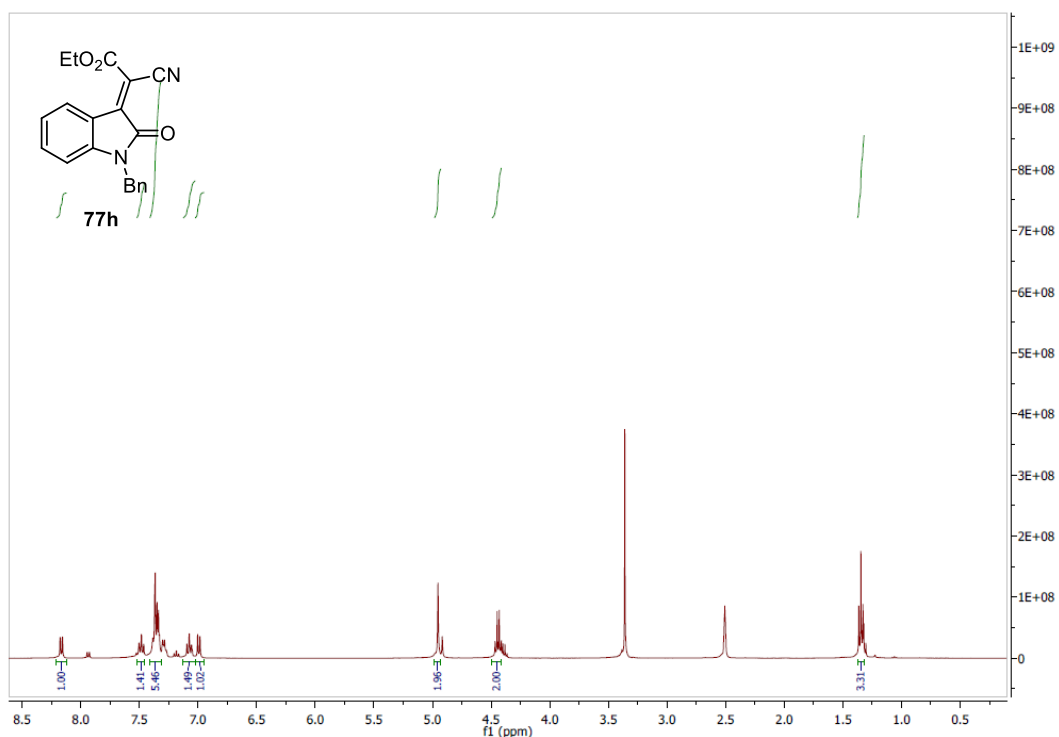


Figure A. 49 <sup>1</sup>H NMR spectrum of **77h**

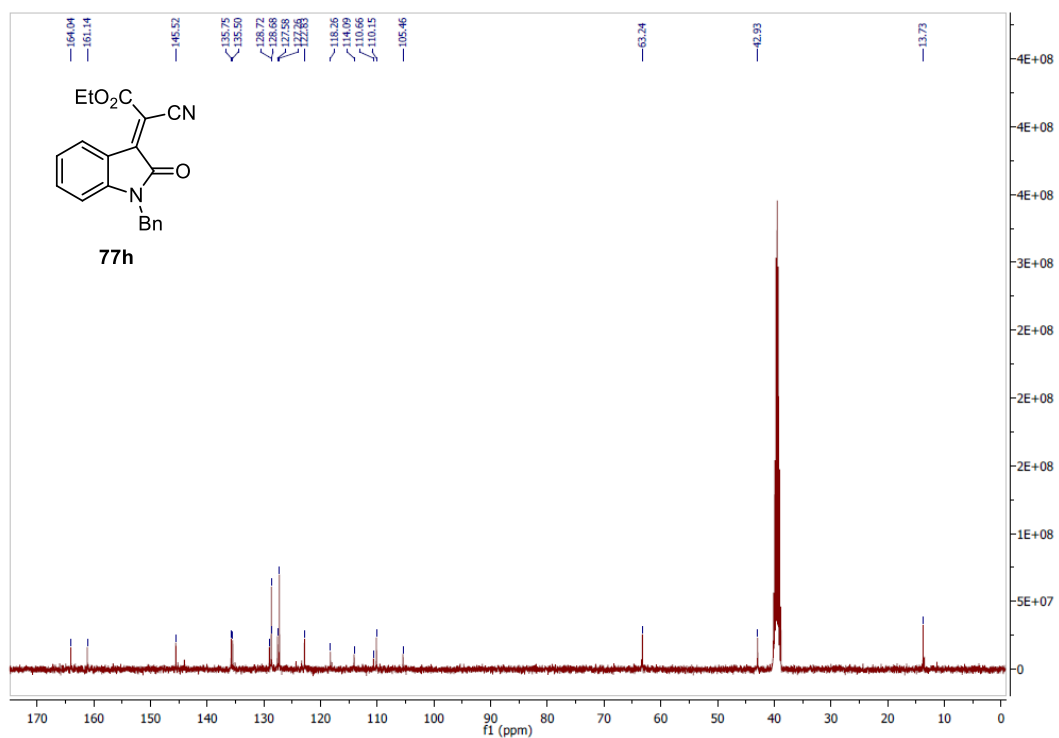


Figure A. 50 <sup>13</sup>C NMR spectrum of **77h**

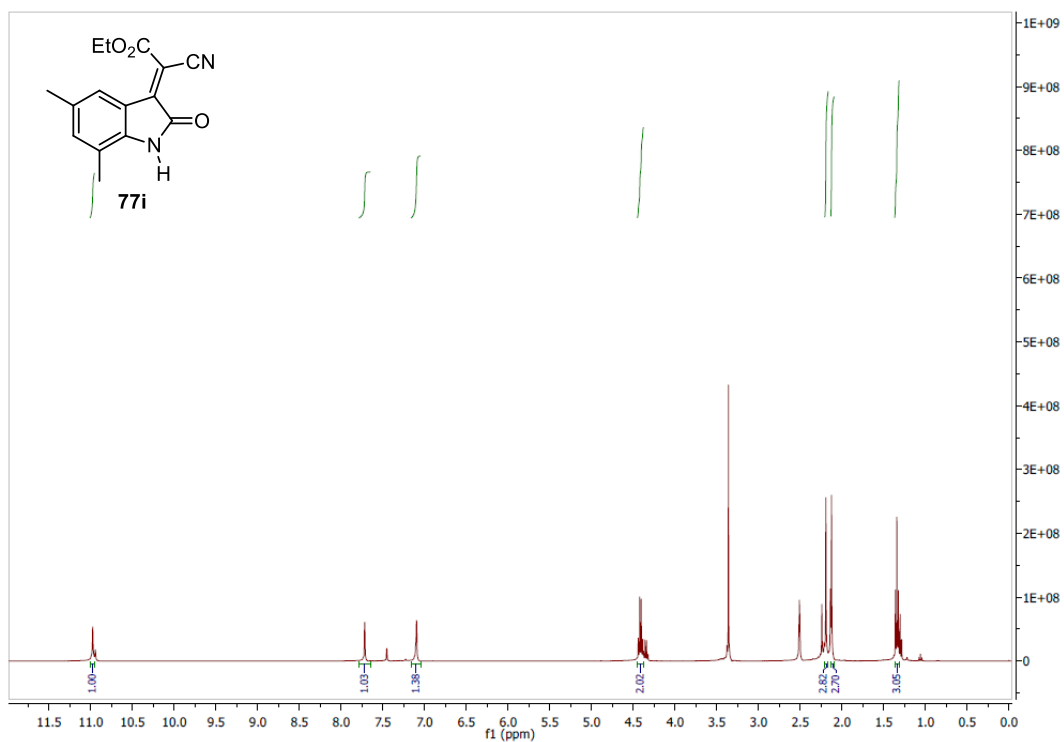


Figure A. 51 <sup>1</sup>H NMR spectrum of **77i**

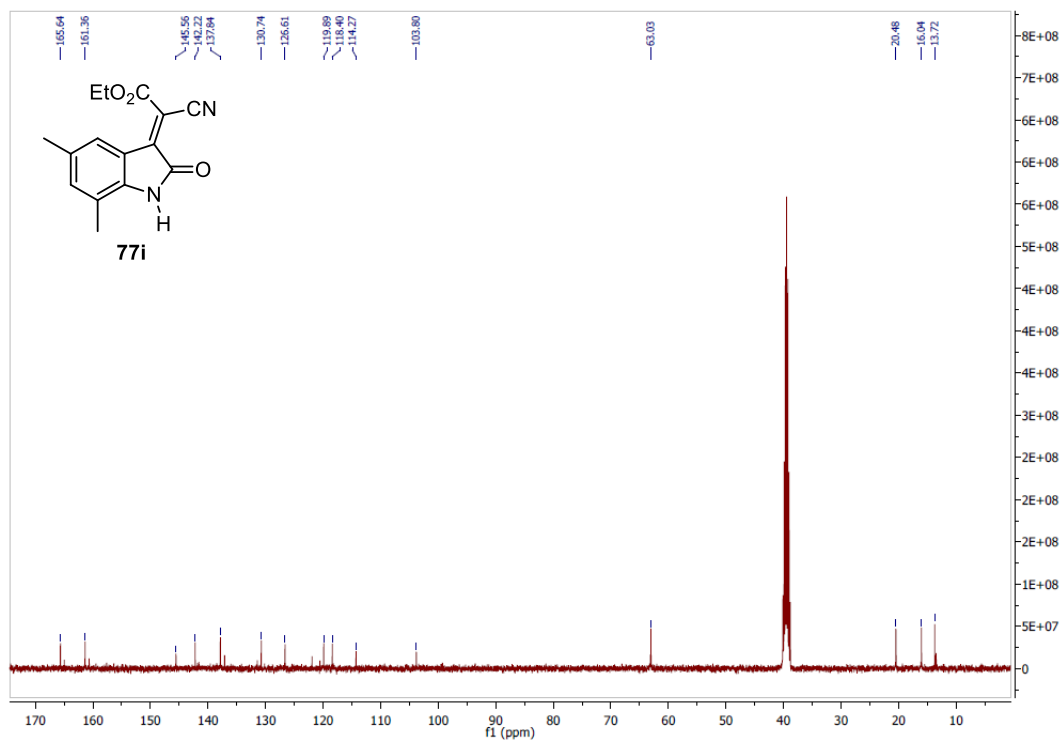
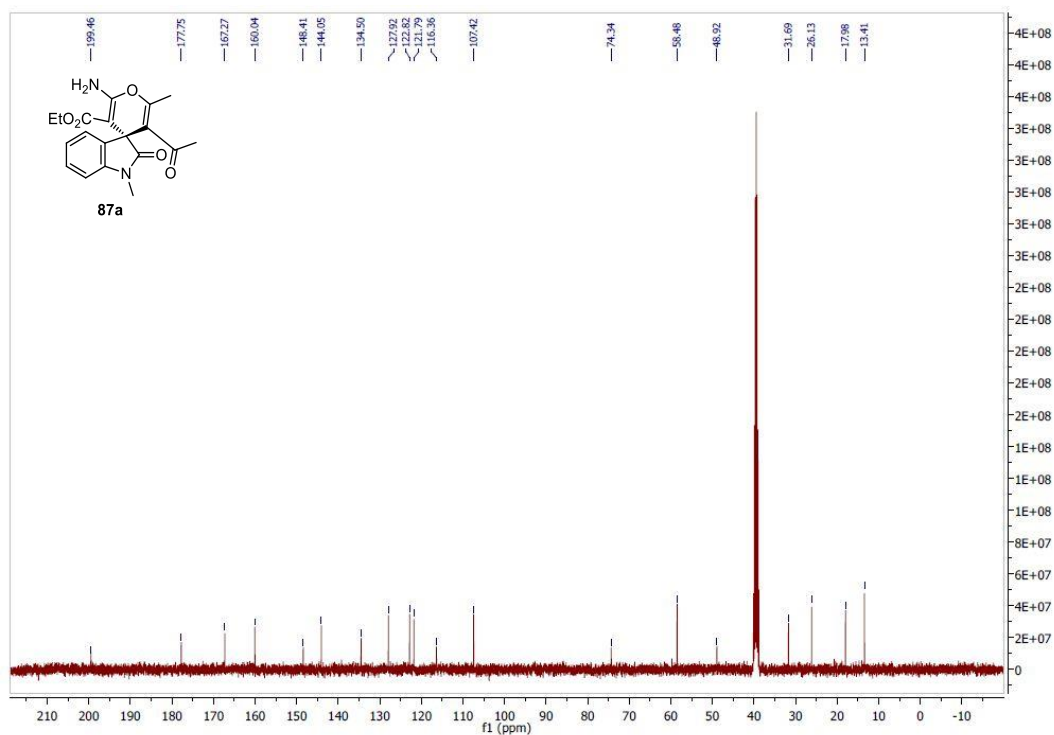
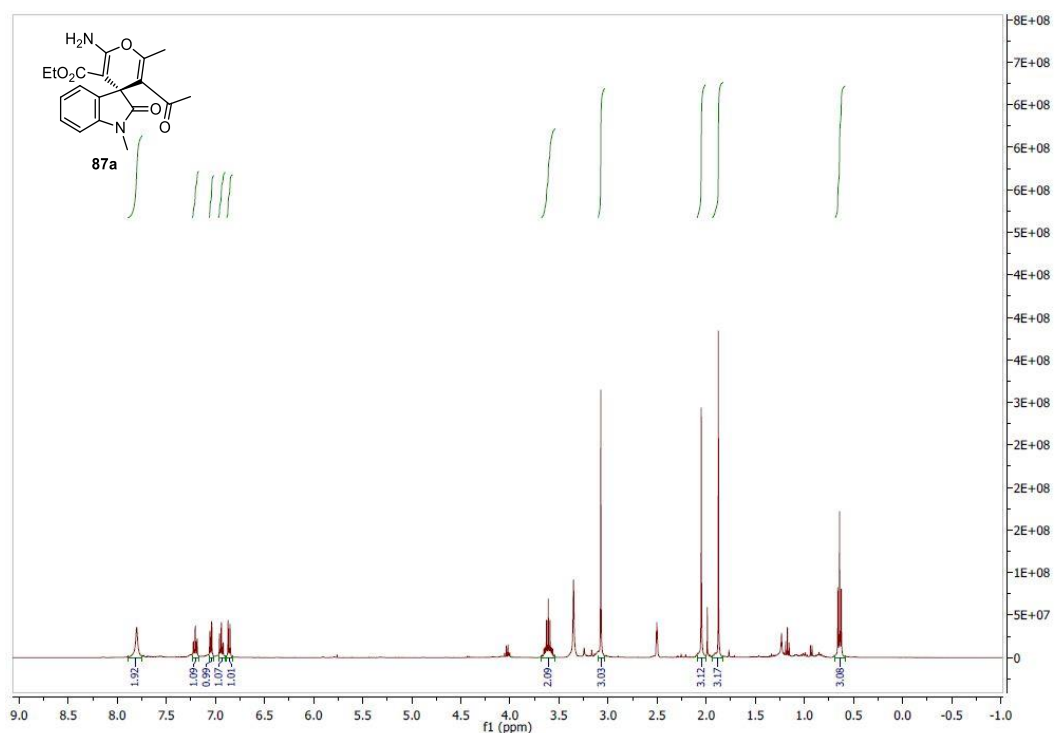
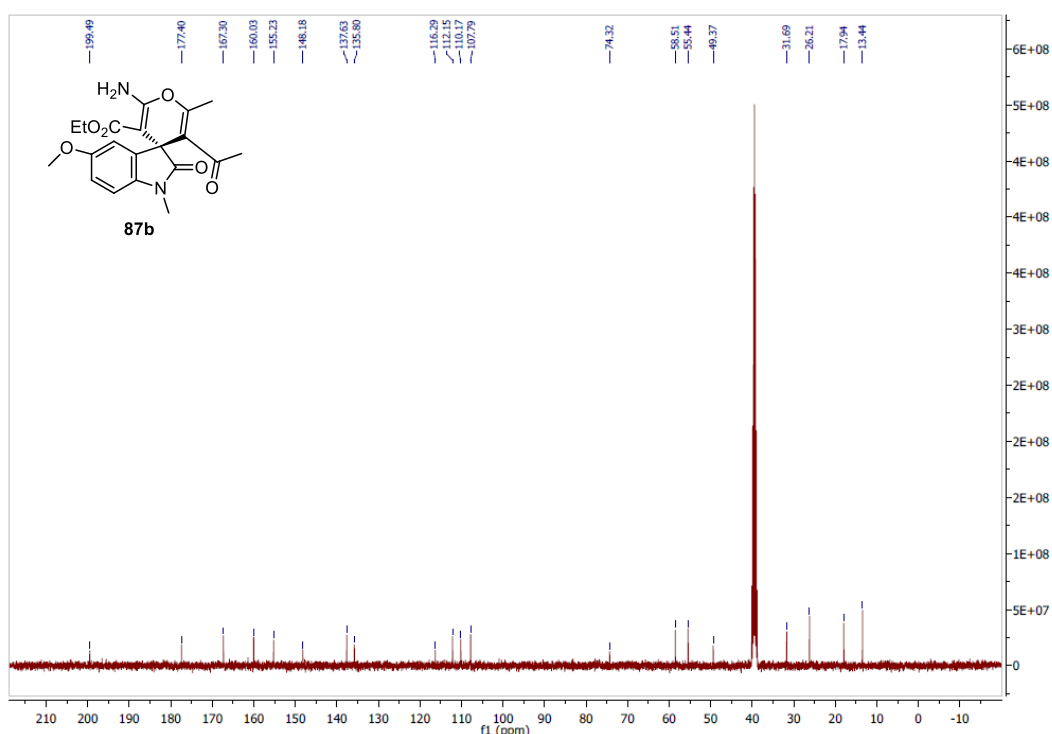
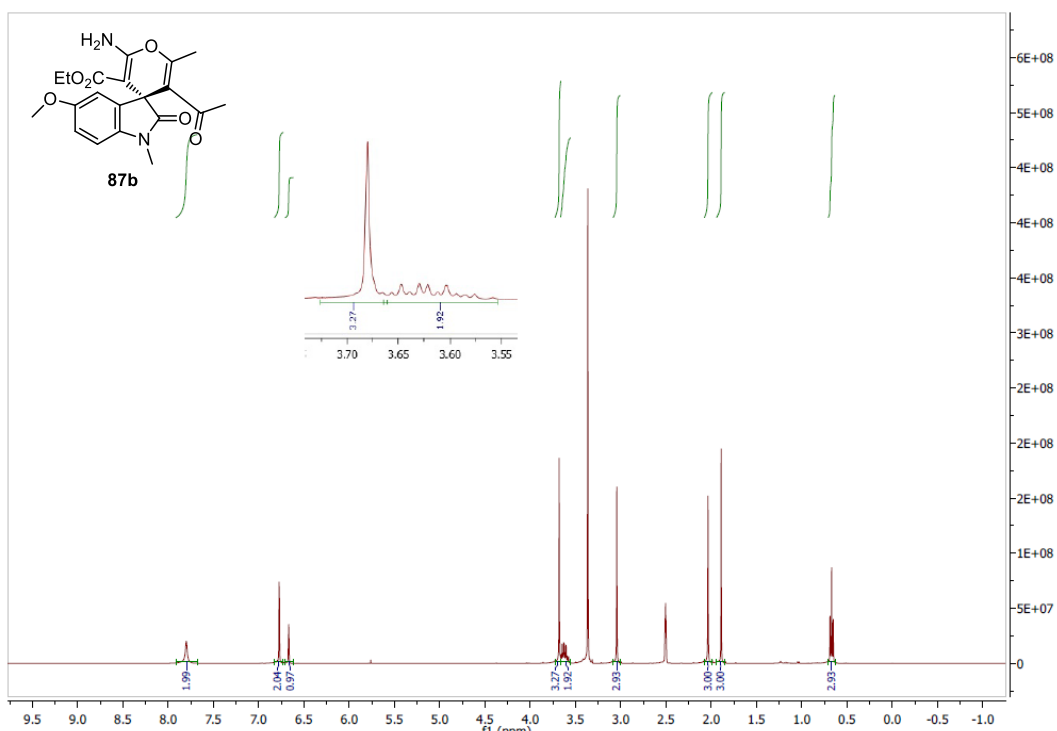
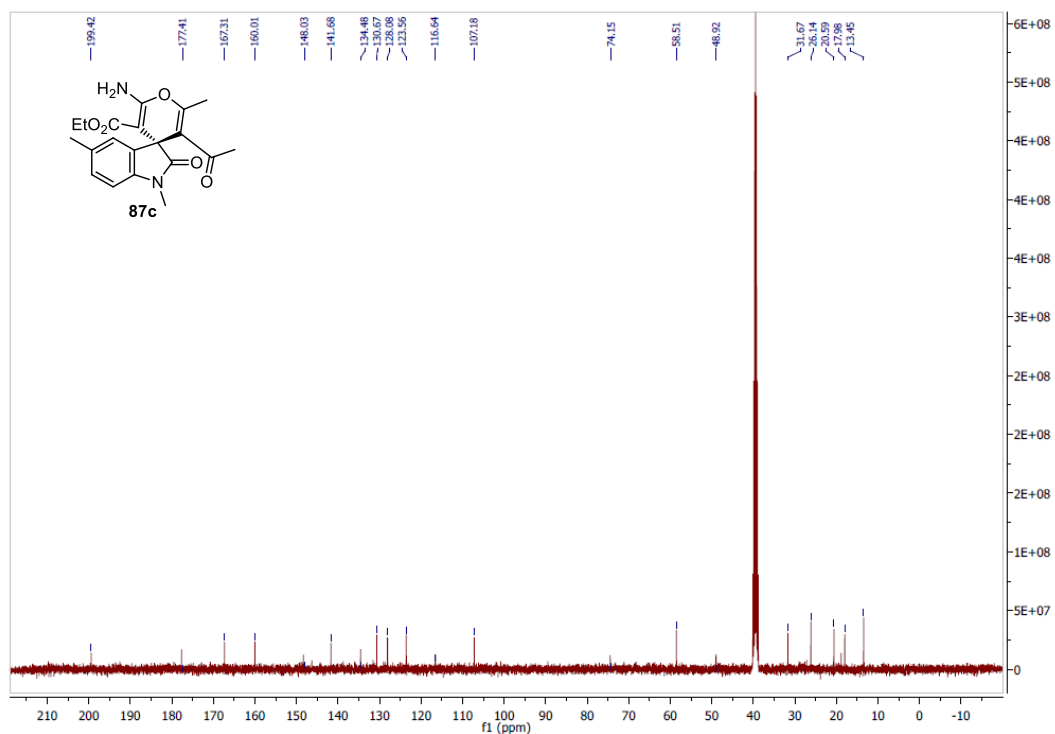
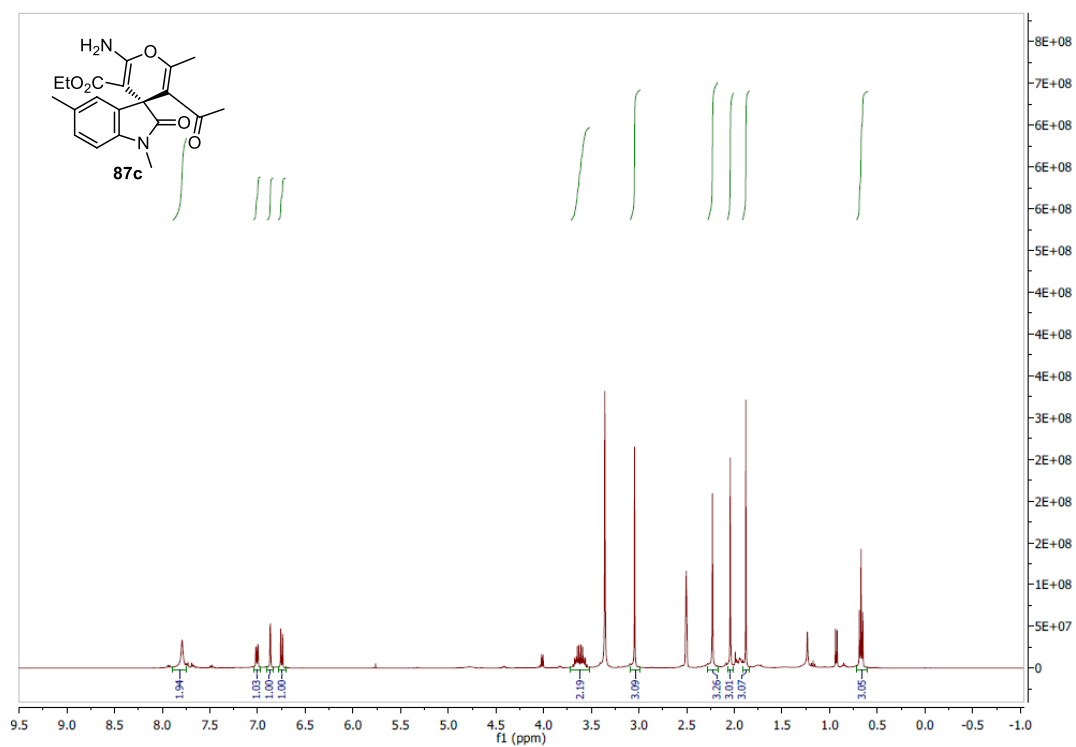


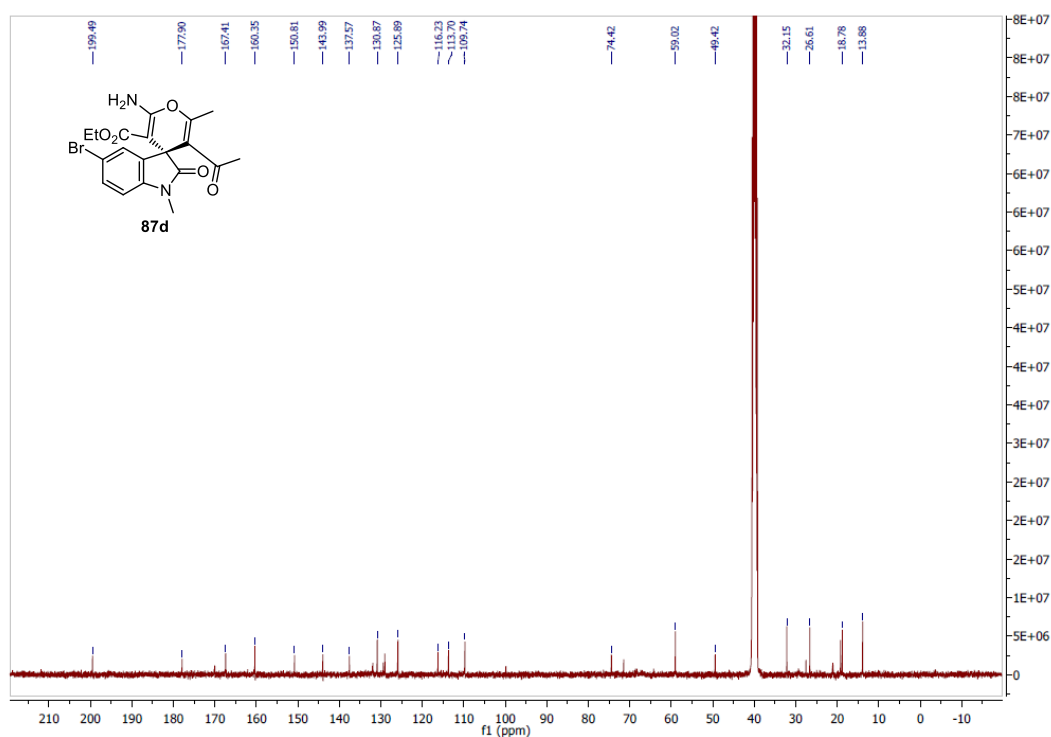
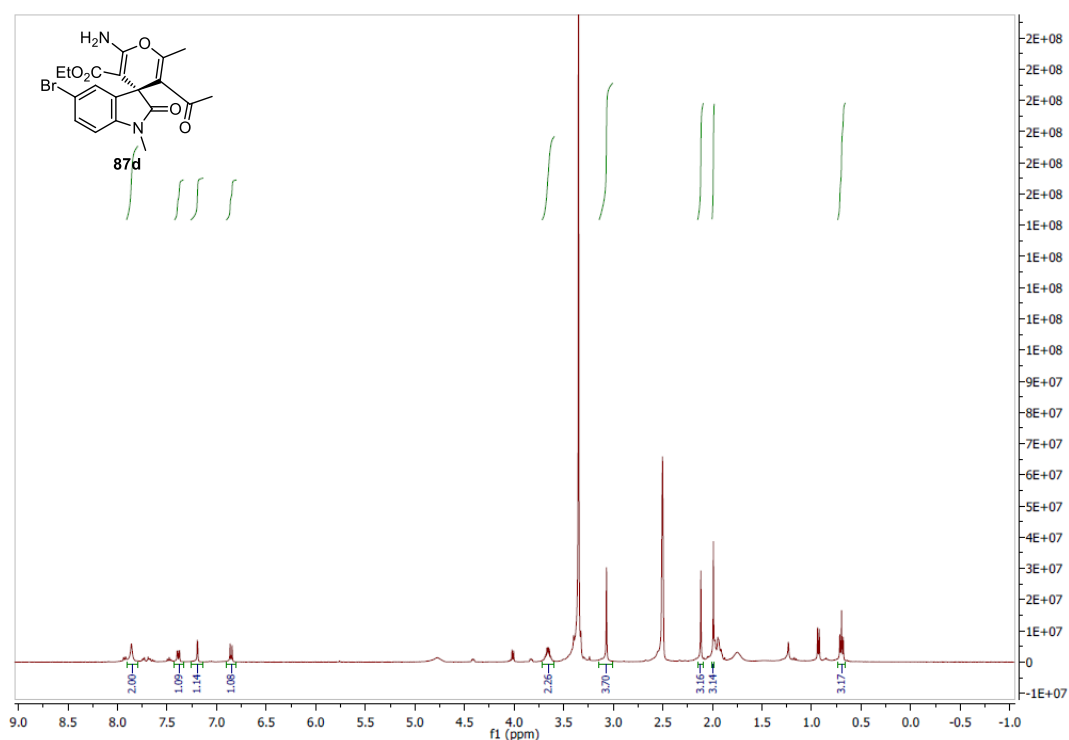
Figure A. 52 <sup>13</sup>C NMR spectrum of **77i**











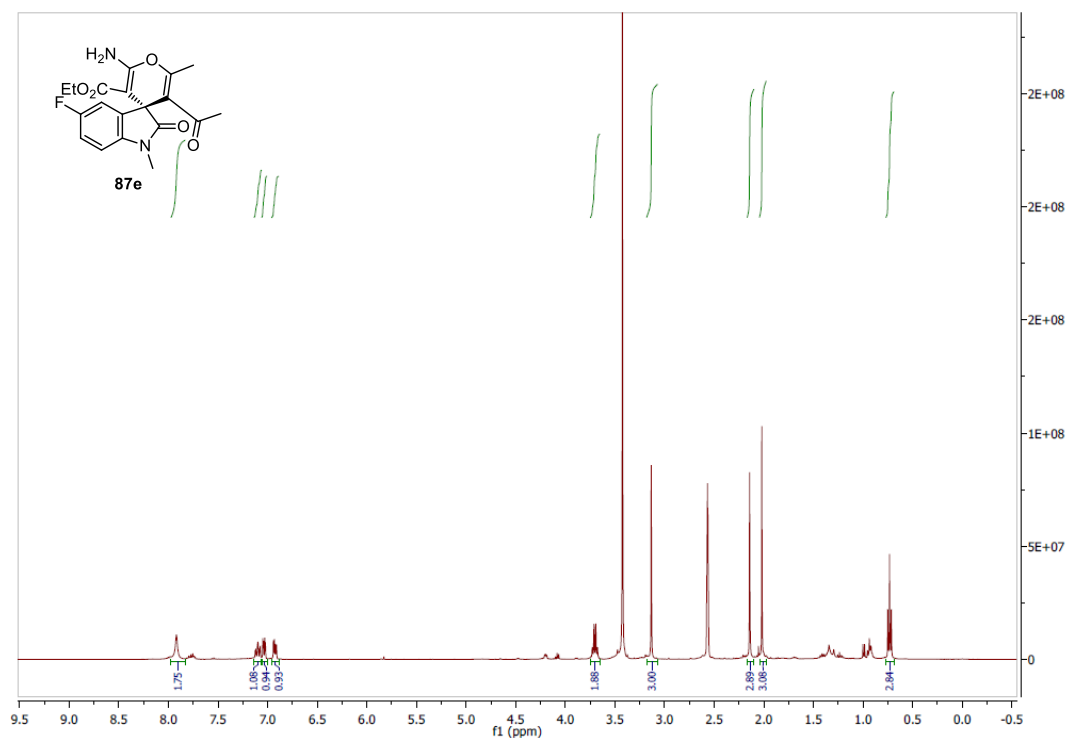


Figure A. 61 <sup>1</sup>H NMR spectrum of **87e**

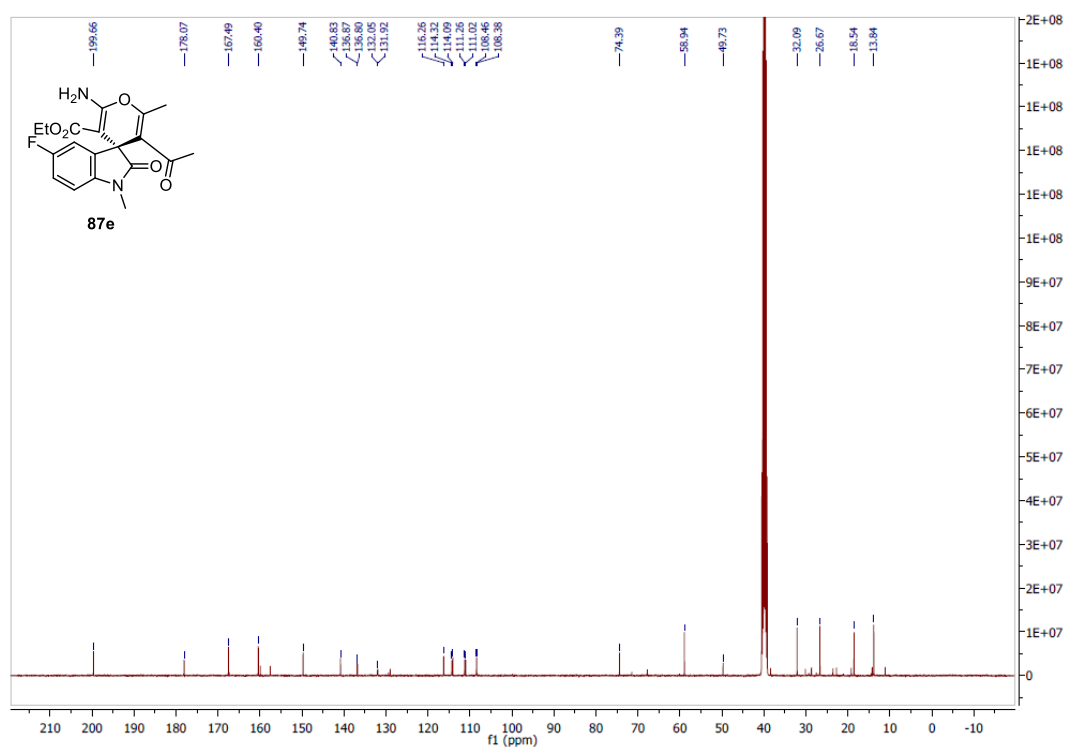
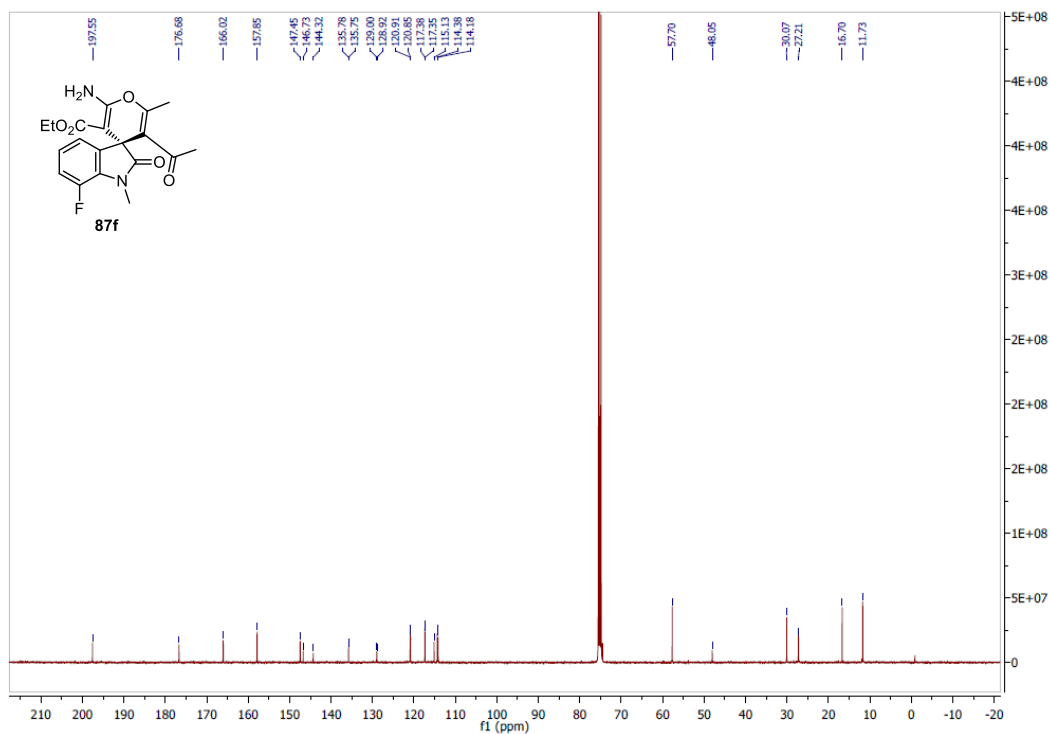
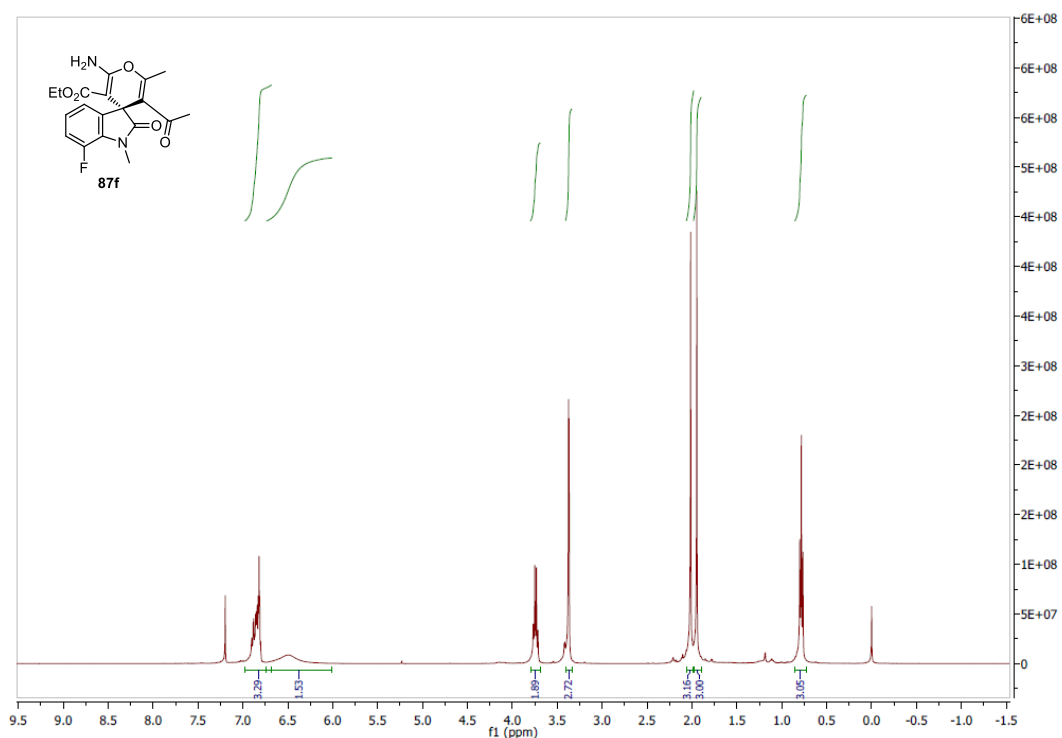
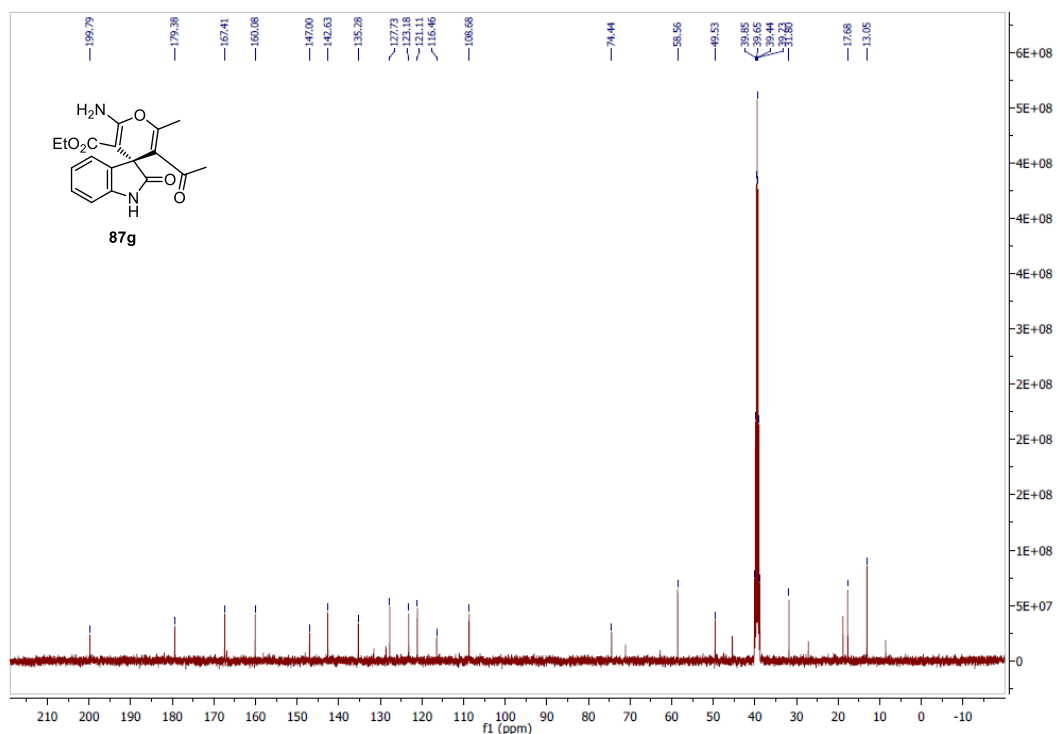
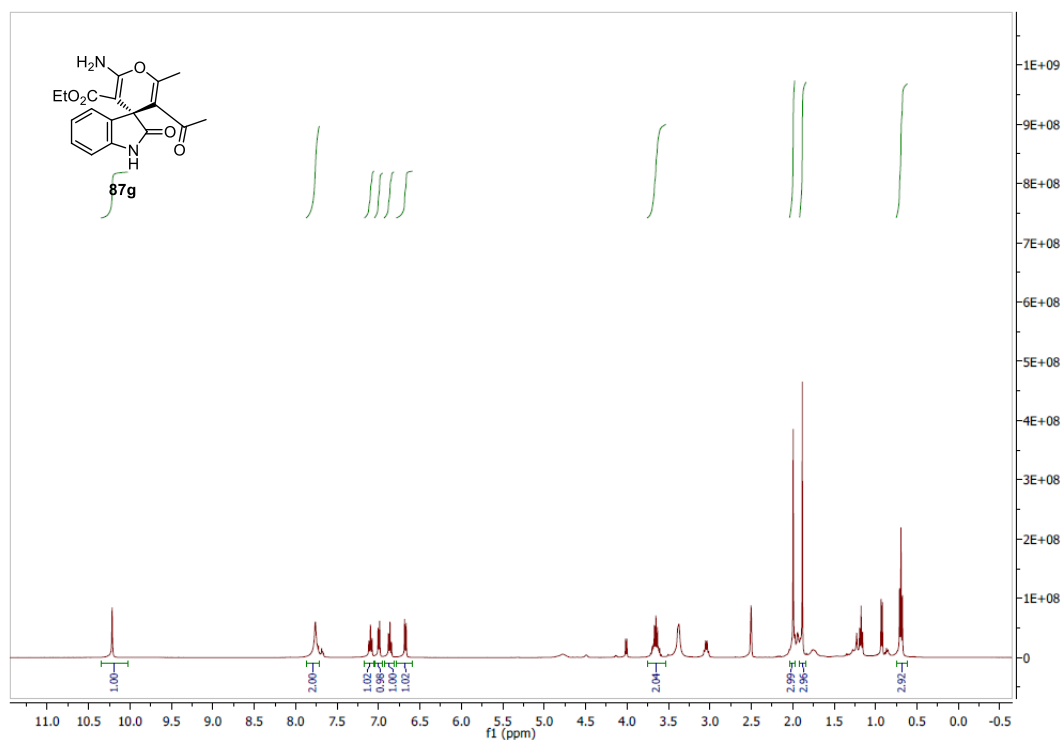
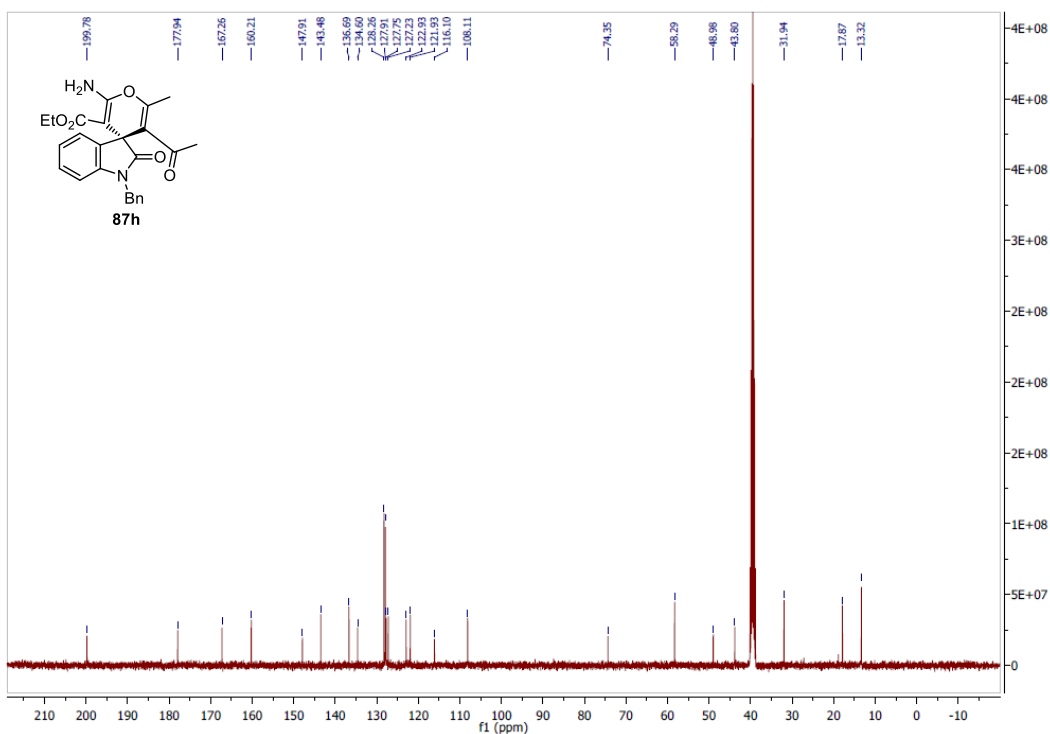
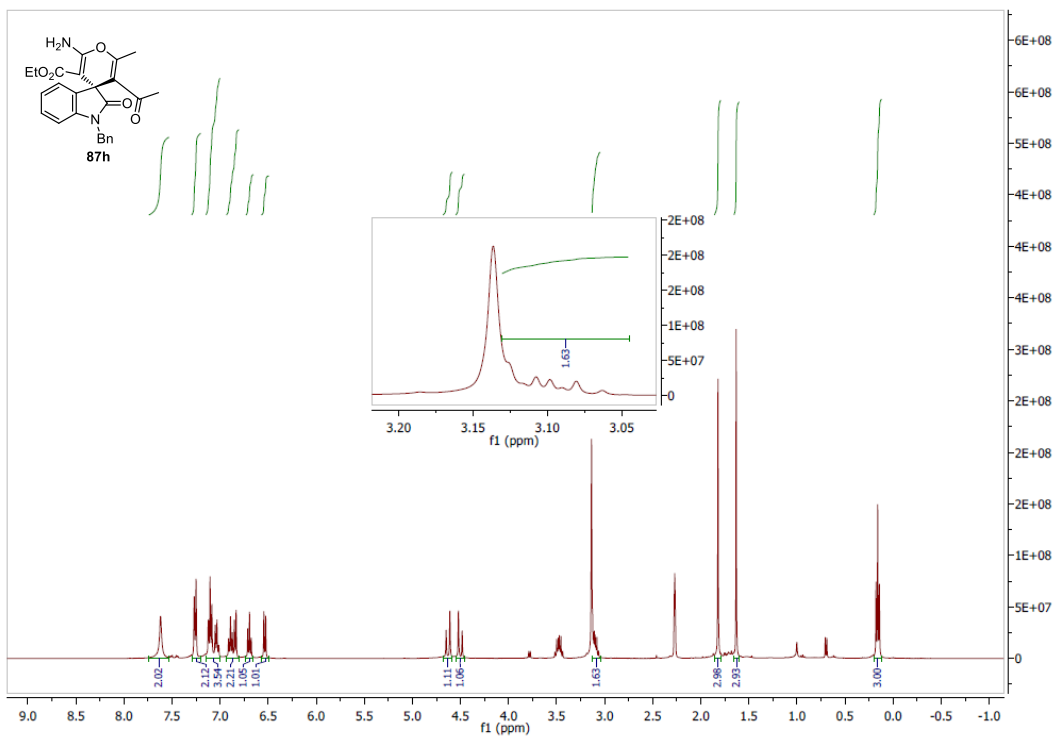
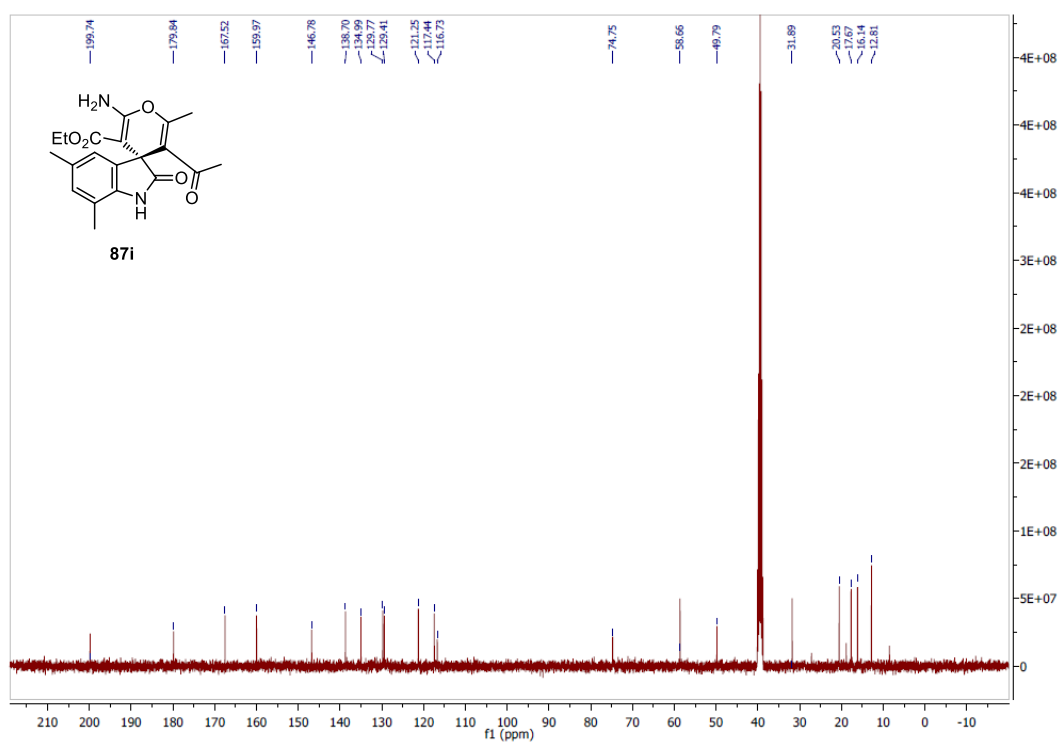
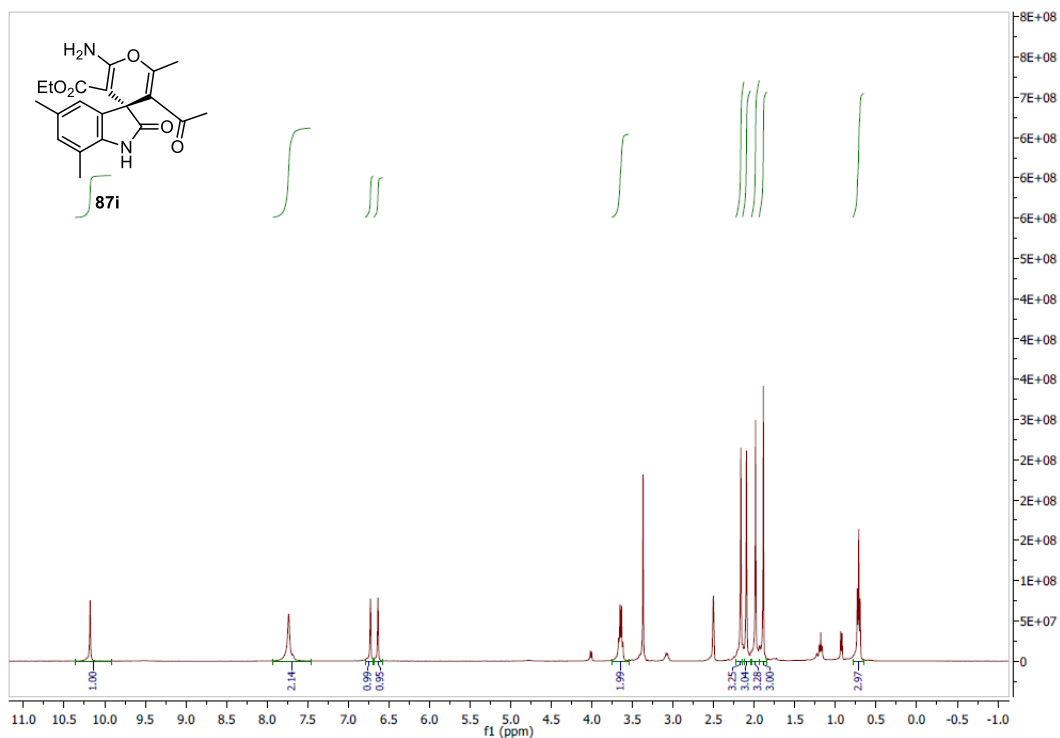


Figure A. 62 <sup>13</sup>C NMR spectrum of **87e**









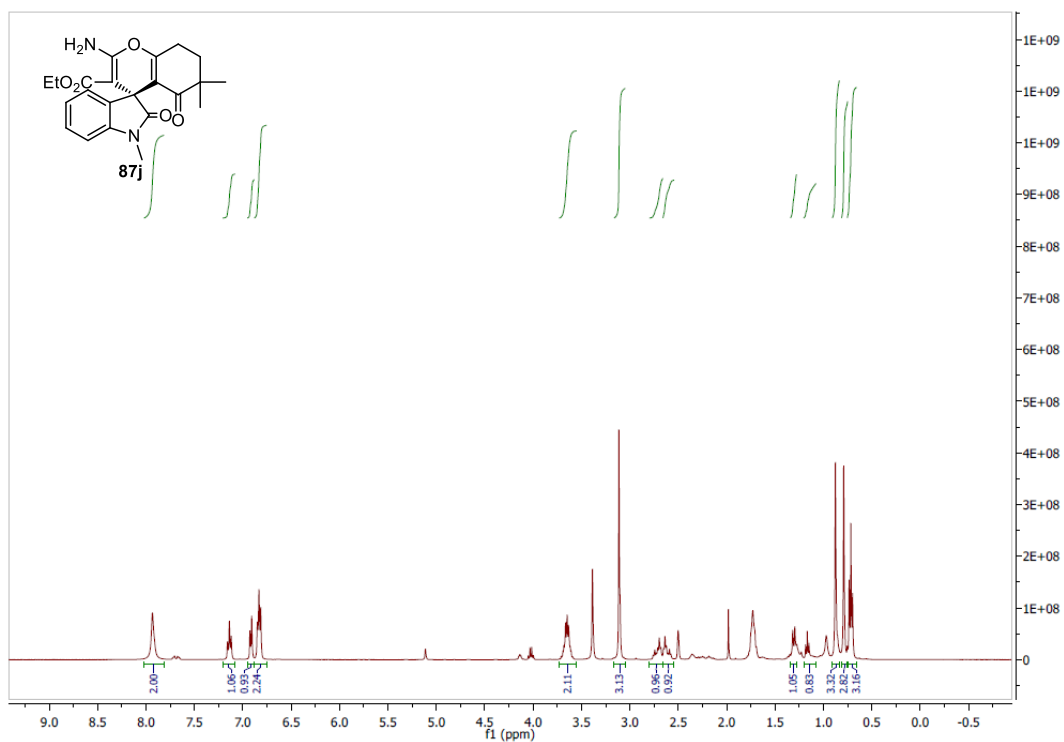


Figure A. 71  $^1\text{H}$  NMR spectrum of **87j**

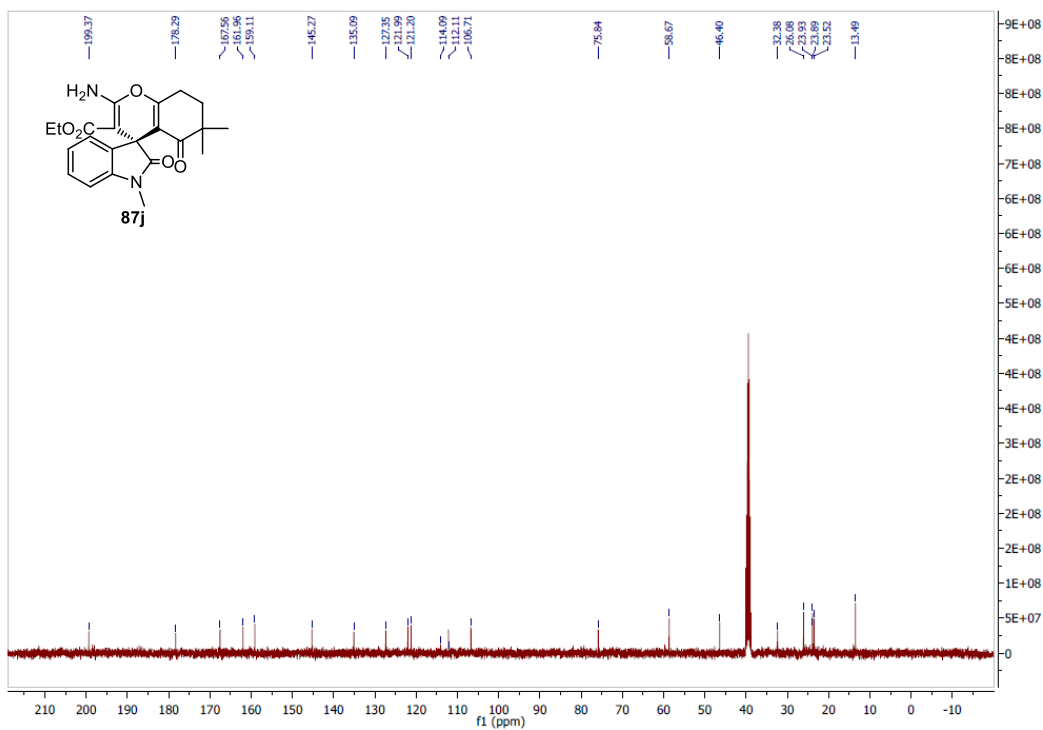
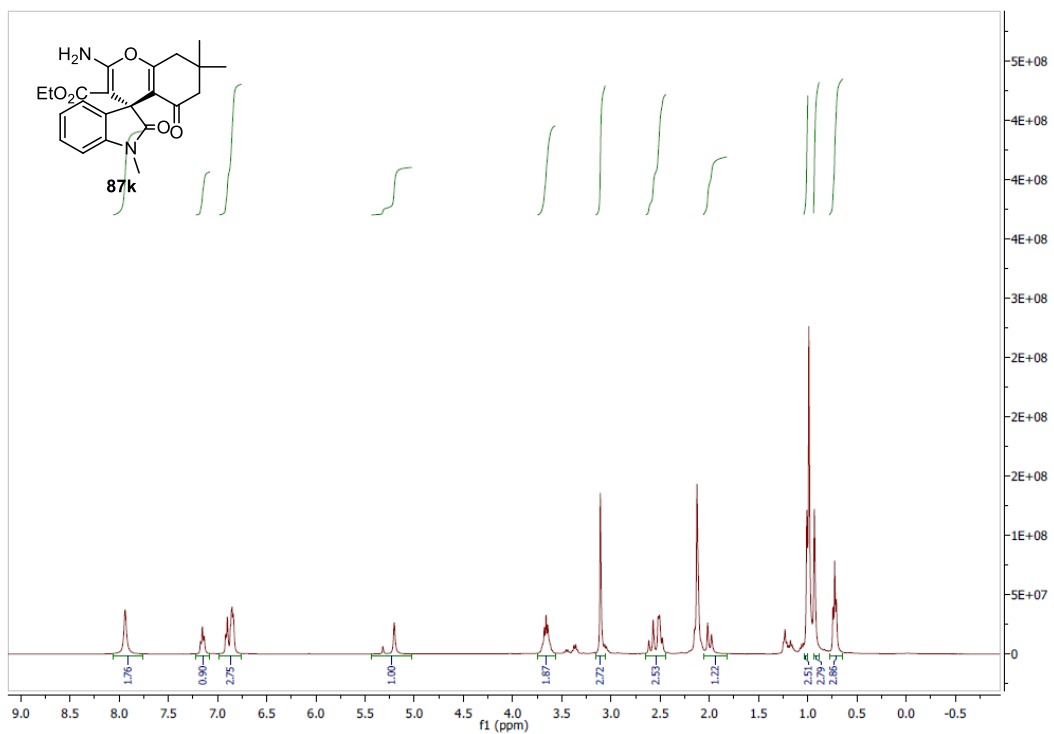
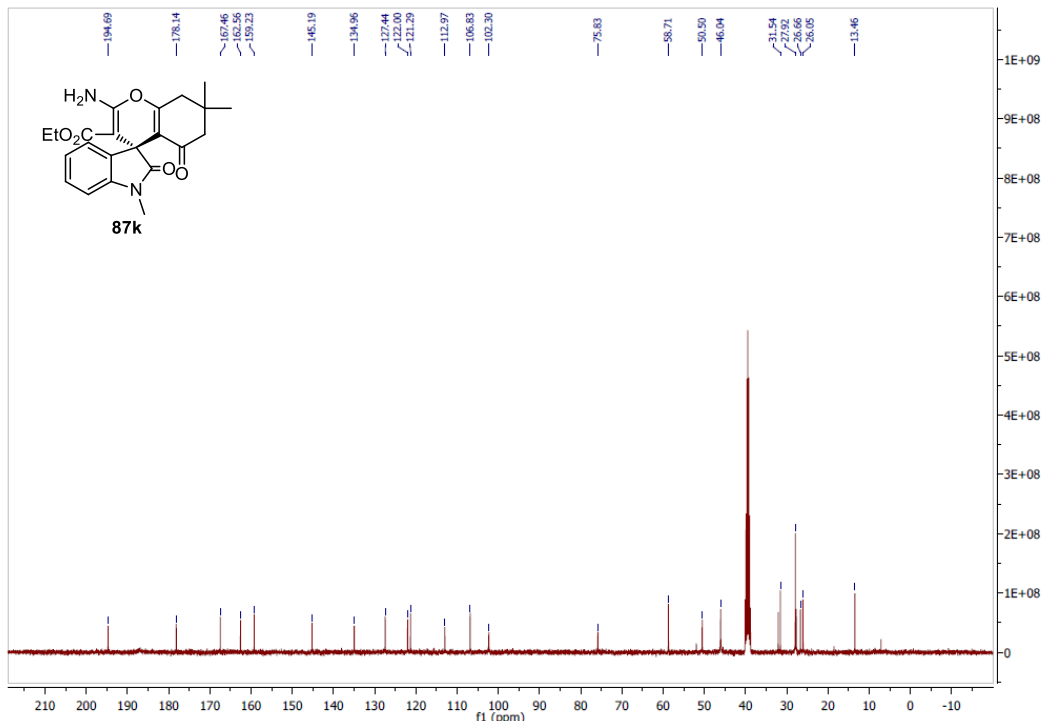


Figure A. 72  $^{13}\text{C}$  NMR spectrum of **87j**

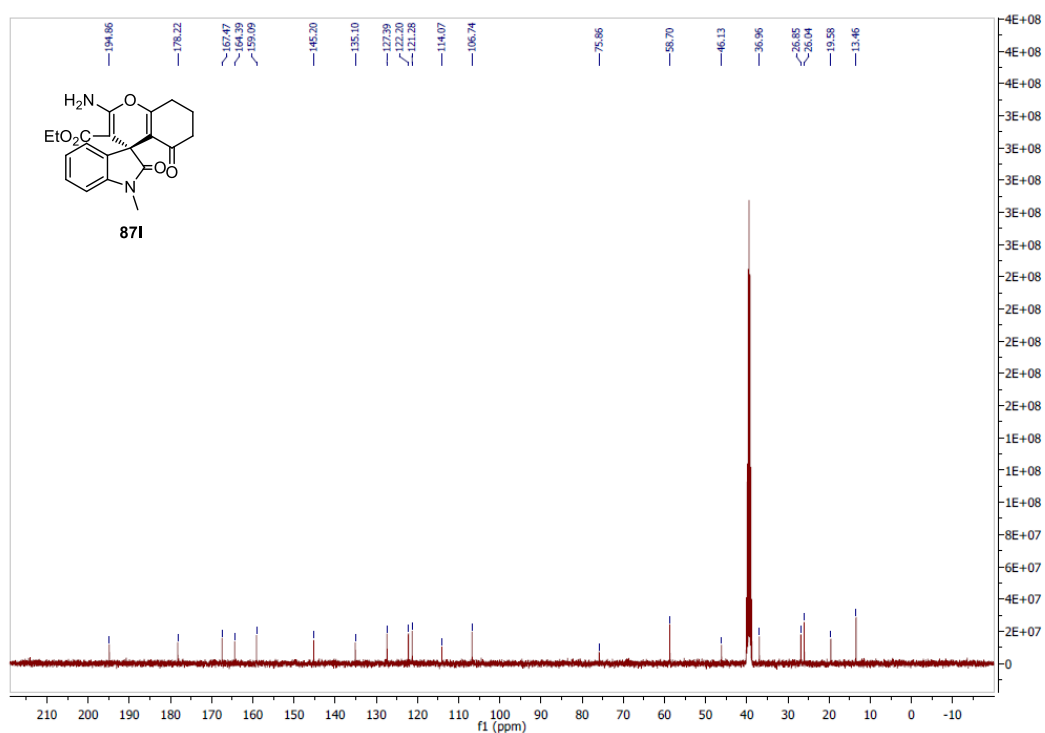
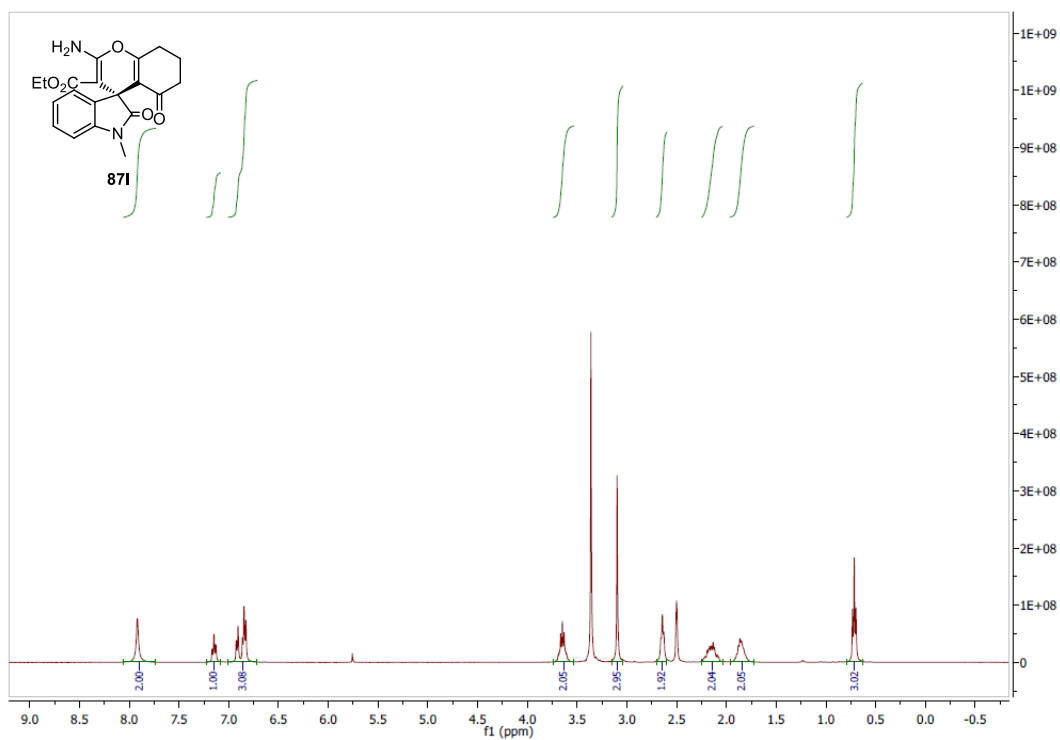


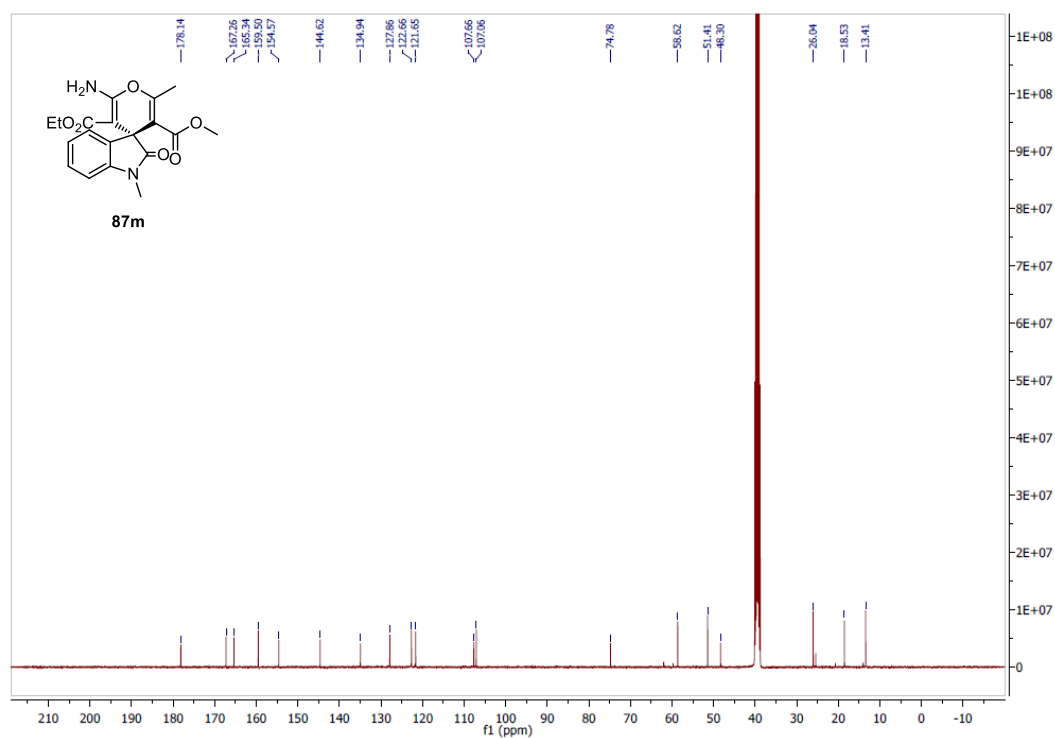
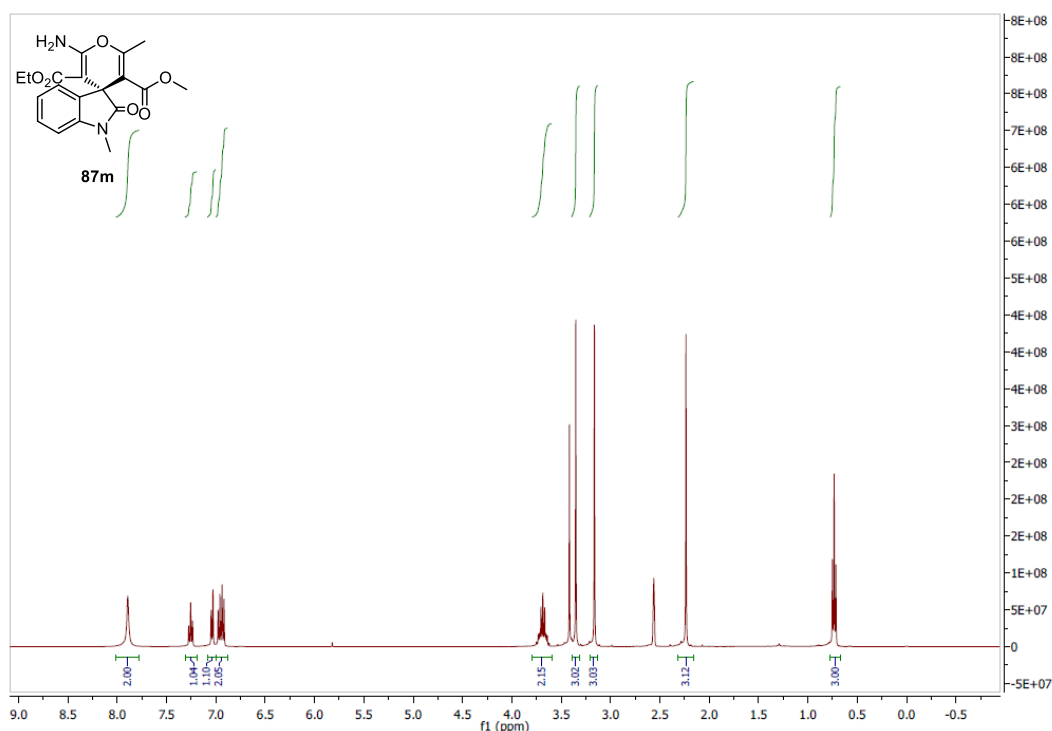


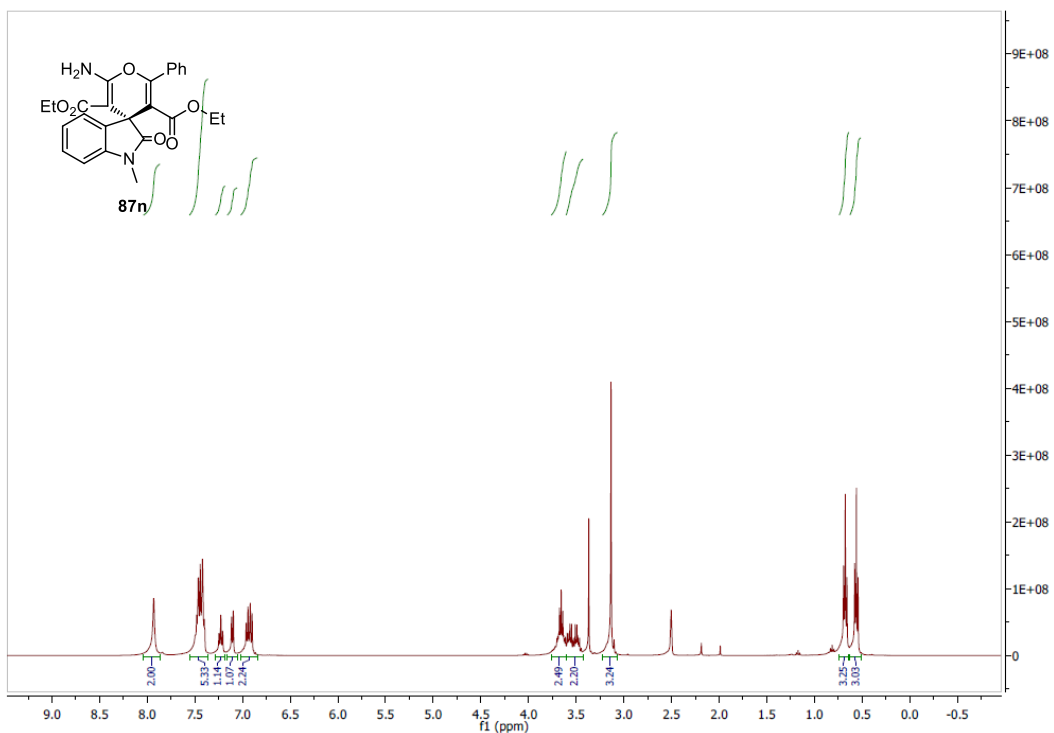
**Figure A. 73**  $^1\text{H}$  NMR spectrum of **87k**



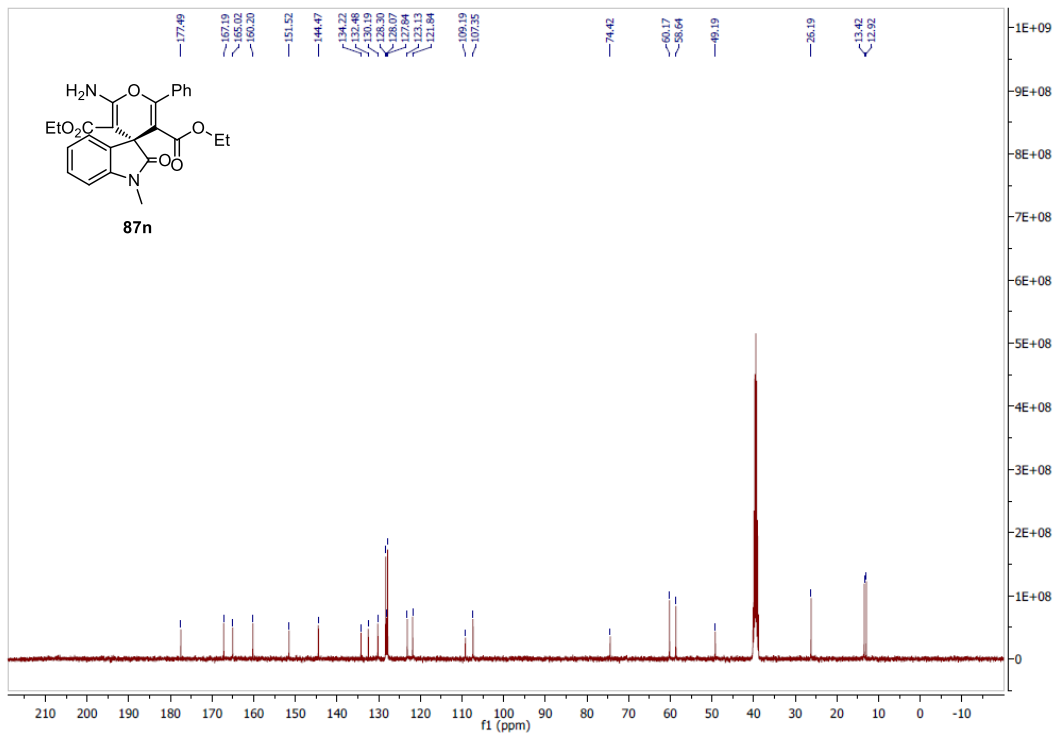
**Figure A. 74**  $^{13}\text{C}$  NMR spectrum of **87k**



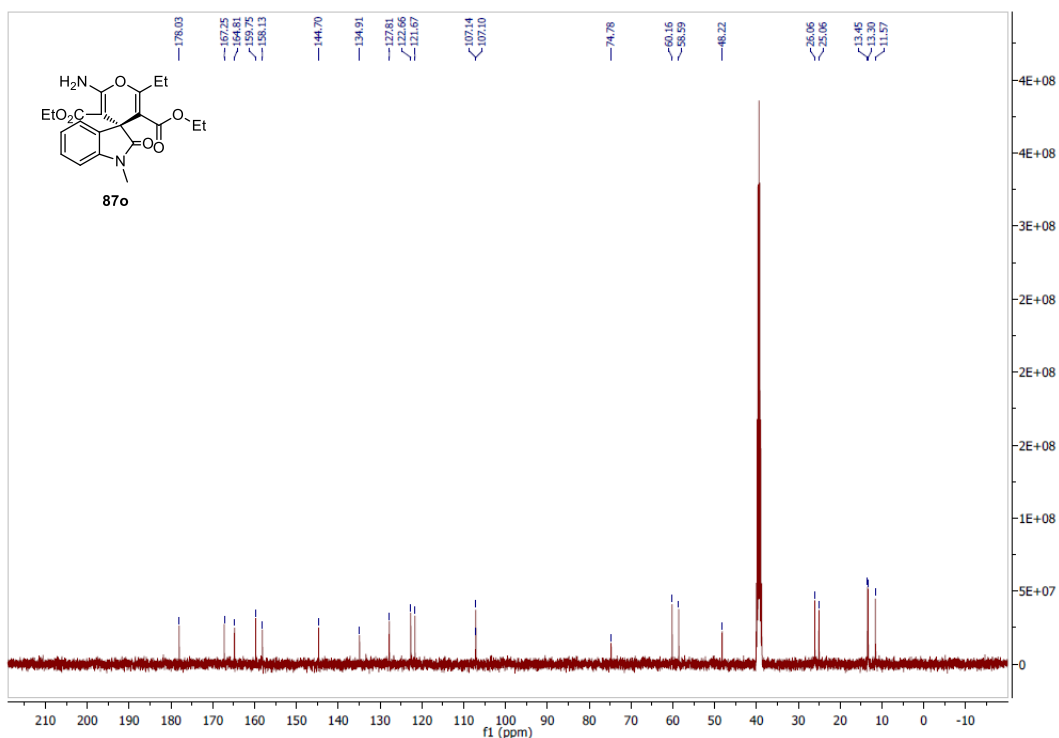
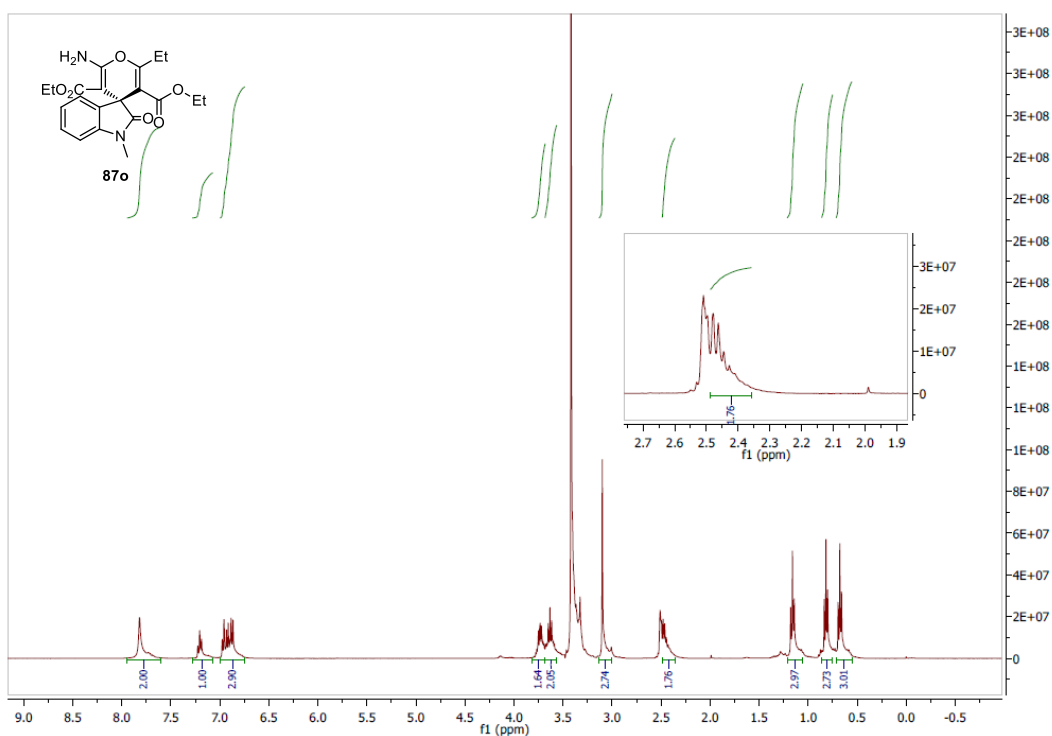


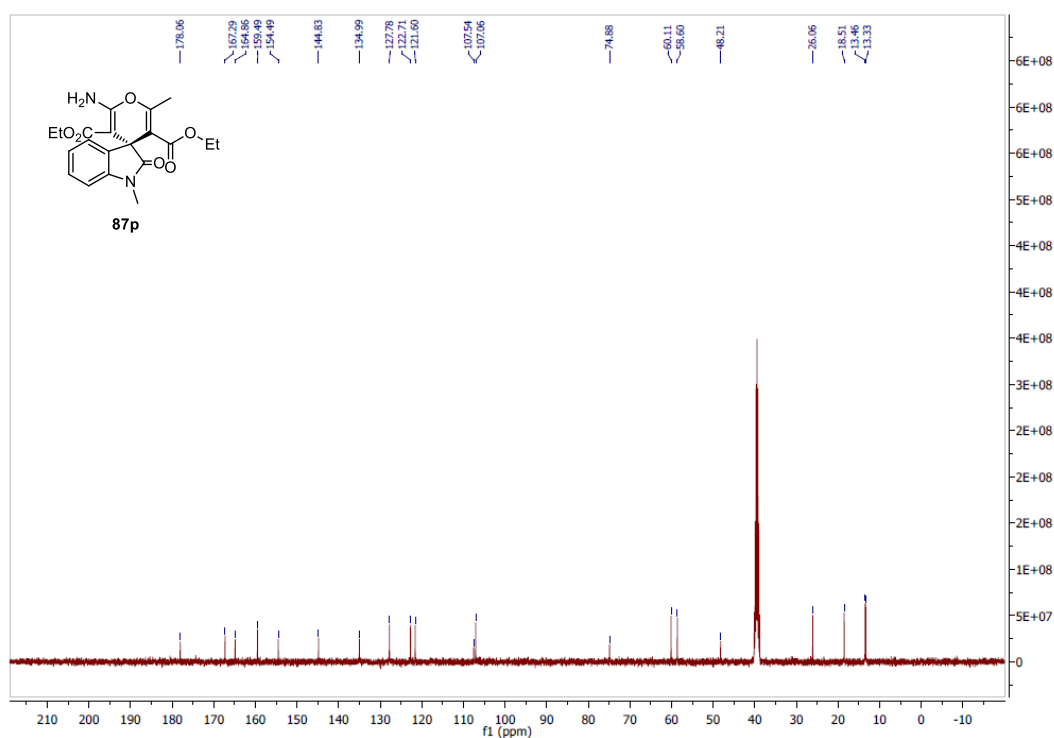
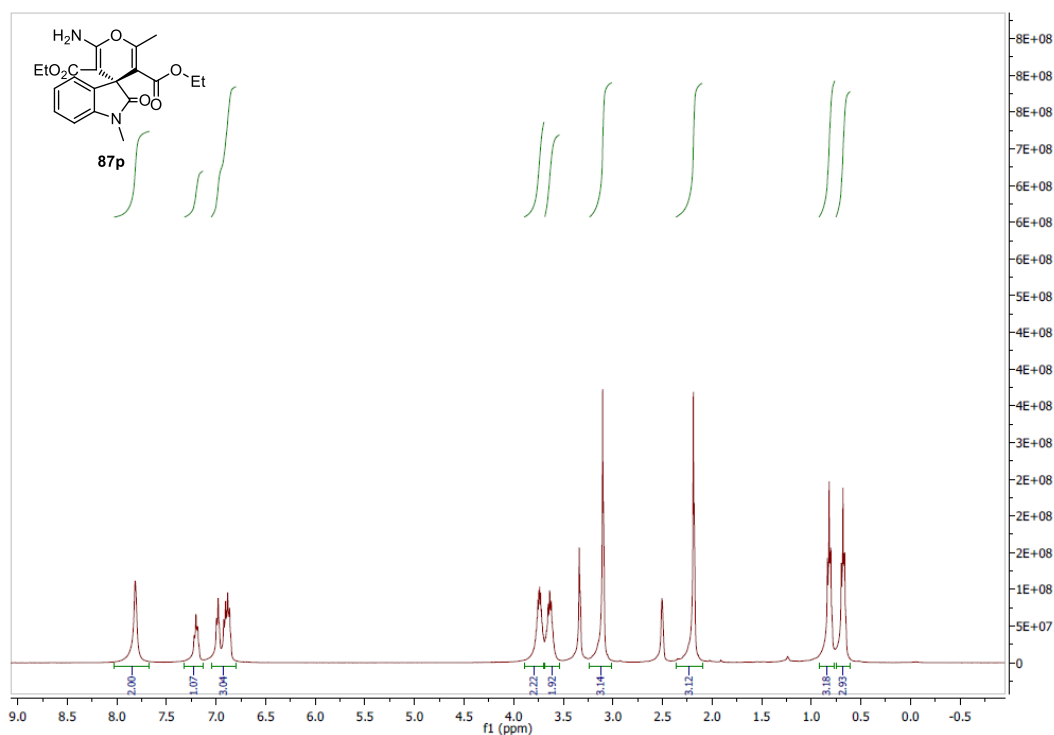


**Figure A. 79**  $^1\text{H}$  NMR spectrum of **87n**



**Figure A. 80**  $^{13}\text{C}$  NMR spectrum of **87n**





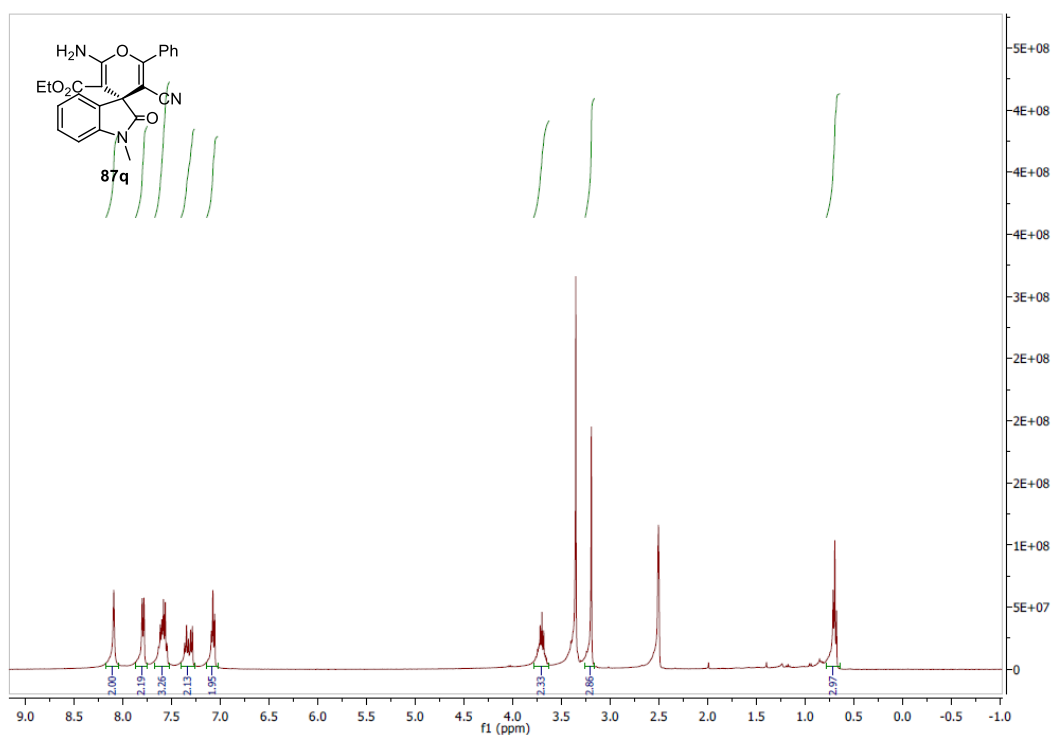


Figure A. 85 <sup>1</sup>H NMR spectrum of **87q**

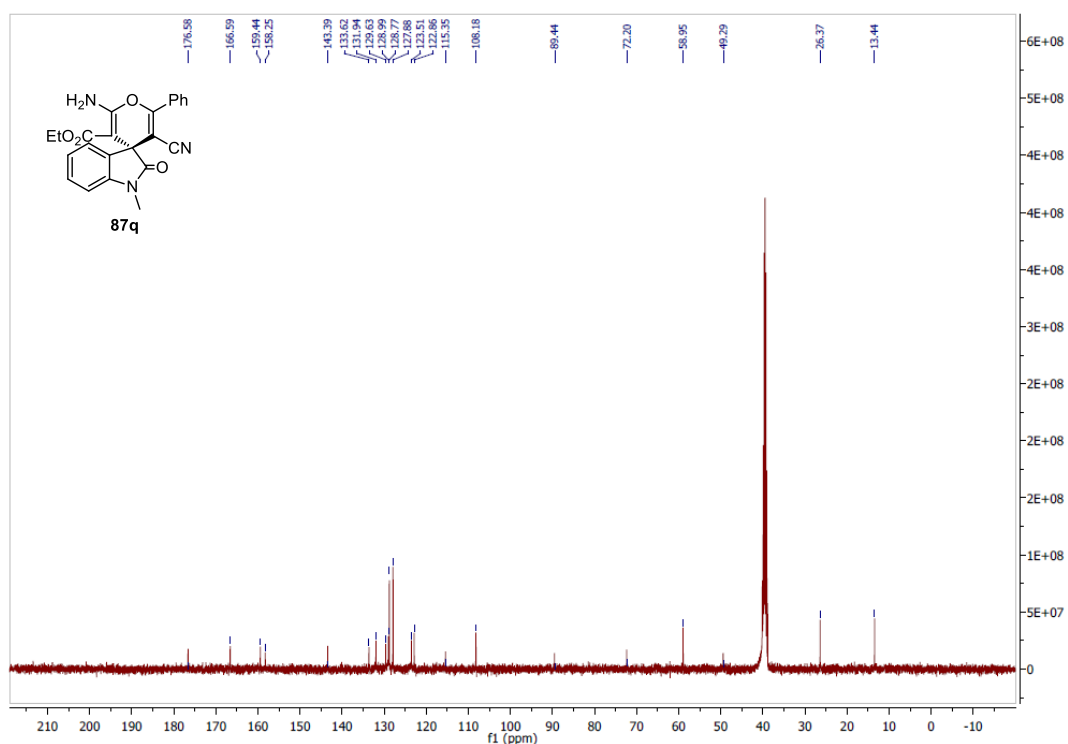


Figure A. 86 <sup>13</sup>C NMR spectrum of **87q**

## B. HPLC CHROMATOGRAMS

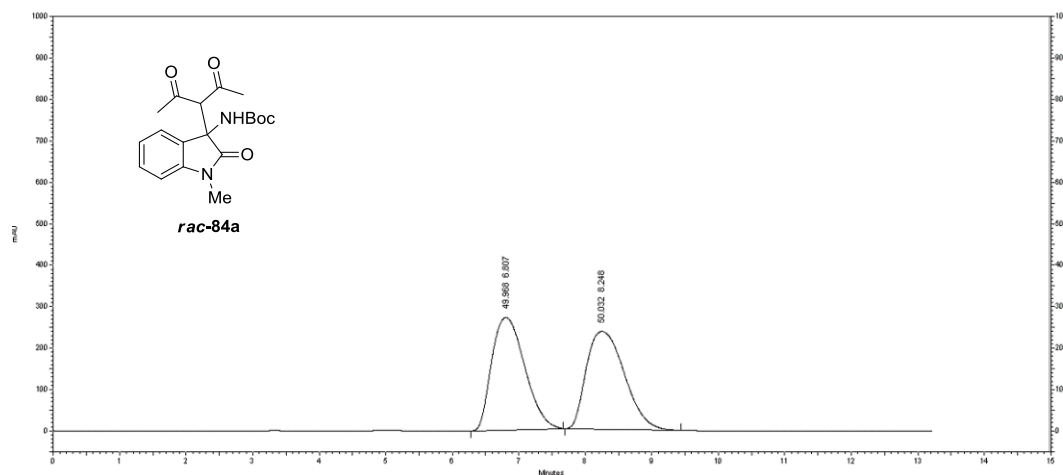


Figure B. 1 HPLC chromatogram of *rac*-84a

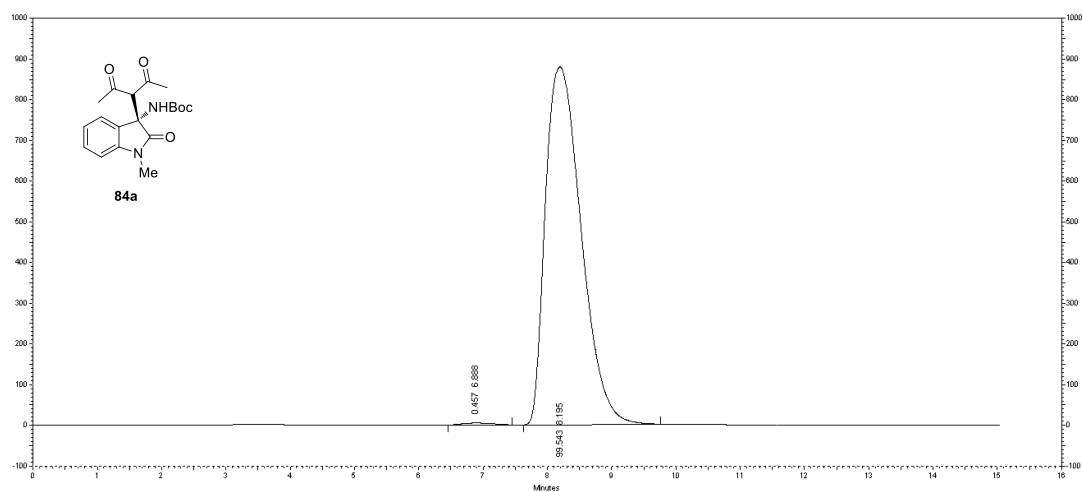
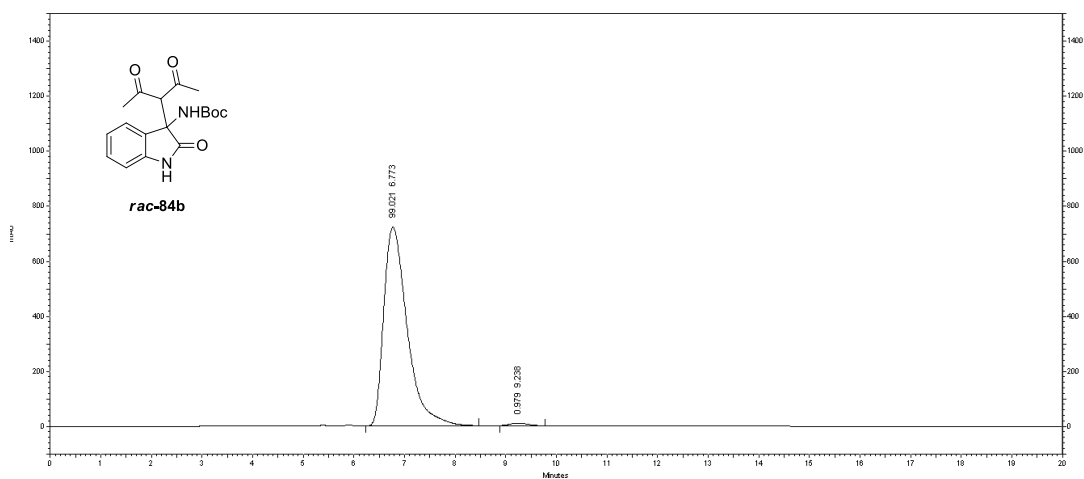
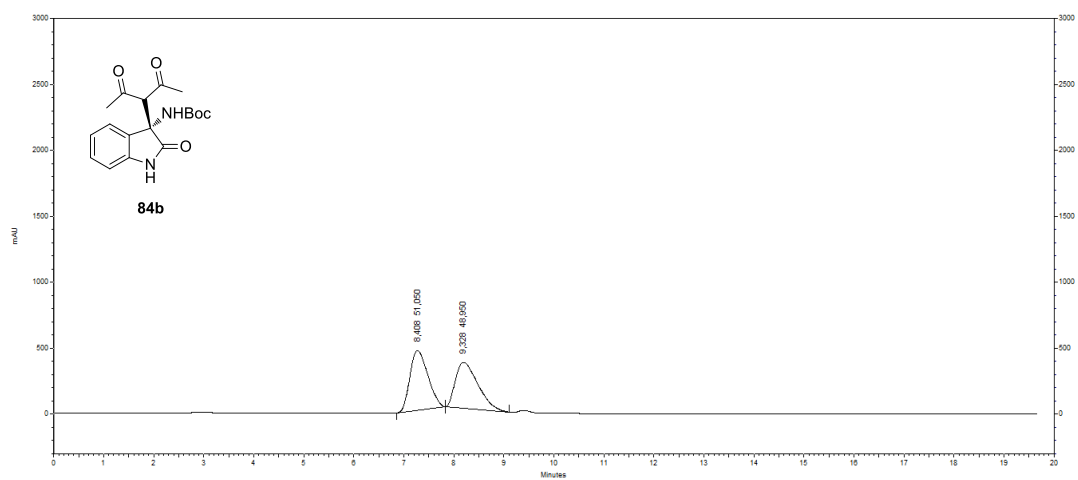


Figure B. 2 HPLC chromatogram of enantiomerically enriched 84a





**Figure B. 3** HPLC chromatogram of *rac-84b*



**Figure B. 4** HPLC chromatogram of enantiomerically enriched **84b**

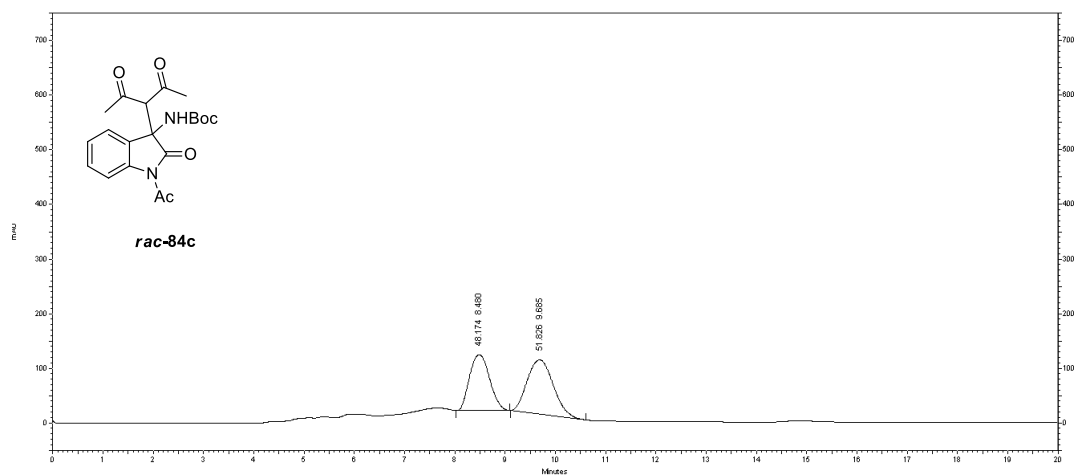


**Figure B. 5** HPLC chromatogram of *rac-84c*

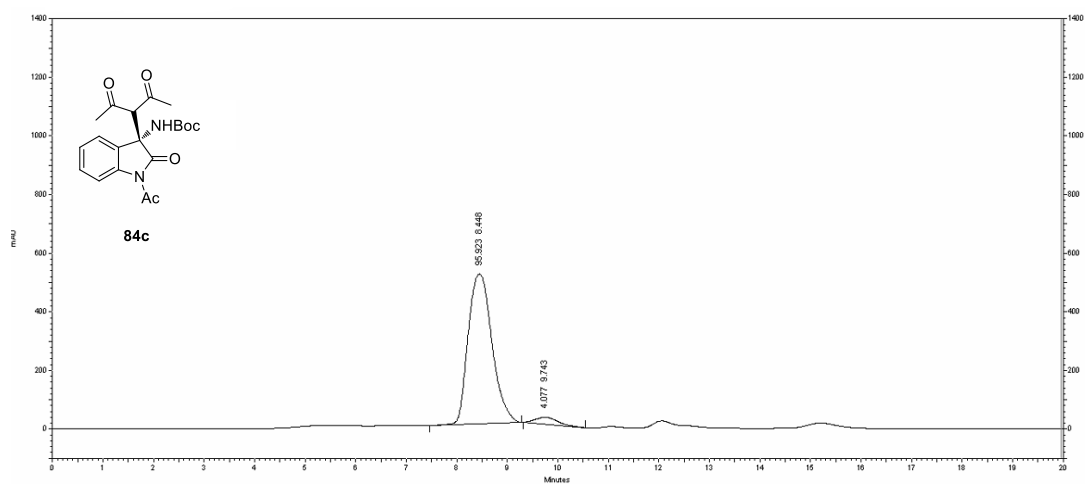


**Figure B. 6** HPLC chromatogram of enantiomerically enriched **84c**

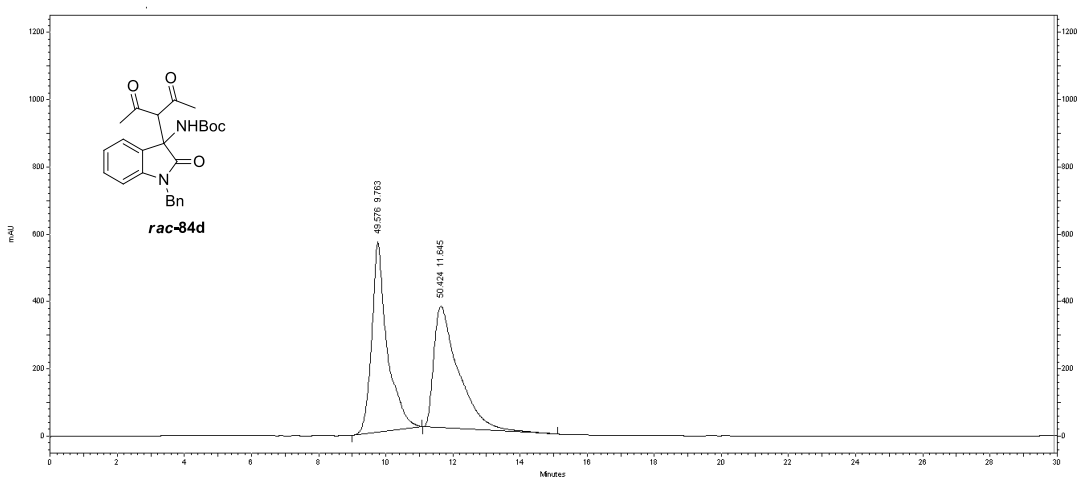


**Figure B. 7** HPLC chromatogram of *rac-84d*

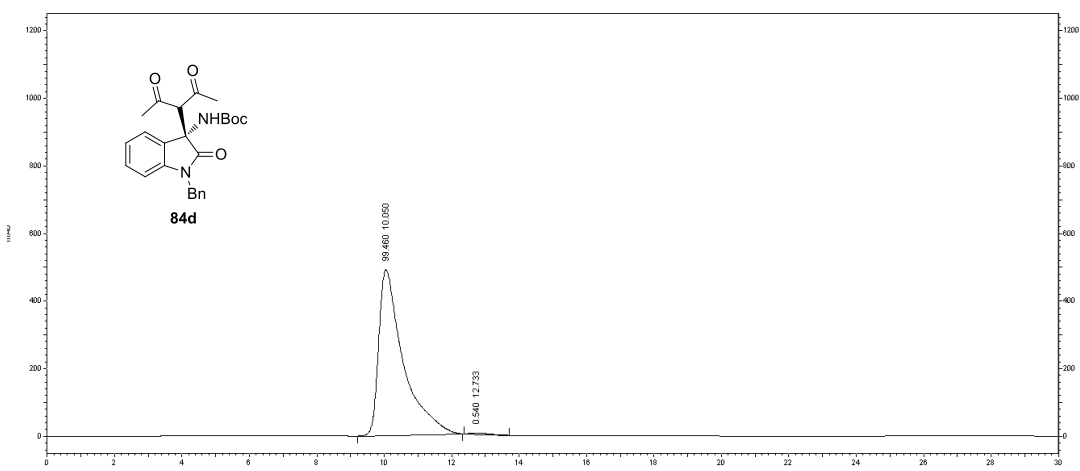


**Figure B. 8** HPLC chromatogram of enantiomerically enriched **84d**

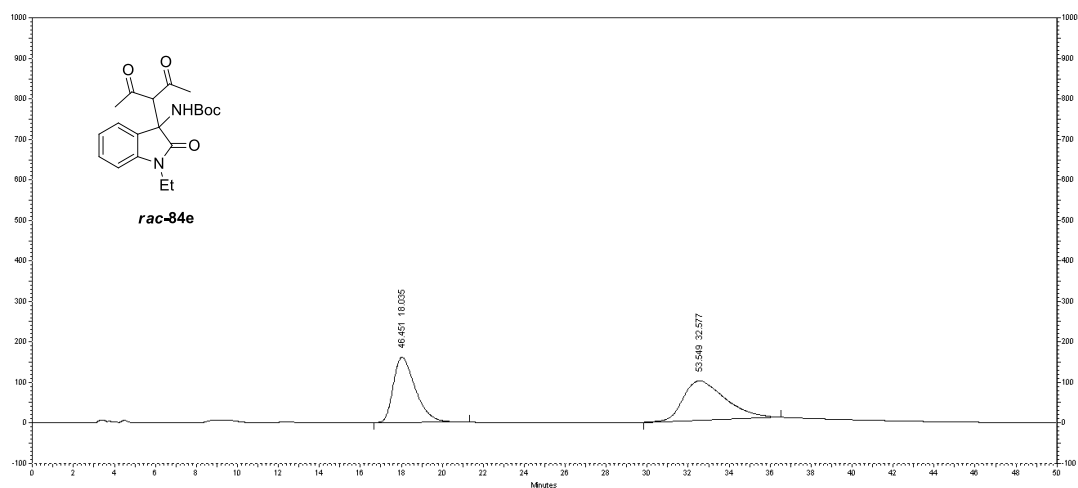


Figure B. 9 HPLC chromatogram of *rac*- 84e

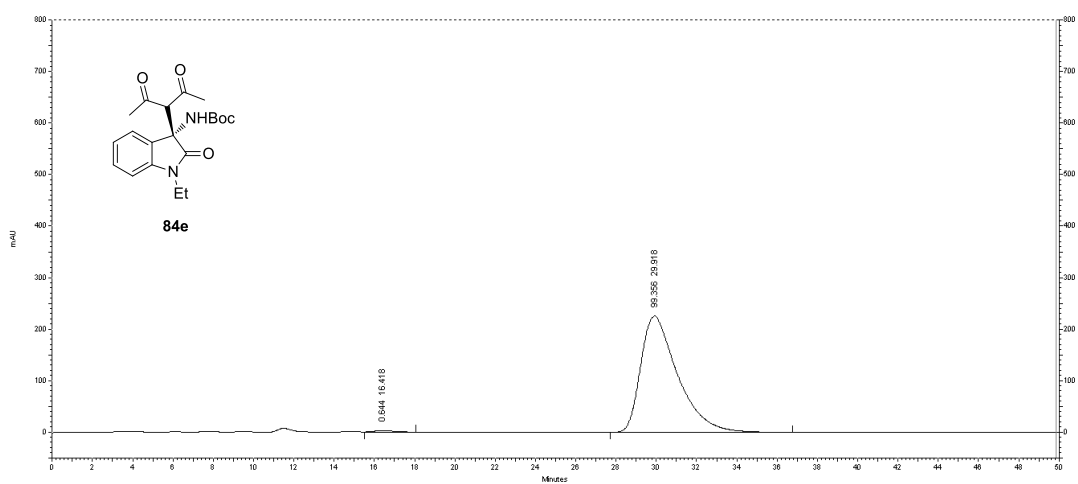
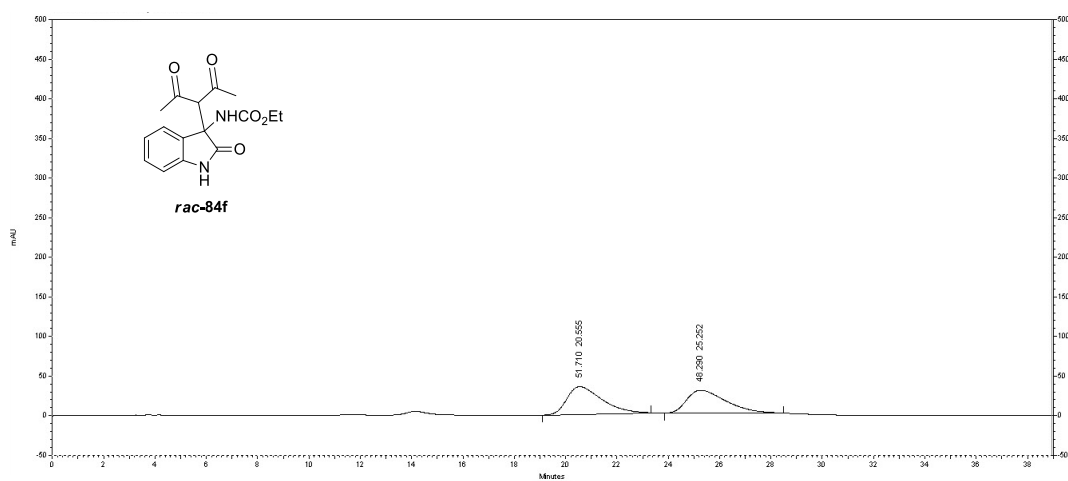
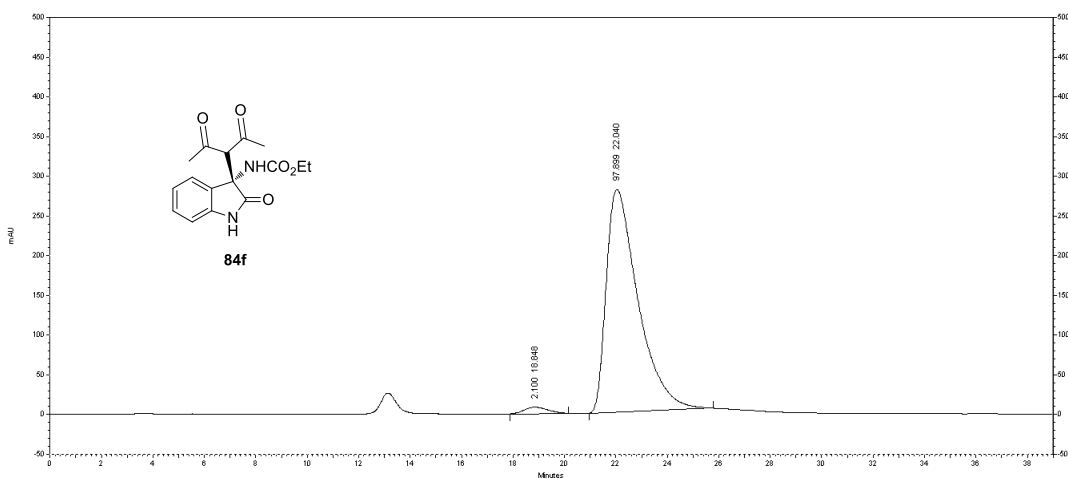


Figure B. 10 HPLC chromatogram of enantiomerically enriched 84e



**Figure B. 11** HPLC chromatogram of *rac*-84f



**Figure B. 12** HPLC chromatogram of enantiomerically enriched 84f

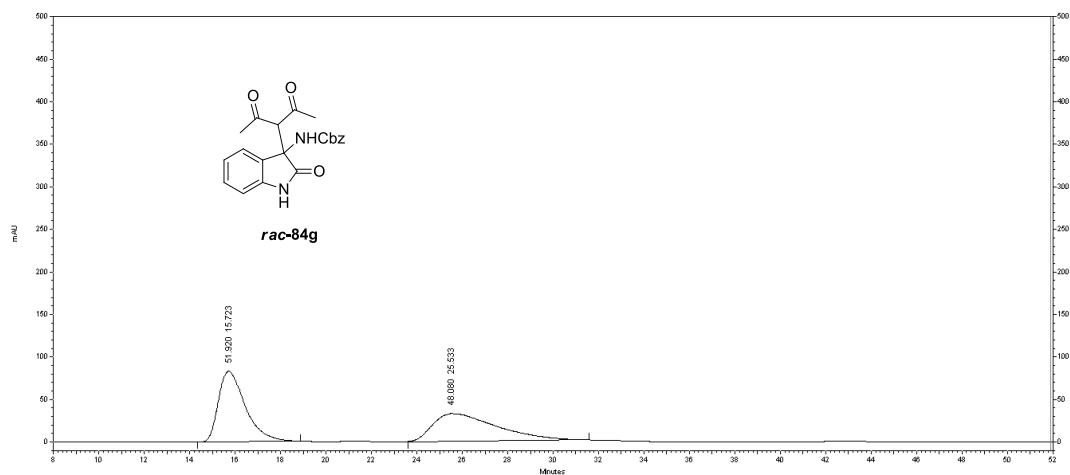


**Figure B. 13** HPLC chromatogram of *rac-84g*

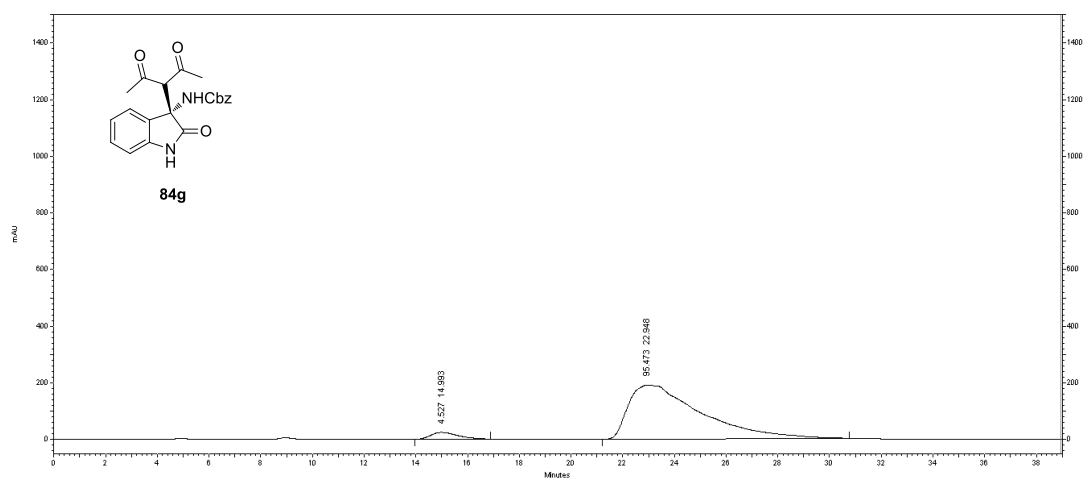


**Figure B. 14** HPLC chromatogram of enantiomerically enriched **84g**

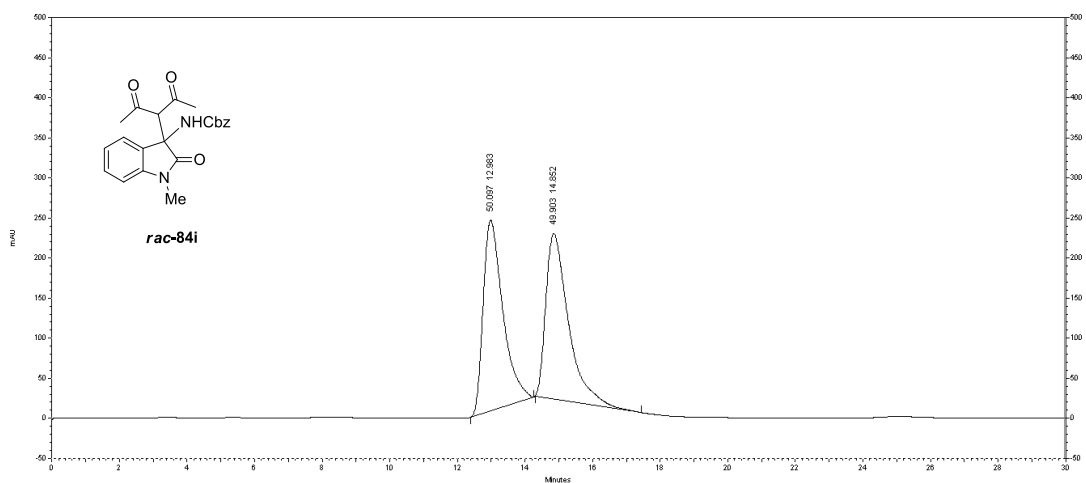


**Figure B. 15** HPLC chromatogram of *rac*-84i

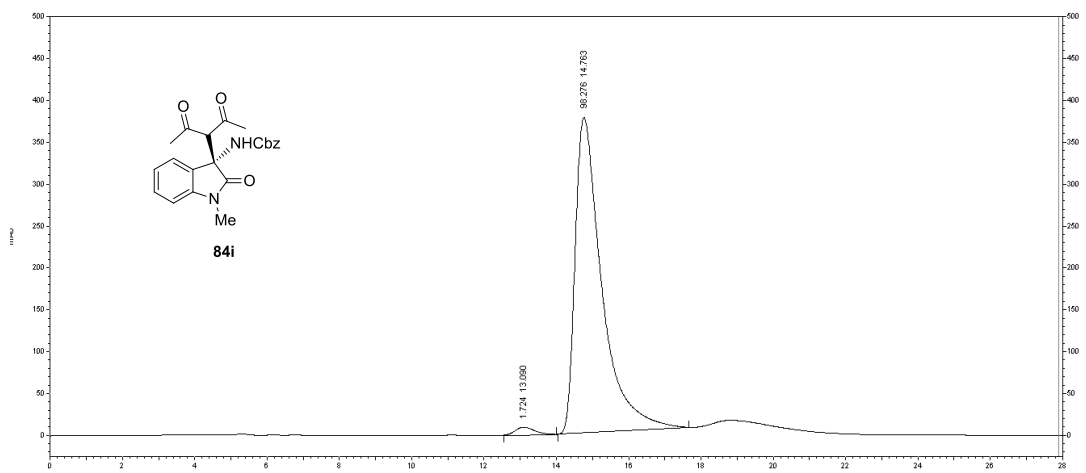


**Figure B. 16** HPLC chromatogram of enantiomerically enriched 84i

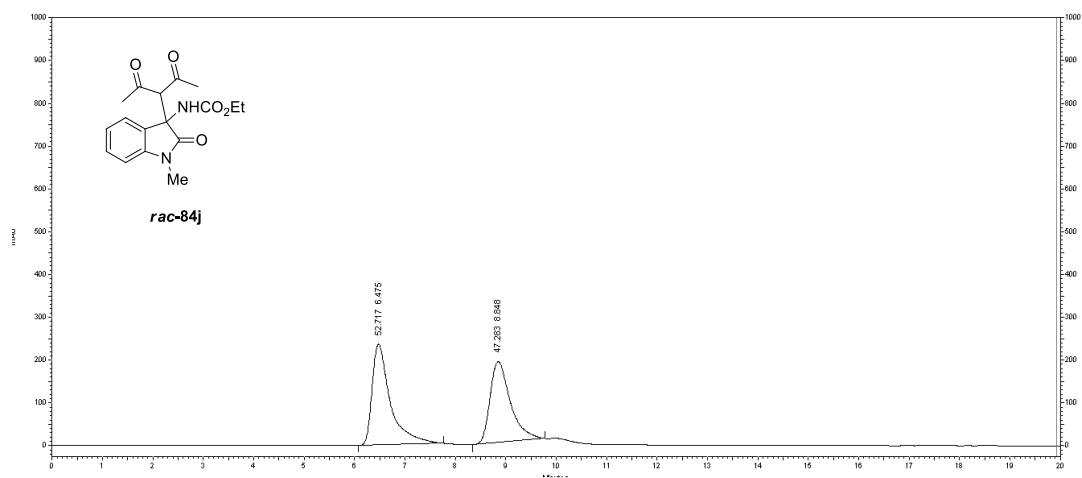


Figure B. 17 HPLC chromatogram of *rac-84j*

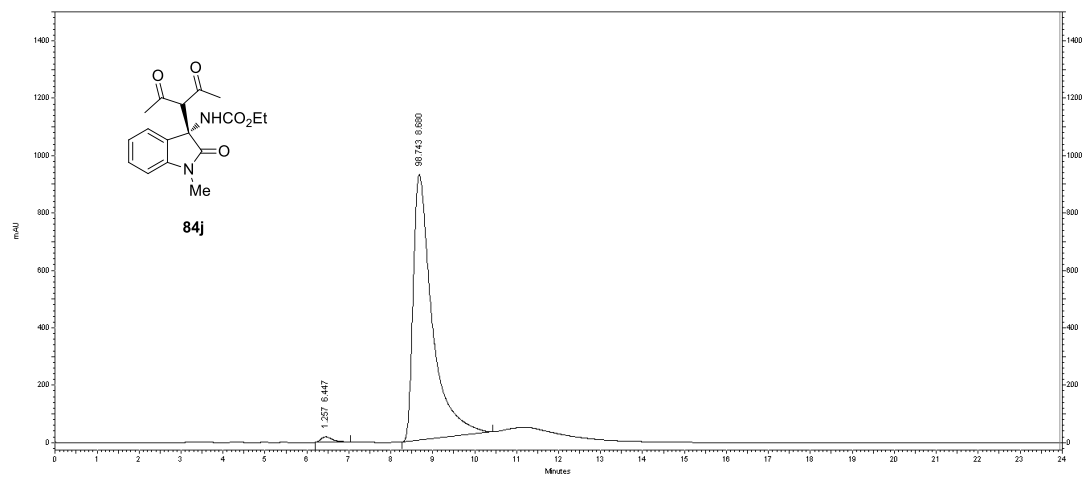
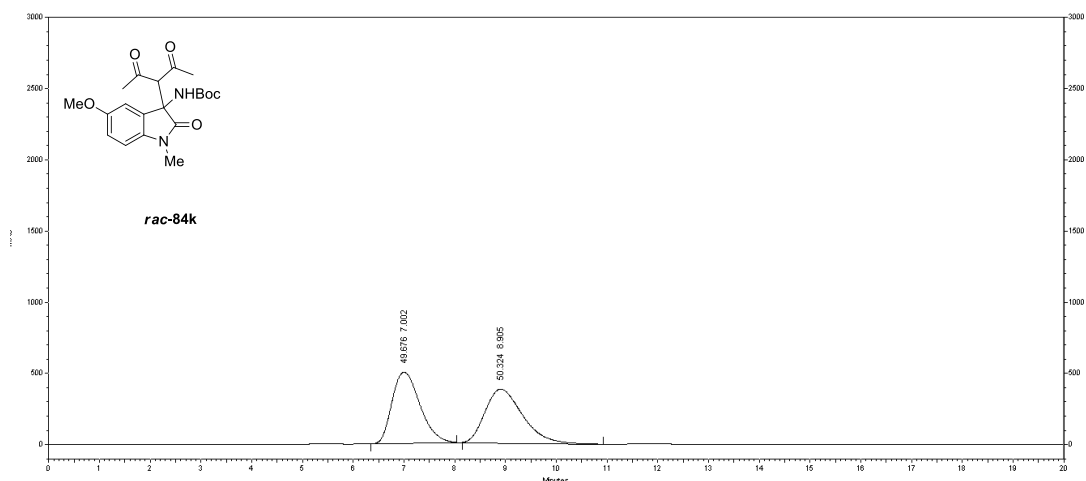
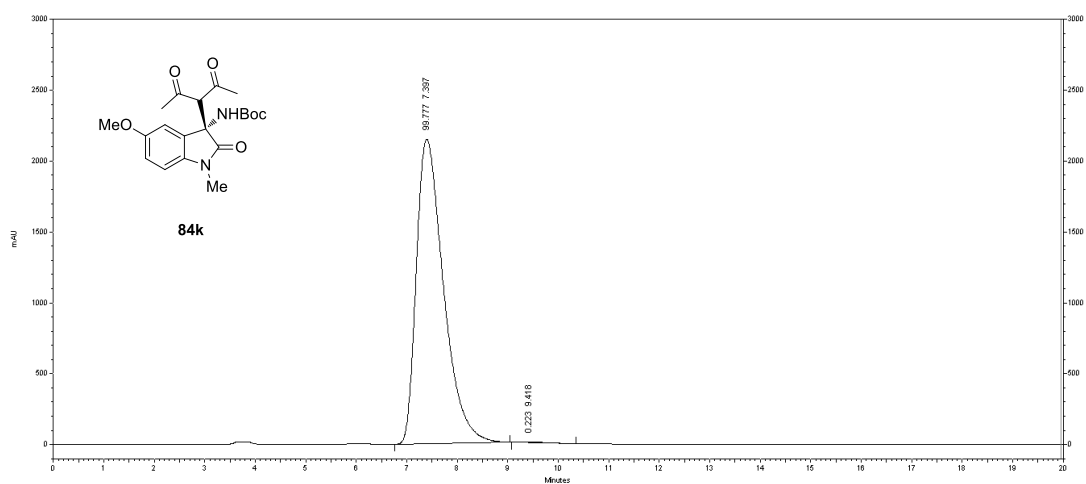


Figure B. 18 HPLC chromatogram of enantiomerically enriched **84j**





**Figure B. 19** HPLC chromatogram of *rac*-84k



**Figure B. 20** HPLC chromatogram of enantiomerically enriched 84k

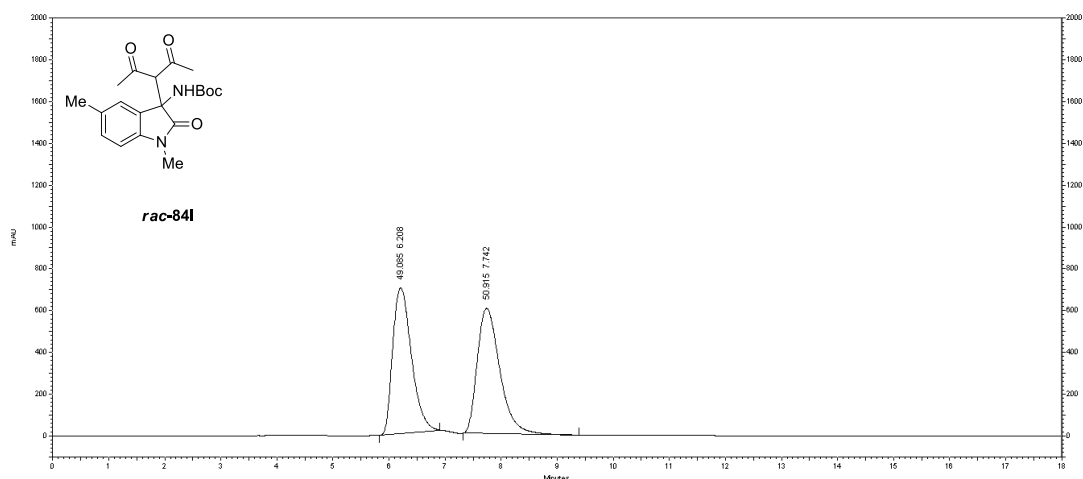


**Figure B. 21** HPLC chromatogram of *rac*-84I

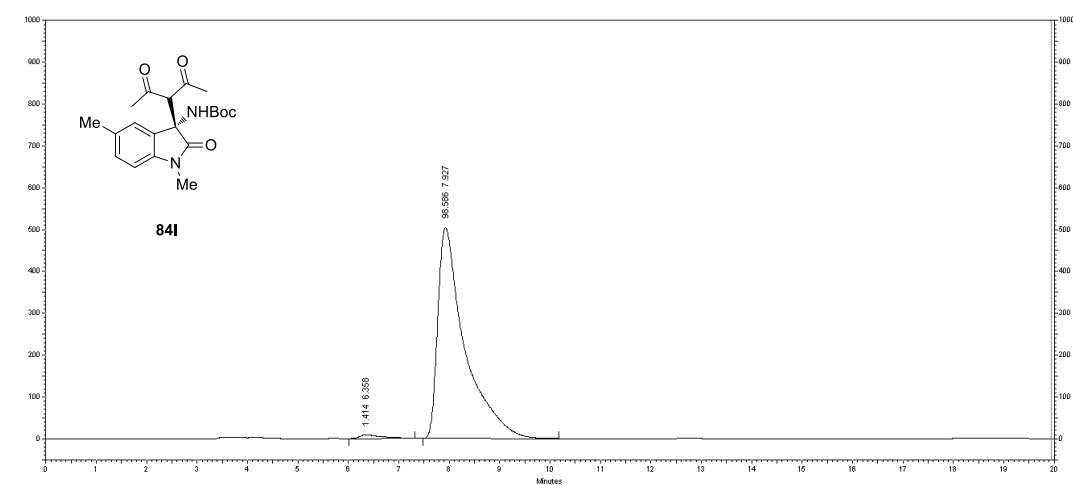


**Figure B. 22** HPLC chromatogram of enantiomerically enriched 84I

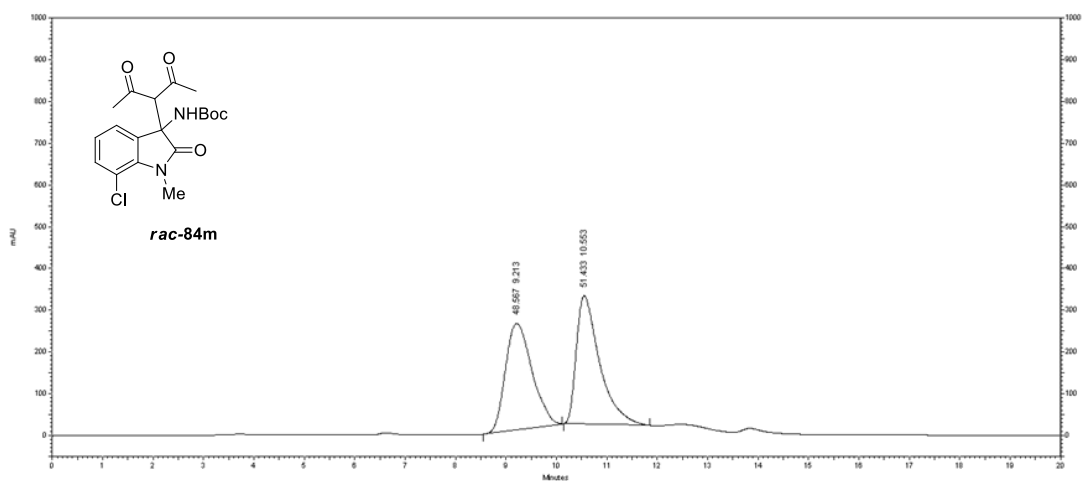


**Figure B. 23** HPLC chromatogram of *rac*-84m

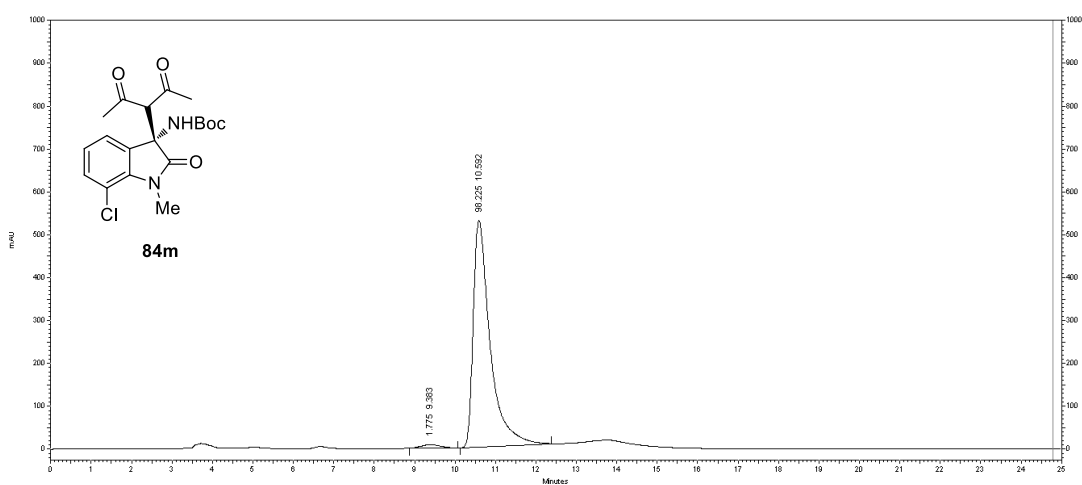


**Figure B. 24** HPLC chromatogram of enantiomerically enriched 84m

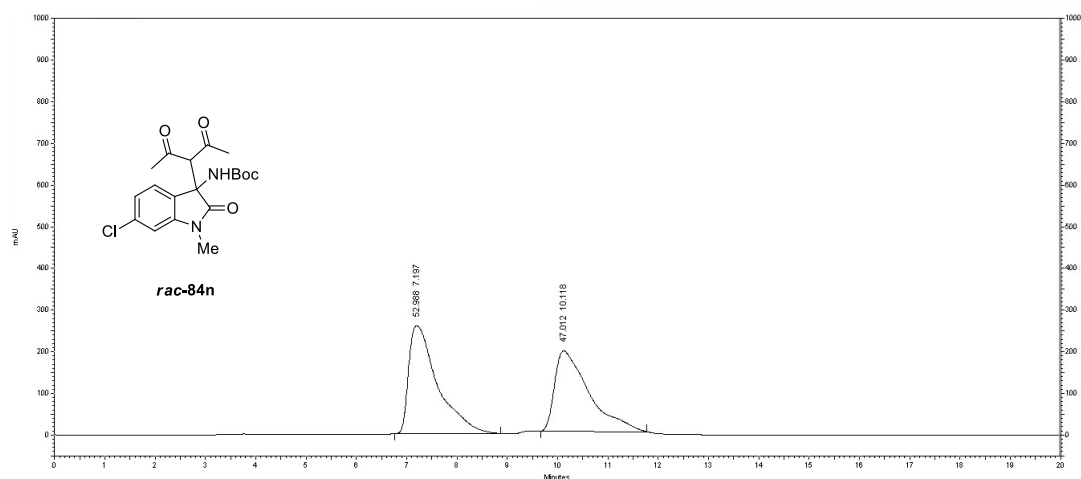


Figure B. 25 HPLC chromatogram of *rac-84n*

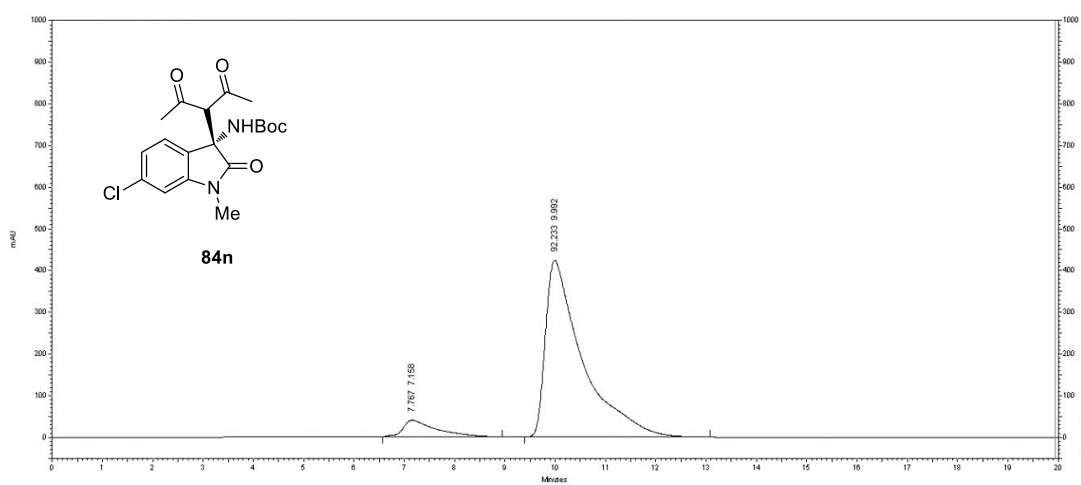
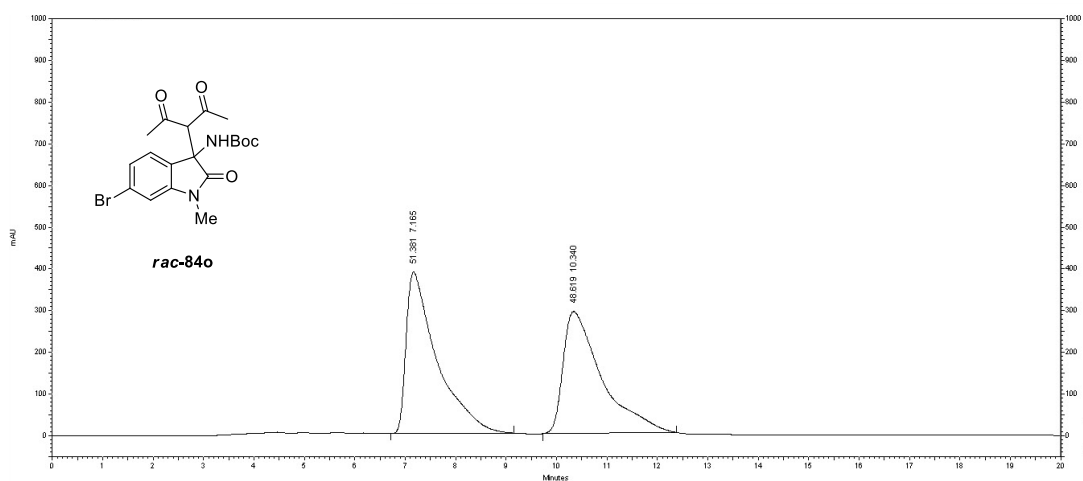
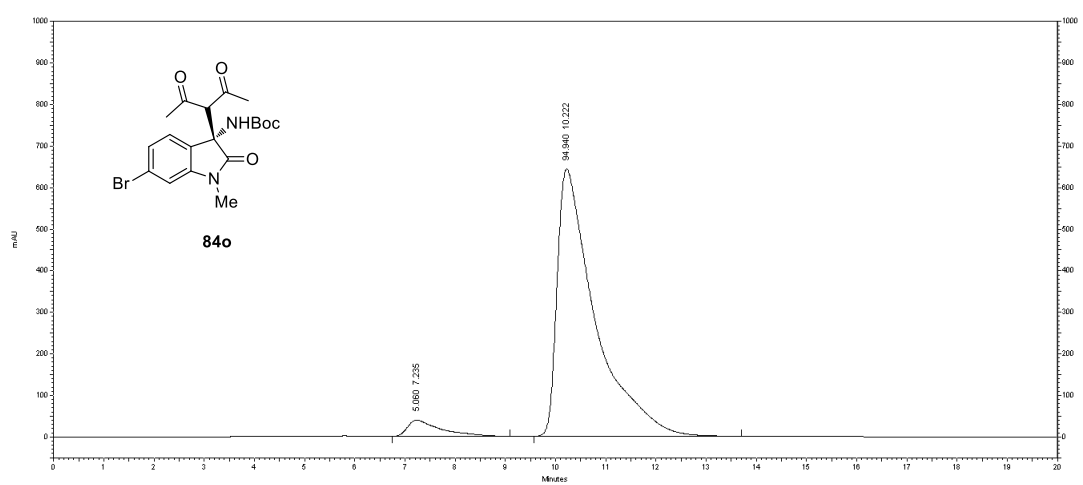


Figure B. 26 HPLC chromatogram of enantiomerically enriched *84n*



**Figure B. 27** HPLC chromatogram of *rac-84o*



**Figure B. 28** HPLC chromatogram of enantiomerically enriched **84o**

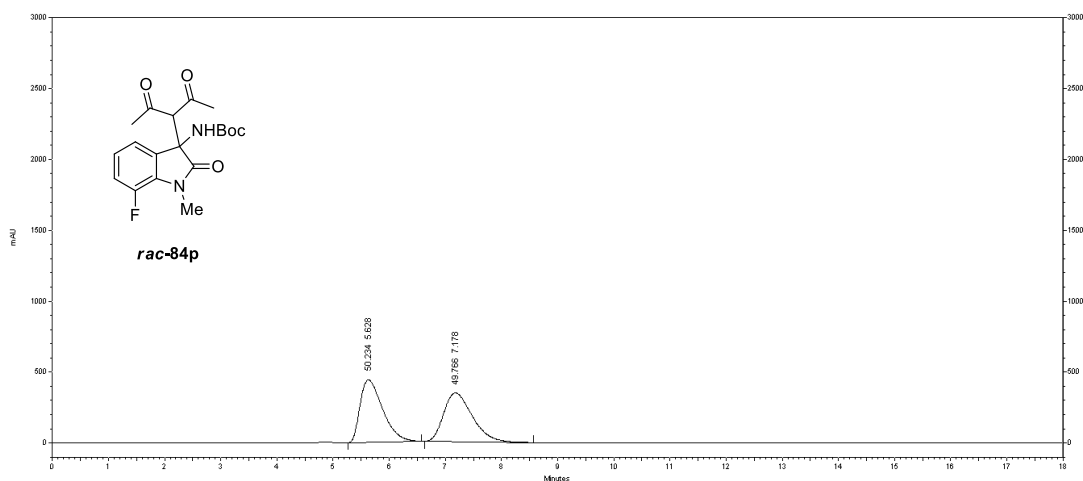


**Figure B. 29** HPLC chromatogram of *rac*-84p

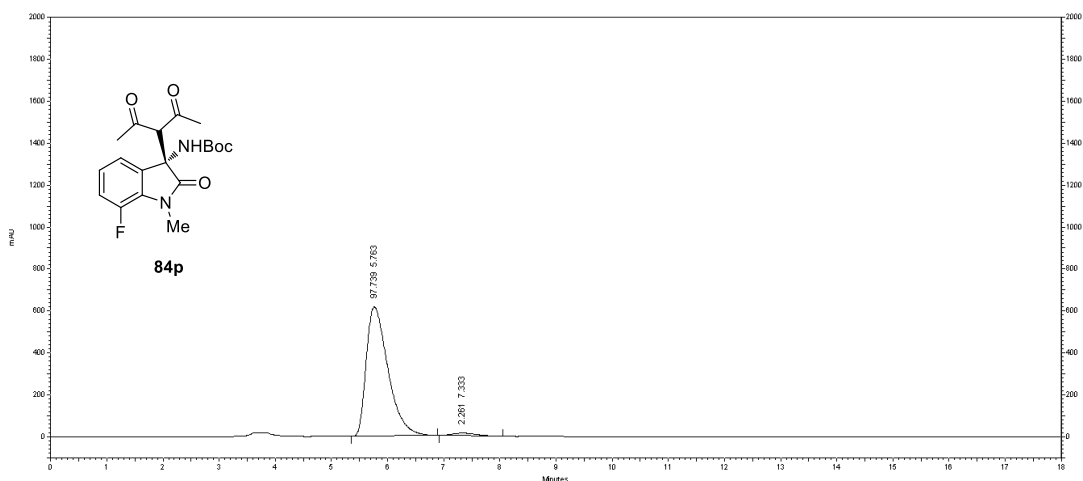


**Figure B. 30** HPLC chromatogram of enantiomerically enriched 84p

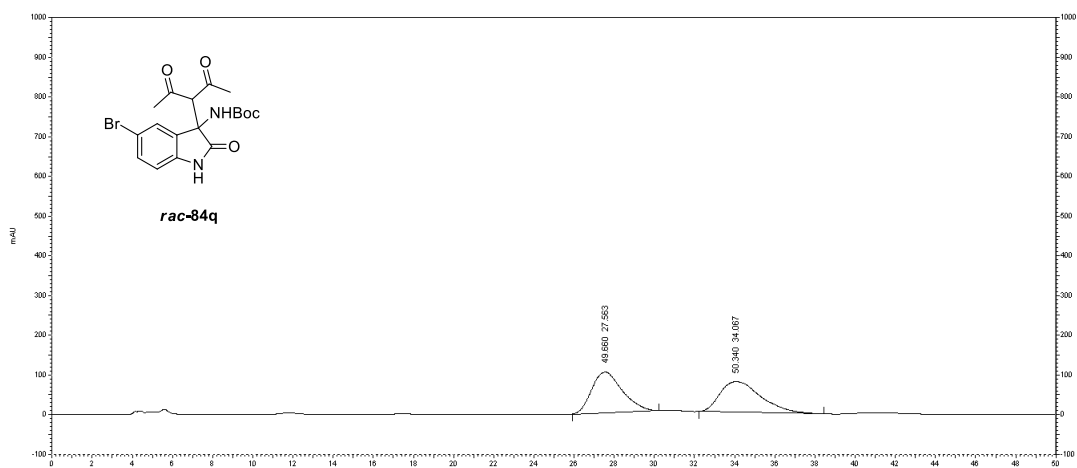


**Figure B. 31** HPLC chromatogram of *rac*-84q

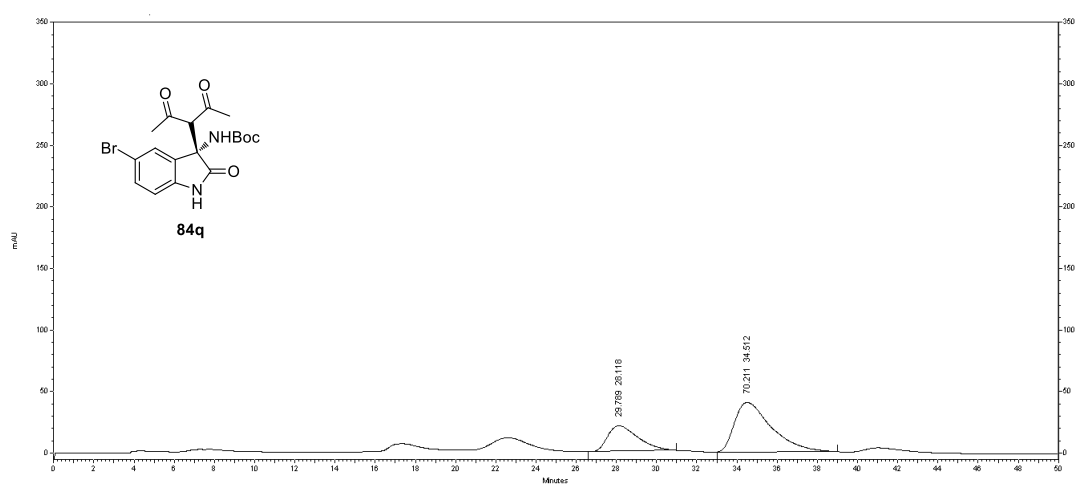


**Figure B. 32** HPLC chromatogram of enantiomerically enriched 84q

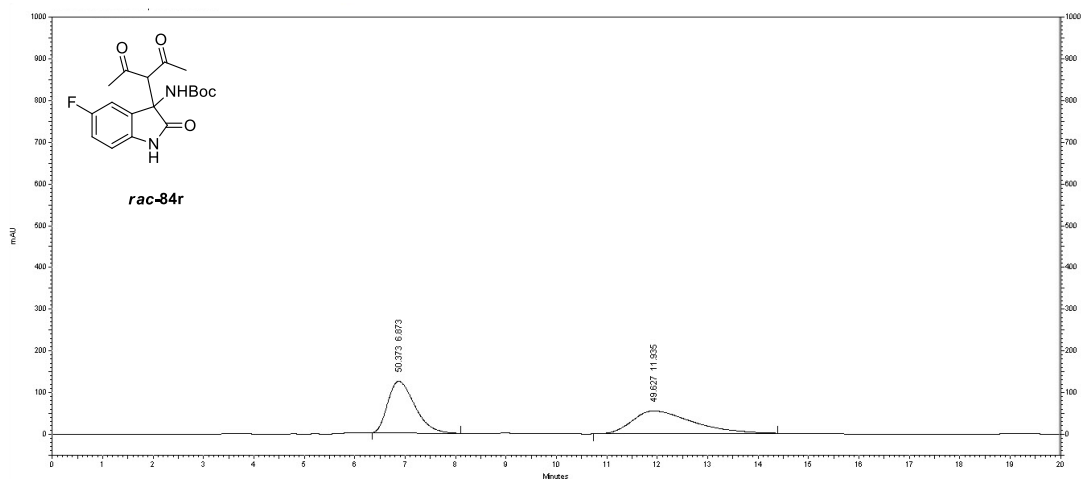


**Figure B. 33** HPLC chromatogram of *rac-84r*

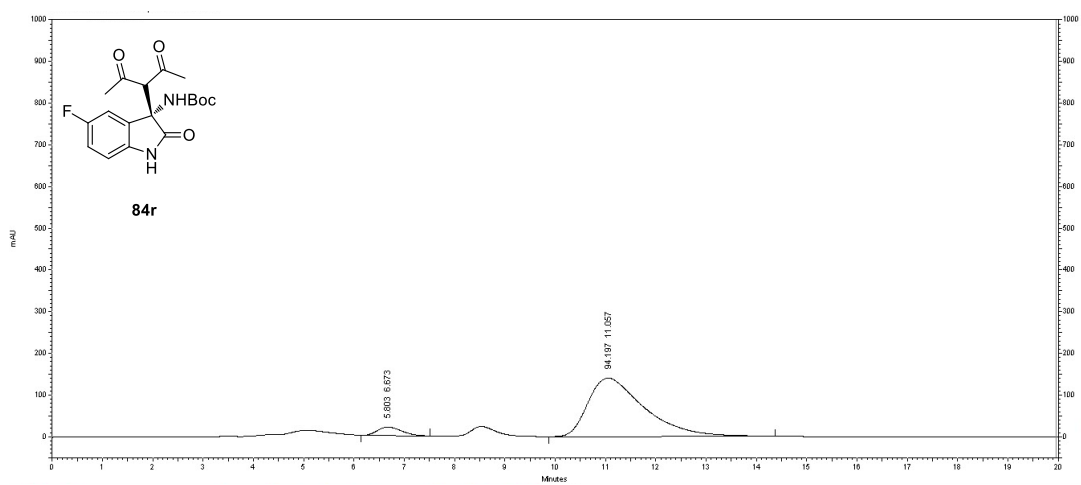


**Figure B. 34** HPLC chromatogram of enantiomerically enriched **84r**



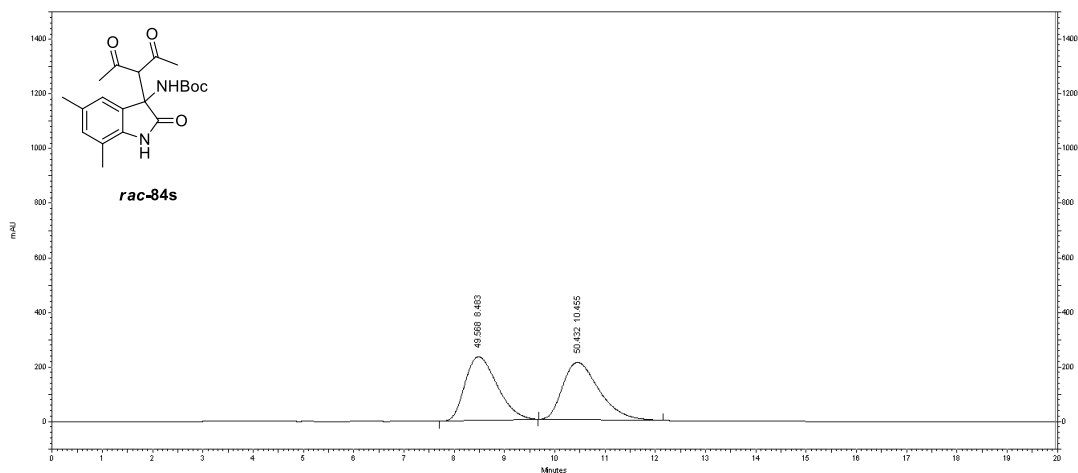


**Figure B. 35** HPLC chromatogram of *rac-84s*

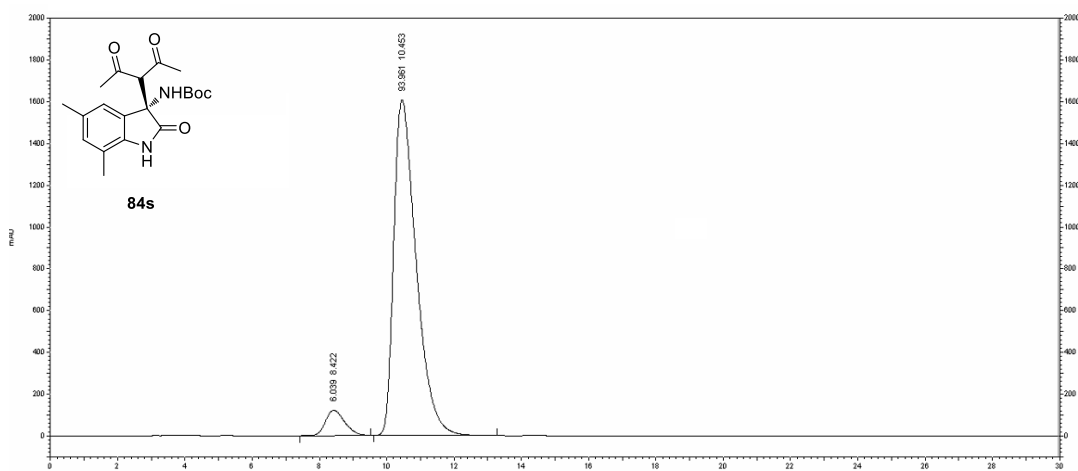


**Figure B. 36** HPLC chromatogram of enantiomerically enriched **84s**

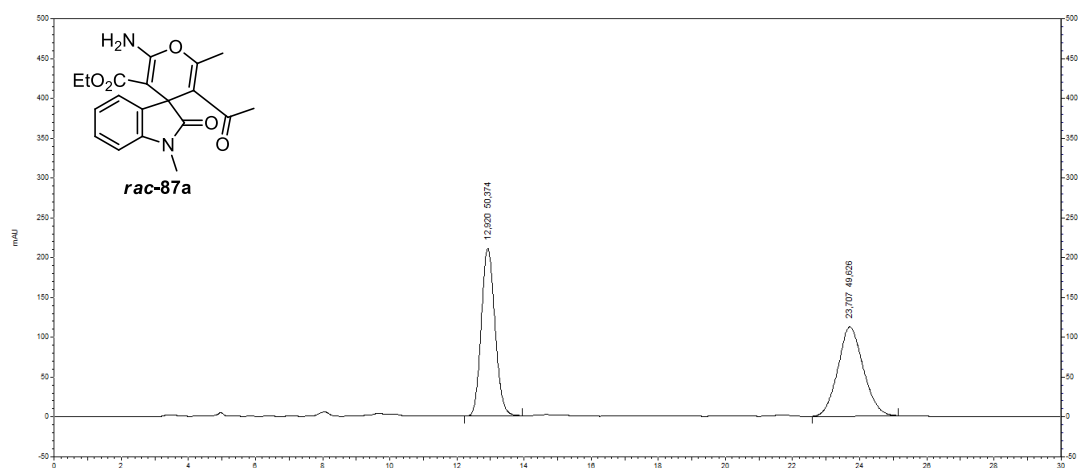


**Figure B. 37** HPLC chromatogram of *rac-87a*

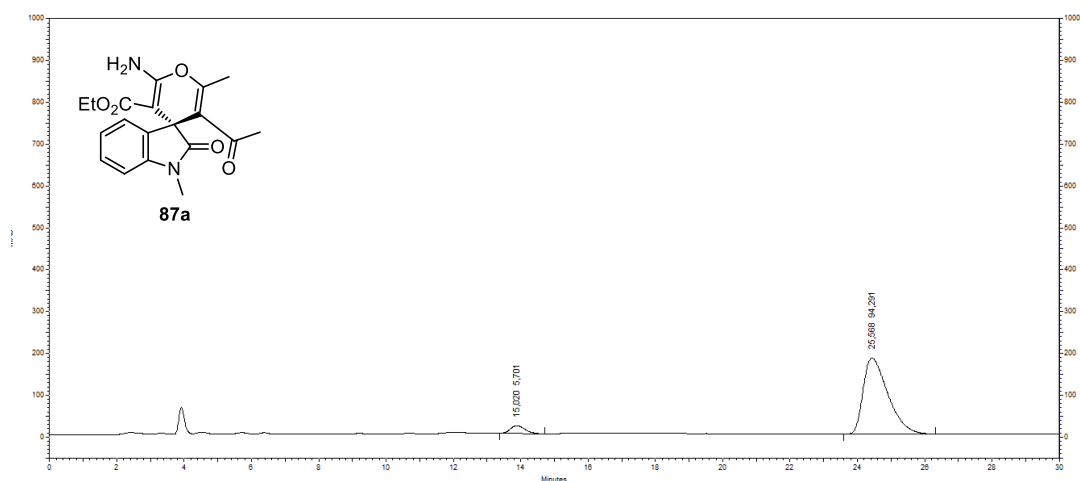


**Figure B. 38** HPLC chromatogram of enantiomerically enriched **87a**

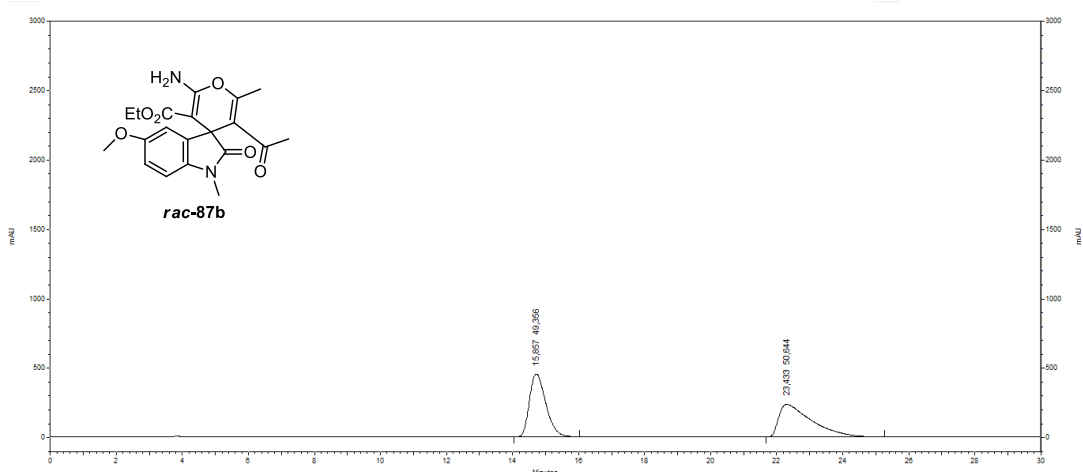


**Figure B. 39** HPLC chromatogram of *rac-87b*

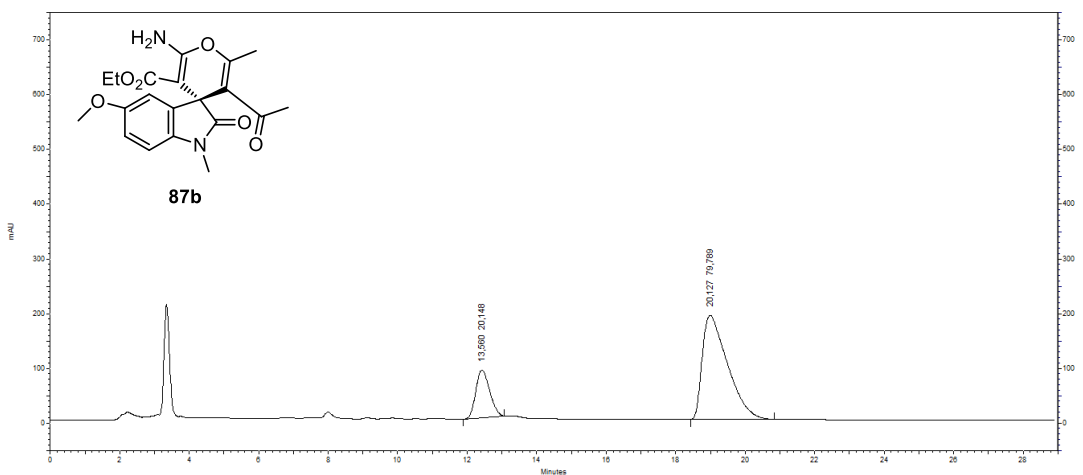


**Figure B. 40** HPLC chromatogram of enantiomerically enriched **87b**

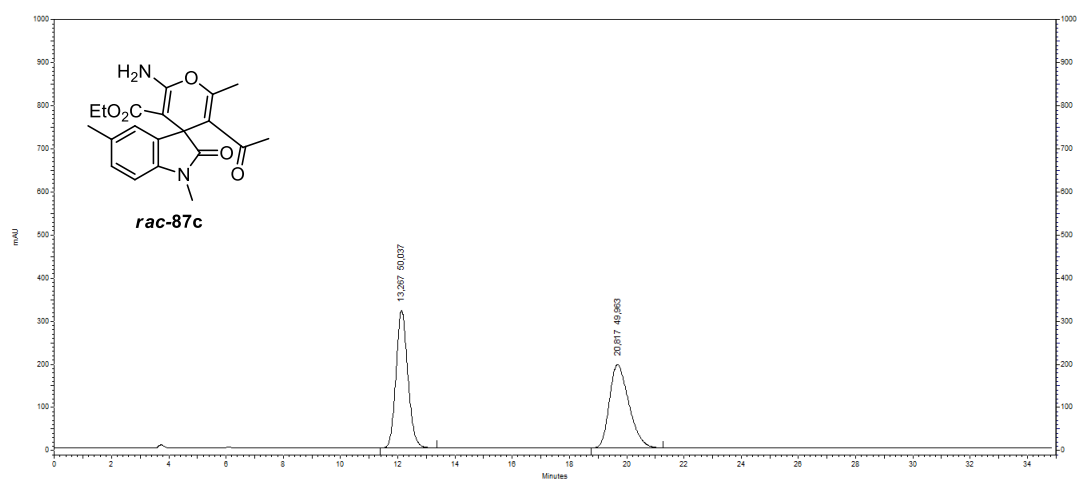


**Figure B. 41** HPLC chromatogram of *rac-87c*

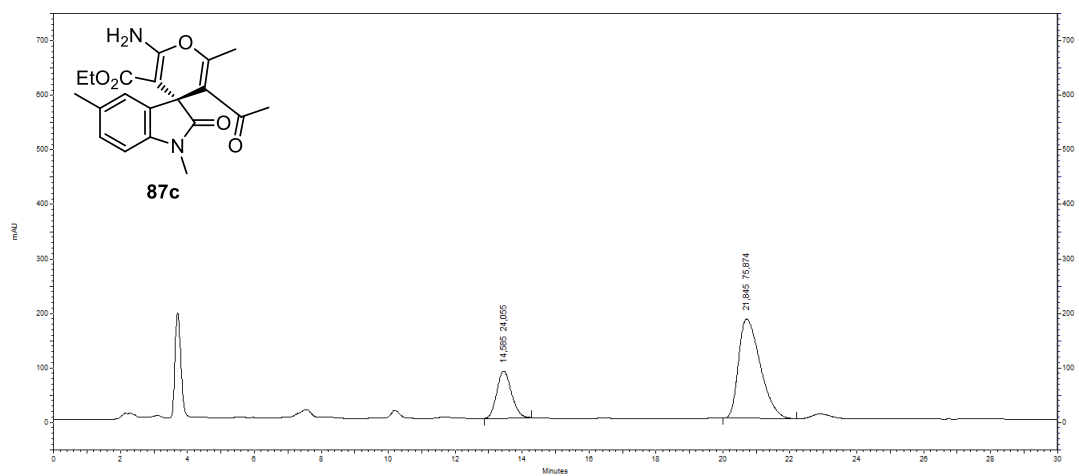


**Figure B. 42** HPLC chromatogram of enantiomerically enriched *87c*

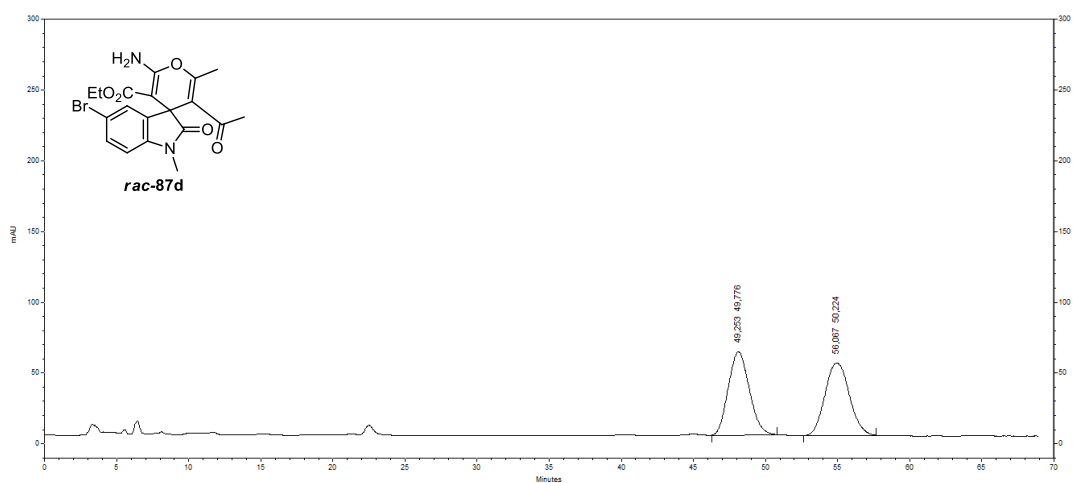


**Figure B. 43** HPLC chromatogram of *rac-87d*

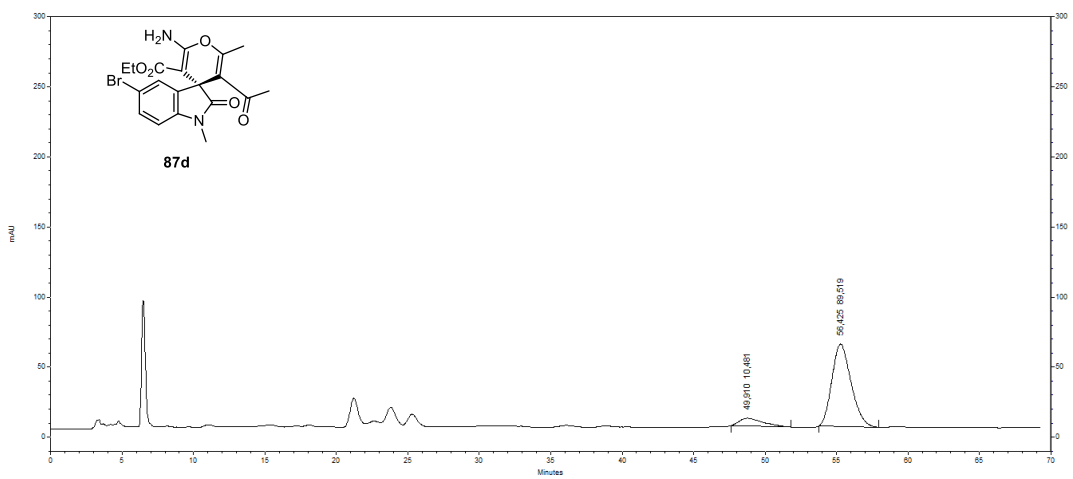


**Figure B. 44** HPLC chromatogram of enantiomerically enriched **87d**

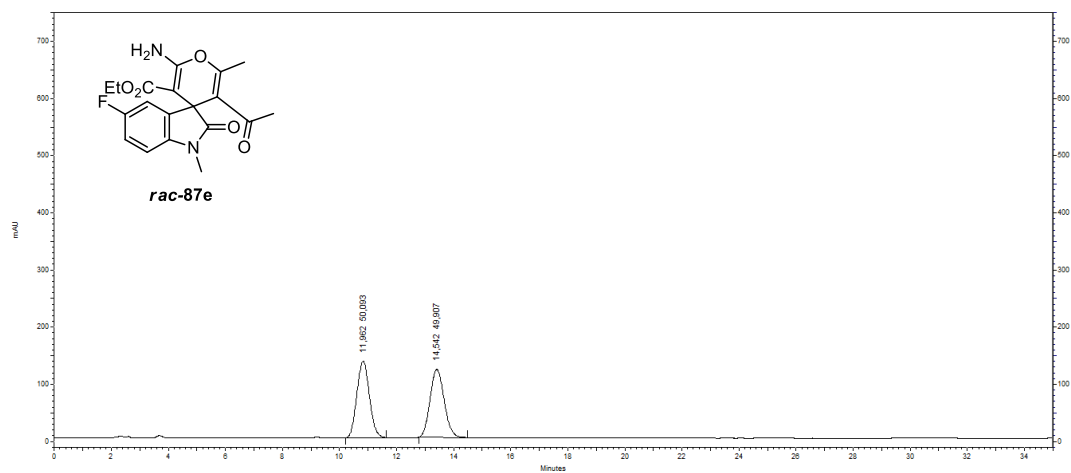


Figure B. 45 HPLC chromatogram of *rac-87e*

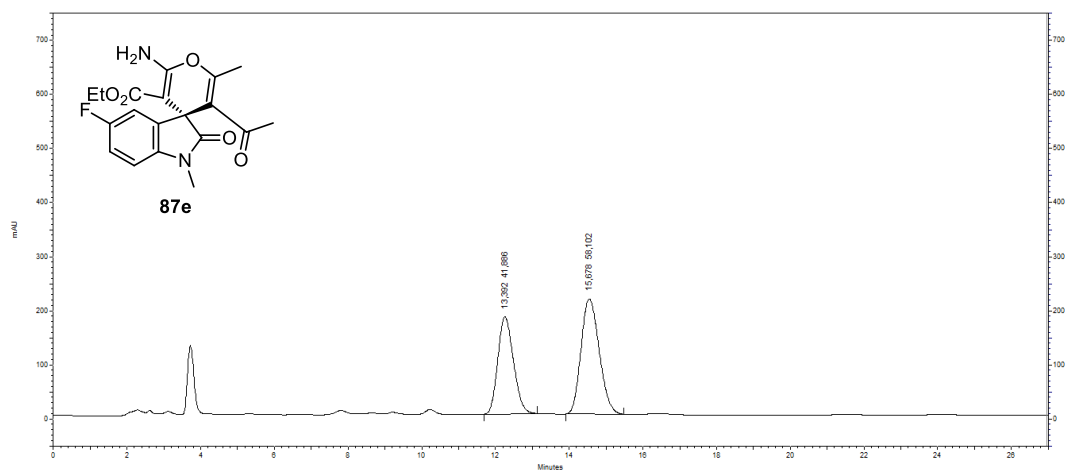
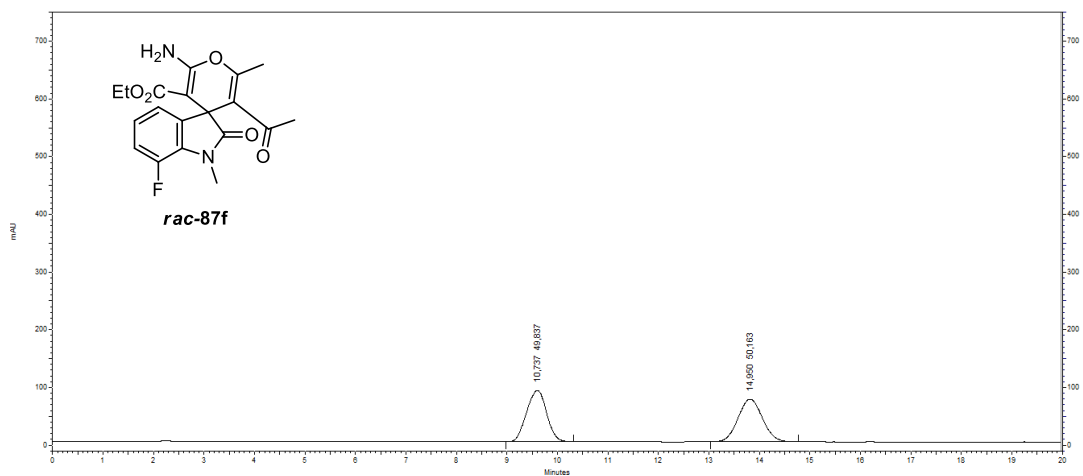
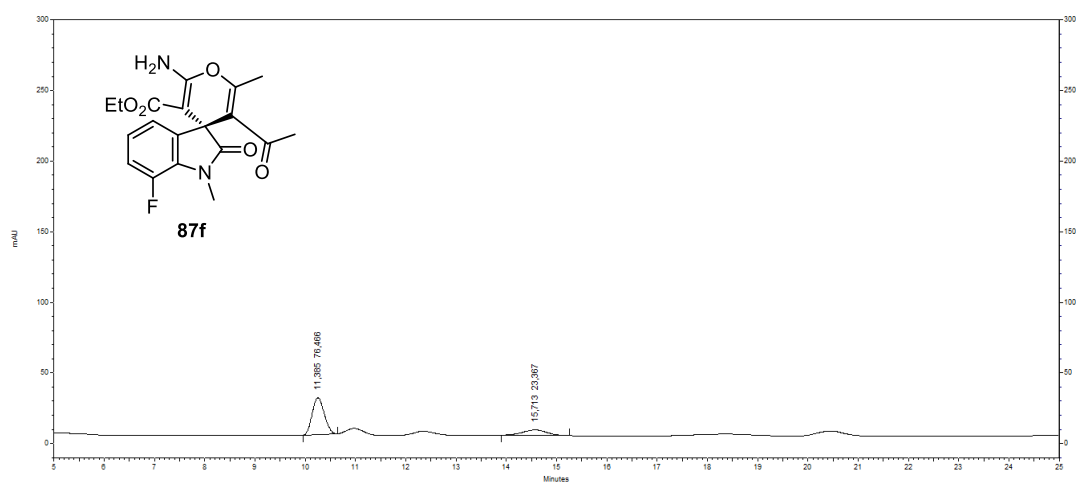


Figure B. 46 HPLC chromatogram of enantiomerically enriched *87e*



**Figure B. 47** HPLC chromatogram of *rac-87f*



**Figure B. 48** HPLC chromatogram of enantiomerically enriched *87f*

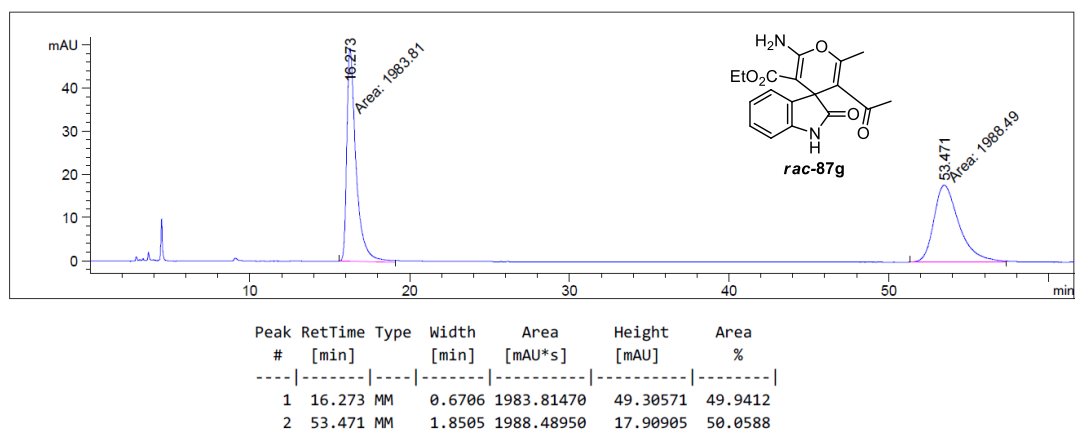


**Figure B. 49** HPLC chromatogram of *rac-87g*

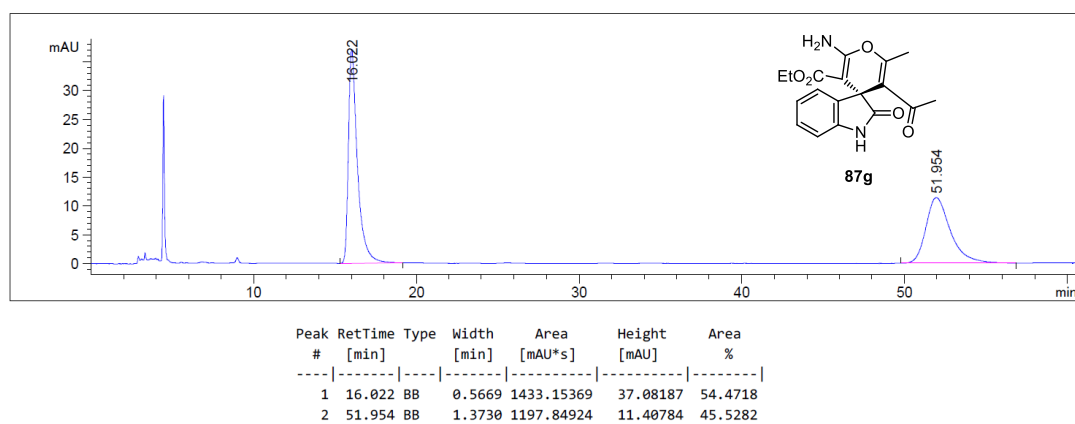


**Figure B. 50** HPLC chromatogram of enantiomerically enriched **87g**



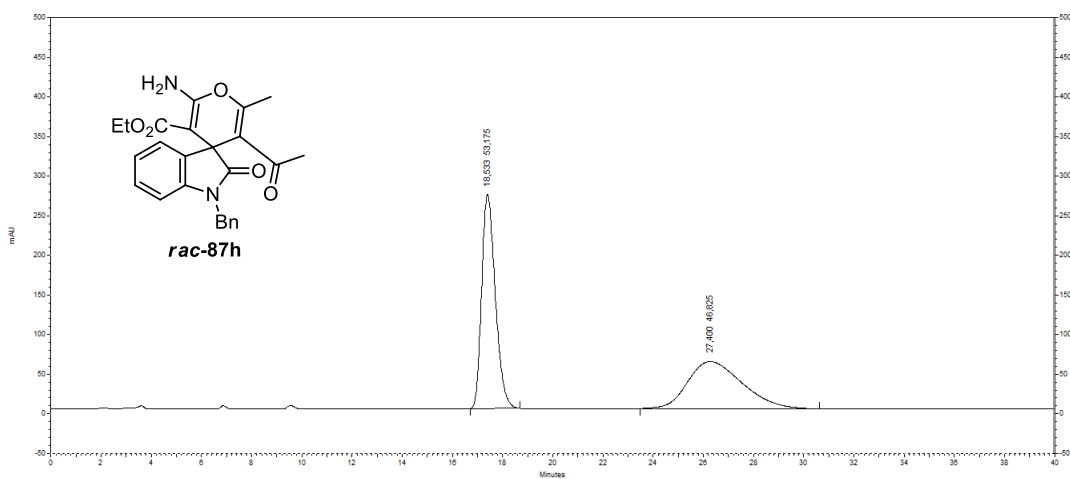


**Figure B. 51** HPLC chromatogram of *rac-87h*

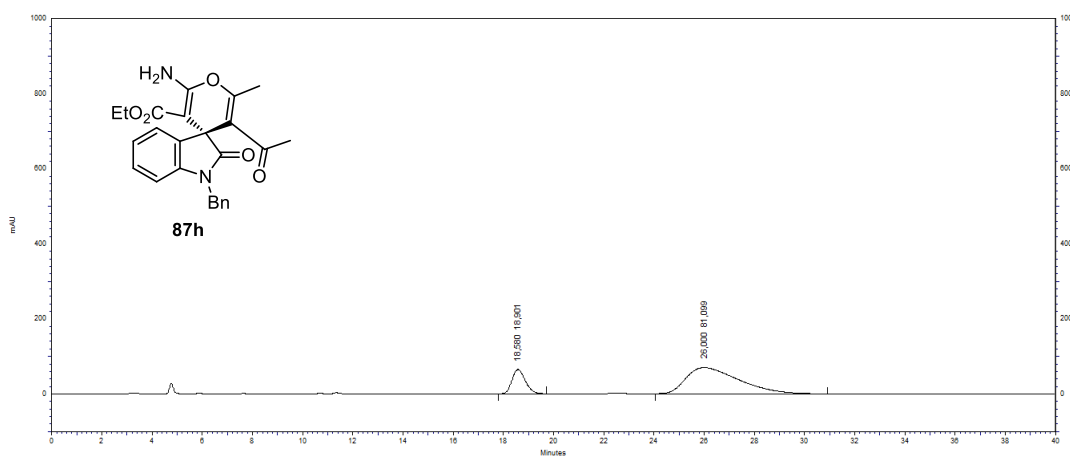


**Figure B. 52** HPLC chromatogram of enantiomerically enriched **87h**

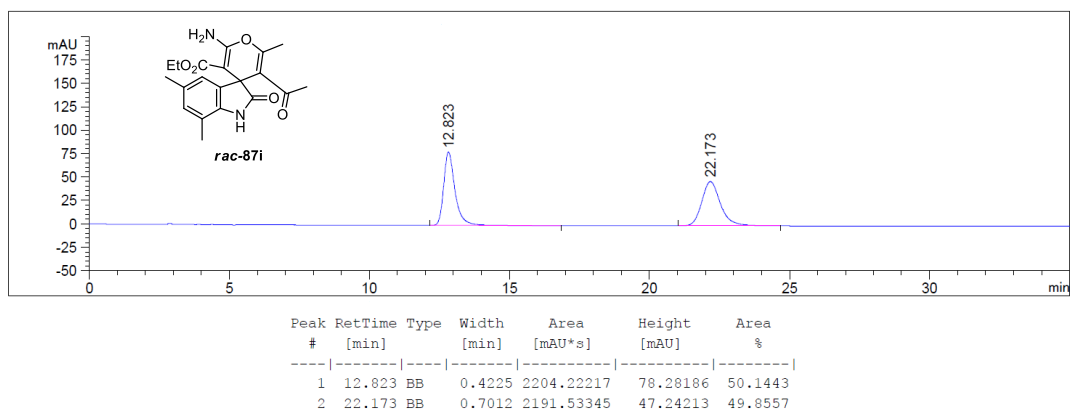


**Figure B. 53** HPLC chromatogram of *rac-87i*

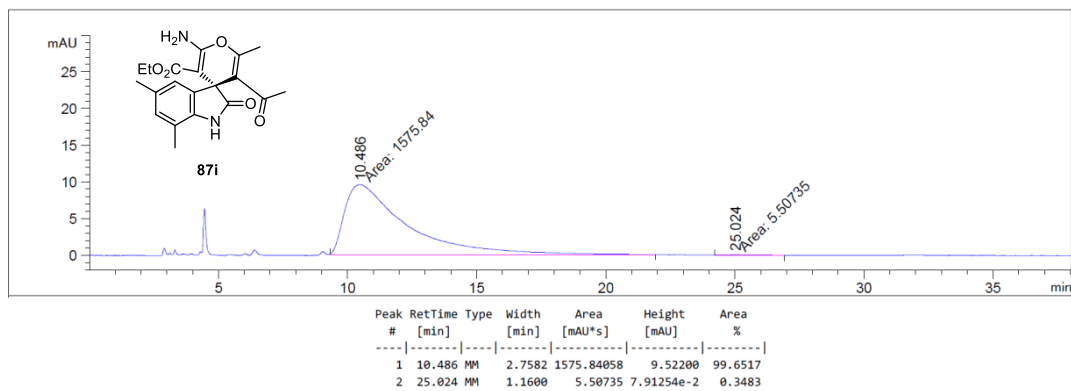


**Figure B. 54** HPLC chromatogram of enantiomerically enriched **87i**

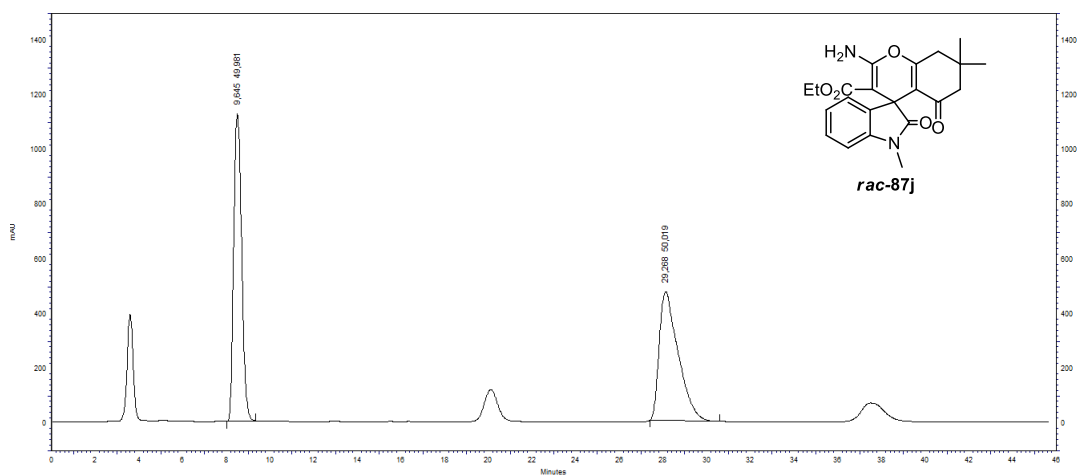


**Figure B. 55** HPLC chromatogram of *rac*-87j

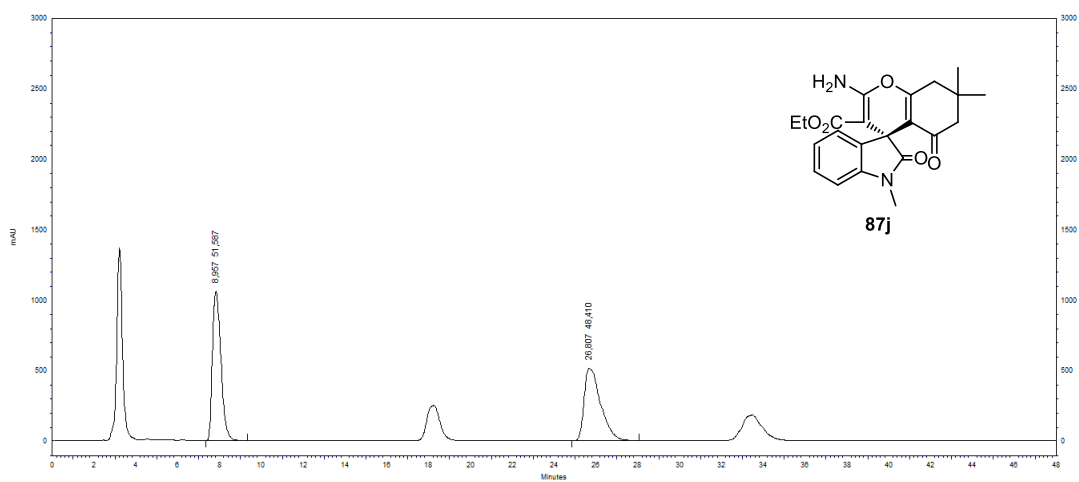


**Figure B. 56** HPLC chromatogram of enantiomerically enriched 87j

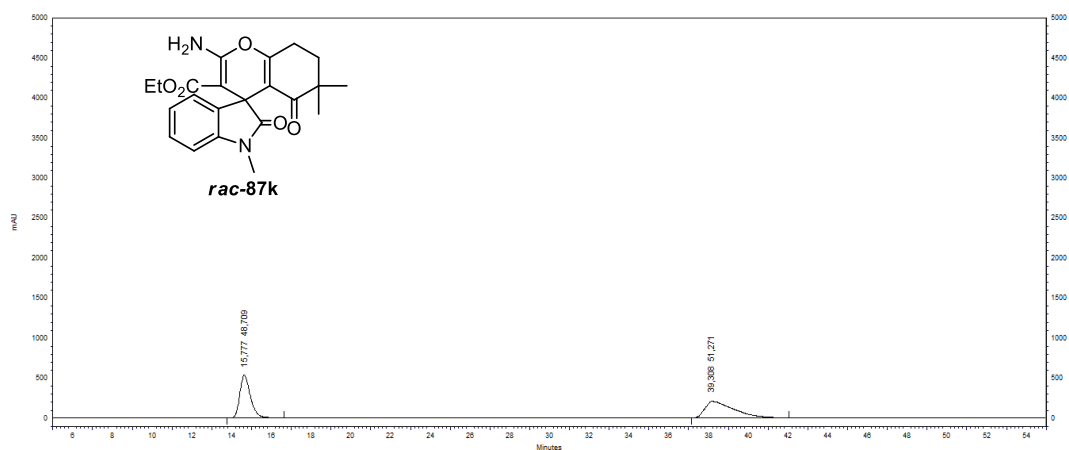


**Figure B. 57** HPLC chromatogram of *rac-87k*

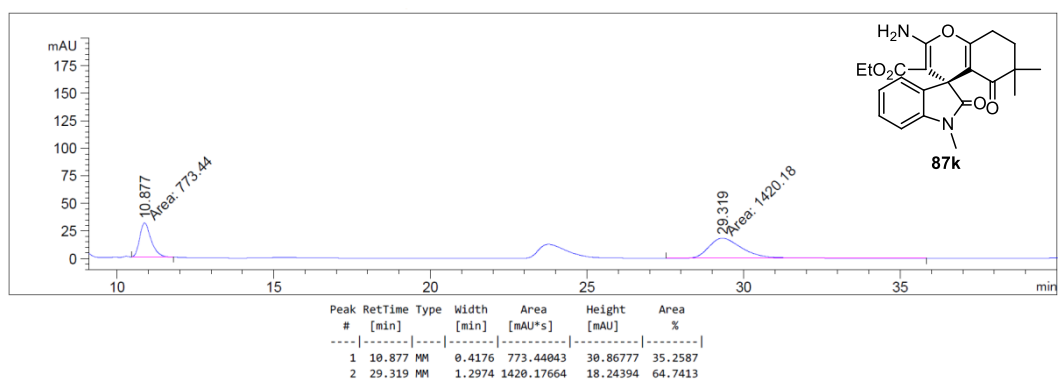


**Figure B. 58** HPLC chromatogram of enantiomerically enriched **87k**

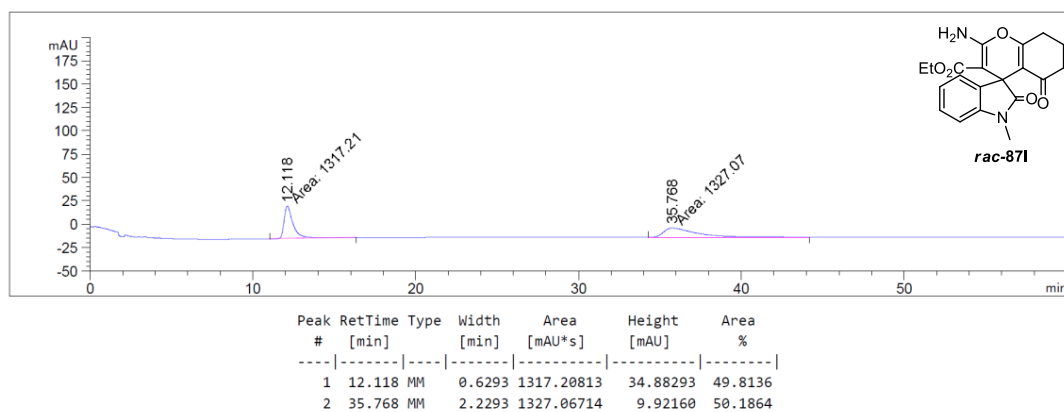


**Figure B. 59** HPLC chromatogram of *rac*-871

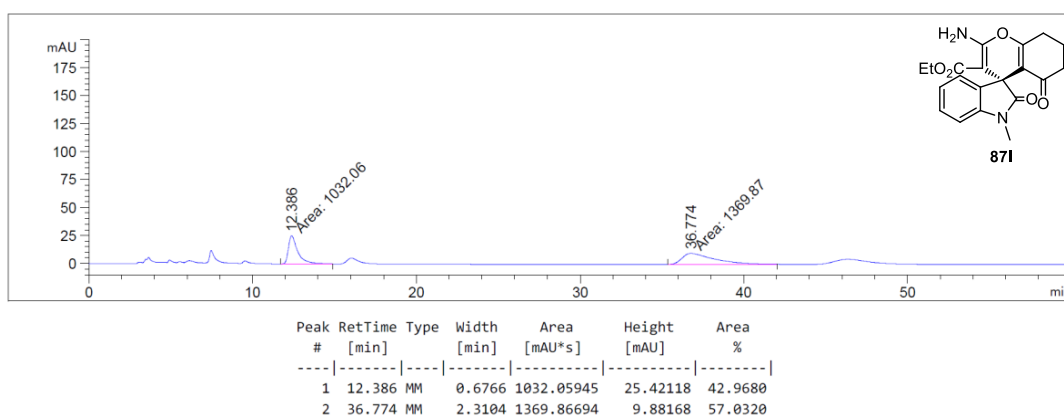


**Figure B. 60** HPLC chromatogram of enantiomerically enriched 871

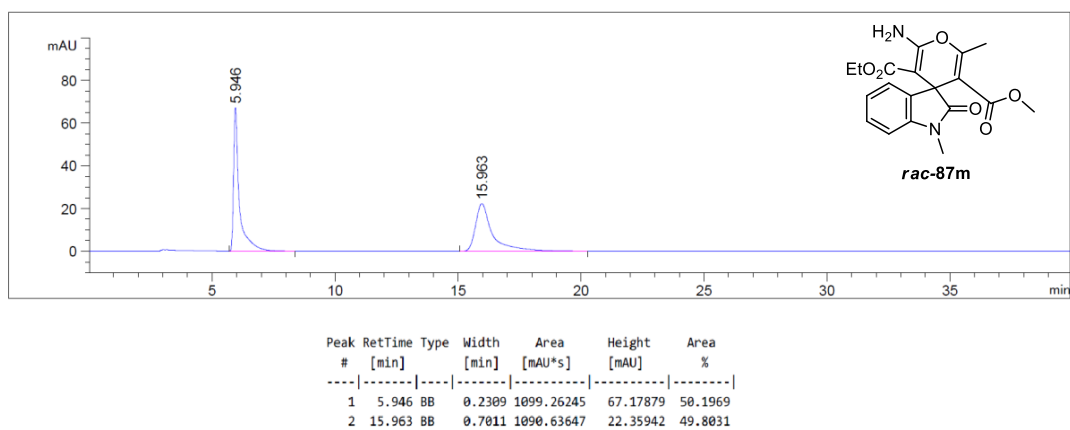


**Figure B. 61** HPLC chromatogram of *rac-87m*

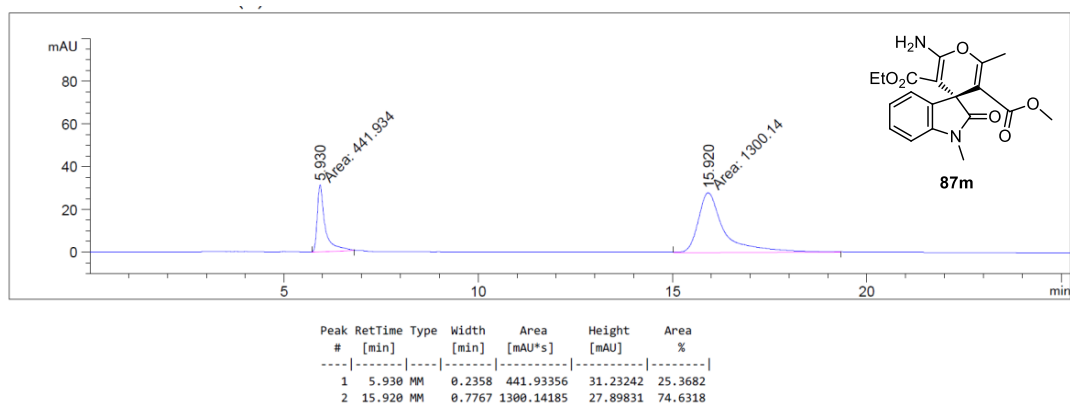


**Figure B. 62** HPLC chromatogram of enantiomerically enriched *87m*

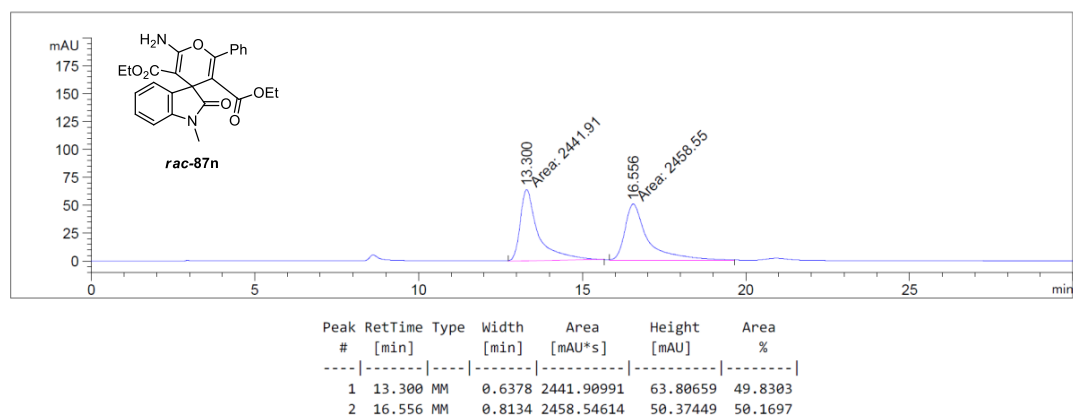


**Figure B. 63** HPLC chromatogram of *rac-87n*

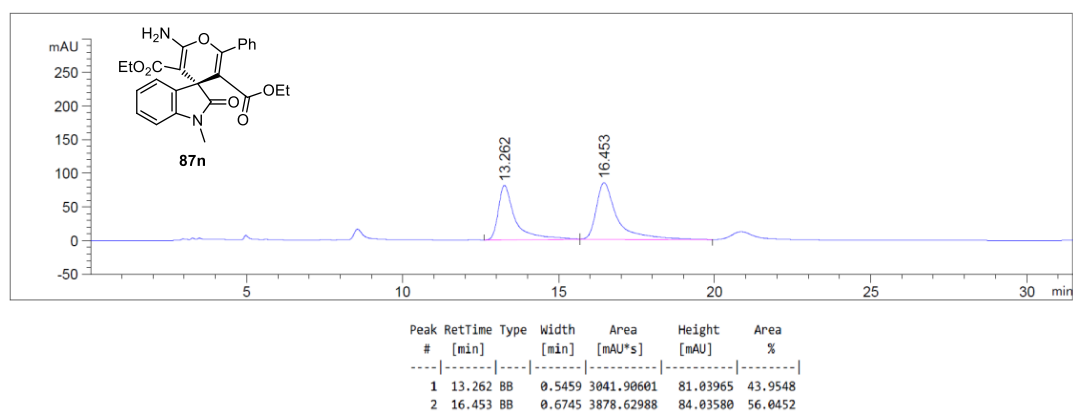


**Figure B. 64** HPLC chromatogram of enantiomerically enriched **87n**

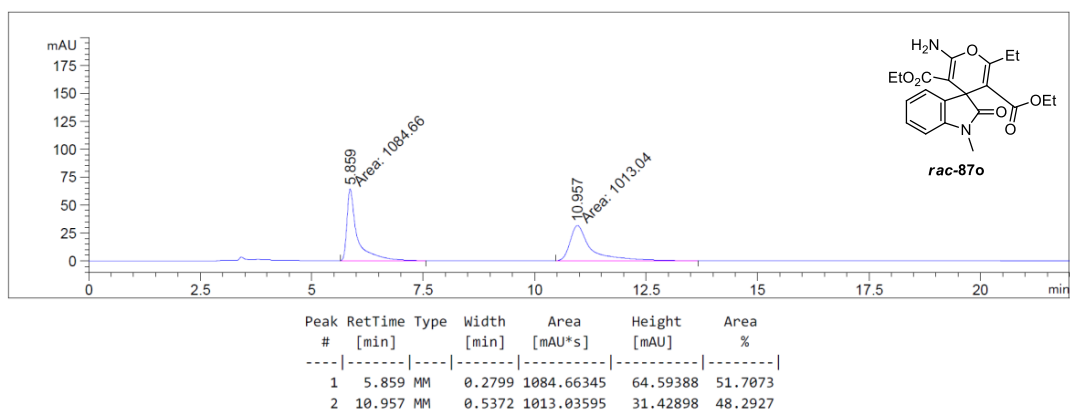


**Figure B. 65** HPLC chromatogram of *rac-87o*

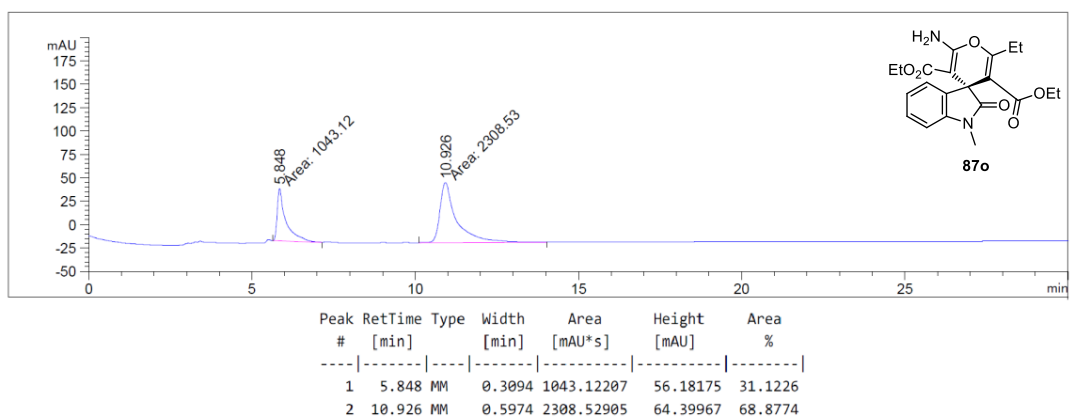


**Figure B. 66** HPLC chromatogram of enantiomerically enriched **87o**



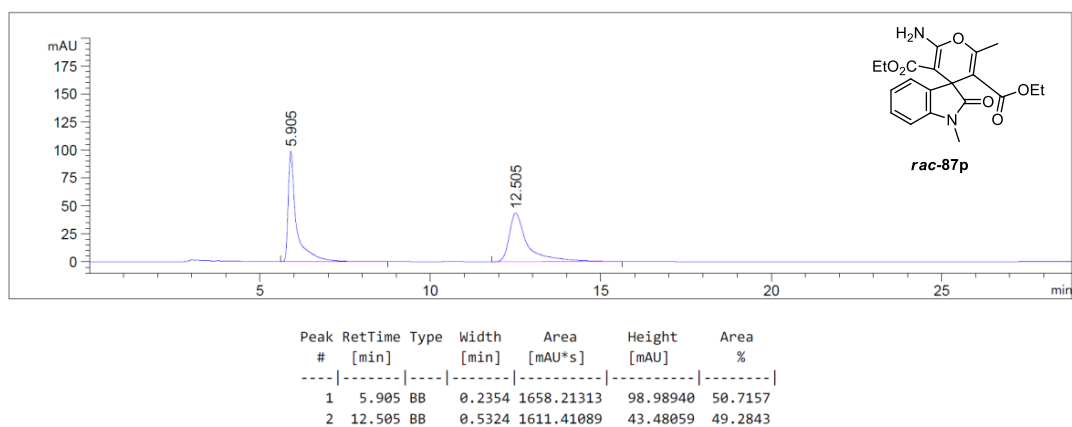


**Figure B. 67** HPLC chromatogram of *rac-87p*

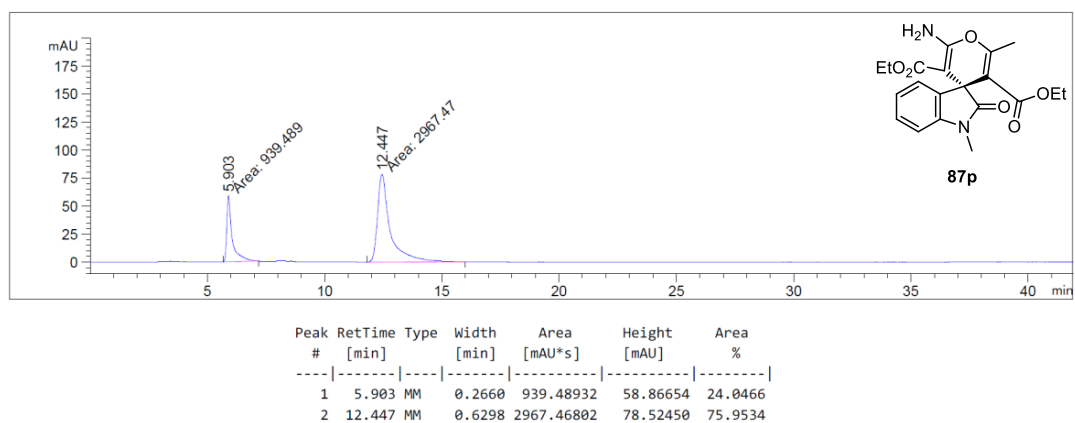


**Figure B. 68** HPLC chromatogram of enantiomerically enriched **87p**

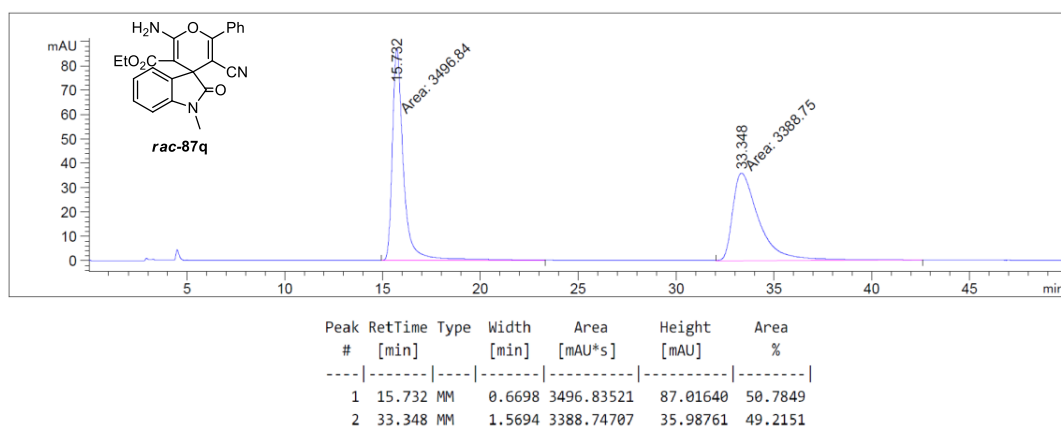


**Figure B. 69** HPLC chromatogram of *rac-87q*

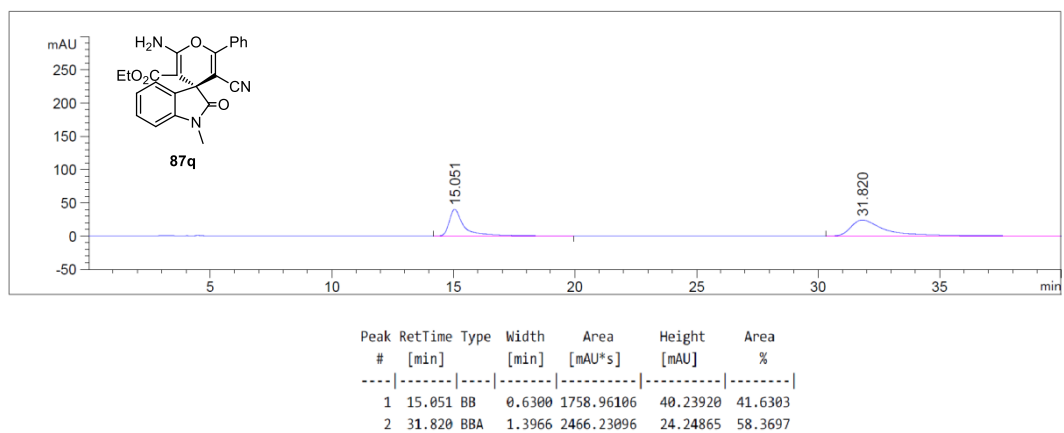


**Figure B. 70** HPLC chromatogram of enantiomerically enriched **87q**

## CURRICULUM VITAE

### PERSONAL INFORMATION

**Surname, Name:** Karaçal, Duygu

### EDUCATION

Degree	Institution	Year of Graduation
MS	METU Chemistry	2013
BS	METU Chemistry	2011
High School	Seyhan ÇEAŞ Anatolian High School, Adana	2006

### FOREIGN LANGUAGES

English: Fluent in speaking

German: Beginner level

### PUBLICATIONS

1. **İşibol, D.;** Karahan, S.; Tanyeli, C. “Asymmetric organocatalytic direct Mannich reaction of acetylacetone and isatin derived ketimines: Low catalyst loading in chiral cinchona-squaramides” *Tetrahedron Lett.* **2018**, *59*, 541-545.